Final Technical Report to U.S. Geological Survey

Award Number: Grant 06HQGR0170

Prinicipal Investigator: Virginia S. Gillerman, Ph.D.

Title:

Geochronology of Iron Oxide-Copper-Thorium-REE Mineralization in Proterozoic Rocks at Lemhi Pass, Idaho, and a Comparison to Copper-Cobalt Ores, Blackbird Mining District, Idaho

December 30, 2008

Research supported by the U.S. Geological Survey (USGS), Department of the Interior, Under USGS award number 06HQGR0170. The views and conclusions contained in this document are those of the authors and should not be interpreted as necessarily representing the official policies, either expressed or implied, of the U.S. government.

Introduction

This MRERP study proposed to investigate the geochronology and petrology of apparently multistage mineralization of copper-gold and iron oxide-thorium-rare earth element deposits in Proterozoic rocks of the Lemhi Pass District, Idaho and Montana. A primary question for the study to answer was whether the Lemhi Pass mineral deposits could be considered as an example of the iron oxide-copper-gold (IOCG) classification of ore deposits. Secondary project goals included a comparison of alteration assemblages for the Lemhi Pass rocks with rocks from the copper-cobalt-gold ores of the Blackbird Mining District, hosted in similar Proterozoic strata approximately 43 miles to the west; and an evaluation of using the electron microprobe to determine chemical ages for monazite geochronology. Previous preliminary work had suggested the presence of a component of Proterozoic-aged mineralization for both the copper-molybdenite mineralization and thorium-REE deposits, as well as a Cretaceous overprint.

Location and Previous Work

The Lemhi Pass Thorium District is located in the Beaverhead Mountains, along the Idaho-Montana border, southeast of Salmon, Idaho (Figure 1). The Lewis and Clark Expedition crossed the Continental Divide at Lemhi Pass in August, 1805. Fieldwork by the Idaho Geological Survey (IGS) started in 2000 as part of a hazard inventory of inactive mine sites. The field crew spent ten days in the area, surveying the Copper Queen mine and several of the larger thorium pits, including the Lucky Horseshoe Mine, Buffalo mine, and Wonder Lode in Idaho (Gillerman and others, 2001; Gillerman and others, 2006). Mines on the Montana side were not examined in 2000.

The Lemhi Pass District is hosted in Proterozoic-age quartzites and siltites of the Apple Creek and Gunsight Formations, overlain by Tertiary-age Challis Volcanics (Staatz, 1979; Evans and Green, 2003). Early prospectors discovered copper-gold mineralization of the Copper Queen mine in 1883 (Umpleby, 1913), along a branch of Agency Creek two miles west of Lemhi Pass. Thorium was discovered there in 1951 and a prospecting boom followed, along with considerable geologic work. Staatz (1979) in USGS Professional Paper 1049A provided a geologic map and the most comprehensive description of the numerous mineral deposits. However, his interpretation that the thorium was related to the Eocene-age Challis volcanics was inconsistent with a number of the IGS crew's field observations, which suggested the Cu and Th mineralization was at least pre-Cretaceous, most likely Proterozoic, in age and had a striking similarity to the Olympic Dam-type Cu-U-Fe Oxide-REE class of mineral deposits (Gillerman and others, 2000; Gibson, 1998).

The 2000 field results and the unusual rocks prompted subsequent geochronological research, limited in scope and described partially in Gillerman and others (2002) and Jercinovic and others (2002). The copper and thorium deposits at Lemhi Pass presented a challenging but unique opportunity to date mineralization using both Th-U-total Pb and Re-Os chronometers on monazite and molybdenite, respectively, and to experiment with

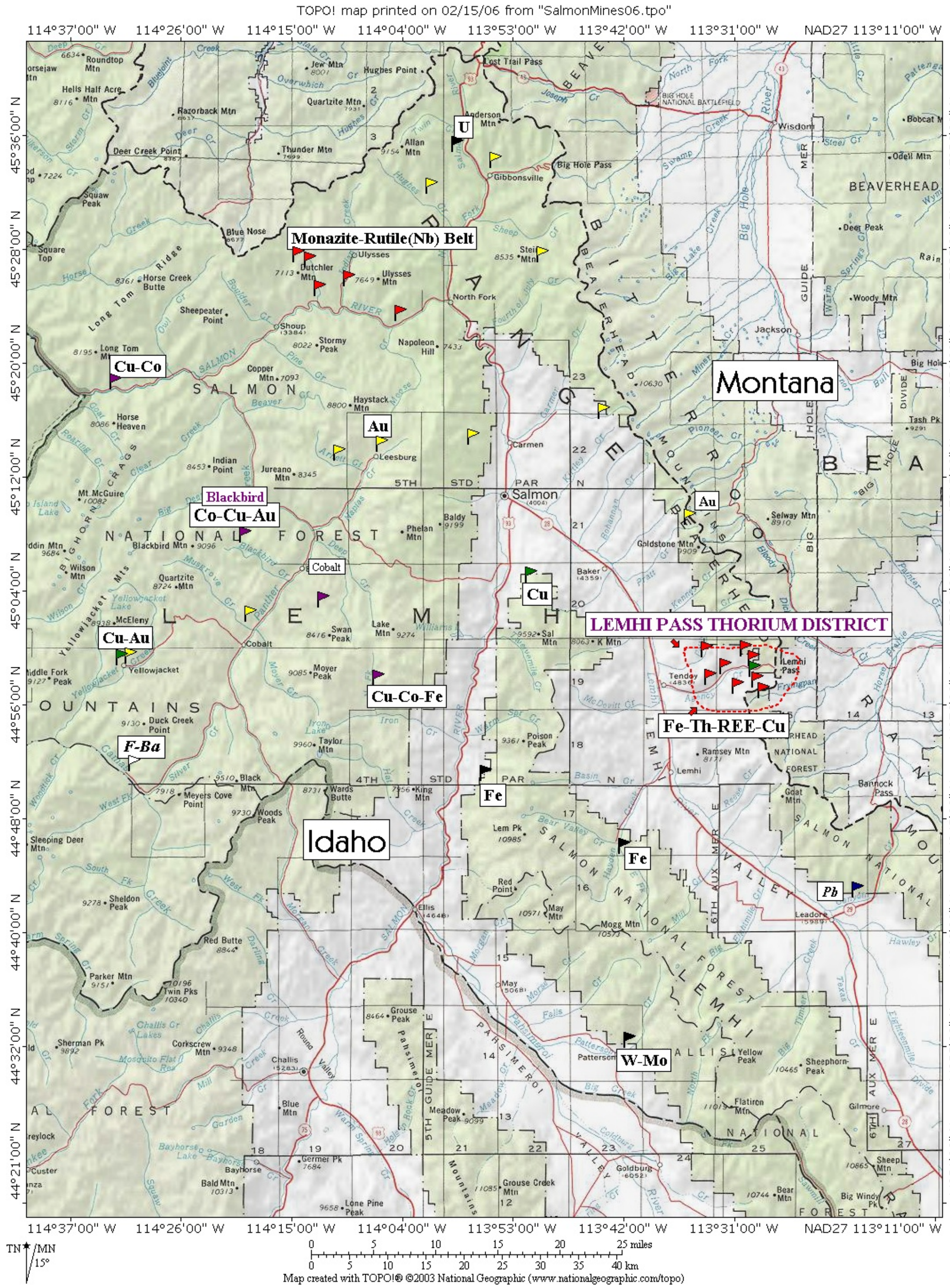

Figure 1. Location Map of the Lemhi Pass Thorium District with additional metallogeny of Salmon region, Idaho.

dating thorite by Th-U-total Pb methods, according to techniques being developed at the University of Massachusetts. Initial results of Electron Microprobe Th-U-total Pb geochronology on zoned monazites in two samples from the Lucky Horseshoe mine showed a complex hydrothermal history with core ages of 800-1100 Ma and younger rims of 200-400 Ma. Colleagues at the electron microprobe facility at the University of Massachusetts were also able to obtain ages on fresh and altered thorite ($ThSiO_4$) reflecting Paleozoic ages and altered domains with Pb loss as young as 100 Ma. In addition, one sample of molybdenite from the waste dump at the Copper Queen mine contained sufficient Re to obtain a Re-Os date of 1053 Ma, matching well the monazite cores (Gillerman and others, 2002). The Proterozoic age did correspond with literature reports of some type of "Grenville-age" thermal event in the region (Anderson and Davis, 1995) but not with any known geologic events in the Salmon region. Lemhi Pass district geology and ore deposits were summarized in Gillerman and others (2003, 2006), and a comprehensive regional geologic map has since been published by the USGS (Evans and Green, 2003).

Given the unusual rocks and unexpected age constraints, additional study seemed warranted. Specific research objectives listed in the ambitious MRERP proposal included better determinations of:

1. Age of mineralization
2. Regional hydrothermal alteration (widespread sodic or potassic alteration is a signature of IOCG systems)
3. Ore Deposit Model – is Lemhi Pass a thorium-rich variant of IOCG's?
4. Comparison to the Idaho Cobalt Belt
5. Comparison to other Idaho thorium deposits

After the initial fieldwork on the project was started, a more realistic assessment of the resources and time available has limited the work on goals 4 and 5 in particular. The geologic complexity and some of the unexpected findings at Lemhi Pass itself focused the study more on that specific district and the Beaverhead Mountains.

Summary of Work Activities and Co-Investigators on Project

Project activities included: 1) fieldwork in late summer of 2006 (plus a shorter time in 2007) involving the principal investigator (PI) and a field crew with a field assistant and two Idaho Geological Survey expert mappers (supported in part by additional funding sources) to do reconnaissance mapping traverses and sampling (see Appendix A for sample waypoint locations); 2) rock-cutting and commercial preparation of a substantial number (approximately 125) of thin sections and polished sections in several batches over two years with ongoing petrographic examination (see Appendix B for brief summary); 3) microprobe analyses at Washington State University of selected polished sections (see Appendix C); 4) geochronology of one intrusive and two detrital zircon samples using SHRIMP U-Pb dating by Dr. Mark Fanning, Australia (see Appendix D for data tables); 5) submittal of one batch of samples, principally intrusives, for whole rock geochemistry by Act Labs of Canada (see Appendix E for full analytical results); 6) submittal of five samples for $^{40}Ar/^{39}Ar$ geochronology at the University of Alaska, Fairbanks, by Dr. Paul Layer (see Appendix F for report); 7) submittal of samples to Dr. Mike Jercinovic at University of Massachusetts, Amherst, for Electron Microprobe Th-U-total Pb geochronology on monazites (see Appendix G for report); and 8) preparation and analysis of 30 samples of feldspar, oxide, and sulfide separates for TIMS (thermal ionization mass spectrometer) analysis of lead isotope ratios at Dr. Mark Schmitz' Isotope Geology Lab at Boise State University (see Appendix H for data tables).

Only a synopsis of the field and petrographic work is included in this summary report. More complete presentations will be included in future publications. Laboratory investigations and basic microprobe analysis used standard analytical procedures; the more difficult and critical issue was finding samples to adequately answer the appropriate questions. Electon microprobe geochronology and microanalysis did require development of new procedures at the University of Massachusetts to study these special monazites and thorites (see Appendix G). A great benefit to the study was additional rock sampling and whole rock geochemistry done by Thorium Energy Inc., and their geologist, Rich Reed of IEG. Some of that data is included in the graphs and discussion in the text, but the full analytical information was retained by them and is not included in this report; some was presented publicly at the SME meeting in February 2008.

Summary of Field Observations and Discoveries

The fieldwork revealed that the district's geology is extremely complex but poorly exposed in many areas, and significant portions of all the published maps are (as expected) in error. A remapping of the Lemhi Pass District was far beyond the objectives of this study. Figure 2 shows major mine locations and general topography.

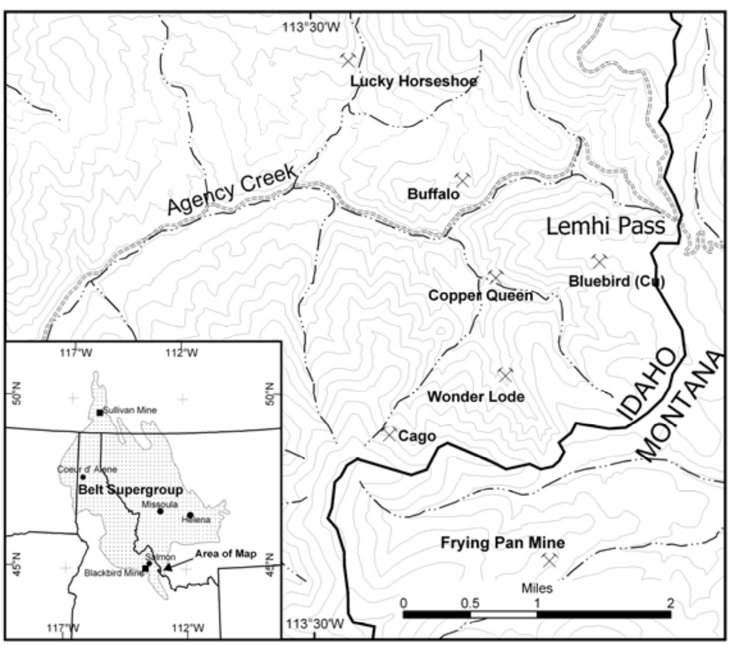

Figure 2. Mine Locations at Lemhi Pass District. The Last Chance mine is about one mile west of the Frying Pan mine in Montana. Note also the location of the Belt Supergroup of Mesoproterozoic clastic sedimentary rocks on the inset map.

Stratigraphic Correlations

A difficulty in mapping was that the Mesoproterozoic quartzite-siltite units (regionally correlative with the Apple Creek and Gunsight Formations in the southeastern most portion of the Belt Supergroup shown in Figure 2) have few marker horizons to map; this study did not find any new ones. However, the predominance of coarser clastic rocks in most of the area lead to an interpretation that most of the district is more likely underlain by the Gunsight Formation, and that the Beaverhead Range metasediments probably have minor facies variations from the type localities and exposures in the Lemhi Range. Some outcrops of more argillaceous and banded lithologies could most likely be classified as upper(?) Apple Creek Formation. There are few age constraints or detailed stratigraphic studies on the Precambrian rocks in the Beaverhead Range, and so two detrital zircon samples from quartzite were collected for age dating and provenance determination using the SHRIMP. Geochronology of the detrital zircons in two samples, DZ-2 and DZ-3, showed probable sedimentation ages of approximately1420-1450 million years ago (Figure 3 and Appendix D). The bar graph pattern (Figure 3) is similar to that from detrital zircon populations of known samples of the Yellowjacket, Apple Creek and western Gunsight Formations (Link, et al., 2007). There are a very few younger grains with ages of about 1370 ma in DZ-2 and DZ-3, which may be due to metamorphism or recrystallization by the 1370 ma suite of megacrystic granites and augen gneiss, exposed further west in the Salmon region (Evans and Zartman, 1990). Because of the regional thrusting which occurred in the Mesozoic, the "original" location of the rocks in the district could have been much further west, closer to the current exposures of the megacrystic granites, but exactly where is unknown.

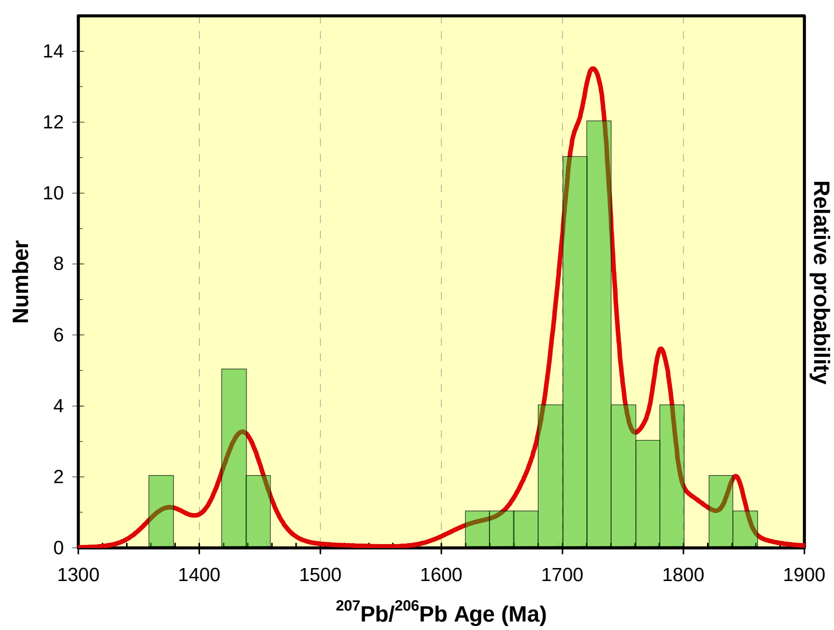

Figure 3. Density plot of youngest ages of detrital zircons in DZ_LP_2. See Appendix D for additional information on both samples.

Structural Interpretation

The structural models in the two most complete district geologic maps, Staatz (1979, USGS Professional Paper 1049-A), and Lund in Evans and Green (2003, I-2765) are radically different (Figures 5 and 6). Staatz's map, at a more detailed scale, defines a number of intersecting normal faults, which cut Tertiary volcanics. He also considered many thorium deposits to be localized along or near the regional-scale Lemhi Pass Fault (Figure 4). Many of the major faults appear to be correctly mapped, but the details of folds and strain fabrics are not included; justification for others is unclear. Lund's map (1:100,000 scale) shows a number of regional thrusts and related normal faults, as well as enigmatic younger over older thrusts. Reed Lewis and Russ Burmester, who have years of experience mapping Proterozoic rocks, could not substantiate the thrusts as they did not see differences in the rock units above and below the thrust faults, in a few traverses. Nor could they see any unequivocal movement direction indicators at the Lucky Horseshoe mylonite zone. However, both the mylonite zone at the Lucky Horseshoe and low angle faults which offset quartz-chalcopyrite veins at the Copper Queen mine clearly indicate that a major low angle flattening, thrust faulting or detachment event has taken place post-mineralization (Figure 7). It seems most compatible with a Mesozoic compressional event and regional thrust faulting. Float of pencil mylonites or strongly elongated quartzite, mapped along the Lemhi Pass Fault, and drag folds at the Lucky Horseshoe and In Trust mines, suggest a complex, and multistage deformation along this very major WNW-trending structure which shows up as a major topographic lineament (Figure 4). After considerable hours in the field, it is my interpretation that both multigenerational thrust faults and normal faults are important, and many of the faults are post-mineral. Deciphering the structural geology and origin of the mylonitization needs more work, but the lack of outcrop or marker beds may preclude any full understanding of the structure.

Figure 4. Lemhi Pass Fault, looking northwest from Lemhi Pass. The fault zone is filled with landslides and Tertiary volcanics. It is interpreted as a Mesozoic or older structure that has been reactivated during the Tertiary.

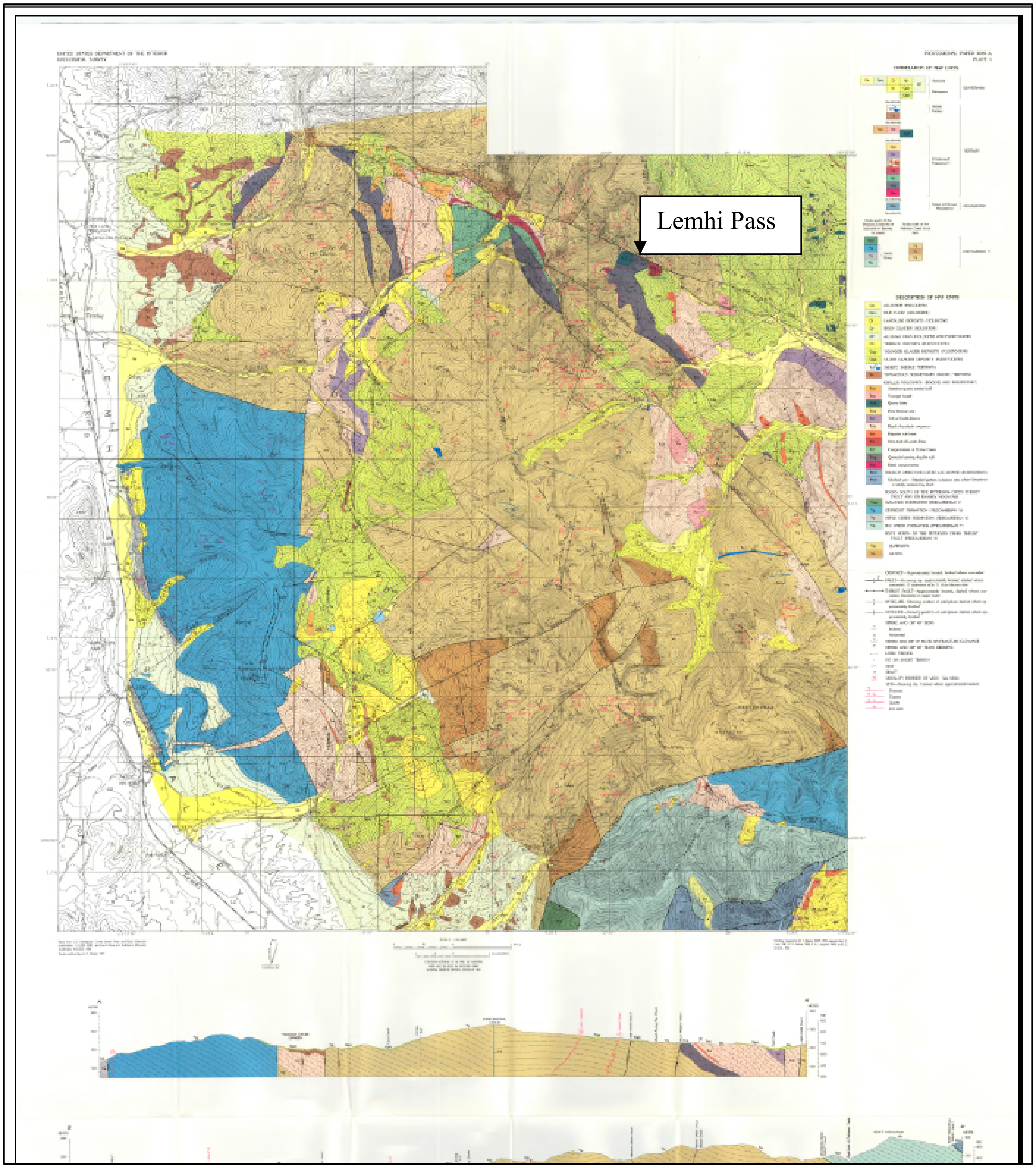

Figure 5. Geologic map of Lemhi Pass District by Staatz, 1979, from USGS Professional Paper 1049-A. The red lines and text are veins; the blue lines are dikes. The tan and brown colors are the quartzite-siltite units, with the brown being more argillaceous. Large block of blue on west side is also Proterozoic quartzite. Blues at south end are Paleozoics.

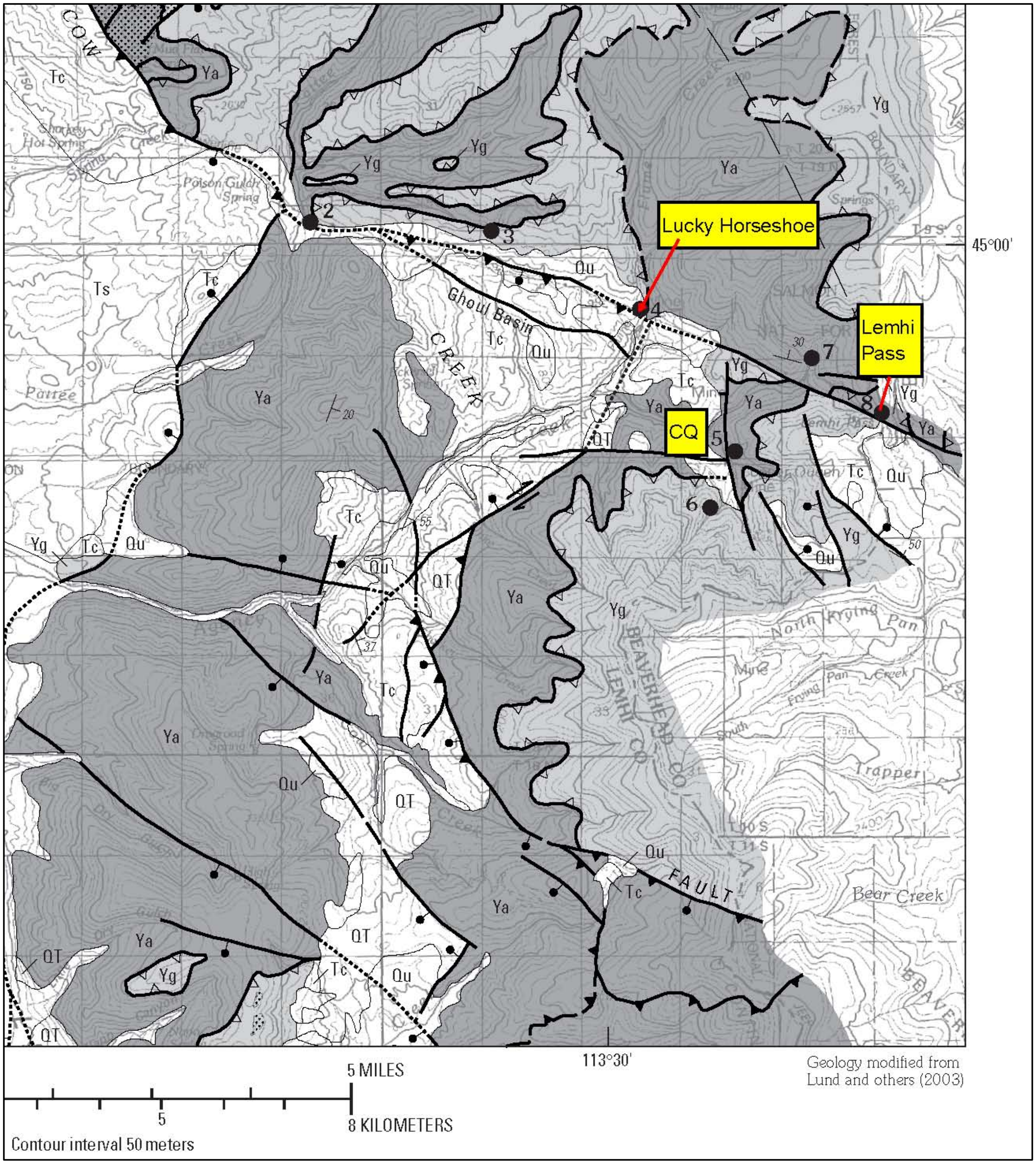

Figure 6. Simplified geologic map by K. Lund of the Lemhi Pass region from USGS Map I-2765 (Evans and Green, 2003). Illustration is from Gillerman, Lund and Evans (2003). Note map pattern of thrust faults and younger over older "thrusts" (open teeth). CQ is Copper Queen mine (locale 5). Detrital zircon sample 2 was from locale 6.

Figure 7. A) Lucky Horseshoe mine cataclasite and mylonite in Th-Fe-REE "schist", looking N30E; B) Gouge and low angle faults cutting quartz-copper vein at Copper Queen mine, adit 3, looking N12E.

Intrusive Rocks

In general, Staatz's map showed the correct rock units, except for some of the Tertiary and Quaternary ones, and was very accurate on the location of the mineralized veins and prospects. Staatz (1979) also mapped a number of intrusive dikes, labeled as "Td" for Tertiary diorite. Additional dikes, sills, and small plugs were discovered by IGS mapping. Anderson (1961) also noted the altered dikes and correctly identified them as lamprophyres. The intrusives range in composition from ultramafic or mafic to syenitic and all have undergone substantial hydrothermal alteration. They do not look at all like the Tertiary volcanics in the district, which are fresh and typical Eocene Challis volcanics. The Tertiary volcanics, including a basal conglomerate or tuff-cobble unit, were deposited on a dissected topographic surface cut into the Precambrian metasediments. The nearest exposures of Paleozoic sediments are approximately 12 miles south of Lemhi Pass.

Mafic dikes have been previously described at the Copper Queen mine, both at the surface and from underground. A fine-grained, altered greenstone dike (sample CQ06-25) with calcite-filled vesicles outcrops prominently at one of the adit portals; the dike is subparallel to the copper vein system. It could be a sill as the bedding attitudes are not well-defined. It has strong propylitic alteration. More interesting are the unweathered mafic dike rocks found on the dump from the Copper Queen shaft, presumably representing those dikes found underground. Schipper (1955) noted that the "propylite dike" on the west side of the mine contains sufficient chalcopyrite and bornite to be classified as ore. He also noted the mineralogy to be largely calcite, epidote, and quartz. One sample of the pyroxene porphyry was cut by a small (5mm wide) vein of calcite with chalcopyrite, pyrite, and galena, all used for lead isotope analysis. The intrusive dike on the Copper Queen dump is a mafic porphyry, which I have informally given the name of "pyroxene porphyry," due to the large euhedral augite crystals, set in a slightly bluish, dark matrix (Figure 8).

Figure 8. Pyroxene Porphyry from Copper Queen mine dump. Sample CQ06-30. Note large euhedral pyroxenes and green altered phenocrysts.

Finer-grained mafic dikes were also mapped in a number of other locations by Staatz and previous workers, including at the Wonder mine, in Frying Pan Creek, Pattee Creek, and along or on either side of the Continental Divide. In thin section, many of these show a similar and distinctive phenocryst assemblage and alteration similar to that of the Copper Queen pyroxene porphyry (Figure 10). In addition to pyroxene, which remains fairly fresh, the phenocryst assemblage includes a distinctive, red brown amphibole (also fairly unaltered) and aggregates of talc, tremolite, and other phases which are interpreted as pseudomorphs after Mg-rich olivine. However, no unaltered olivine was seen preserved; cross-sections are 6-sided in places. Geochemistry and petrography suggests that these are alkaline basalts in composition, perhaps bordering on more ultramafic, and that they should be classified as true lamprophyres. The intense to moderate propylitic alteration is consistent over a wide area, extending at least from the Saddlehorn prospect in the south to at least as far north as the Lucky Horseshoe and from the Frying Pan Creek to Pattee Creek.

Two other, more localized and unusual mafic intrusives were discovered. One, noted by Anderson (1961) on Pattee Creek, is a biotite lamprophyre (sample PCL), very highly altered and actually plotting chemically as an ultramafic rock. The other, not shown on any previous maps of the district, is referred to as the Lucky Horseshoe sill (Figure 9, 11). It is well exposed over a short distance along the road to and just east of the adit below the Lucky Horseshoe mine and just above Flume Creek. Samples LH06-23 and 07WP120 are of this rock, an aphanitic to very fine-grained black to very dark gray massive sill approximately 1 meter thick.

Figure 9. Lucky Horseshoe sill, looking northerly at Waypoint 120.

Figure 10 (next page). Petrography of Pyroxene Porphyry Dike Sample BL06-3. The highly birefringent minerals are tremolite blades, interpreted as replacing Mg-rich olivine. Brown phenocryst is amphibole. Large colorless phenocryst in upper left is augite. A. Uncrossed polarizers, B. Crossed polarizers.

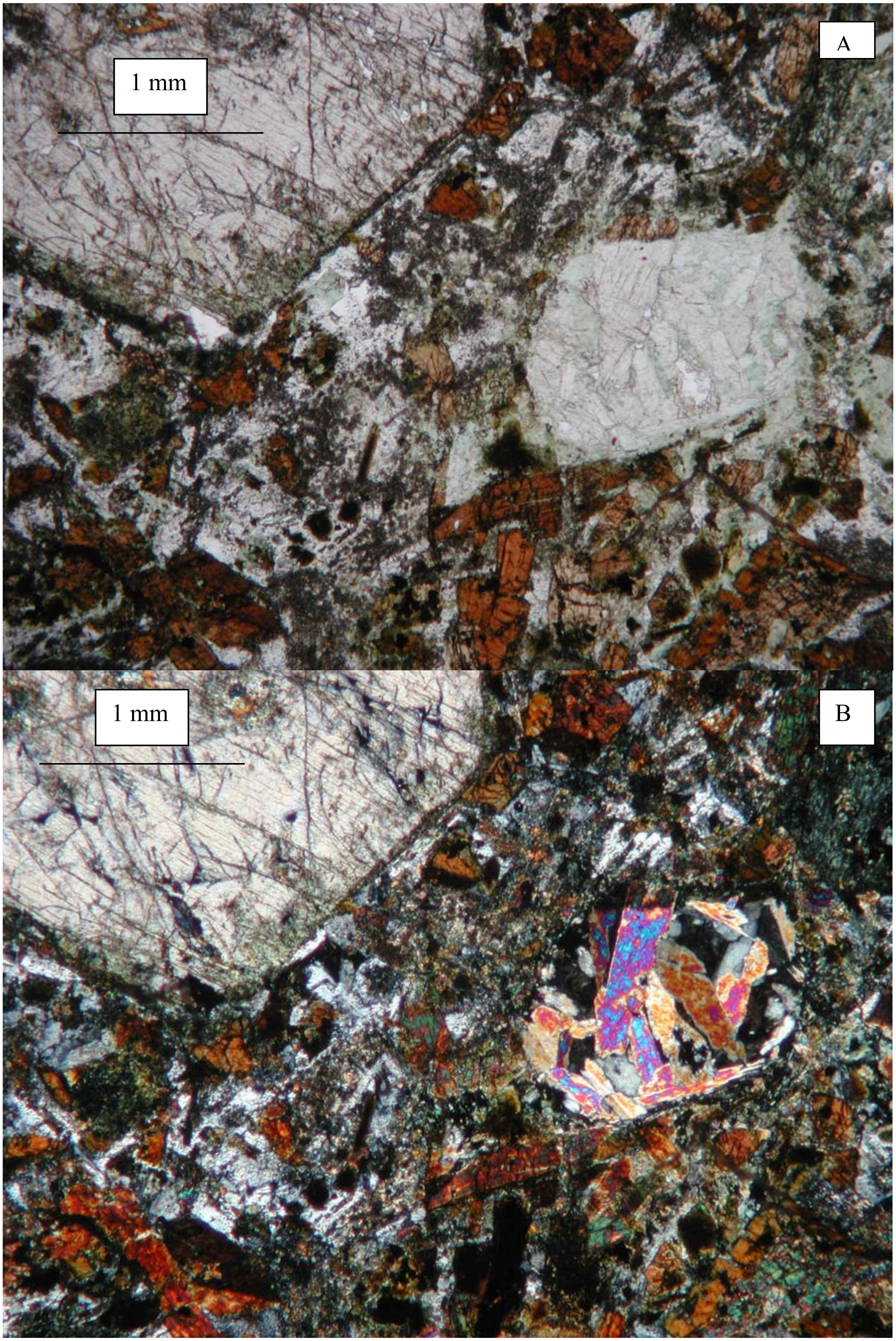
A
1 mm
B
1 mm

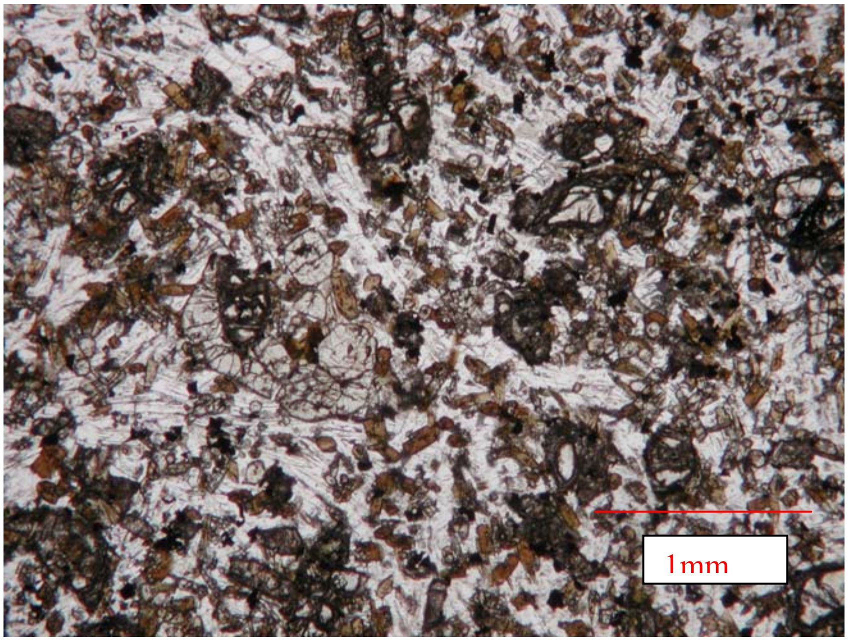

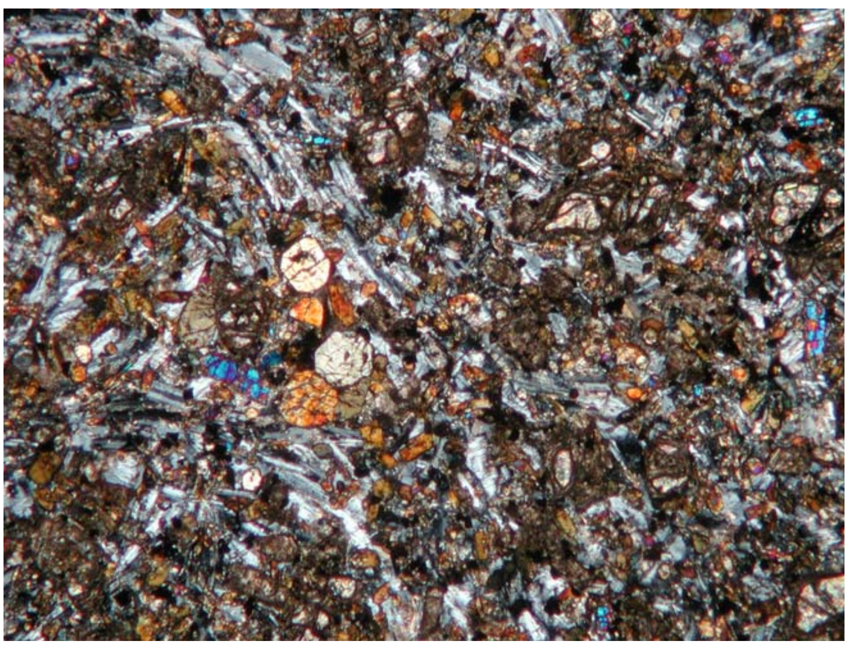

Figure 11. Lucky Horseshoe Sill in thin section, sample 07WP120. Top half is uncrossed polars, bottom half is crossed polarizers. Note fresh euhedral colorless pyroxene phenocrysts, brown amphibole phenocrysts, and fine-grained masses of very highly birefringent, slightly tan colored mineral, some of which show tabular to wedge-shaped outlines. This is a dusty brown carbonate mineral(Fe-rich magnesite), shown better in enlarged slides below. Some looks as if it could be a primary phenocryst, but it is probably a replacement of olivine. Carbonate veins, of more typical dolomitic composition, also cut the sill and infill vugs, locally with barite and celestite. Some of opaques may be chromite, from reconnaissance microprobe and SEM results. Matrix is hard to discern but includes plagioclase of intermediate composition.

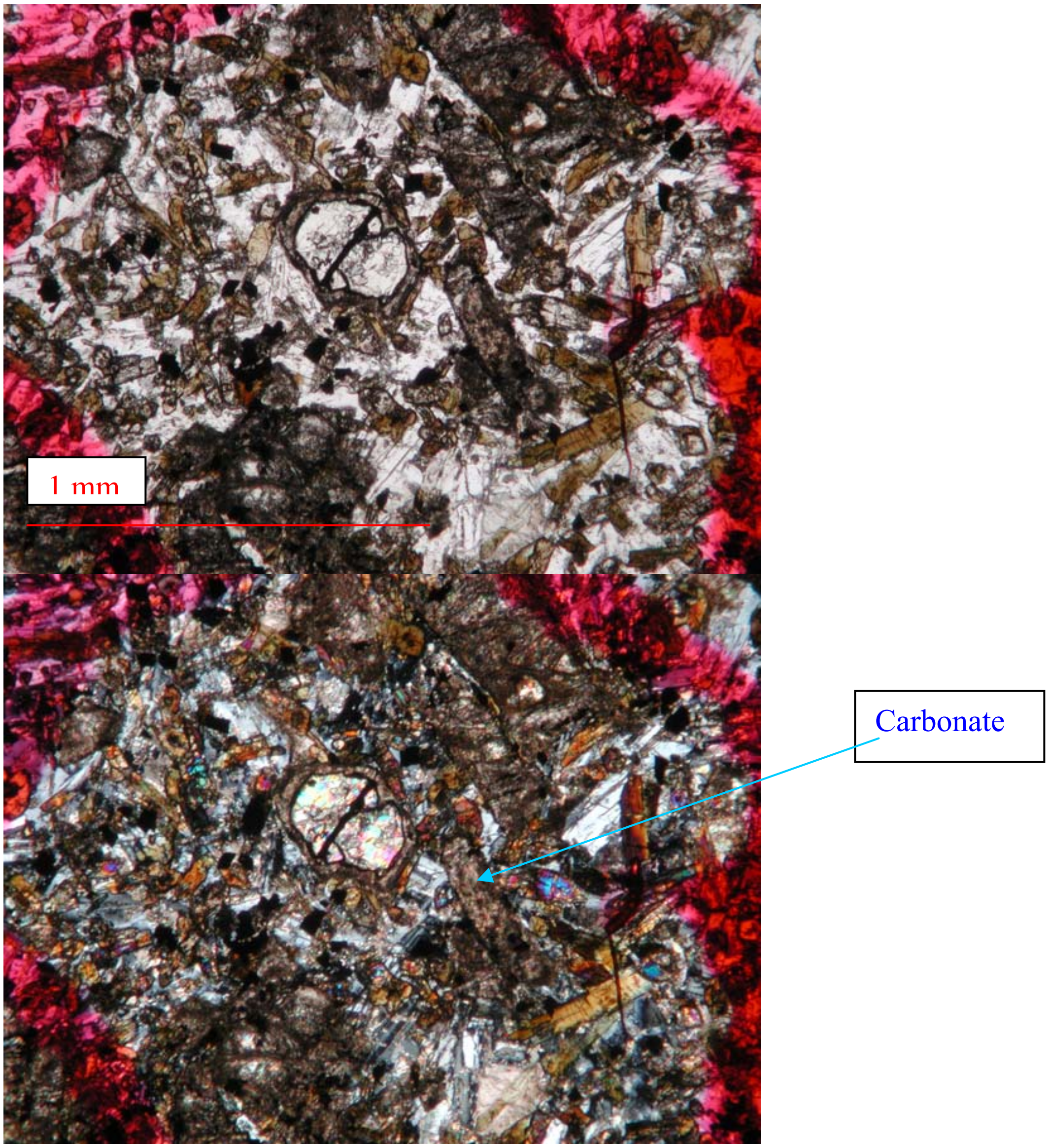

Figure 12. Magnesite "phenocrysts" and replacements in Lucky Horseshoe sill, sample 07WP120. Note fresh hornblendes and feldspar matrix coexisting with carbonate.

As seen in Figures 11 and 12, presumed olivine phenocrysts in the sill are replaced by ferroan magnesite, and other phenocrysts include pyroxene and brown hornblende in matrix of relatively fresh feldspar. Carbonate veins and vug-fillings include probable barite and celestite, suggesting that the unusual carbonate alteration of a possible ultramafic sill may be related to the nearby thorium-REE-iron deposits.

The most significant discovery of the field mapping was discovery of a syenite body exposed in a large trench just west of the Continental Divide in the heart of the district (Figure 13). It is shown on an old thesis map (Hansen, 1983) as a Tertiary syenite but not on any more recent work, and it is not on Staatz's map. The trench exposure is over 20 meters long and the syenite is exposed in at least two additional prospects and further north in a tiny dozer scrape south of the Bluebird copper prospect.

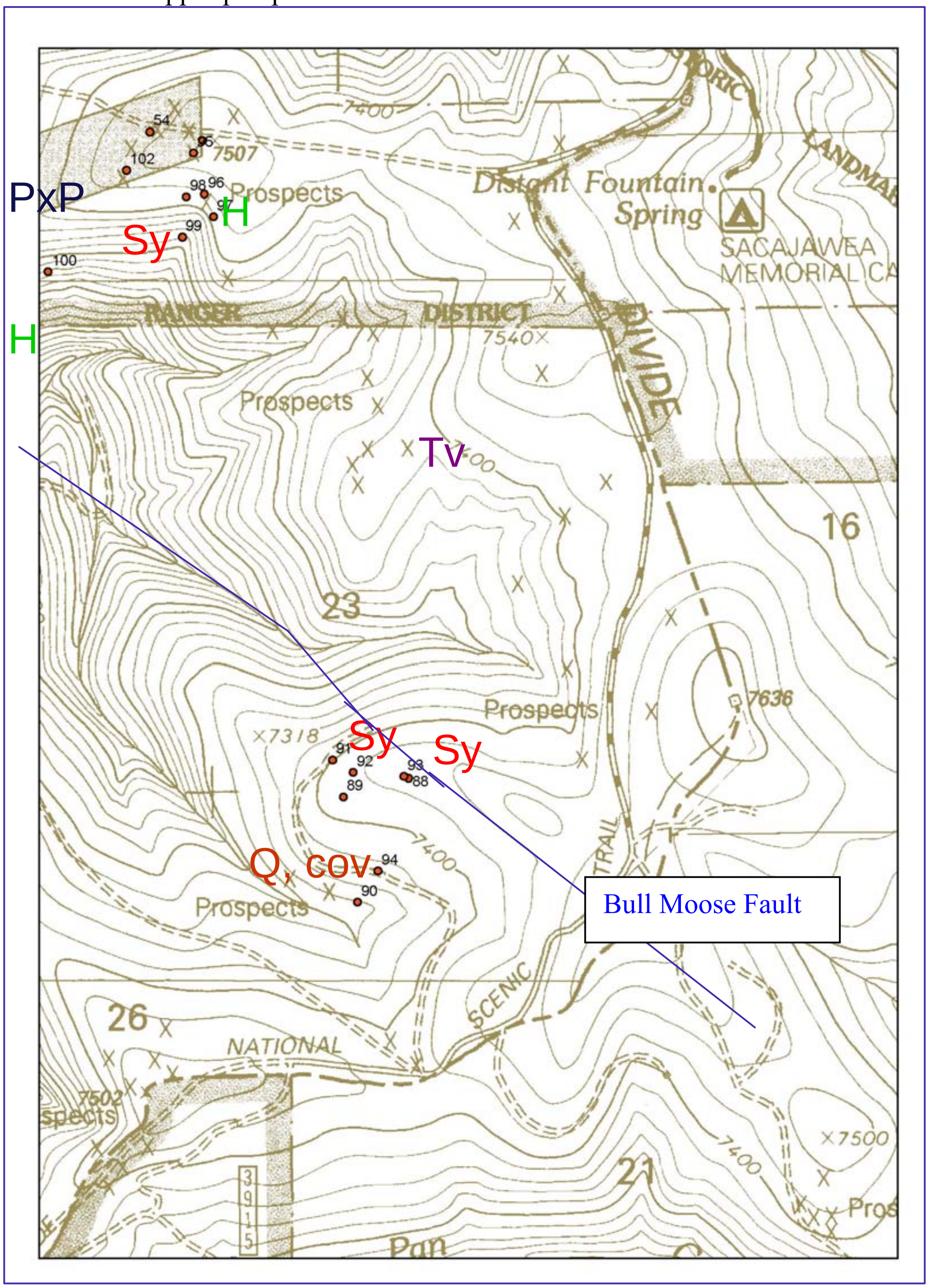

Figure 13. Locations of syenite (SY) exposures. H = hornfels, PxP = pyroxene porphyry, Tv = Tertiary volcanic cover, Q = Quaternary cover.

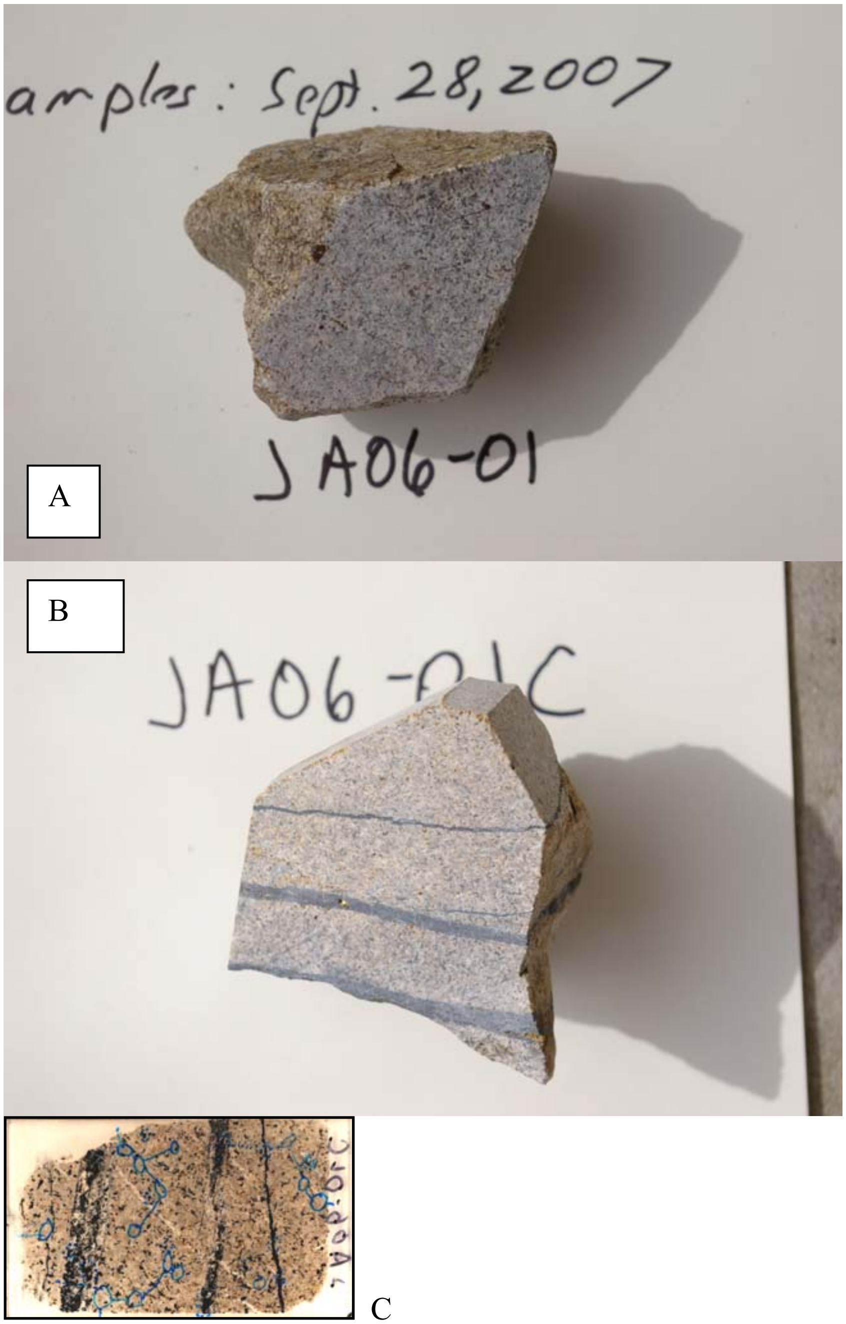

Figure 14. Syenite from trench in hand specimen. Sample A is most typical, but Sample B and the polished section in C show cross-cutting specular hematite alteration. Blue circles are ink for microprobe markings.

The tan-colored syenite consists largely of inclusion-rich potassium feldspar with few mafics and local specular hematite alteration. It outcrops only in dozer cuts and does not exhibit any deformational fabric where seen, but it looks “old” (Figure 14, 15).

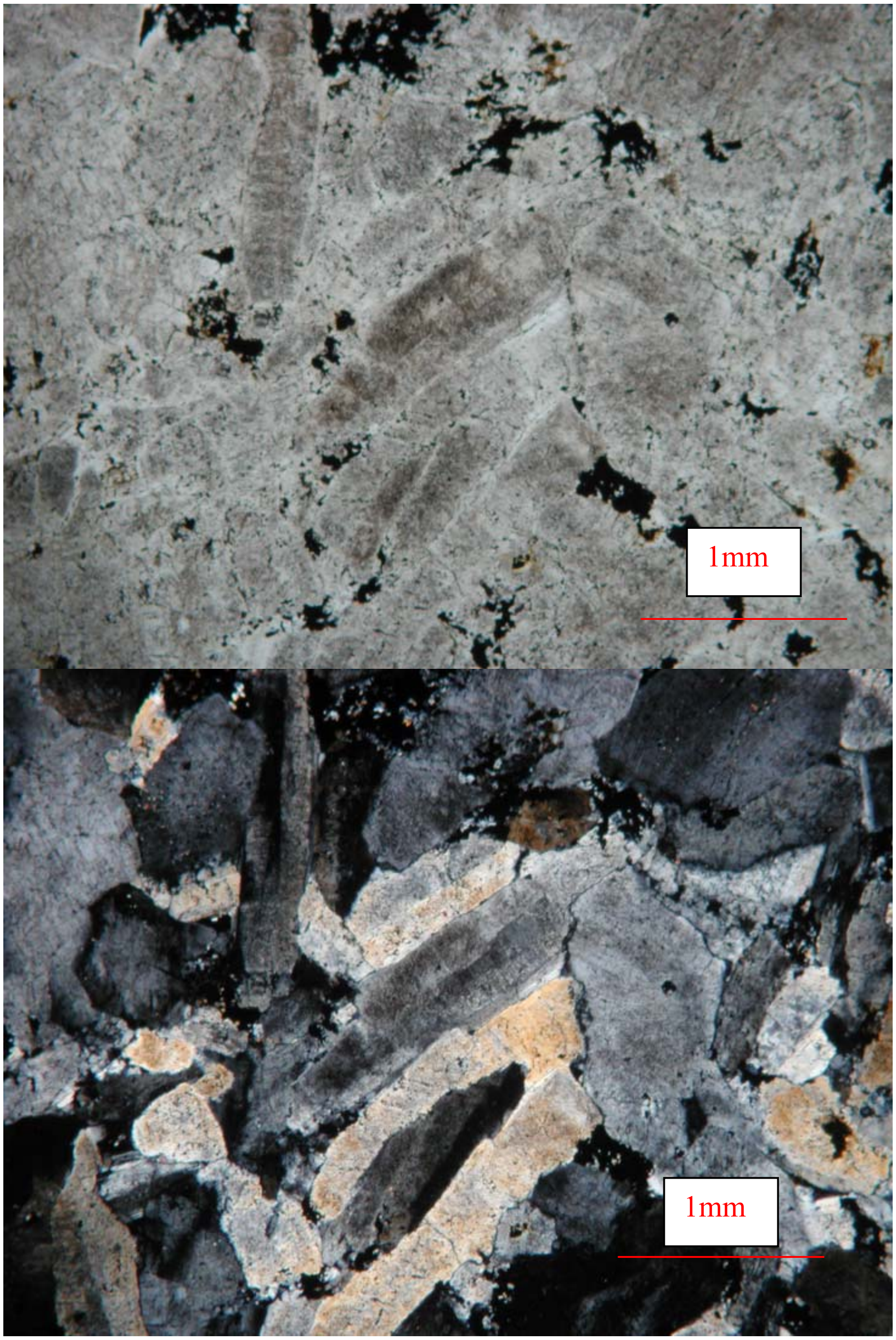

Figure 15. Syenite sample JA06-01D in thin section; top is uncrossed polars, bottom is crossed polars. Inclusion-rich cores are potassium feldspar; clearer rims are albite.

The syenite sample (BL06-05) did contain remnant biotite, presumably magmatic, but syenite samples (JA06-01) from the trench locality further south had little if any biotite, and all mafics were replaced by specular hematite. Zircon and rutile were noted in thin section; quartz is sparse and interstitial.

As specular hematite is a major component of the thorium-REE veins, and the hematite veins do not exhibit obvious wall rock alteration envelopes against the syenite, a working hypothesis was that they are related or that the hematite alteration was close in time and/or temperature to crystallization of the syenite. The albitic rims may represent a type of fenitization or sodic type of alteration (Figure 15).

A large sample of syenite was crushed and zircons separated for U-Pb geochronology on the SHRIMP at ANU. A good age date of 529.1 Ma plus or minus 4.5 Ma (1 std) was obtained (Figure 16).

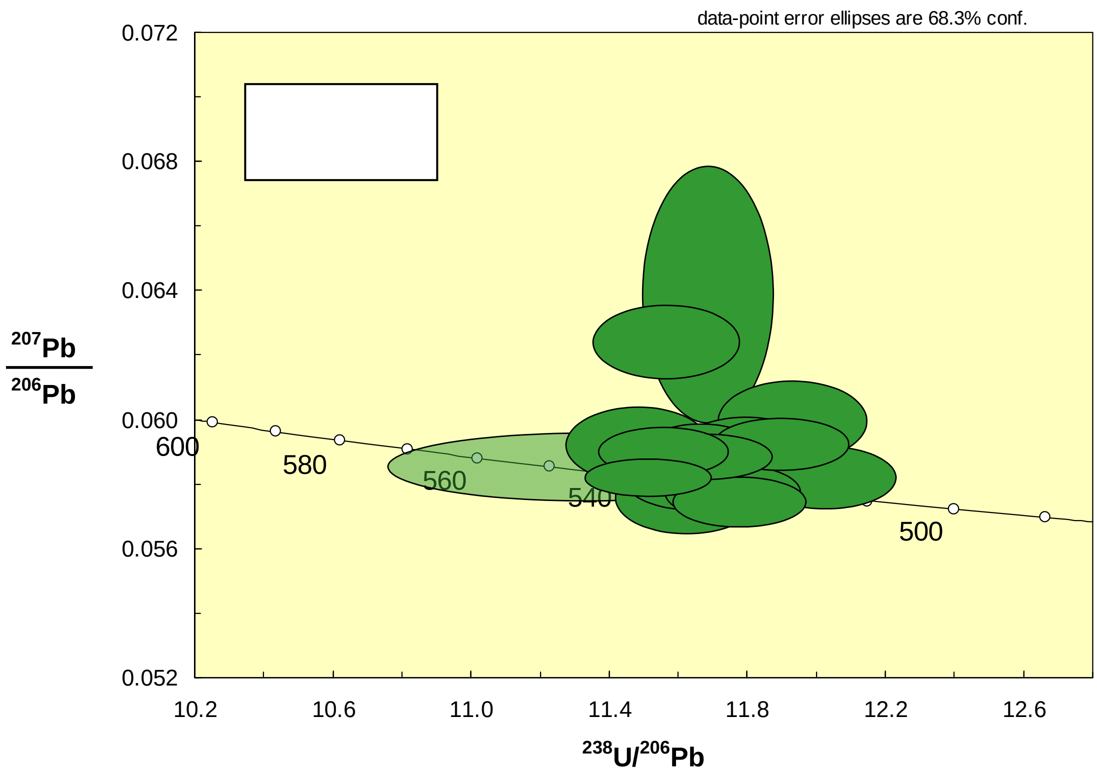

Figure 16. Geochronology for Lemhi Pass syenite sample JA06-01A. The best age of crystallization is 529 Ma +/- 4.5 Ma or Lower Cambrian. More details are in Appendix D.

Summary of Mineralization and Hydrothermal Alteration

Staatz (1979) and previous literature, as well as the thesis of Gibson (1998) present more comprehensive descriptions and maps of the veins. Gillerman, et al. (2006) includes detailed surveyed maps of surface workings at some of the major properties, including the Copper Queen, Lucky Horseshoe and Cago mines.

Copper Deposits

Several copper veins are known in the district, but the Copper Queen mine is the only one of significance and the best exposed vein system. A good description of the Copper Queen with level maps is available in the thesis of Schipper (1955) and Sharp and Cavender (1962). The mine was developed down approximately 400 feet and the workings flooded. All the copper veins have an assemblage of quartz-chalcopyrite-bornite with minor gold. Pyrite is very rare. Molybdenite is found locally at the Copper Queen in samples on the dump and mentioned in the literature. The wall rock at the Copper Queen is very quartzitic and alteration is hard to define but appears to be minimal. The rocks show a weak color anomaly and have a vague “baked” or “hornfels” appearance. Schipper (1955) notes argillaceous, calcareous quartzite on the western part of the mine. There are local specular hematite veins, but they are not clearly tied to the copper veins. In some samples, the bornite looked boudinaged, not unexpectedly considering the shearing and faulting evident in the adit walls (Figure 17). Quartz in the veins near the low angle fault system is intensely sheared and strained. The host rock is a micaceous quartzite but in some samples the muscovite mica appears to be replaced by potassium feldspar, and in one vein sample microcline is present. Other samples have coarse epidote but the paragenesis is questionable. As noted, the mafic intrusive rocks exhibit a ubiquitous, moderate to intense propylitic alteration. At the Copper Queen, Schipper (1955) described finding a “cross-cutting” radioactive veinlet which formed later than the main copper veins but contains both copper and thorium. This is evidence that the copper mineralization predates, but may be partly overlapping with, the main thorium veins sets. Schipper (1955) also records assays of 3-5% copper as chalcopyrite-bornite-calcite mineralization in the greenstone dike.

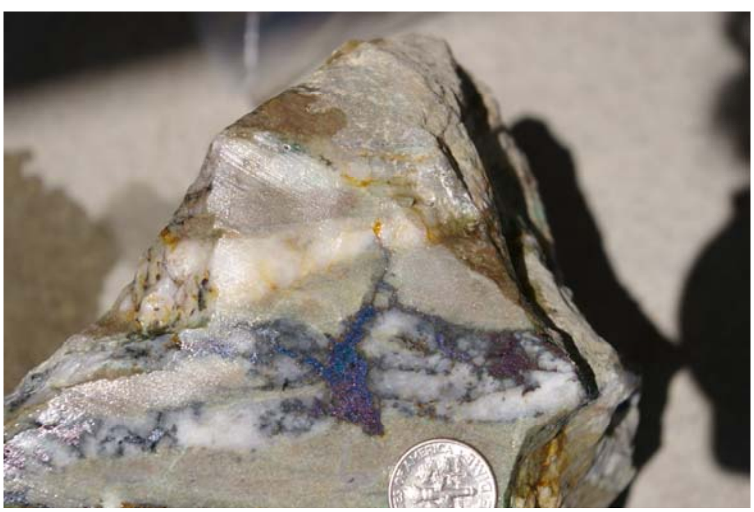

Figure 17. Bornite in possible pull-aparts of boudinaged quartz-copper vein, Copper Queen mine. No clear alteration envelope, but diffuse hornfels(?) in quartzite wall rock.

An outcrop of good epidote-bearing calc-silicate hornfels (Waypoint 97) was mapped about 1000 feet southeast of the Bluebird copper vein and a large outcrop of brown-stained baked quartzite (Waypoint 113) with numerous barren quartz veins, some with trace epidote and perhaps albite selvages was mapped in the bottom of the canyon a half mile east of the Copper Queen. Thus, alteration suggests a speculative possibility of a "dry" buried intrusive at depth in the center of the district and near the copper prospects.

Thorium and Rare Earth Element (REE) Deposits

Most of the thorium deposits in the district are quartz veins, and the quartz has a distinctive waxy to greasy luster. It is typically fine-grained and strongly colored in shades of pink to brown as a result of the abundant hematite and thorite. The veins are steep to moderately dipping, of variable size, but share an assemblage of quartz-hematite-thorite with alkali feldspar and lesser but variable amounts of apatite, monazite, biotite, barite, carbonate, fluorite, allanite, and many other minerals (Figure 18). Thin sections from the Cago vein and others show that the muscovite in the host quartzite is converted to potassium feldspar adjacent to the vein, though alteration extends only a few feet away from the vein. Though reported as microcline (Staatz, 1979), the feldspar is hard to recognize since it lacks typical microcline twinning. Locally, albite twins are visible, but most of the potassium feldspar is untwined and occurs in patchy masses near the veins. Microprobe analyses also detected albite and rutile in altered zones. Brecciation and crackle veins are common to all the thorium deposits, and multi-generational strained quartz is typical.

Figure 18. Pink quartz-potassium feldspar-specular hematite-thorite vein from the Cago prospect. The white outer envelope contains additional K-feldspar plus albite and rutile.

One deposit, the Lucky Horseshoe, is classified as a “replacement” deposit, in more argillaceous wall rocks. Unlike most of the deposits, it has not been affected by extensive supergene weathering, and the original mineralogy and texture are well-preserved. The ore rocks, essentially specularite schist and breccia, are strongly sheared and in places mylonitic with a nearly horizontal fabric (Figures 19, 20). Because the deposit has been partially excavated and ripped up, the original vein orientations and structure are unknown, but in thin section and the preserved 3-dimensional outcrop, it is obvious that the rocks are strongly sheared, brecciated, and cataclastic in nature with a near-horizontal schistocity. At least one probable fold nose is exposed in the pit (Gillerman and others, 2006). The near-horizontal fabric, plus the lack of mineralization exposed in an adit driven underneath the open pit level, support the interpretation of a horizontal geometry rather than a vertical or steeply dipping vein, but no drilling has been done to test this hypothesis. Lucky Horseshoe ores contain some of the highest REE concentrations in the district (Staatz, 1979). In thin section, the biotite layers contain as much as 25% of monazite (Figure 19). Textures are extremely complex and probably record multiple deformation and metamorphic events that pre-date to post-date the mineralization (Figure 21).

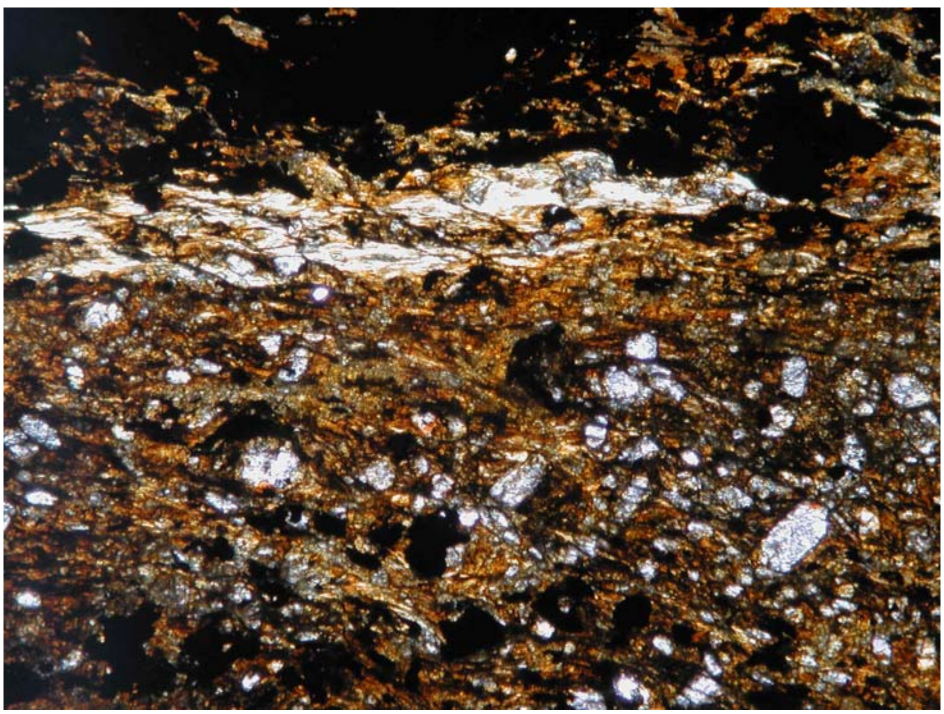

Figure 19. LH-12 (kcv-9) under high magnification and plain light. Brown biotite, opaques (hematite-thorite) and monazite (high relief colorless grains abundant in lower half of slide). Image is approx. 2.7 mm across. Note the preferred orientation and shear fabric.

Dominant minerals in the Lucky Horseshoe ores are hematite, potassium feldspar, biotite, and monazite and thorite. Much of the biotite is brown, especially where less affected by deformation or subsequent events. Other micas are green biotite (especially in sheared or veined zones) and muscovite. Albite is locally present, plus allanite, fluorite, barite, minimal quartz, and carbonate; a variety of other minerals are reported in the literature.

Figure 20. Lucky Horseshoe mine. Top photo (A) shows cataclasite with radioactive thorium ore. Black color is due to biotite and hematite. Tan-colored clasts are feldspar and/or apatite. Bottom Photo B shows some of the tan alkali feldspar veins which are peripheral, especially in the hanging wall of the deposit. Thin sections and geochemical analyses indicate the tan veins have both Na and K feldspars.

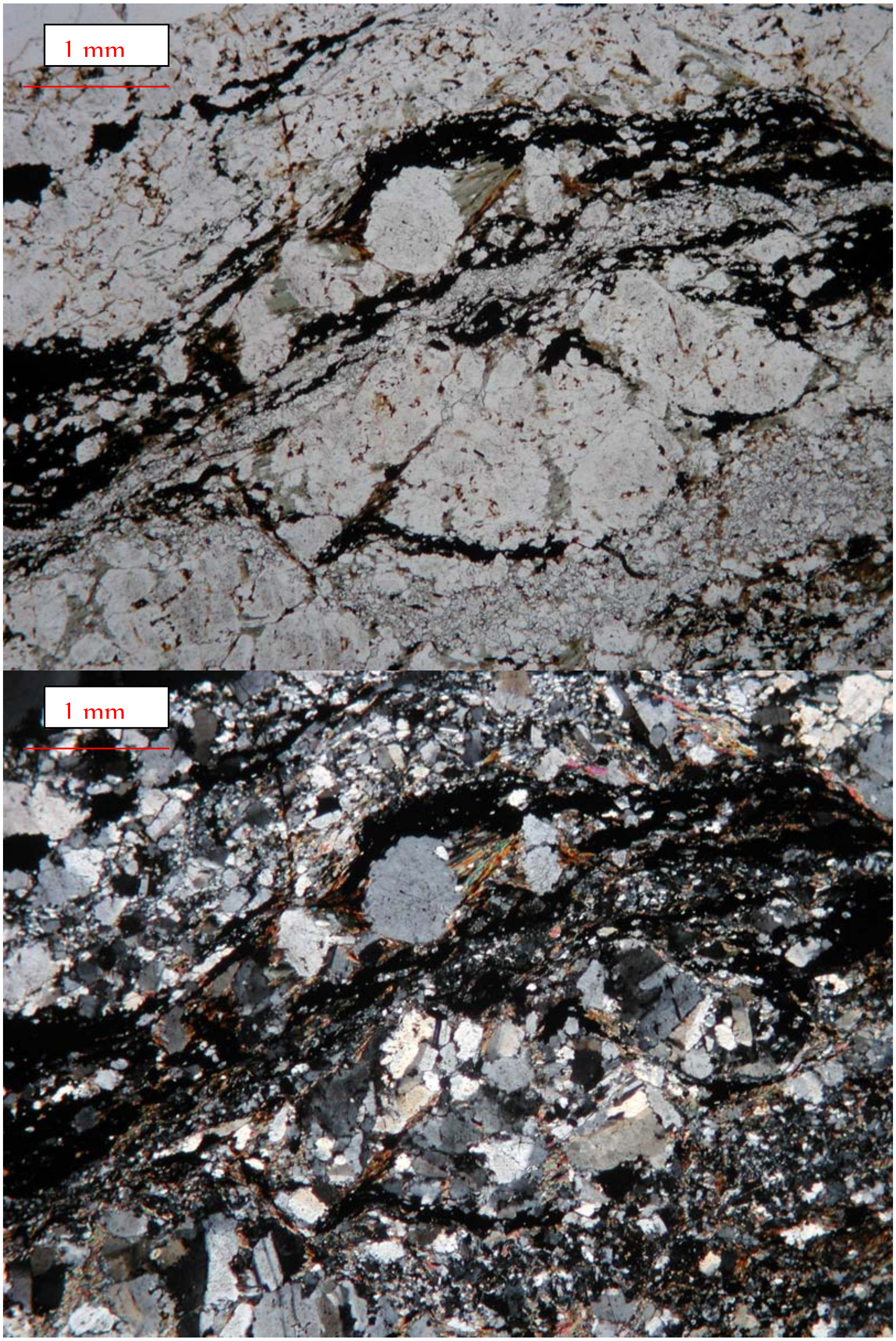

Figure 21. LH06-24B, Lucky Horseshoe cataclasite. Top (A) is plain light; Bottom (B) is in crossed polarizers. Note clasts are aggregates and the metamorphic biotite is growing or recrystallized within pressure shadows of the clasts. Also note some similar textures of the feldspar aggregates in the clasts to the texture of the syenite.

Mineral Compositions

Both the electron microprobe and scanning electron microscope were used to facilitate mineral identification and to analyse mineral compositions. Unfortunately, access to both of these was limited by time, distance, funds, and equipment breakdowns and replacements. In particular, local access to good SEM facilities or a microprobe with qualitative imaging would have been very useful.

With the exception of the monazite and thorite used for the EMPA geochronology, the remaining electron microprobe work was done at Washington State University on a Cameca electron microprobe with visual optical lens capability. This was helpful in selecting grains. Laboratory manager Scott Cornelius did a superb job with the instrument setup and standard selection.

Blackbird Mining District

The USGS has been undertaking a new study of mineralization in Proterozoic Basins, and part of that is a new look at the Blackbird Copper-Cobalt District, located a few tens of miles west of Lemhi Pass and hosted in similar rocks (Figure 1). In cooperation with that Blackbird project, microprobe analyses of garnets and biotites, specifically, were completed. Results are in Table 1 and Table 2, as well as Appendix C. In addition, scapolite and chloritoid were analysed and those results are tabulated in Appendix C.

Garnet, biotite, and chloritoid at Blackbird all show extreme iron enrichment, and chloritoid, though less abundant as a coarse blue porphyroblast, is typical of metamorphosed iron formations. Also of interest is the element zoning in the garnets. Cores have higher manganese contents, and lower magnesium, than the rims. One hypothesis is that they grew under prograde metamorphic conditions, with the rims forming at higher temperatures than the cores. A subsequent and visually distinct retrograde rim was avoided in the probe analyses.

Biotites greatly favor iron over magnesium in their compositions. Also of interest is the fairly low amount of F and Cl, with Cl being 2-4 times more abundant than F. Scapolite in the regional host rock contains 2 weight percent Cl (Appendix C), but it is present only locally in the stratigraphic section.

Table 1. Blackbird Mining District Garnets. RMet1 is from the RAM deposit metallurgical core; BZ is from Blacktail Pit. Both rocks are garnet-biotite schists. Chloritoid is also present in the BZ sample (see Appendix C).

Representative Mineral Compositions, Formulas and End-Members: Blackbird Mining District Samples
Determined by Electron Microprobe, Washington State University

Sample	**RMet1, pt. E3**	**RAM deposit**		Sample	**BZ-06A1, ptE1**	
Wt. % Oxides	Garnet Core	Garnet - Int.	Garnet Rim	Garnet Core	Garnet - Int.	Garnet Rim
SiO2	35.36	35.84	35.4	34.55	34.87	35.18
TiO2	0.06	0.19	0.06	0.04	0.06	0.03
Al2O3	19.77	19.84	20.16	19.43	20.2	19.94
FeO t	32.41	32.82	33.57	37.06	38.49	39.36
MnO	2.58	2.04	0.83	2.55	1.92	1.28
MgO	0.26	0.33	0.71	0.37	0.47	0.46
CaO	6.42	7.02	6.59	1.56	1.81	1.51
Na2O	0	0	0	0.01	0.04	0.04
K2O	0	0.01	0	0	0.01	0
F, Cl zero						
Total	96.86	98.08	97.32	95.57	97.87	97.81
	Cations					
Si	2.982	2.982	2.962	2.985	2.946	2.973
Ti	0.004	0.012	0.004	0.003	0.004	0.002
Al -IV						
Al-VI	1.964	1.945	1.988	1.979	2.011	1.986
Fe	2.286	2.284	2.348	2.678	2.72	2.782
Mn	0.184	0.144	0.058	0.186	0.138	0.092
Mg	0.033	0.04	0.089	0.047	0.059	0.058
Ca	0.58	0.625	0.591	0.144	0.164	0.137
Na	0	0	0	0.002	0.006	0.007
K	0	0.002	0	0	0.001	0
Formula Total	20.032	20.034	20.04	20.024	20.048	20.036
Fe/(Fe+Mg)	0.99	0.98	0.96	0.98	0.98	0.98

Table 2. Analyses of Blackbird Micas. Yac is from Apple Creek Fm. Outside of mine area, RMet1 is from RAM deposit, BZ is Blacktail Pit, HE is Hawkeye portal.

Sample Average	**Yac-06A, biotite**	**RMet1, biotite**	**BZ-06A1, biotite**	**He-06A, biotite (brn/grn)**	**RMet1, Muscovite**
Wt. % Oxides - Averages	Biotite	Biotite	Biotite	Biot. brown/grn	Muscovite
SiO2	32.82	31.71	30.29	31.03	45.07
Al2O3	16.39	16.90	17.30	17.13	33.57
TiO2	2.72	2.10	1.38	0.70	0.26
FeO if 50% Fe+2	11.89	13.38	14.79	14.14	1.32
Fe2O3 calc at 50%	13.22	14.88	16.44	15.72	1.47
MnO	0.30	0.04	0.04	0.03	0.00
MgO	5.97	4.39	2.32	4.33	0.62
CaO	0.00	0.00	0.01	0.00	0.00
Na2O	0.04	0.13	0.06	0.07	0.49
K2O	9.59	9.35	9.25	9.38	10.44
F	0.24	0.25	0.13	0.32	0.31
Cl	0.65	0.42	0.78	0.78	0.00
(H2O)	3.51	3.51	3.38	3.34	4.23
TOTAL - w/ corrections	97.07	96.86	95.94	96.66	97.66

Lemhi Pass Mineral Compositions

In order to help classify the intrusive rocks, representative samples of the syenite and mafic intrusives were examined, as well as some of the alteration minerals associated with the thorium veins. Given the complexity of the rocks, the amount of probe work could easily have been doubled, had more time and funds been available. Additional details are in Appendix C.

Table 3: Zoning of alkali feldspar in the syenite, traverse across a single feldspar grain.

Weight Percent Oxide on Grain Traverse	**Na2O**	**K2O**
Un 79 JA06-01C, Feldspar Trav., rim, pt. B1	7.72	5.91
Un 80 JA06-01C, Feldspar Trav., rim/core, pt. B2	0.35	16.37
Un 81 JA06-01C, Feldspar Trav., core, pt. B3	0.38	16.53
Un 82 JA06-01C, Feldspar Trav., core middle, pt. B4	0.75	16.04
Un 83 JA06-01C, Feldspar Trav., core, pt. B5	0.39	16.76
Un 84 JA06-01C, Feldspar Trav., rim/core, pt. B6	11.76	0.12
Un 85 JA06-01C, Feldspar Trav., rim, pt. B7	9.73	3.06

Table 4: Compositions of selected mafic minerals at Lemhi Pass

	Biotites				Amphiboles	
	Syenite	**Th ore**	**Th ore**	**Th ore**	**Px Porphyry Phenos**	
Sample (Averages)	BL06-05	LH-12c	LH-12c2	LH01-1a	CQ06-30A1	CQ06-30A1
color	brown	brown	green	gn/brwn	red brown	clear -alt.
Wt. % Oxides						
SiO2	32.25	38.19	38.23	41.67	35.63	55.50
Al2O3	11.24	11.24	11.11	11.72	13.13	0.95
TiO2	1.96	0.19	0.12	0.28	5.70	0.02
FeO if 50% Fe+2	16.01	4.94	5.02	5.53	4.35	5.89
Fe2O3 calc at 50%	17.81	5.50	5.59	6.15	7.26	2.18
MnO	0.78	0.10	0.11	0.10	0.12	0.23
MgO	1.18	19.64	19.97	19.31	11.92	19.22
CaO	0.28	0.02	0.12	0.05	11.95	12.85
Na2O	0.03	0.03	0.05	0.05	2.12	0.22
K2O	8.68	10.24	10.28	10.47	1.35	0.04
F	0.90	4.03	4.84	NA	0.33	0.00
Cl	0.53	0.02	0.02	0.03	0.05	0.01
(H2O)	2.96	1.98	1.61	4.13	1.76	2.12
TOTAL - w/ corrections	94.11	94.41	95.03	99.47	95.53	99.24

Table 5. Representative Feldspars from Lemhi Pass

Feldspars	Cores	Rims		Orangy	clearer/outer?
Sample Number	BL06-05	BL06-05		CA06-B1	CA06-B1
Wt. % Oxides	**syenite**			**Cago Th vein**	**Envelope?**
SiO2	63.28	67.08		64.52	70.91
Al2O3	19.04	20.58		18.87	20.62
Fe2O3	0.06	0.10	as FeO	0.09	0.03
CaO	0.01	0.22		-0.03	0.06
Na2O	0.45	11.24		0.34	10.93
K2O	16.20	0.41		16.36	0.13
BaO	0.21	0.01		na	na
Total	99.24	99.65		100.14	102.67

A curious feature of the feldspars probed in both the syenite and the Cago and Lucky Horseshoe thorium deposits at Lemhi Pass is the bimodal composition with both Na-rich and K-rich varieties, often in the same thin section. The pinker K-feldspar is dominantly orthoclase in composition, but the clearer rims are albitic. Few in-between compositions were found, and the amount of calcium plagioclase in the albite is minimal. Though less distinct, both feldspar compositions are also present in the Lucky Horseshoe deposit. Timing and exact zoning are poorly constrained, though as in the Cago vein, the more sodic phases appear to be either an outer zone or possibly later.

In comparison to the Blackbird District, biotites from the Lucky Horseshoe mine at Lemhi Pass have F >> Cl, with 4% F at Lemhi Pass versus only 0.25 % F in the Blackbird ores. TiO_2 content of the biotite in the Blackbird ore is comparable to that in the Lemhi Pass syenite. TiO_2 in the red-brown amphibole (oxyhornblende or hastingsite?) of the pyroxene porphyry at Lemhi Pass is very high (over 5%), but TiO_2 in the ore zone biotite at the Lucky Horseshoe is very low. Overall, the biotites from the Lucky Horseshoe ores are significantly more phlogopitic in composition.

The clear or colorless alteration amphibole with the composition in Table 4 is a tremolite, interpreted as one of the alteration products of olivine phenocrysts in the pyroxene porphyry. Pyroxene compositions are augitic.

Geochemistry

Intrusive Rocks

Complete whole rock analyses of the syenite and mafic intrusives are in Appendix E. Major elements are listed in Table 6 below. All analyses were done by Activation Laboratories in Canada.

Analyte Symbol	C-Total	Total S	F	SiO2	Al2O3	Fe2O3(T)	MnO	MgO	CaO	Na2O	K2O	TiO2	P2O5	LOI	Total
Unit Symbol	%	%	%	%	%	%	%	%	%	%	%	%	%	%	%
Detection Limit	0.01	0.01	0.01	0.01	0.01	0.01	0.001	0.01	0.01	0.01	0.01	0.001	0.01	0.01	0.01
Analysis Method	IR	IR	FUS-ISE	FUS-ICP	FUS-ICP	FUS-ICP	FUS-ICP	FUS-ICP	FUS-ICP	FUS-ICP	FUS-ICP	FUS-ICP	FUS-ICP	FUS-ICP	FUS-ICP
JA06-01	0.03	< 0.01	< 0.01	63.48	15.1	8.01	0.044	0.1	0.1	5.78	4.79	0.26	0.06	0.76	98.48
JA06-01C	0.02	< 0.01	< 0.01	64.09	13.6	10.77	0.033	0.06	0.1	4.87	4.92	0.296	0.07	0.44	99.24
BL06-05	0.04	< 0.01	0.04	62.2	16.27	7.88	0.123	0.31	0.32	5.95	5.55	0.305	0.14	0.74	99.79
07WP129	0.02	< 0.01	0.05	73.41	12.96	1.95	0.028	0.23	0.18	2.6	6.48	0.339	0.08	0.82	99.08
CQ06-25B	0.26	0.11	0.18	46.49	15.27	12.27	0.157	6.98	7.38	3.14	2.75	2.554	0.53	3.39	100.9
CQ06-30B	0.33	0.13	0.14	45.25	13.94	11.1	0.186	8.94	9.78	2.78	1.91	1.86	0.51	3.49	99.75
BL06-03	0.04	0.02	0.14	44.96	13.44	11.7	0.172	10.35	10.05	2.37	1.68	2.041	0.52	2.35	99.63
LH06-23B	3.62	0.05	0.09	41.2	10.82	10.07	0.181	10.68	8.32	1.81	1.96	0.845	0.25	13.44	99.58
07WP120	2.45	0.07	0.09	44.65	11.09	10.37	0.193	10.28	8.91	1.83	1.95	0.871	0.26	9.74	100.1
LH06-24B	0.02	< 0.01	0.44	48.95	11.99	19.78	0.028	1.89	3.43	5.12	2.86	0.163	3.41	0.77	98.38
07WP127B	3.93	0.13	0.5	3.97	0.74	8.03	0.606	1.25	23.35	0.07	< 0.01	0.014	18.92	14.23	71.16

Table 6. Whole rock chemistry from Lemhi Pass. The first three samples listed (JA06-01 and BL06-05) are syenite with about 63% silica and about 5-6% each of Na2O and K2O. 07WP129 is a granite from near Leadore. CQ06-25B is the Copper Queen greenstone dike, CQ06-30B and BL06-03 are pyroxene porphyries from the Copper Queen and Bluebird areas, LH06-23B and 07WP120 are samples of the carbonate-rich mafic sill by the lower Lucky Horseshoe adit, and LH-6-24B is of the Lucky Horseshoe breccia ore. For comparison, 07WP127B is from a carbonatite sample on the Roberts property west of Shoup (Anderson, 1958).

The syenite contains about 25-30 ppm thorium and moderately high alkalis, subequal in amount between potassium and sodium, and very low calcium. The mafic rocks seem to have a slightly alkaline character (Figure 22) and are low in silica with only about 45% $SiO_{2,}$ rather low for basalt and approaching the value for peridotites, based on representative igneous rock analyses (Winter, 2001). The mafic pyroxene porphyries fit the definition of a true lamprophyre as a dark, porphyritic mafic rock with biotite and/or amphibole phenocrysts and normally rich in alkalis (Winter, 2001, p. 363). If the syenite and mafic porphyries are of approximately the same age (see geochronology discussion below), they are interpreted to comprise a bimodal assemblage of continental alkalic magmatism, most likely rift-related. In spite of considerable searching in thin section, no feldspathoids or clear evidence of silica undersaturation or ultraalkaline mineralogy was found. Hydrothermal alteration has obviously affected the rocks, and makes classification more difficult.

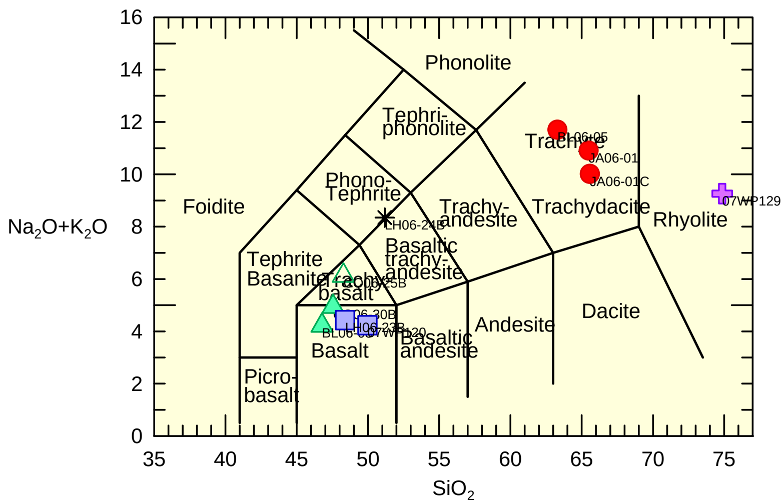

Figure 22. Total alkali-silica plot (normalized) for same samples. Red circles are syenite; green triangles are mafic dikes; blue squares are Lucky Horseshoe sill and purple is regional granite.

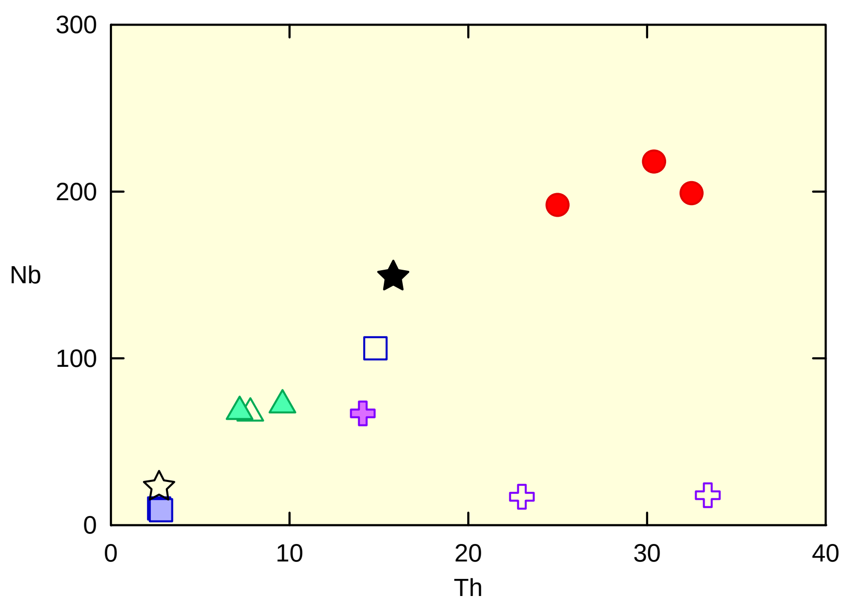

Figure 23. Nb versus Th for intrusive samples in diagram above, plus two additional mafic to ultramafic rocks(black stars) in the district and two samples of the regional Precambrian megacrystic granite (open purple crosses). The syenite (red circles) seems to be the most enriched in Th and Nb as well as alkalis and REE.

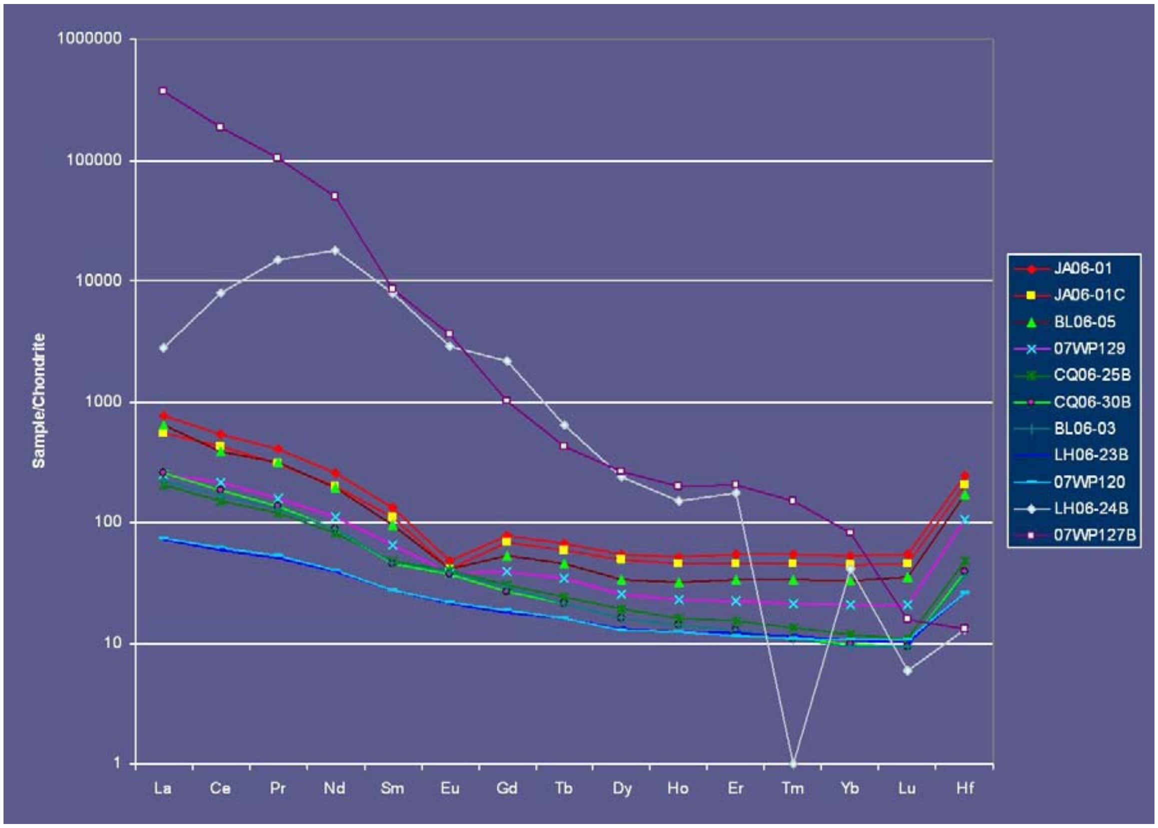

Figure 24. REE spider diagram for selected intrusives and ore sample. Note standard Eu anomaly for the syenite, and the flat to slightly elevated Eu pattern of the mafic porphyries. Also note the difference in ore sample LH06-24B with an extreme Nd-enrichment versus standard LREE enriched pattern of North Fork carbonatite (07WP127B).

The syenite shows the highest enrichment in Nb, Th, and REE of the intrusives sampled in the Lemhi Pass District (Figures 23, 24). It also shows a modest negative Eu anomaly. The mafic porphyries and greenstone show flatter patterns with a hint of a positive Eu anomaly, and the Lucky Horseshoe sill shows lower REE fractionation relative to chondritic values, appropriate for the basaltic chemistry of the rocks and probable mantle derivation.

In contrast to the intrusives, rare earth element compositions of the thorium-REE veins show a definitely unusual pattern of middle rare earth (MREE) enrichment relative to chondritic values (Figure 25). This has been noted by previous workers in the Lemhi Pass District. It is of both geologic and economic interest since neodymium is currently used in several high tech applications, such as magnets. The other middle rare earths are also of considerable economic importance, but carbonatites and other easily mined REE deposits tend to be LREE-enriched.

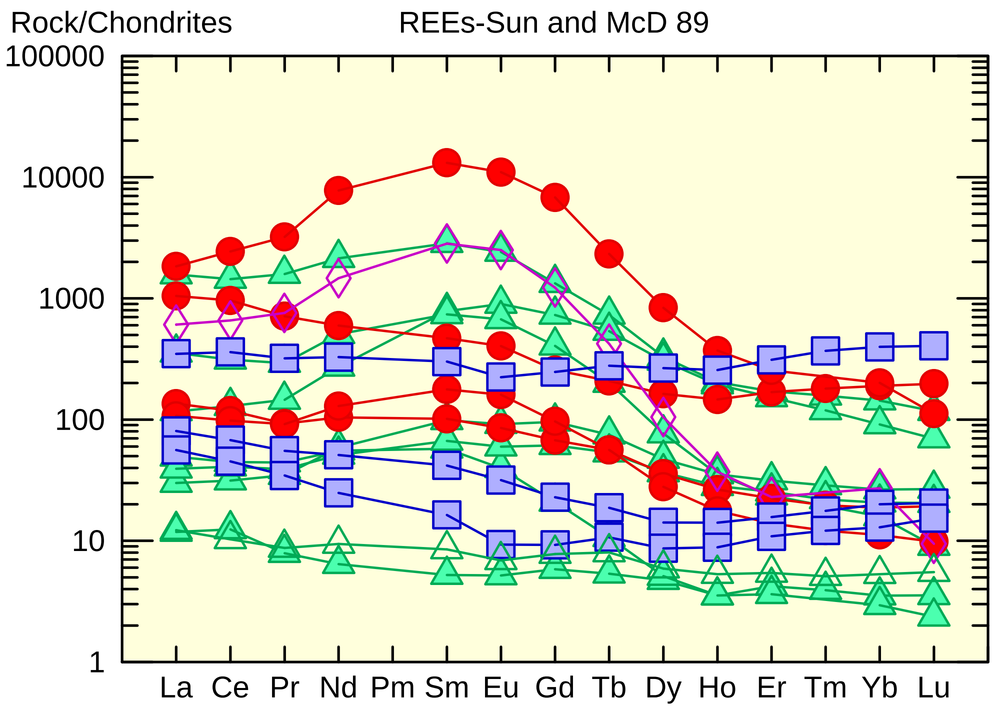

Figure 25. A number of vein samples from data supplied by Thorium Energy. Note the middle rare earth enrichment of many of the samples. This has been noted by earlier workers in both government (Staatz et al., 1972b), industry, and by Samson and Wood (2005). It remains an unexplained and unique characteristic of the Lemhi Pass District.

Monazite Geochemistry

As monazite is the major rare earth element bearing mineral in the deposits and is particularly abundant at the Lucky Horseshoe, I was interested to look at its composition. Scanning electron microscopy provided a quick look at several samples with monazite (Figure 26). SEM scans of thorite showed just Th and silica peaks, suggesting fairly pure thorite in the fresh sections examined.

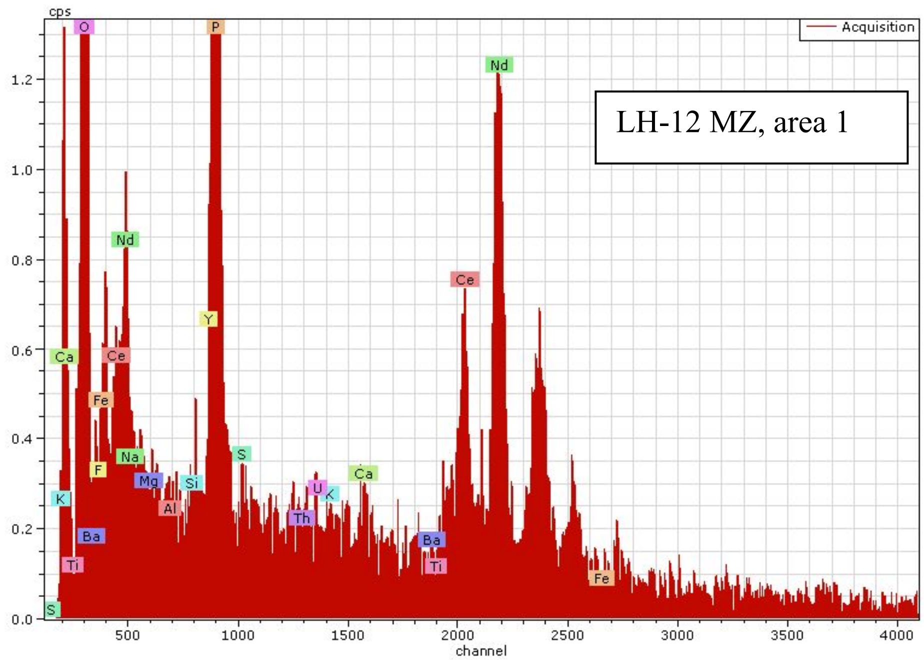

Figure 26a. EDS spectra of monazite in LH-12 ore from Lucky Horseshoe mine. Note high Nd and Ce peaks and lack of large La peak.

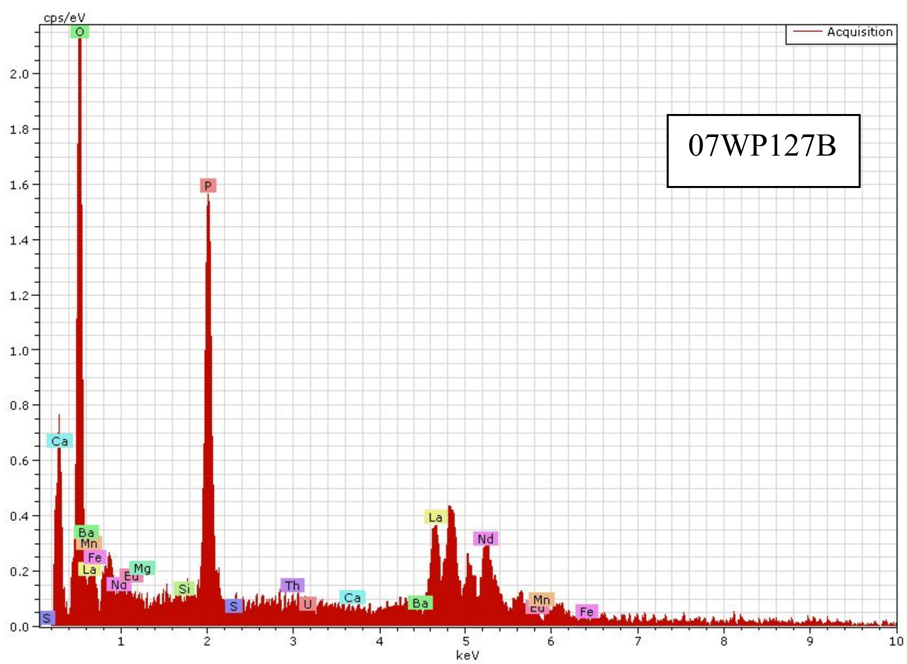

Figure 26b. EDS spectra from 07WP127B monazite from Roberts South prospect near North Fork. Note standard LREE dominance of La and Ce peaks, typical of a carbonatite. Scale is different from LH-12 spectra.

Figure 27. Monazite compositions determined by electron microprobe at WSU. Eu was not analysed for (NA). Four samples from the Lucky Horseshoe mine show an average of 35% Nd oxide, while sample 07WP127B from the Roberts carbonatite shows standard La and Ce LREE enrichment. A sample from the Sunshine Lode of the Blackbird district is also Ce dominant. Analyses are in Appendix C.

Monazites, both rim and cores, from the Lucky Horseshoe mine are the most enriched in Nd of any reported in the literature, based on a modest survey; the Lucky Horseshoe monazites contain 35 weight percent Nd oxide (Figure 27). The exact reason is unknown. Also different is the mineral's color – or lack of it. Mineral separation of the Lucky Horseshoe monazite for geochronology proved extremely difficult, because, unlike standard amber or yellow monazites, Lucky Horseshoe monazite is virtually indistinguishable by color from common grains like feldspar. It is a "dishwater grey to soapy tan" color at best.

The most compositionally analogous (i.e. MREE-enriched) monazite example found in the literature is that described by Laval (1998). He describes "grey monazite", a slightly thoriferous monazite of sedimentary, diagenetic origin that forms REE-zoned ovoid grains. Nd_2O_3 contents of the three grey monazite analyses given in his paper are in the 21-25% range, but CeO_2 contents are still greater (> 40%). At Lemhi Pass, both La and Ce oxide contents are lower and Nd oxide is higher.

Geochronology

Feldspars and Hornblendes with $^{40}Ar/^{39}Ar$

Five samples were analysed by Dr. Paul Layer for $^{40}Ar/^{39}Ar$ geochronology and thermal history. His full report is in Appendix F. Only the most important or representative results are included here. In summary, potassium feldspars from three thorium veins were examined, the Lucky Horseshoe deposit, and the Cago, and ThO_2 veins (Sample 07WP119). Of those, the ThO_2 is the furthest south and most remote from the syenite or any presumed intrusive center. An earlier, unpublished study on biotite from the Lucky Horseshoe (LH) mine, as well as from the Blackbird District, showed evidence of partial resetting of LH biotites and complete resetting (or thermal closure) at Blackbird in the 120-150 Ma range. Regionally, the Lucky Horseshoe mine shows the greatest deformation, interpreted as syn and post-mineralization, which may have contributed to its resetting. Other vein deposits do not contain biotite. Thus, feldspars were used (Figure 28). Feldspars have closure temperatures of 150-350^{o} C, somewhat lower than biotite. The two samples from the ThO_2 mine and the Lucky Horseshoe show saddle ages of 112 Ma and 56 Ma, respectively. The ThO_2 mine area does not display the intense mylonitization present at the Lucky Horseshoe. The spectra suggest a period of Tertiary to Cretaceous reheating and a primary age or thermal event near or older than 200 Ma. This is not sufficient to pin down an exact age of mineralization and feldspar precipitation, but it is definitive proof that the feldspar is not Eocene, as interpreted by earlier workers (Staatz, 1979), and the feldspar could be much older, most likely pre-Jurassic in age.

Hornblende closes to argon diffusion at much higher temperatures (about 550^{o} C), so an attempt was made to date the red-brown hornblende in the pyroxene porphyry. A sample of pyroxene porphyry (07-CQ09 HO#1) from the Copper Queen mine dump and a sample of coarse hornblende from the pegmatitic mafic rock clast in the calcite breccia at location #77 of Staatz (1979) were analysed. The hornblende in the breccia pipe has crystals several centimeters in diameter and is surrounded by a matrix of coarse calcite which might have protected the hornblende from alteration or recrystallization. The hornblende is tan, slightly lighter but of a similar color to that in the pyroxene porphyry dikes. It is probably related to a pyroxene porphyry dike adjacent to the calcite matrix breccia, which Staatz (1979) interpreted as a carbonatite. Results are shown in Figure 29.

The hornblende spectra from the Copper Queen pyroxene porphyry is “messy” but suggests thermal resetting perhaps about 400 Ma, though it continues to step up to older ages. The hornblende sample (07LOC77BP HO#3) is from the coarse hornblende megacryst in the breccia pipe and exhibits a very nice plateau age of 558 Ma +/- 1.6 Ma. This is statistically older than the age of the syenite, suggesting mafic magmatism predated the syenite (529 Ma) and igneous activity may have spanned 30 million years or more, possibly in discrete pulses. Considerable additional work is needed to more fully describe this Latest Precambrian to Early Cambrian magmatism, but the geochronology presented here provides definitive evidence for an early Paleozoic igneous event, most likely with bimodal and mildly alkaline signatures. Field and petrographic evidence is compatible, though not definitively, with the mafic intrusives being older than the syenite. Copper mineralization cuts the mafic porphyries and could be related to the mafic magmatism. Based on the cross-cutting hematite vein (Figure 14) and possible clasts of syenitic feldspars in the Lucky Horseshoe cataclasite (Figure 21), field and petrographic evidence suggests the Th-REE-hematite mineralization postdates the syenite.

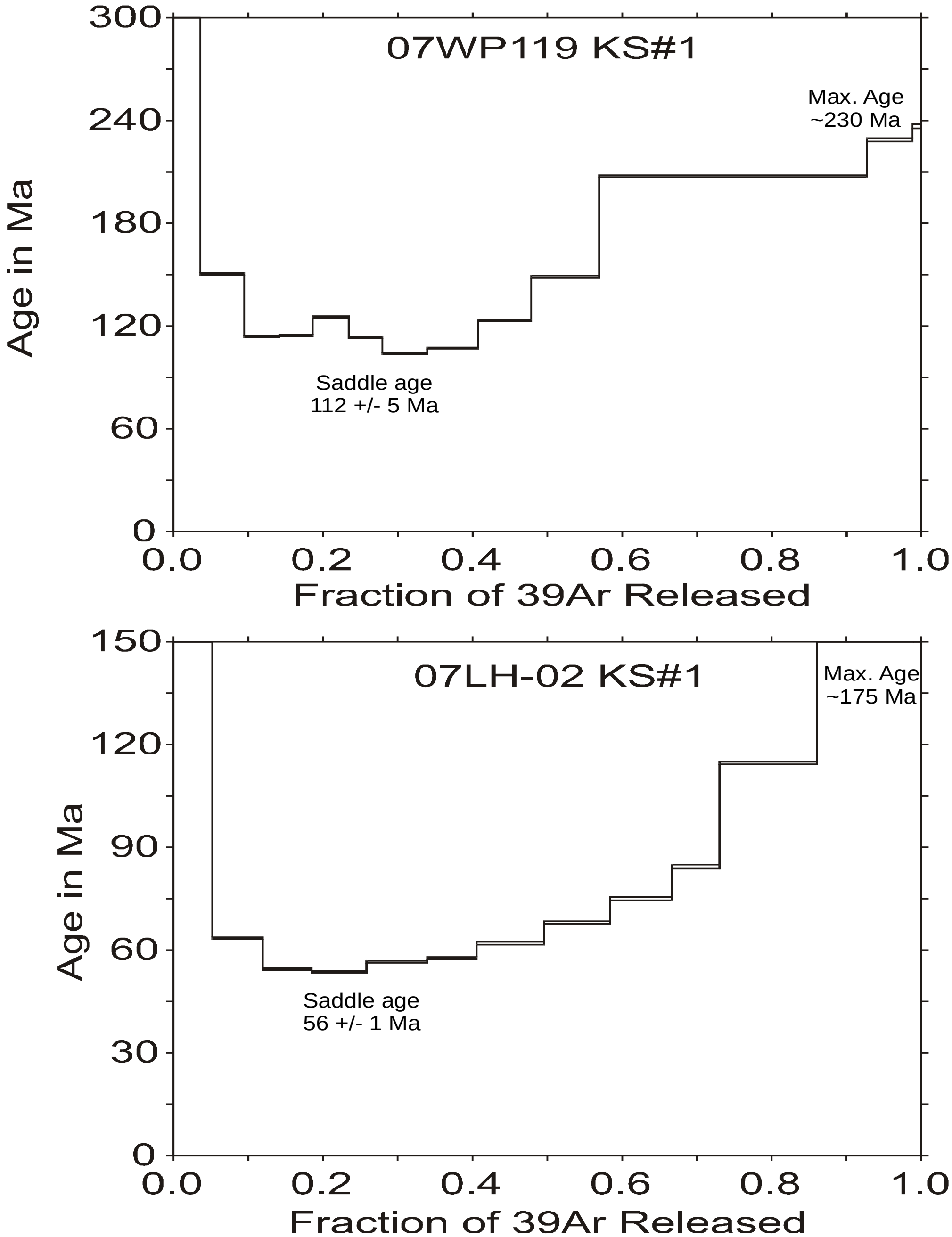

Figure 28. Feldspar $^{40}Ar/^{39}Ar$ geochronology for sample 07WP119 KS#1 from the ThO_2 vein on the south end of Lemhi Pass District, and for 07LH-02 KS#1 from the Lucky Horseshoe mine. The potassium feldspar is intimately associated with the thorite veins and deposits. Both samples show “saddle ages” indicative of Tertiary to Cretaceous thermal resetting. However, the maximum ages of approximately 200 Ma suggest that the feldspars retain a component of Jurassic or older crystallization.

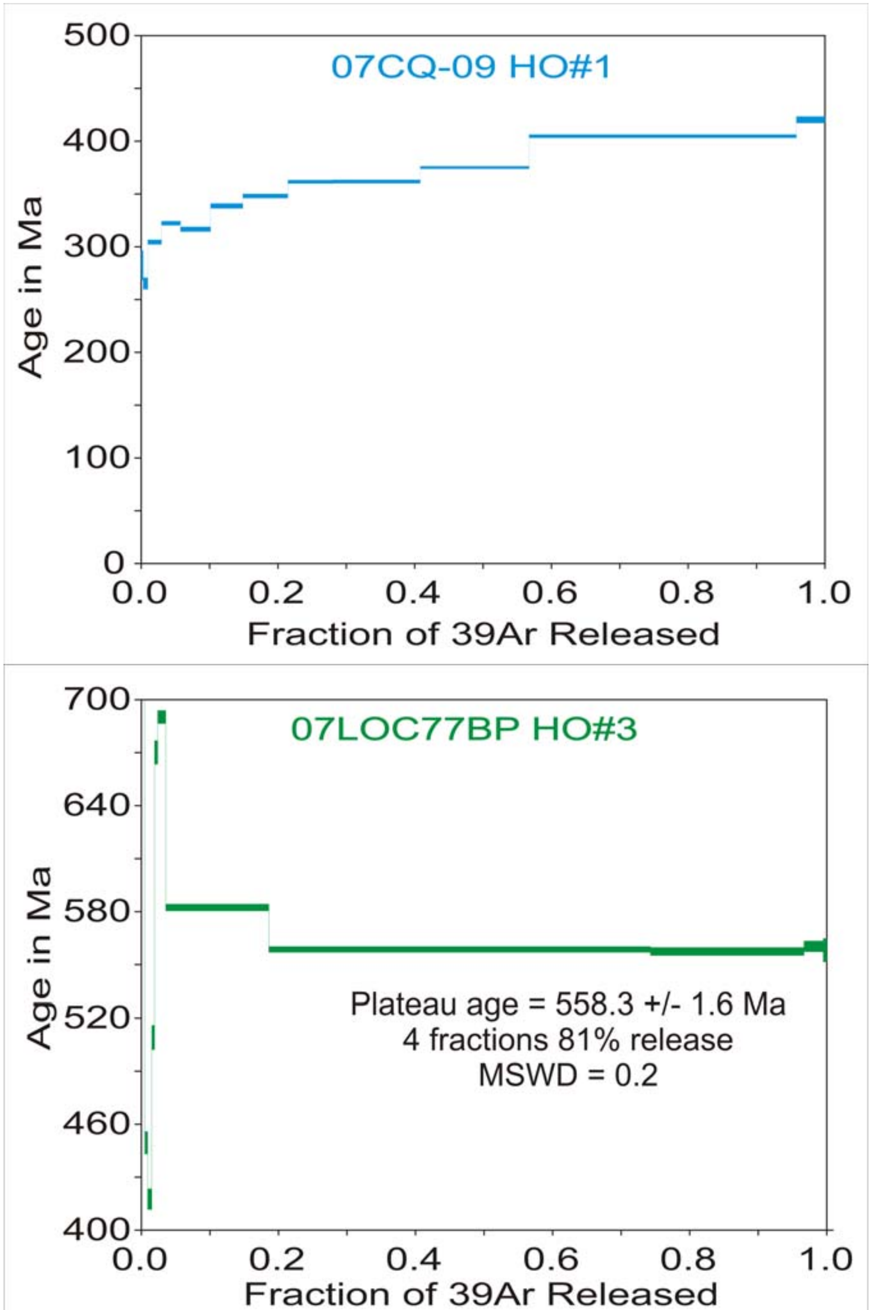

Figure 29. Hornblende geochronology. The upper spectra (07CQ-09 HO#1) is from the Copper Queen pyroxene porphyry and shows a messy spectra that was reset perhaps about 400 Ma but continues to step up to older ages. The lower sample (07LOC77BP HO#3) is from the coarse hornblende megacryst in the breccia pipe and shows a very nice plateau age of 558 Ma.

Electron Microprobe Geochronology on Thorite and Monazite

Preliminary work in 2002 (Jercinovic, et al., 2002) and this study's more comprehensive work done at the University of Massachusetts showed the utility of microanalysis of monazites and thorites for Th-U-total Pb geochronology (by measuring chemical amounts of U, Th, and total Pb). The full report of Dr. Mike Jercinovic is included in Appendix G and only a brief summary of the results is included in this section. In spite of the unusual low actinide contents (below 0.5 wt. % total) of the abundant monazite at Lemhi Pass and the Lucky Horseshoe mine in particular, the electron probe microanalysis (EPMA) on their new, unique Cameca SX-Ultrachron at the University of Massachusetts achieved some impressive results. The spatial resolution and in situ analysis are especially important for documenting chemical and age zoning and altered or unaltered domains. While monazite in metamorphic rocks has frequently been dated by this means, there are fewer examples in the literature of dating monazite in mineralized systems and fewer of good quality thorite ages. While U and Pb contents are quite low in the Lemhi Pass monazites, one advantage is that the overall Pb content of the hydrothermal thorium-REE deposits seem to be low (based on whole rock geochemistry), thus minimizing the common lead problem. While a few vein analyses contained a few hundred ppm of lead, most had only 50 ppm or less, while thorium was over 1000 ppm. In addition, Dr. Matt Kohn used a Laser Ablation-ICPMS for reconnaissance U-Pb geochronology analysis on two Lucky Horseshoe monazite samples. His results suggest that radiogenic lead greatly dominates over common lead in the Lucky Horseshoe thorium deposit.

Summary results from the University of Massachusetts EMPA study are in Figures 30 and 31. In the report, Dr. Jercinovic notes: *"Monazite from the Lucky Horseshoe mine is exceptionally high in Nd and Pr (~ 35wt.% Nd2O3, ~ 5wt.% Pr2O3), and commensurately low in La and Ce compared to most monazite worldwide (see example analyses, Table 6). Thorium concentrations in the bulk monazite (by far the most volumetrically significant) in the samples for this study is generally below 0.6 wt.% (Table 6). There is also clear evidence, in most monazite samples, of higher Th rims and fracture fillings (see Figure 1). This higher Th monazite (1-2 wt.% in general, see Table 6), can be interpreted as precipitating later than the bulk, low-Th monazite via textural evidence."*

Conclusions of the report (Appendix G), are:
"Summary Evidence of two episodes of monazite growth is preserved in samples from the Lemhi Pass Th-REE District of Idaho and Montana, illustrated in Figure 5. The initial episode, at which time the major Th-REE mineralization appears to have taken place, occurred ca. 350 Ma. The actinide content of this monazite is exceptionally low, and the Nd-Pr content exceptionally high, relative to typical igneous or metamorphic monazite (for example, see Williams et al., 2007). Thorium concentrations are generally below 6000 ppm, and concentrations of U generally below 100 ppm in the Lemhi Pass region bulk monazite. This monazite is, however, associated with major mineralization of thorite (ThSiO4). A second episode of ca. 100 Ma monazite growth is also suggested. This monazite occurs generally as thin (less than 5 micrometers) rims on the bulk monazite or as fracture fillings. The later monazite is significantly higher in Th, generally 1-2 wt.% Th, but reaching nearly 5 wt.% in some samples (06CTCAr). There is no suggestion of mineralization older than late Devonian based on monazite EPMA geochronology, and a second episode (although volumetrically

minor) of cretaceous mineralization is implied. EPMA of thorite from the Lemhi Pass Th-REE District yields data compatible with ages suggested by monazite. Although easily rendered metamict with subsequent hydrolyzation (Lumpkin and Chakoumakos, 1988) some small (generally below 10 micrometer) areas within some thorite grains remain. Analysis of these areas yields ages similar to coexisting monazite, and are compatible with mineralization at ca. 350 Ma and ca. 100 Ma (see Figure 5). Radiogenic Pb concentrations in thorite are expected to be somewhat variable due to the effects of metamictization, therefore the spread of apparent ages is correspondingly larger for thorite relative to monazite in Figure 5. There is no suggestion of ages appreciably older than ca.350 Ma, or significantly younger than ca. 100 Ma based on thorite analyses."

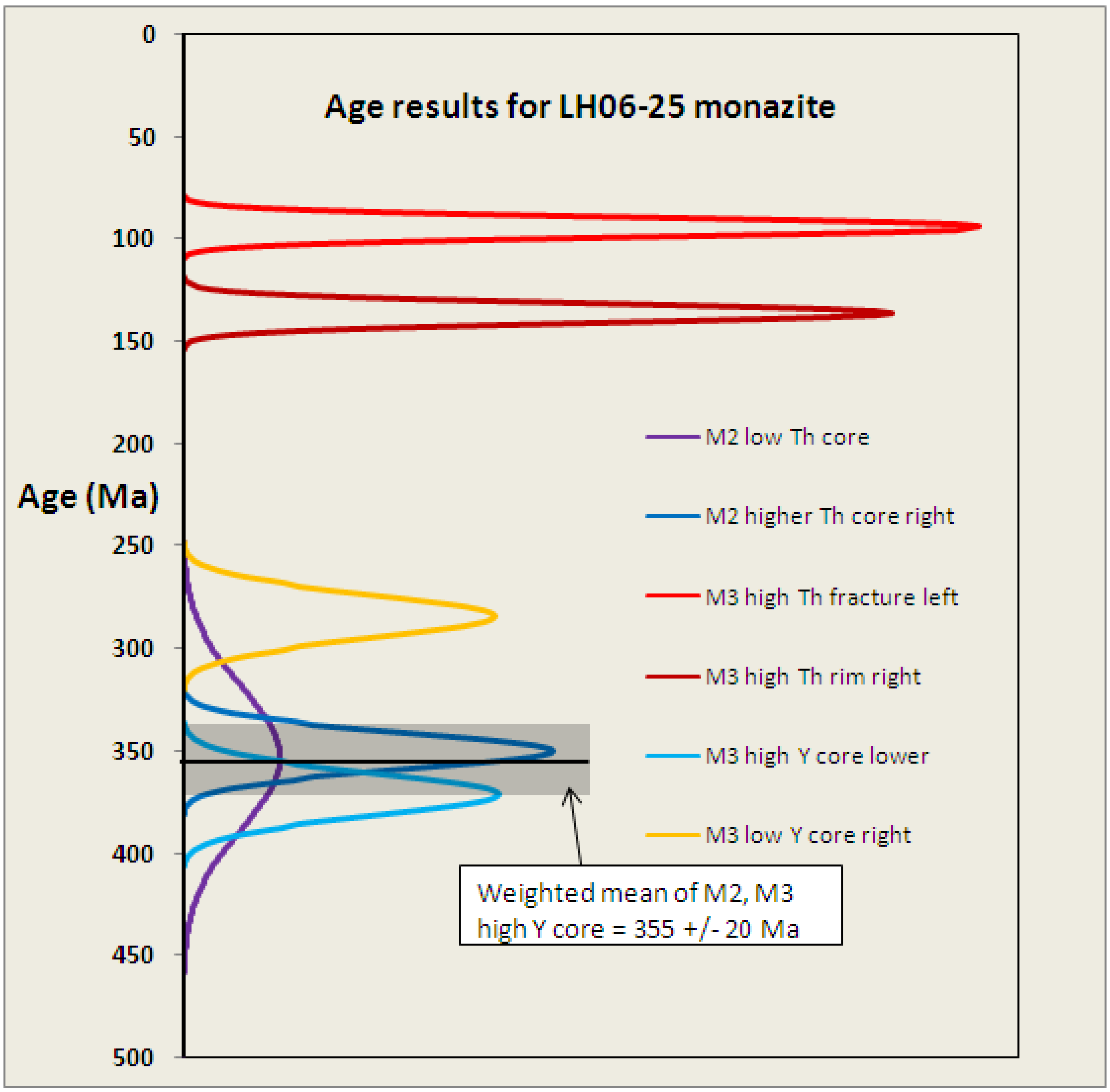

Figure 30, (Figure 2 in report in Appendix G). Histogram representation of age results for LH06-25 monazite. Histograms represent age and error as normal distribution around weighted mean age of analyses in each domain. A separate weighted mean of the cumulative results of M2 monazite and M3 high Y core results is shown.

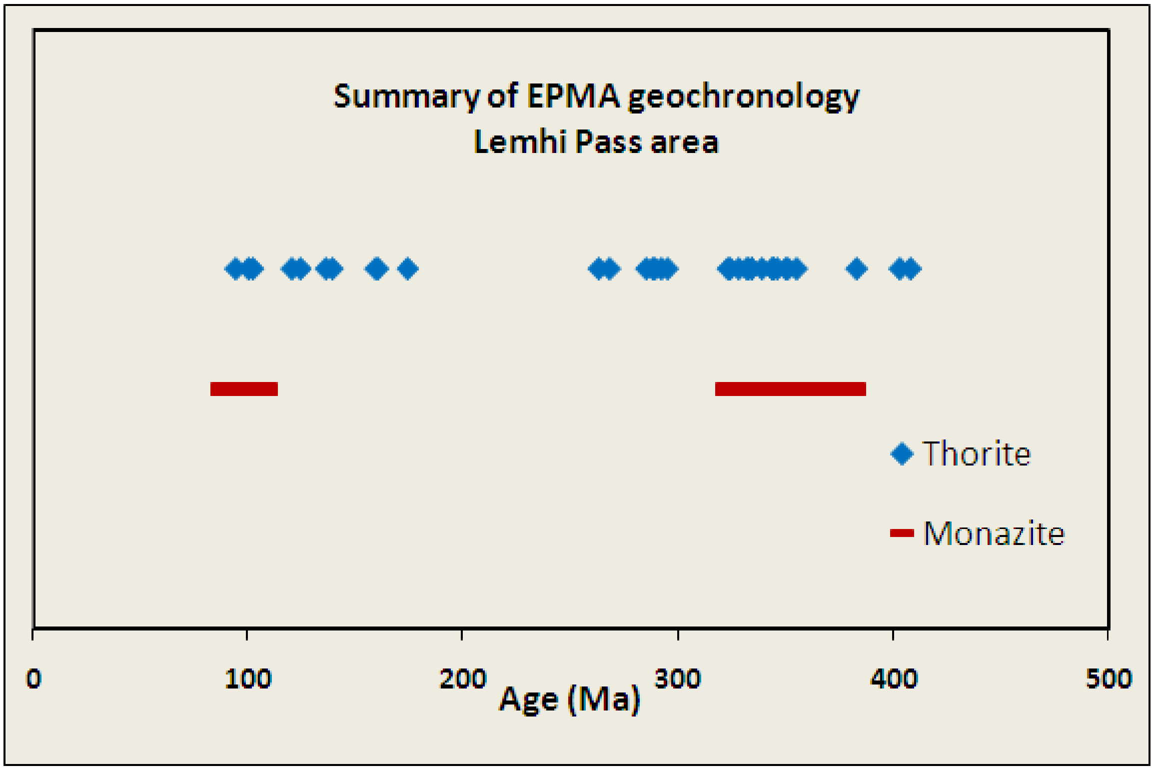

Figure 31, (Figure 5 in report). Summary of EPMA geochronology results, analyses from all domains, all samples (see Tables 4 and 5). Monazite data are from Table 8, representative of 2σ errors of weighted means. Thorite values are from Table 9 in report from Dr. Jercinovic (Appendix G). Note the overlapping range of monazite and thorite ages, centered on 350 Ma.

Thus, the best estimate of primary thorium mineralization is ca.350 Ma, or in the range 300-400 Ma, Late Devonian to early Mississippian in age, and considerably younger than the age of crystallization of the Cambrian syenite (Figure 31). Recrystallization and remobilization of thorium and lead in the Cretaceous is not surprising and is most likely related to intrusion of the Idaho Batholith, and associated regional metamorphism and thrusting.

Lead Isotope Measurements

Lead isotope compositions were measured in a suite of igneous and vein potassium feldspars, and district and regional sulfide and oxide minerals, in an attempt to test the genetic associations, if any, of igneous rocks and mineralized veins. The mineral separation and laboratory work was conducted principally by a Boise State University student, Michelle Gordon, under supervision of the PI and Dr. Mark Schmitz, of the Isotope Geology Lab at Boise State University. All analyses are of mineral separates. Oxide and sulfide minerals underwent bulk dissolution in aqua regia, under the assumption that measured ratios estimate the initial isotopic composition for these low U/Pb phases. For the feldspars, a sequential mixed acid (HNO_3-HCl-HF) leaching process, modified after Housh and Bowring (1991), was done to remove alteration zones or U or Th-bearing inclusions which could compromise the measurement of initial Pb compositions. The preferred fraction was the second HF leach aliquot. Pb was separated from dissolved samples by double-pass anion exchange chromatography in dilute HBr media. Isotope ratios were measured by thermal ionization mass spectrometry using static Faraday analysis on the Isoprobe-T mass spectrometer at Boise State University. Measured ratios were corrected for instrumental fractionation (0.11%/a.m.u.) based upon repeated measurement of the NBS-981 and 982 standards, and are listed in Appendix H and Table 7. Figure 32 shows the location of the regional samples analysed.

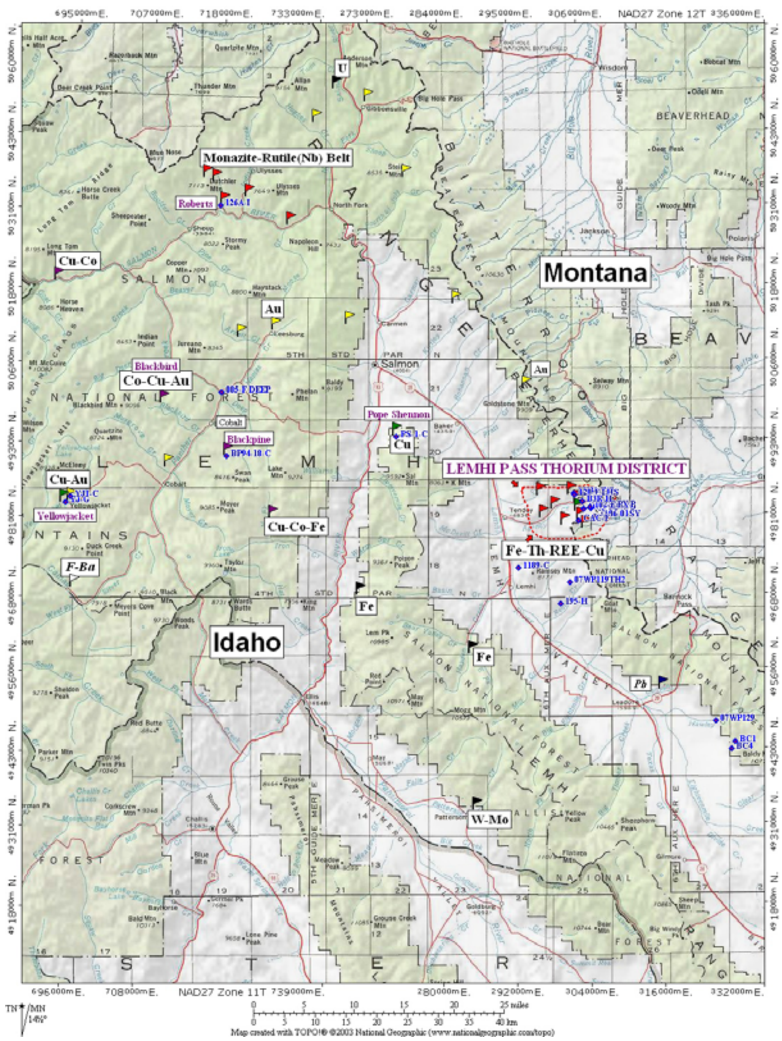

Figure 32. Location of lead isotope samples (blue text with waypoints), plus regional metallogeny.

Table 7a. Lead Isotope Analyses for Igneous and Vein Feldspars, Oxides, and Sulfides.

Sample	Mineral	Rock	Locale	$^{208}Pb/^{204}Pb$	%se	$^{207}Pb/^{204}Pb$	%se	$^{206}Pb/^{204}Pb$	%se	$^{208}Pb/^{206}Pb$	%se	$^{207}Pb/^{206}Pb$	%se
Regional Intrusives (magmatic compositions)													
07WP129 KF-P	feldspar	granite	Leadore	38.132	0.047	15.631	0.046	18.093	0.046	2.1075	0.005	0.86384	0.004
07WP129 KF-C	feldspar	granite	Leadore	37.976	0.036	15.658	0.036	18.044	0.035	2.1049	0.004	0.86771	0.003
085-F	feldspar	alkali syen/gabbro	Deep Creek	39.409	0.007	15.729	0.007	19.545	0.007	2.0163	0.001	0.80484	0.001
099-F	feldspar	syenite	Bluebird	39.628	0.002	15.672	0.002	19.354	0.002	2.0475	0.000	0.80973	0.000
Altered Intrusives													
BC4-F	feldspar	granite	Bull Canyon	44.754	0.009	15.963	0.009	23.879	0.009	1.8743	0.002	0.66850	0.001
102-F	feldspar	mafic porphyry	Bluebird	42.604	0.005	15.861	0.004	21.388	0.004	1.9920	0.002	0.74157	0.001
JA06-01A KF-C	feldspar	syenite	Continental Divide	40.293	0.016	15.809	0.015	20.361	0.015	1.9790	0.003	0.77644	0.002
Regional Fe or REE Mineralization													
195-H	hematite	vein	Loc. 195 Fe mine	38.288	0.002	15.655	0.002	18.688	0.002	2.0488	0.001	0.83772	0.001
126A-I	ilmenite	carbonatite	Roberts Prospect	38.420	0.005	15.646	0.004	18.692	0.003	2.0638	0.002	0.84049	0.001
Th-REE-Fe Mineralization													
JA06-01C HM	hematite	vein	Continental Divide	42.977	0.003	15.984	0.003	22.515	0.003	1.9089	0.001	0.70994	0.001
LH06-24B HM	hematite	vein	Lucky Horseshoe	400.057	0.016	16.364	0.016	30.014	0.016	13.3286	0.001	0.54518	0.002
B3r-H	hematite	vein	Buffalo Mine	41.607	0.002	15.806	0.002	19.995	0.002	2.0809	0.001	0.79502	0.001
LH06-24B KF-C	feldspar	vein	Lucky Horseshoe	97.440	0.012	15.956	0.012	23.001	0.012	4.2364	0.001	0.69370	0.002
LH33-F	feldspar	vein	Lucky Horseshoe	45.897	0.006	15.988	0.006	23.123	0.006	1.9850	0.001	0.69145	0.001
CAC-F	feldspar	vein	Cago Mine	46.264	0.011	15.871	0.010	21.370	0.010	2.1648	0.002	0.74261	0.001
Cu Mineralization													
CQ06-30B GA	galena	vein	Copper Queen Mine	41.023	0.008	15.849	0.006	20.112	0.004	2.0397	0.004	0.78803	0.002
CQ06-30B PY	pyrite	vein	Copper Queen Mine	40.926	0.004	15.803	0.003	20.105	0.002	2.0356	0.002	0.78598	0.001
CQ06-52 CP	chalcopyrite	vein	Copper Queen Mine	42.316	0.001	15.881	0.001	21.564	0.001	1.9624	0.001	0.73648	0.000
1CQ-26 MO	molybdenite	vein	Copper Queen Mine	40.337	0.005	15.745	0.004	19.487	0.002	2.0700	0.002	0.80799	0.001
07CQS-R BN	bornite	vein	Copper Queen Mine	43.577	0.002	15.964	0.002	22.317	0.002	1.9527	0.001	0.71533	0.001
YJ-G	galena	vein	Yellowjacket Mine	39.350	0.017	15.652	0.013	17.729	0.010	2.2194	0.008	0.88284	0.004
YJ1-C	chalcopyrite	bxa	Yellowjacket Mine	39.672	0.008	15.735	0.006	18.619	0.004	2.1307	0.004	0.84507	0.002
1189-C	chalcopyrite	vein	Napo Can.	38.944	0.003	15.658	0.002	18.151	0.002	2.1455	0.001	0.86266	0.001
BP94-18-C	chalcopyrite	vein	Blackpine Cu-Co prospect	45.131	0.003	16.302	0.002	26.056	0.002	1.7321	0.001	0.62566	0.001
PS-1-C	chalcopyrite	ore	Pope Shennon Mine	45.109	0.003	15.987	0.003	22.307	0.003	2.0222	0.001	0.71668	0.001

Notes: %se is the relative 1-sigma standard error on the measured ratio; fractionation uncertainty imposes the following minimum absolute uncertainties(1-sigma): $^{208}Pb/^{204}Pb$, 0.019; $^{207}Pb/^{204}Pb$, 0.007; $^{206}Pb/^{204}Pb$, 0.008; $^{208}Pb/^{206}Pb$, 0.0009; $^{207}Pb/^{206}Pb$, 0.0004.

Table 7b. Summary Sample Descriptions. See appendix H for more information.

Lemhi Pb: Gillerman

Sample	Type	Rock type	Location
Regional Intrusives (magmatic compositions)			
07WP129 KF-P	feldspar, L2	Leadore Pink Granite	Leadore – Hawley Crk.
07WP129 KF-C	feldspar, L2	Leadore Granite	Leadore – Hawley Crk.
085-F	feldspar, L2	Ord. mafic alkali Syenite?	Napias/Deep Creek –very fresh
099-F	feldspar, L1	LP Syenite	Bluebird area (=BL06-05)
Altered Intrusives			
BC4-F	feldspar, L2	Bull Canyon granite-alt.	South of Leadore area
102-F	feldspar, L1	Pyroxene Porph (alt.)	Bluebird area (=BL06-03)
JA06-01A KF-C	feldspar, L2	LP Syenite (Hm alt.)	Continental Divide
Regional Fe or REE Mineralization			
195-H	hematite	Spec. Hm vein	Loc. 195 Fe mine
126A-I	ilmenite	Carbonatite Bxa	Roberts Prospect, North Fork
Th-REE-Fe Mineralization			
JA06-01C HM	hematite	LP syenite – Hm vein	Continental Divide
LH06-24B HM	hematite	Th ore	Lucky Horseshoe
B3r-H	hematite	Hm-Th-(Cp) vein	Buffalo Mine, LP District
LH06-24B KF-C L2	feldspar, L2	Th ore	Lucky Horseshoe
LH33-F	feldspar, L2	Vein hw to LH Th ore	Lucky Horseshoe
CAC-F	feldspar, L2	Th vein envelope	Cago mine
Cu Mineralization			
CQ06-30B GA	galena	PbCu Vein in Px Porph	Copper Queen (CQ) mine
CQ06-30B PY	pyrite	Mineralized Px Porph	CQ mine
CQ06-52 CP	chalcopyrite	Cu_{vein}	CQ mine
1CQ-26 MO	molybdenite	Cu-Mo vein	CQ mine
$07CQS\text{-}R_{BN}$	bornite	Bornite-qz vein	CQ mine
YJ-G		Qz-Galena vein	Yellowjacket mine
YJ1-C	chalcopyrite	Chalcopy. Bxa	Yellowjacket mine
1189-C	chalcopyrite	Chalcopy. Vein	Napo Canyon, S of district
BP94-18-C	chalcopyrite	Qz-Cp vein	Blackpine Cu-Co prospect
PS-1-C	chalcopyrite	Cu ore	Pope Shennon Mine

galena

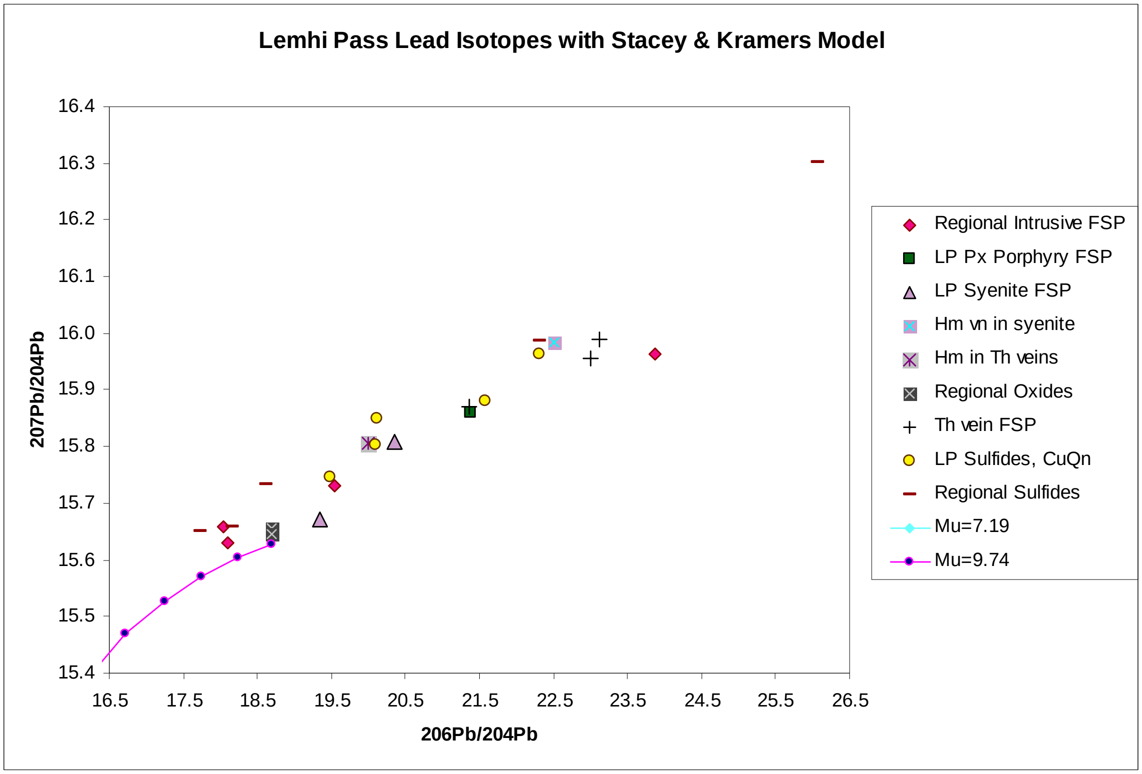

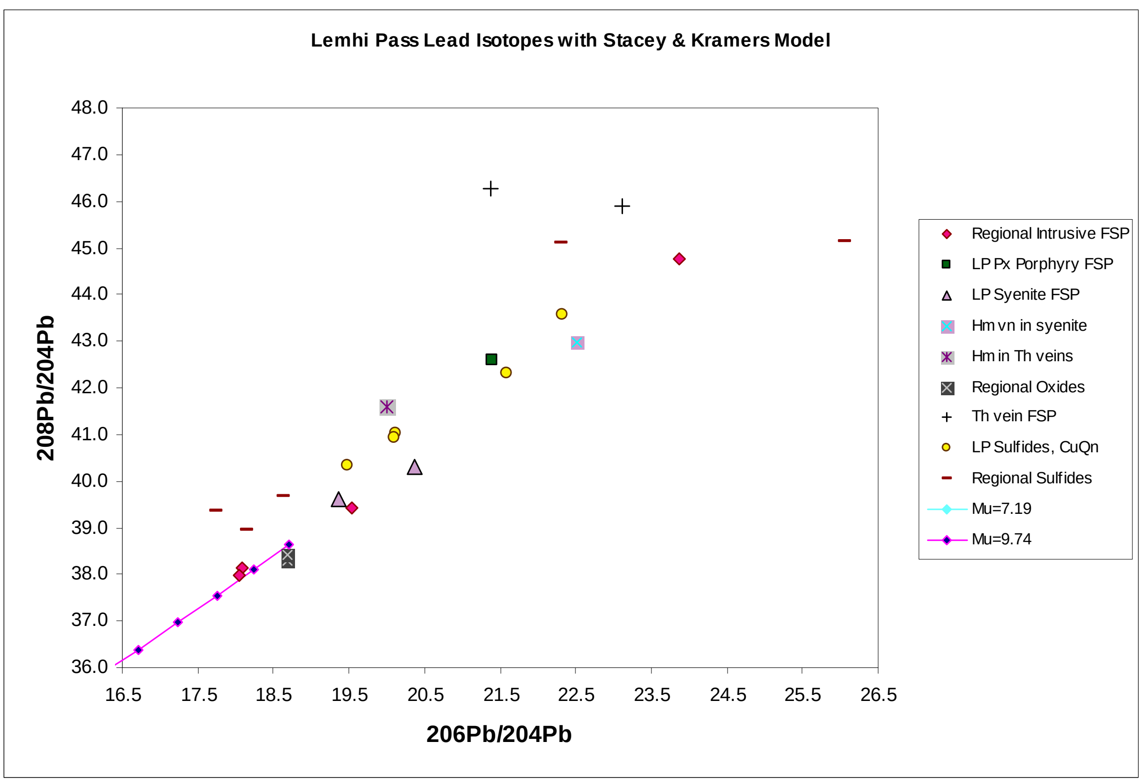

Figure 33a and 33b. Lead isotope results relative to ^{204}Pb with curves from 2-stage model of Stacey and Kramer.

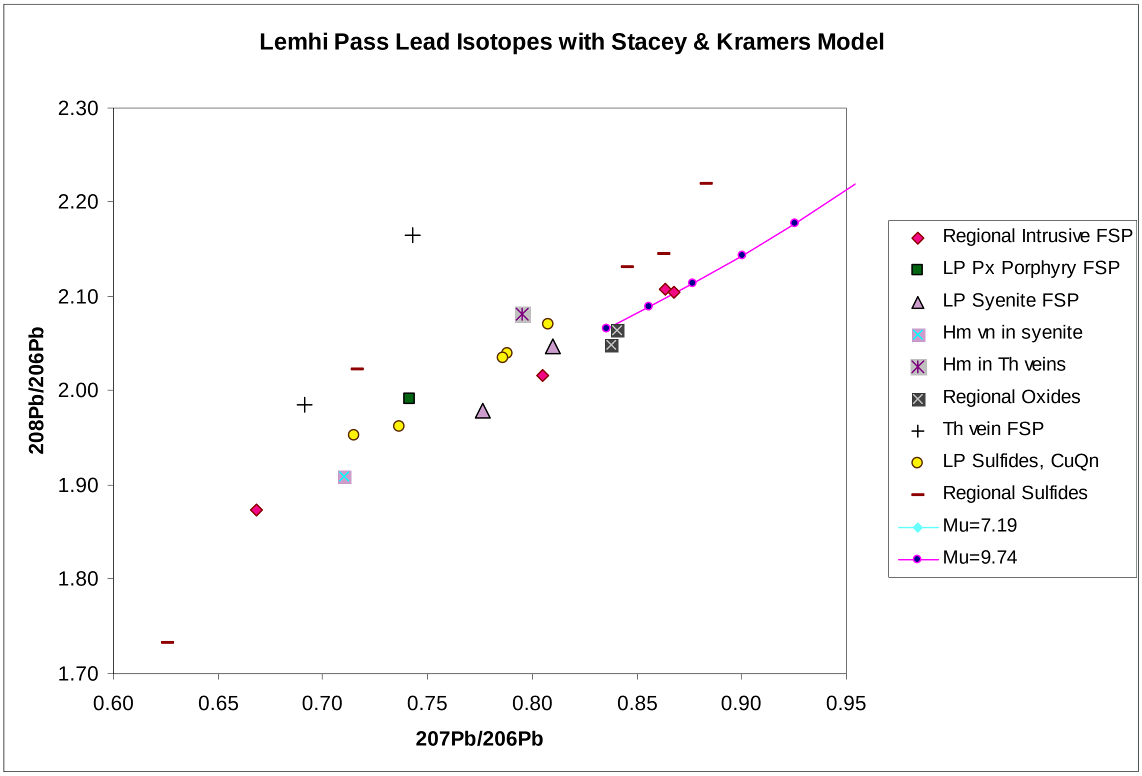

Figure 34. Lead isotope ratios relative to ^{206}Pb.

The objective of the lead isotope study was to determine if a correlation exists between the common lead in the intrusive rocks (as measured in igneous feldspar), the common lead in the sulfide veins, and/or the common lead in the thorium veins (measured in both feldspars and hematite). If the ratios are similar, then the hypothesis was that this would support a genetic connection between the veins and the intrusives with both of them sharing a common lead isotopic source reservoir. Both regional intrusives and Lemhi Pass district intrusives were sampled; likewise some regional hematite veins and copper sulfide veins, as well as district copper and thorium veins were analysed and are graphed with different symbols (Figure 33, 34).

The most unradiogenic or "primitive" lead sources still lie slightly above (at greater 207/204 ratios) the Stacey and Kramers crustal growth curve (Stacey and Kramers, 1975). Several attempts were made to model the data using higher values of μ, or ^{238}U/^{204}Pb, and a third stage of crustal evolution. Most of the data points still remain to the more radiogenic (or future time) side of such curves, but a simple, reasonable fit to the most primitive points was made by changing the second-stage to μ=10 as shown in Figure 35 where key points are labeled. Among the samples of intrusive rocks, both unaltered and altered rocks were sampled for lead isotopes. It is likely that the least or unaltered samples are most representative of magmatic lead isotope reservoirs. However, it is noteworthy that, with the exception of the Tertiary volcanics, no samples of truly fresh igneous rocks were seen in the Lemhi Pass district. Propylitic alteration is extensive in the mafic dikes and specular hematite veins locally cut the syenite.

Results of lead isotope study

The very fresh Deep Creek alkali gabbro pluton (085-F), dated as Ordovician (Evans and Zartman, 1988) has an isotopic lead composition between that of the two Lemhi Pass syenite samples. It is described by Evans and Zartman (1988) as an equigranular, alkali-feldspar syenite to alkali-feldspar quartz syenite with an Ordovician age of around 500 Ma but with some inherited lead or lead loss possible in the zircons. Our sample analysed had substantial mafic minerals, including biotite, and extremely fresh feldspar. On Figure 35, it is still one of the least radiogenic samples. The Leadore granite intrusion, 07WP129, sits close to the modeled curve and a reasonable model age of 503 million years can be calculated (Appendix H). It is located in the Beaverhead Range south of Lemhi Pass, and the analysed sample had only very minor deuteric alteration of plagioclase; it is a pink granite and has the least radiogenic composition (206/204, 207/204 is 18.044, 15.658).

Within the Lemhi Pass district, sample 099-F is the least altered intrusive and considered most likely to represent a "magmatic" value. It is syenite (62% SiO_2 with $Na_2O+K_2O > 11\%$; sample BL06-05 in Table 6) with magmatic biotite preserved but still has some specular hematite alteration. It plots below the model curve but is more radiogenic than 07WP129. Sample JA06-01A KF-C is potassium feldspar from the syenite (dated at 529 Ma) exposed in the trench near the Continental Divide; it has abundant interstitial specular hematite with no biotite left. Its isotopic signature is significantly more radiogenic (20.361, 15.809) than 099-F (19.354, 15.672). A hydrothermally altered pyroxene porphyry, 102-F, is also radiogenic. The most radiogenic intrusive analysed is sample BC4-F from the Bull Canyon stock south of Leadore. Feldspars in this purple granite are partially altered to muscovite plus hematite. Sample BC4 seems too altered and too radiogenic (23.879, 15.963) for a primary magma and is interpreted as having an enriched lead composition more indicative of alteration than any magmatic signature. It is only a few miles south of the least radiogenic sample 07WP129.

Two oxide samples of unusual regional mineralization were analysed. Though from very different types of deposits, the regional specular hematite vein (195-H) and the Roberts carbonatite (126A-I) overlap and are among the lowest in $^{206}Pb/^{204}Pb$ and $^{207}Pb/^{204}Pb$ ratios (18.688, 15.655), plotting in between 07WP129 and 099-F. Though the ages are unconstrained, it does present the possibility of a common lead isotopic reservoir for the hematite vein and the Paleozoic intrusives.

The lead isotopic values of regional sulfides cover a wide range, with copper vein, 1189, and the Yellowjacket sulfides (YJ-G, YJ1-C), being among the least radiogenic. The Yellowjacket chalcopyrite had minor secondary limonite and so the galena sample (15.652, 39.350) may be a better indication of the lead isotopic value for the Yellowjacket base metal mineralization. An intrusive suite of Paleozoic age has also been mapped near the Yellowjacket mine (Evans and Green, 2003). A sample of chalcopyrite (PS-1-C) from the Pope Shennon mine, near Salmon, was substantially more radiogenic (22.307, 15.987) than the other regional sulfides with the exception of BP94-18-C from the Blackpine copper-cobalt district. The Blackpine chalcopyrite plots in the upper right corner of Figure 35 with values (26.056, 16.302) much more radiogenic than the others.

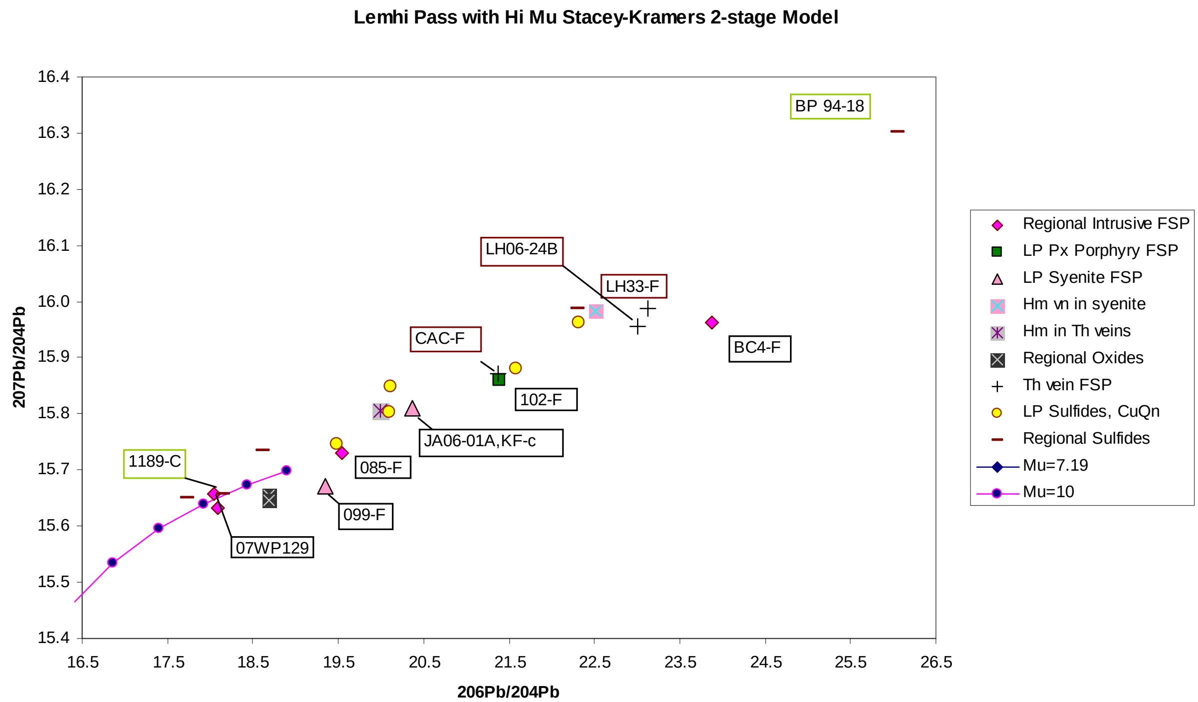

Figure 35. Lead isotope results in $^{207}Pb/^{204}Pb$ versus $^{206}Pb/^{204}Pb$ graph with higher μ=10 curve.

Sulfides from the Copper Queen mine at Lemhi Pass show a wide variation in their lead isotopic composition, perhaps reflecting subsequent deformation and/or metamorphism, or dual mineralizing events. The molybdenite sample (1CQ-2b MO) preserves the least radiogenic value (19.487, 15.745). Molybdenite was previously dated by ReOs at about 1 Ga in age (Gillerman et al., 2002) but that date was barely within analytical limits, and this study has not confirmed that age. Still, it is possible that molybdenite is either less susceptible to later recrystallization than other sulfide minerals, or that multiple aged veins exist. Two samples of galena (late vein) and pyrite (disseminated and in vein) cutting a mineralized pyroxene porphyry dike (CQ06-30B) plot close together (20.112, 15.849) in the middle of the graph, but two other copper samples from a quartz-chalcopyrite vein (CQ06-52 CP) and a bornite vein (07CQS-R BN) cutting the quartzite are considerably more radiogenic (22.317, 15.964 on bornite). The two copper samples were collected from the surface and could be affected by the deformation and thrusting described earlier. The mineralized mafic porphyry samples (CQ06-30B) from the mine dump are probably less affected by later structural events if they are from a deeper level, as well as being more chemically isolated by the intrusive wall rock.

Several samples of feldspar or hematite associated with the thorium-rare earth mineralization were analysed with acceptable results for common lead. Least radiogenic (19.995, 15.806) of those was a hematite vein with a trace of chalcopyrite from the Buffalo mine (B3r-H). A sample of feldspar in the envelope to the Cago vein (CAC-F) was more radiogenic, while two samples from the Lucky Horseshoe mine, LH33-F (23.123, 15.988) and LH06-24B KF-C, plotted close to a sample of hematite (22.515, 15.984) from a vein that cuts the syenite.

Interpretation of isotope results

In summary, a correlation is possible between the least radiogenic regional intrusives and some regional sulfides or oxides. Geologic evidence also suggests a spatial association between some of the Paleozoic intrusions and minor base metal mineralization, particularly at Yellowjacket but also at Leadore. At Lemhi Pass, the Copper Queen sulfides, as well as the syenite and mafic porphyry samples, occupy a considerable isotopic range which is tentatively interpreted as reflecting both variable hydrothermal alteration of the intrusives and perhaps mixing of more radiogenic fluids during formation or remobilization of base metal mineralization. It is quite possible that fluids with more radiogenic lead introduced during thorium mineralization have recrystallized some sulfides, or that the fluids responsible for the thorium deposition overlap in time/space/isotopic composition with those of the copper mineralization. Field relations show that the bulk of copper mineralization post-dates the mafic intrusives, which are both altered and mineralized, and the thorium post-dates the copper veins. Geochronology indicates that the mafic porphyries predate the syenite, as discussed earlier. Lead isotope values from the feldspars associated with the thorium veins are more radiogenic than the least-altered syenite (099-F) but close to the lead isotopic value of the hematite vein cutting the syenite, suggesting a genetic link to the specular hematite alteration. But that lead is far more radiogenic than lead from any known, unaltered intrusions of likely magmatic composition.

Sample BC4-F may be an example of this more strongly U and Th-enriched hydrothermal alteration affecting an intrusive rock. BC4-F is from the thorium-anomalous granite intrusion south of Leadore, at Bull Canyon (Staatz and others, 1972; Figure 32). The feldspar sample BC4-F is highly enriched in $^{206}Pb/^{204}Pb$ and more moderately enriched in $^{207}Pb/^{204}Pb$. However, the unusual granite is a rose to dark purple in color and is quite altered. The feldspars, which appear to have been perthitic alkali feldspar originally, are in the process of being converted to hematite and a muscovite phase. Matrix (or perhaps interstitial plagioclase) is largely fine-grained sericite. Quartz is unaffected and no mafics were seen in the few sections examined. Graphic intergrowths of quartz and feldspar are common, suggesting eutectic, low temperature growth, possibly in a water-rich environment. Accessory zircon or monazite and sphene seem to be partly under attack by the hydrothermal fluids responsible for the unusual alteration (Figure 36). In short, the enriched lead isotope signature is probably as much hydrothermal as magmatic, though additional work would be needed to evaluate this hypothesis.

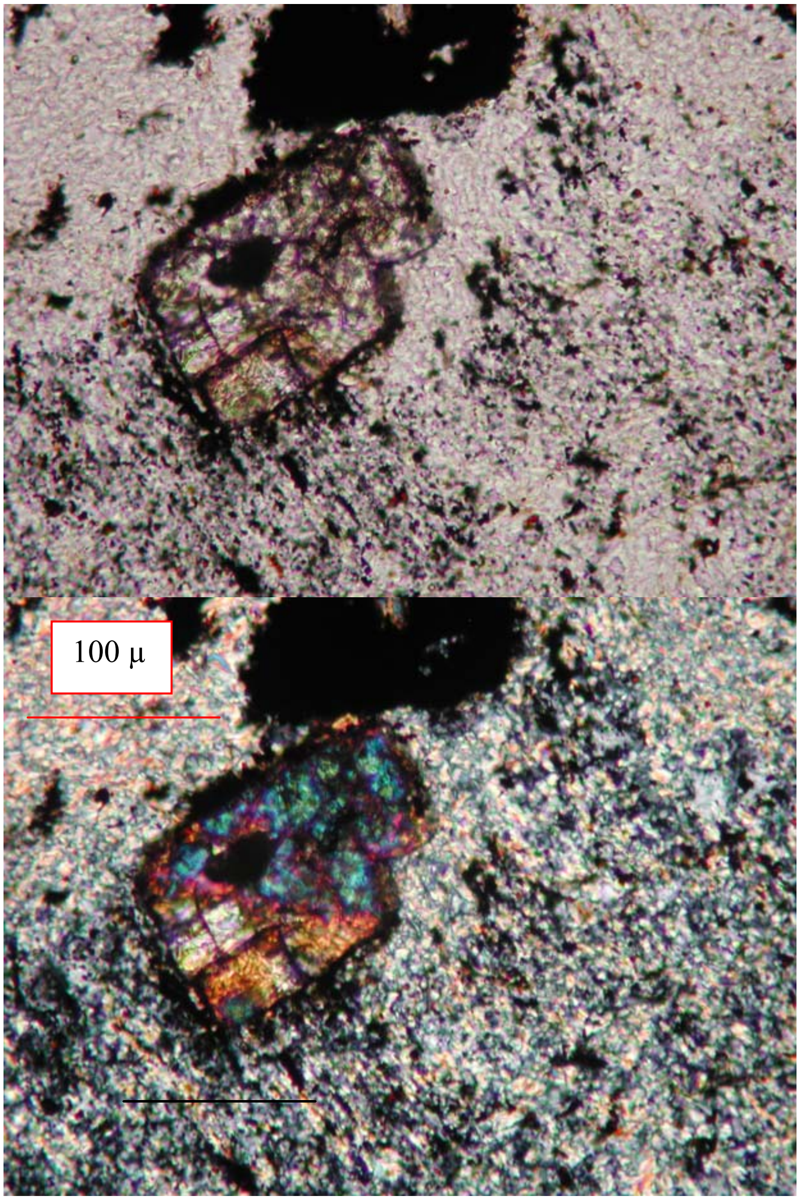

Figure 36. Euhedral Monazite (?) in hematite-sericite altered feldspar in Bull Canyon stock, sample 08BC1-2. Other grains show more intense alteration of the monazite. No microprobe data is available for this thin section sample.

<u>Cobalt Deposits</u>

There is one more radiogenic sample, BP94-18-C, which sits in the upper right corner of the graph (Figure 35). There is a considerable gap between it and the other samples. Sample BP94-18 is chalcopyrite from a quartz-chalcopyrite vein in drill core from the Blackpine copper-cobalt mine (Figure 32). Its highly radiogenic lead isotopes are typical of those reported from more metamorphosed copper-cobalt horizons (thought to be Precambrian exhalatives or sediment-hosted sulfides) in the Blackbird District (Panneerselvam, et al., 2004).

Blackbird Co-Cu ores have ranges of $^{206}Pb/^{204}Pb$ = 30.8-40.4; $^{207}Pb/^{204}Pb$=16.8-17.6; and $^{208}Pb/^{204}Pb$=49.7-63.9 and are interpreted to reflect leaching of lead from the host Yellowjacket Formation by basinal brine or metamorphic fluid circulation (Panneerselvam, et al., 2004). Other explanations for the Blackbird deposits invoke Proterozoic, syngenetic, volcanic-related exhalative solutions localized along a rift basin (Nash and Hahn, 1989). Some combination of the two theories for the origin of the Blackbird deposits may better fit the geologic and isotopic data. The isotopic gap between the Blackpine sample and the Lemhi Pass and other regional samples is suggestive of different processes, metal/fluid sources, and probably timing of mineralization, with the Lemhi Pass and other regional sulfide samples crystallized from fluids tapping a less radiogenic lead source, possibly involving a greater amount of magmatically derived lead.

Conclusions of lead isotope study

In conclusion, the lead isotope data from the Lemhi Pass District and other nearby deposits sampled is interpreted to reflect mixing of juvenile magmatic lead represented by the unaltered igneous intrusives with a more U and Th-enriched crustally-derived, hydrothermal lead component. The thorium veins, the hematite vein cutting the syenite, some of the copper veins, and the Bull Canyon altered intrusive appear to contain a significantly higher proportion of the crustal-derived lead, and they also reflect increasing hydrothermal alteration and metasomatism. The source of the more radiogenic component could be magmatic – perhaps a buried intrusion derived from a lead reservoir of continental derivation – or it could be hydrothermally derived from leaching radiogenic lead from Precambrian or Paleozoic sediments, or both.

General Conclusions and Discussion

Important major results of this MRERP study are listed below. Additional interpretation and analysis of the large amount of data collected is ongoing and more will be published.

- Lemhi Pass District hosts at least two unusual and previously undescribed and undated intrusive suites of Latest Precambrian to Early Cambrian age: a syenite (approximately 530 Ma, based on U-Pb date on zircons) and mafic porphyries (in part 560 Ma based on $^{39}Ar/^{40}Ar$), probably alkaline lamprophyres, plus other altered mafic rocks. The intrusives are interpreted to represent a bimodal, alkaline suite with rift-related affiliation in a continental setting. More work is planned on their geochemistry, but they are very unusual rocks for Idaho.

- The mafic intrusives are propylitically to calc-silicate altered over a wide geographic area, and one unusual mafic or ultramafic sill shows Mg-carbonate replacement of igneous phenocrysts, suggesting fluids of very high CO_2 content. Timing of the alteration is unknown. Some thorium and copper deposits are spatially associated with intrusive dikes, suggesting related structural settings.

- Local epidote-bearing hornfels and one area of "dry" quartz veins in the center of the district are compatible with a buried pluton of some type.

- Alteration and stratigraphic variation in the Mesoproterozoic metasediments is subtle to indistinguishable. The metasediments have detrital zircons that correlate temporally with and share similar provenance to the Apple Creek and Gunsight Formations further west. More detailed mapping is needed to understand the structural setting, but the Lemhi Pass Fault is a major WNW-trending shear zone, probably with drag folds. The Lucky Horseshoe mylonite has sheared and recrystallized the thorium-REE mineralization there. The mylonite most likely represents a Mesozoic thrust complex, as does the low angle, brittle fault zone that displaces copper veins at the Copper Queen mine stopes.

- Hydrothermal alteration in the metasediments around the copper veins is poorly developed but seems to include local potassium feldspar, carbonate, and epidote. The mafic intrusives are strongly propylitically altered. Hydrothermal alteration around the thorium-REE veins and replacements is better developed, though only on a scale of centimeters to meters in width, approximating the width of the vein. It includes strong potassium feldspar replacement of the muscovite quartzite, with local sodium feldspar and some rutile outwards of that. Specular hematite is ubiquitous and early as well as being intergrown with thorite and quartz.

- Based on petrographic evidence, feldspar veins surrounding the Lucky Horseshoe mine, and resulting clasts within the Lucky Horseshoe cataclasite/mylonite, could include syenite dikes, or related alkali metasomatism (fenites?). One clast of crystalline monazite, plus metamorphic fabrics of biotite growing in pressure shadows around feldspar clasts, confirms that the deformation and metamorphism largely postdates thorium mineralization. However, multiple orogenic events are likely, before, during and after mineralization.

- Argon geochronology and thermochronology indicate regional-scale resetting during the Tertiary and Cretaceous of vein feldspars and biotites in the thorium veins. Hornblendes from the mafic porphyries record maximum ages as old as 560 Ma, but possibly as younger (to 400 Ma) as well.

- The only direct age on the copper mineralization is the original Re-Os age on molybdenite in the Copper Queen vein. This study could not substantiate the 1.05 Ga age, and it is considered as questionable due to the extremely low levels of Re. Both copper and thorium-REE mineralization are considered to be Paleozoic (or latest Precambrian for the copper) based on their cross-cutting relationship to dated intrusives and the electron microprobe ages (approximately 350 Ma) on monazite and thorite. The best interpretation of the window of mineralization is from 550 to 350 million years ago, with the copper most probably being deposited in the earlier portion (i.e. Cambrian) and the thorium somewhat later in the Devonian. Multiple periods of base metal sulfide mineralization are quite possible as some thorium veins do contain minor copper, though it is unclear if the copper is remobilized or primary.

- Lead isotopes indicate possible correlations of the regional Paleozoic intrusions with some copper mineralization, particularly at the Yellowjacket mine, but some of the Copper Queen mine sulfides and the thorium-REE mineralizing fluids show a trend to more U and Th-enriched, crustally derived source of lead. No Devonian intrusions are known, though other undated Paleozoic plutons exist in the Beaverhead Range, and large areas of gravel cover are present in the valley. Lead may have been derived from a buried plutonic source or from leaching of continental sediments. Multistage mineralization is quite possible.

Rare earth geochemistry of Lemhi Pass and Iron oxide – copper – gold (IOCG) deposits

While many of the structural and mineralogical characteristics of Lemhi Pass mineralization are similar to those present in IOCG deposits, such as the giant Olympic Dam deposit in Australia, other features are not. And IOCGs constitute a very diverse group of deposits, not all of which have rare earth data available in the literature. Geochemical signatures of rare earth deposits have been used to help distinguish deposit types (Samson and Wood, 2005; Castor and Hedrick, 2006), though a full review is beyond the scope of this report. Samson and Wood (2005) included the Lemhi Pass veins in their study. They note the unusual rare earth signature (MREE enriched) of the Lemhi Pass veins, in contrast with LREE enriched carbonatites (inc. the carbonate breccia at Staatz' locale #77). Their plots of Lemhi Pass veins on a normalized La vs. Eu/Eu* graph show a position below (i.e. less enriched in La) the values for either the Olympic Dam IOCG deposit or the Bayan Obo carbonatite and also outside the fields of rocks from the Missouri iron oxide REE deposits and others in Australia (Figure 37). Olympic Dam is unusually enriched in rare earths compared to other IOCG deposits, perhaps because of the granitic host rocks.

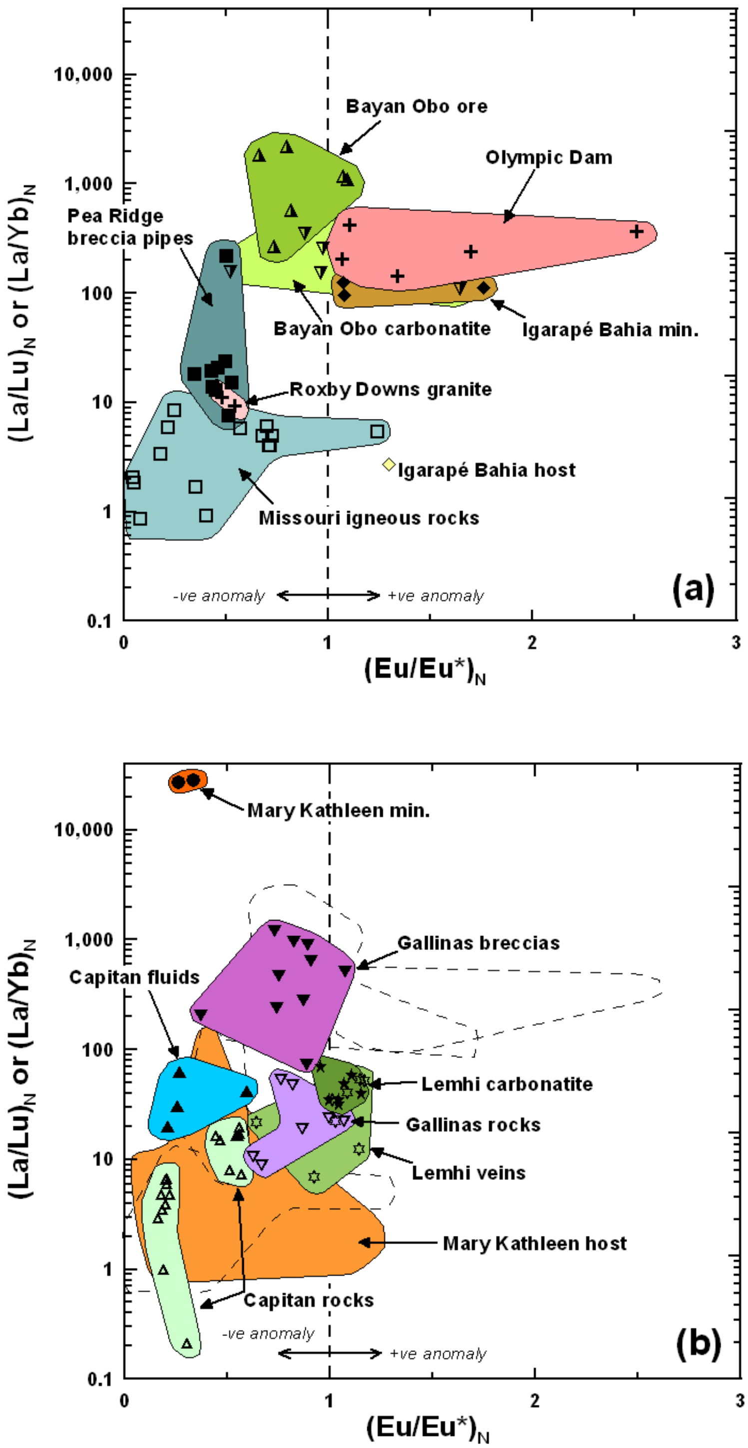

Figure 37. From Samson and Wood (2005), showing different rare earth deposits distinguished by their different normalized La/Lu ratio versus normalized Eu/Eu* content. They include data for Lemhi Pass veins, which are outside of the data fields for Olympic Dam and IOCGs (top diagram), but overlap some of the iron deposits. New analytical data is similar to their Lemhi Pass data.

Figure 38 shows a similar plot of La/Gd versus Eu/Eu* modified from Castor and Hedrick (2006) with addition of new vein geochemical analyses from Lemhi Pass (Reed and Gillerman, 2008). The Lemhi Pass vein samples partially overlap the field of peralkaline REE deposits and the field of iron-REE deposits. The veins are quite distinct from the LREE-enriched carbonatites, including those at North Fork, a few tens of miles northwest of Lemhi Pass, along the monazite-rutile belt. Castor and Hedrick (2006) also discuss the more HREE-enriched pattern typical of large low grade igneous, peralkaline rare earth deposits and the mixed signatures of various vein deposits, such as at Lemhi Pass.

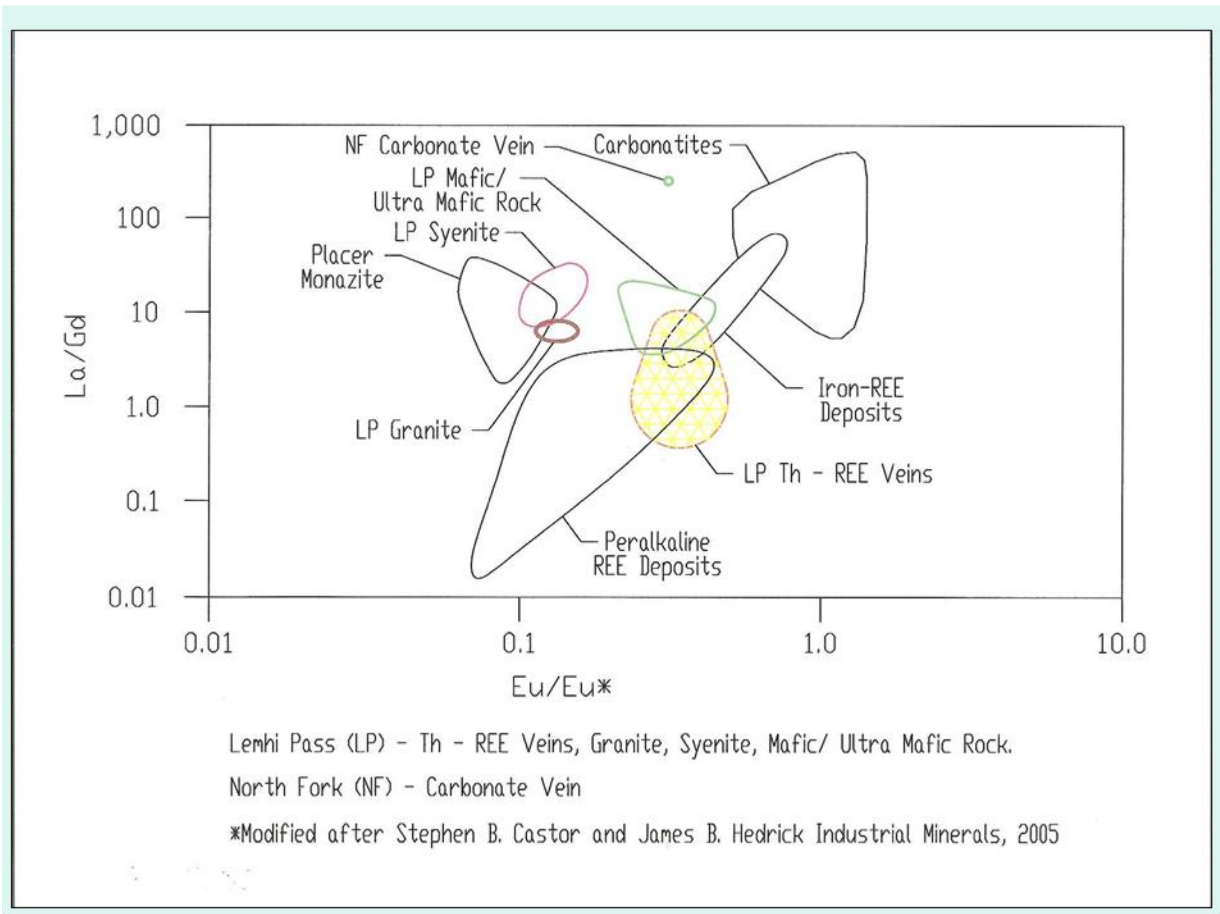

Figure 38. Plots of La/Gd versus Eu/Eu* for suite of Lemhi Pass rocks in comparison to values from literature for various types of deposits (from Reed and Gillerman, 2008, after Castor and Hedrick, 2006).

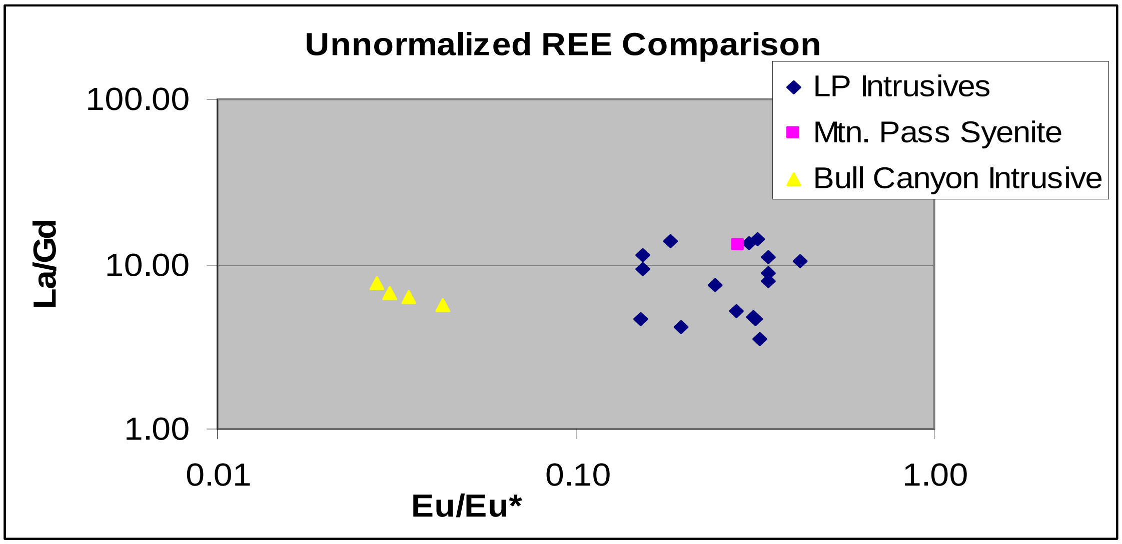

Figure 39. La/Gd vs. Eu/Eu* plot of Lemhi Pass intrusive rocks compared to a syenite from the Mountain Pass carbonatite complex, California, and to altered granite from Bull Canyon pluton, Leadore, Idaho. Note the much lower Eu/Eu* for the Bull Canyon rocks.

Figure 39 shows the much lower Eu/Eu* for the Bull Canyon rocks in comparison to the Lemhi Pass intrusives (all types), along with one sample of fresh syenite at Mountain Pass, California. All four Bull Canyon samples show a distinctly low Eu/Eu* value, evidence of a huge negative Eu anomaly on a REE spider diagram (Figure 40); they also have only 0.02 wt. % CaO. One possible interpretation would be that Eu was mobilized out of the rocks as divalent Eu during hydrothermal alteration. Divalent Eu is more soluble than the trivalent Eu (Samson and Wood, 2005). The Bull Canyon samples still contain 18-35 ppm Th, or approximately the same amount as the Lemhi Pass syenite (25-33 ppm, 3 samples). So, while both the Lemhi Pass syenite and Bull Canyon stocks are anomalous in thorium and rare earths, compared to typical igneous rocks, they are not themselves mineralized, except in iron.

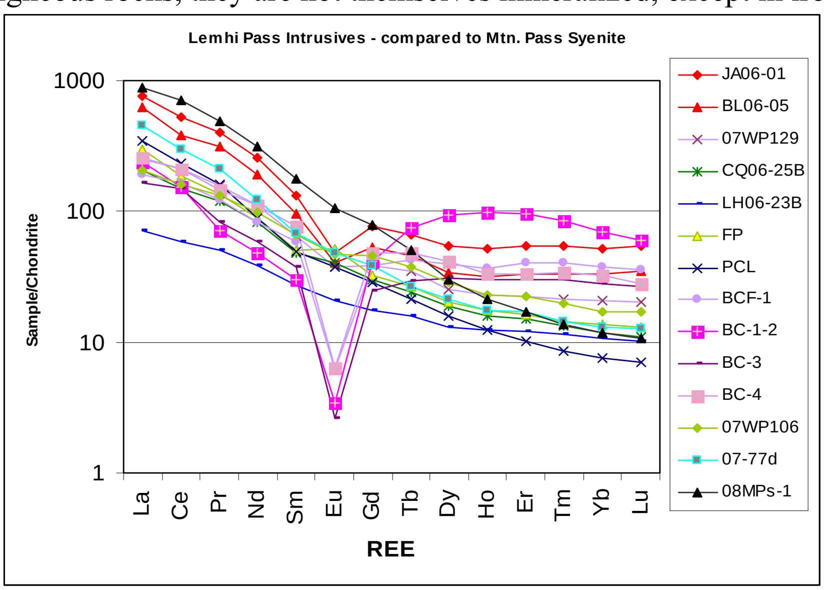

Figure 40. REE spider diagram for Lemhi Pass intrusives and Bull Canyon stock samples.

Discussion on Origin of Lemhi Pass Deposits

The multiple methods of geochronology used in this study strongly suggest the existence of two significant geologic events at Lemhi Pass – a latest Precambrian to Cambrian (560-520 Ma) bimodal mafic/syenite magmatic episode, probably with associated copper and base metal mineralization, and a later, 350 Ma, or late Devonian period of thorium-REE-hematite mineralization and vein formation. The Th-REE-Fe mineralization could correspond to a lengthy time interval from 300-400 Ma, approximately. As essentially no magmatic rocks of Devonian age are known in Idaho, but some "sedex" and MVT-type mineralization has been described in central and eastern Idaho (Figure 41 from Lund, 2008, and summary therein), it seems possible that the Lemhi Pass veins, including their unique REE signature, could be related to regional-scale hydrothermal circulation through the sedimentary and upper crustal package in response to whatever triggered other "sedex" and MVT mineralization.

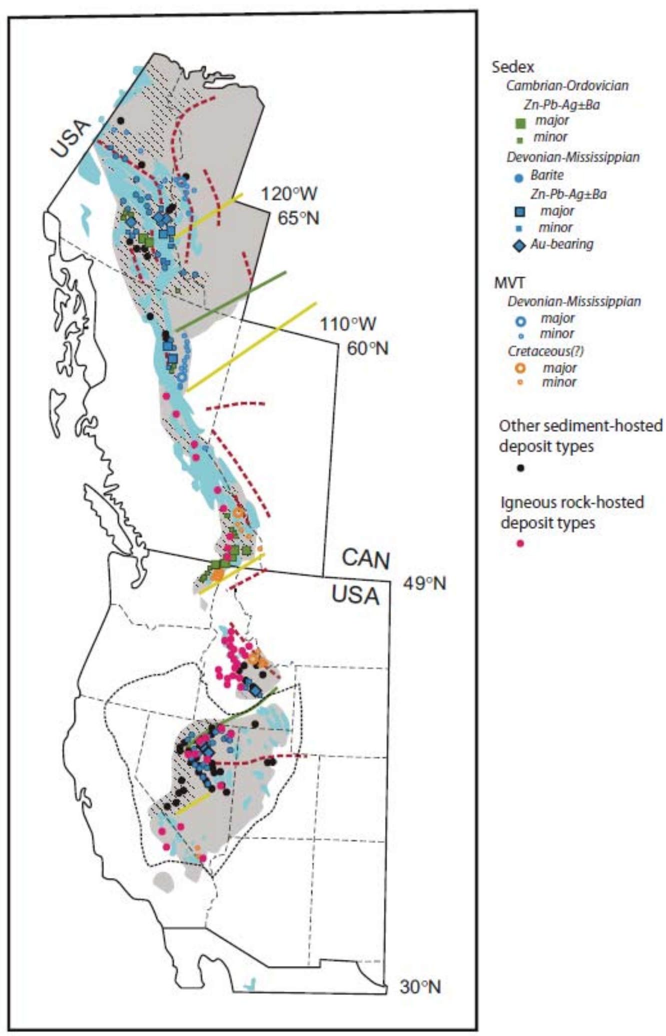

Figure 41. Figure 5 from Lund, 2008, showing mineral deposit types along the, rifted Paleozoic margin to western Laurentia.

The Lemhi Pass fault zone may be an inherited portion of this rifted margin, and the multiple intrusives at Lemhi Pass are interpreted to be related to extensional settings along the Paleozoic rifted margin over a protracted period of geologic history.

Strong or abundant regional alteration has not been recognized in the Proterozoic siltites and quartzites at Lemhi Pass or elsewhere in the Salmon region, and regional mapping available for eastern Idaho does not include alteration mapping. But using a model similar to some IOCG types of deposits, metals and lead could be associated with a widespread, regional hematite-bearing alteration of earlier, lithophile-rich intrusions, including hypothetical buried ones in the Beaverhead Range and adjacent areas. However, the abundant apatite and fluorine signatures of the district, along with the large volume of the thorium and rare earths, locus of fracturing and vein localization, are hard to explain with a standard "sedimentary leaching" model.

The iron oxides, apatite, rare earths and fluorine are also signatures of more typical thorium deposits - those associated with alkaline intrusive-(+- carbonatite) complexes, such as at the Powderhorn District in Colorado (Van Gosen and Lowers, 2007; Staatz and others, 1980). Some combination of a crustally derived, igneous source of metals, and modification by regional hydrothermal circulation seems necessary to explain the Th-REE suite and the lead isotope results at Lemhi Pass. Thus, the existence of a buried Paleozoic-age pluton seems likely, though its location has been obscured by later structural displacements.

In particular, Lemhi Pass and the Paleozoic syenite intrusive and thorium mineralization may be related to a Paleozoic belt of syenites and carbonatite/intrusive complexes with Th-REE veins which trend through New Mexico and Colorado (Figure 42).

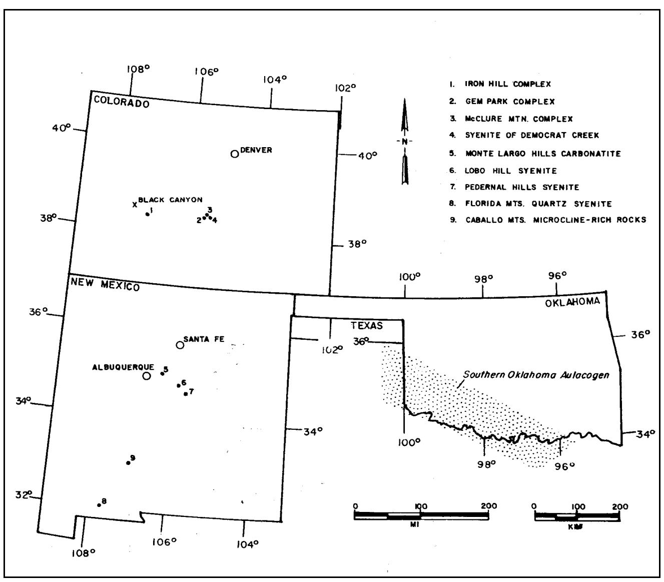

Figure 42. Paleozoic syenites of New Mexico and Colorado. From Loring and Armstrong, 1980. The Colorado alkalic complexes host Th, REE, Ti, Nb, and other mineralization; they are Cambrian in age (Olson and others, 1977).

At Lemhi Pass, the substantial age separation, nearly 200 million years, between the mafic to syenitic igneous rocks and the vein monazites and thorites, as well as the lead isotopic differences and discrete geographic loci of mineralization for the Th-REE-Fe versus copper mineralization, argue against the original hypothesis that the district represents a Th-rich variant of an Olympic Dam or IOCG type of deposit. It is possible that the consistent electron microprobe ages of 300-400 Ma on both monazites and thorites represent a complete recrystallization of earlier thorium-REE mineralization, but that also seems doubtful.

However, lead isotope signatures, the unique MREE-enriched rare earth chemistry, and altered intrusives at Lemhi Pass also suggest that regional hydrothermal alteration and fluid flow, with possible metal leaching from crustal sources, such as buried intrusives, may have had a role in formation of the thorium-rare earth veins and deposits. Extensive, regional-scale calcic-sodic alteration and fluid flow is a hallmark of IOCG deposits (Corriveau, 2006; Williams and others, 2005). It is possible that an altered and mineralized, buried or eroded, Cambrian pluton of unknown composition could simply have served as a metal source for Devonian fluid flow and mineralization. It is also possible that a buried pluton of Devonian (300-400 Ma) age was directly involved in the genesis of a more typical peralkaline thorium-rare earth magmatic-related ore system. A multistage sequence of ore-forming processes and geologic events certainly seems required to produce the unique deposits at Lemhi Pass. Additional study of both the district and the region will be needed to more fully understand the genesis of these unique deposits.

In summary, two possible models for the Lemhi Pass District are hypothesized. Both recognize a regional-scale Late Precambrian to early Paleozoic, bimodal intrusive event, probably with accompanying base metal mineralization in the region. The first model postulates magmatic-hydrothermal Th-REE-Fe mineralization related to a buried or unknown, Devonian-age alkaline intrusive with radiogenic lead compositions. The second model forms the Th-REE-Fe veins and replacements during the Devonian in a hydrothermal (to metamorphic) setting with regional fluid flow leaching metals and volatile components from earlier Paleozoic (Cambrian?), Th-REE-P mineralized intrusive complexes, plus continentally derived, U and Th-enriched sediments and earlier copper deposits in part. A combination of both models is also possible. Regardless of the exact origin of the Lemhi Pass base metal and thorium mineralization, it is dominantly of Paleozoic age with remobilization, thermal resetting, and probably some metamorphism and alteration, along with structural disruption during Cretaceous and Tertiary times.

References Cited and Selected Others

Anderson, A.L., 1958, Uranium, thorium, columbium, and rare earth deposits in the Salmon region, Lemhi County, Idaho: Idaho Bureau of Mines and Geology Pamphlet 115, 81p.

Anderson, A.L., 1961, Geology and mineral resources of the Lemhi quadrangle, Idaho, Lemhi County, Idaho: Idaho Bureau of Mines and Geology Pamphlet 124, 111 p.

Anderson, H.E., and Davis, D.W., 1995, U-Pb geochronology of the Moyie sills, Purcell Supergroup, southeastern British Columbia: implications for the Mesoproterozoic geological history of the Purcell (Belt) basin: Canadian Journal of Earth Sciences, v. 32, p.1180-1193.

Austin, S.R., Hetland, D.L., and Sharp, B.J., 1970, Mineralogy of the Lemhi Pass thorium and rare-earth deposits: Idaho Bureau of Mines and Geology Mineral Resources Report 11, 10 p.

Bell, Keith, ed., 1989, Carbonatites—Genesis and evolution: London, Unwin Hyman, approx. 400p.

Castor, S.B., and Hedrick, J.B., 2006, Rare earth elements, *in* Kogel, J.E., Trivendi, N.C., Barker, J.M., and Krukowski, S.T., eds., Industrial minerals and rocks – commodities, markets, and uses (7^{th} ed.): Society for Mining, Metallurgy, and Exploration, Inc. (SME), Littleton, CO, p. 769-792.

Corriveau, L, 2006, Iron oxide copper-gold (+-Ag+-Nb+-P+-REE+-U) deposits: A Canadian Perspective: Internet pdf accessed 12-2008, http://gsc.nrcan.gc.ca/mindep/synth_dep/iocg/index_e.php

Doe, B.R., and Sanford, R.F., 1995, Lead isotope characteristics of ore systems in central Idaho, *in* Worl, R.G., et al., eds., Geology and mineral resources of the Hailey 1o x 2o quadrangle and the western part of the Idaho Falls 1^{o} x 2^{o} quadrangle, Idaho: U.S. Geological Survey Bulletin 2064 A-R, p. M1-M29.

Evans, K.V., and Green, G.N., 2003, compilers, Geologic map of the Salmon National Forest and vicinity, east-central Idaho: U.S. Geological Survey Miscellaneous Investigations Map I-2765, scale 1:100,000.

Evans, K.V., and Zartman, R.E., 1990, U-Th-Pb and Rb-Sr geochronology of middle Proterozoic granite and augen gneiss, Salmon River Mountains, east-central Idaho: Geological Society of America Bulletin, v. 102, p. 63-73.

Evans, K.V., and Zartman, R.E., 1988, Early Paleozoic alkalic plutonism in east-central Idaho: Geological Society of America Bulletin, v. 100, p. 1981-1987.

Gibson, P.E., 1998, Origin of the Lemhi Pass REE-Th deposits, Idaho/Montana: petrology, mineralogy, paragenesis, whole rock chemistry and isotope evidence (unpublished M.S. thesis): University of Idaho, Moscow, Idaho, 320 p.

Gibson, P., and Wood, S.A., 1997, Geochemistry and mineralogy of the Lemhi Pass Th-REE deposits: Mineral Deposits, Papunen (ed.), Balkema, Rotterdam, p. 945-948.

Gillerman, V.S., Fanning, C.M., Link, P.K., Layer, P., and Burmester, R.F., 2008, Newly Discovered Intrusives at the Lemhi Pass Thorium-REE Iron Oxide District, Idaho: Cambrian Syenite and Mystery Ultramafics - Signatures of a Buried Alkaline Complex or Two Systems?[abs.]: Geological Society of America Abstracts with Programs, v. 40:1, p. 51.

Gillerman, V. S., Jercinovic, M.J., and Stein, H.J., 2002, U-Pb and Re-Os geochronology suggest a multistage Precambrian-Mesozoic history for thorium and copper mineralization, Lemhi Pass, Idaho [abs.]: Geological Society of America Abstracts with Programs, v. 34:6, p. 337.

Gillerman, V.S., Lund, K., and Evans, K.V., 2003, Stratigraphy, structure, and mineral deposits of the Lemhi Pass area, central Beaverhead Mountains, eastern Idaho: Northwest Geology, v. 32, p. 134-146.

Gillerman, V.S., Otto, B.R., and Griggs, F.S., 2006, Site inspection report for the abandoned and inactive mines in Idaho on U.S. Bureau of Land Management property in the Lemhi Pass area, Lemhi County, Idaho: Idaho Geological Survey Staff Report S-06-4, 170 p.

Gillerman, V.S., Otto, B.R., and Griggs, F.S., 2001, Site inspection report for the abandoned and inactive mines in Idaho on U.S. Bureau of Land Management property in the Lemhi Pass area, Lemhi County, Idaho: contract report to the Bureau of Land Management, 168 p.

Gillerman, V.S., Otto, B.R., and Griggs, F., 2000, Lemhi Pass Thorium District: a variant of Proterozoic iron oxide (Cu-U-Au-REE) deposits?[abs.]: Geological Society of America Abstracts with Programs, v. 32:7, p. A-83.

Hansen, P.M., 1983, Structure and stratigraphy of the Lemhi Pass area, Beaverhead Range, Southwest Montana and east-central Idaho (unpublished M.S. thesis): Pennsylvania State University, Pennsylvania, 112 p.

Hitzman, M.W., Oreskes, N., and Einaudi, M.T., 1992, Geological characteristics and tectonic setting of Proterozoic iron oxide (Cu-U-Au-REE) deposits: Precambrian Research, v. 58, p. 241-287.

Housh, T.B., and Bowring, S.A., 1991, Lead isotopic heterogeneities within alkali feldspars; implications for the determination of initial lead isotopic compositions: Geochimica et Cosmochimica Acta, v. 55(8), p. 2309-2316.

Jercinovic, M.J., Gillerman, V.S., and Stein, H.J., 2002, Application of microprobe geochronology to hydrothermal monazite and thorite, Lemhi Pass District, Idaho [abs.]: Geological Society of America Abstracts with Programs, v. 34:6, p. 172.

Jones, A.P., Wall, F., and Williams, C.T., eds., 1996, Rare Earth Minerals, chemistry, origin and ore deposits: Mineralogical Society Series #7, Chapman & Hall: London, England, 372 p.

Kohn, M.J., and Vervoort, J.D., 2008, U-Th-Pb dating of monazite by single-collector ICP-MS: Pitfalls and potential: Geochemistry Geophysics Geosystems, v. 9, Q04031, doi: 10.1029/2007GC001899.

Laval, M., 1998, Properties and geology of grey monazite: a possible new resource of REE: Canadian Institute of Mining Special Volume 50, p. 193-204.

Link, P.K., and Fanning, C.M., 2003, Detrital zircon ages from the Yellowjacket, Apple Creek and Gunsight Formations, Blackbird mining district, Salmon River Mountains, central Idaho: Northwest Geology, v. 32, p. 206-207.

Link, P.K., Fanning, C.M., Lund, K.I., and Aleinikoff, J.N., 2007, Detritial-zircon populations and provenance of Mesoproterozoic strata of east-central Idaho, U.S.A.: correlation with Belt Supergroup of southwest Montana, *in* Link, P.K., and Lewis, R.S., eds., Proterozoic Geology of Western North America and Siberia, SEPM Special Publication No. 86, p. 101-128.

Linnen, R.L., and Samson, I.M., eds., 2005, Rare-element geochemistry and mineral deposits: Geological Association of Canada Short Course Notes 17, 342 p.

Loring, A.K., and Armstrong, D.G., 1980, Cambrian-Ordovician syenites of New Mexico, part of a regional alkalic intrusive episode: Geology, v. 8, p. 344-348.
Lund, K., 2008, Geometry of the Neoproterozoic and Paleozoic rift margin of western Laurentia: Implications for mineral deposit settings: Geosphere, April 2008, v. 4:2, p. 429-444.
Mackin, J.H., and Schmidt, D.L., 1957, Uranium and thorium-bearing minerals in placer deposits in Idaho: Idaho Bureau of Mines and Geology, Mineral Resources Report No. 7, 9 p.
Mariano, A.N., 1989, Nature of economic mineralization in carbonatites and related rocks, *in* Bell, Keith, ed., Carbonatites—Genesis and evolution: London, Unwin Hyman, p. 149-176.
Nash, J.T., and Hahn, G.A., 1989, Stratabound Co-Cu deposits and mafic volcaniclastic rocks in the Blackbird mining district, Lemhi County, Idaho: Geological Association of Canada Special Paper 36, p. 339-356.
Newton, J., LeMoine, D., Adams, C.N., Anderson, A.L., and Shively, J.A., 1960, Study of two Idaho thorite deposits: Idaho Bureau of Mines and Geology Pamphlet 122, 53p.
Olson, J.C., and Hedlund, D.C., 1981, Alkalic rocks and resources of thorium and associated elements in the Powderhorn district, Gunnison County, Colorado: U.S. Geological Survey Professional Paper 1049–C, 34 p.
Olson, J.C., Marvin, R.F., Parker, R.L., and Mehnert, H.H., 1977, Age and tectonic setting of lower Paleozoic alkalic and mafic rocks, carbonatites, and thorium veins in south-central Colorado: U.S. Geological Survey Journal of Research, v. 5, no. 6, p. 673–687.
Olson, J.C., Shawe, D.R., Pray, L.C., and Sharp, W.N., 1954, Rare-earth mineral deposits of the Mountain Pass district, San Bernardino County, California: U.S. Geological Survey Professional Paper 261, 75 p.
Panneerselvam, K., Macfarlane, A.W., and Salters, V.J.M., 2006, Provenance of ore metals in base and precious metal deposits of central Idaho as inferred from lead isotopes: Economic Geology, v. 101, pp. 1063-1077.
Panneerselvam, K., Macfarlane, A., and Salters, V., 2004, Lead isotope constraints on the origin of Proterozoic sediment-hosted cobalt-copper ores of central Idaho [abs.]: Geological Society of American Abstracts with Programs, v. 36:5, p. 517.
Reed, R., and Gillerman, V., 2008, Thorium and rare earths in the Lemhi Pass region, Idaho: SME Annual Meeting Program, p. 90-91.
Ross, G.M., Parrish, R.R., and Winston, D., 1992, Provenance and U-Pb geochronology of the Mesoproterozoic Belt Supergroup (northwestern United States): implications for age of deposition and pre-Panthalassa plate reconstructions: Earth and Planetary Science Letters, v. 113, p. 57-76.
Samson, I.M., and Wood, S.A., 2005, The rare earth elements: behaviour in hydrothermal fluids and concentration in hydrothermal mineral deposits, exclusive of alkaline settings, *in* Linnen, R.L., and Samson, I.M., eds., Rare-Element Geochemistry and Mineral Deposits: Geological Association of Canada, GAC Short Course Notes 17, p. 269-297.
Sanford, R.F., and Wooden, J.L., 1995, Sources of lead in ore deposits of central Idaho, *in* Worl, R.G., et al., eds., Geology and mineral resources of the Hailey 1o x 2o quadrangle and the western part of the Idaho Falls 1^{o} x 2^{o} quadrangle, Idaho: U.S. Geological Survey Bulletin 2064 A-R, p. N1-N24.
Schipper, W.B., 1955, The Tendoy Copper Queen mine (unpublished M.S. thesis): University of Idaho, Moscow, Idaho, 38 p.

Sha, G.S., Vervoort, J.D., Watkinson, A.J., Doughty, P.T., Prytulak, J., Lee, R.G., and Larson, P.B., 2004, Geochronologic constraints on the tectonic evolution of the Boehls Butte-Clearwater core complex; evidence from 1.01 Ga garnets: Geological Survey of America Abstracts with Programs,v. 36:4, p. 72.
Sharp, W.N., and Cavender, W.S., 1962, Geology and thorium-bearing deposits of the Lemhi Pass area, Lemhi County, Idaho, and Beaverhead County, Montana: U.S. Geological Survey Bulletin 1126, 76p.
Slack, J.F., Aleinikoff, J.N., Belkin, H.E., Fanning, C.M., Ransom, P.W., 2008, Mineral chemistry and SHRIMP U-Pb geochronology of Mesoproterozoic polycrase-titanite veins in the Sullivan Pb-Zn-Ag deposit, British Columbia: Canadian Mineralogist, v. 46, pp. 361-378.
Slack, J.F., 2006, High REE and Y concentrations in Co-Cu-Au ores of the Blackbird District, Idaho: Economic Geology, v. 101:2, p. 275-280.
Staatz, M.H., 1979, Geology and mineral resources of the Lemhi Pass thorium district, Idaho and Montana: U.S. Geological Survey Professional Paper 1049-A, 90p.
Staatz, M.H., Bunker, C.M., and Bush, C.A., 1972a, Thorium distribution in a granite stock near Bull Canyon, Lemhi County, Idaho: U.S. Geological Survey Professional Paper 800-B, p. B51-B56.
Staatz, M.H., Hall, R.B., Macke, D.L., Armbrustmacher, T.J., and Brownfield, I.K., 1980, Thorium resources of selected regions in the United States: U.S. Geological Survey Circular 824, 32 p.
Staatz, M.H., Shaw, V.E., and Wahlberg, J.S., 1972b, Occurrence and distribution of rare earths in the Lemhi Pass thorium veins, Idaho and Montana: Economic Geology, v. 67, p. 72-82.
Stacey, J.S., and Kramers, J.D., 1975, Approximation of terrestrial lead isotope evolution by a two-stage model: Earth and Planetary Science Letters, v. 26, p. 207-221.
Umpleby, J.B., 1913, Geology and ore deposits of Lemhi County, Idaho: U.S. Geological Survey Bulletin 528, 182 p.
Van Gosen, B.S., and Lowers, H.A., 2007, Iron Hill (Powderhorn) carbonatite complex, Gunnison County, CO—A potential source of several uncommon mineral resources: Mining Engineering, v. 59, no. 10, p. 56-62.
Williams, P.J., Barton, M.D., Johnson, D.A., Fontbote, L., de Haller, A., Mark, G., Oliver, N.H.S., and Marschik, R., 2005, Iron oxide copper-gold deposits: geology, space-time distribution, and possible modes of origin: Economic Geology 100th Anniversary Volume, pp. 371-405.
Winter, J.D., 2001, An Introduction to Igneous and Metamorphic Petrology: Prentice-Hall, New Jersey, 697 p.

Publications Resulting from MRERP Grant # 06HQGR0170

<u>Completed</u>

Gillerman, V., Layer, P., Jercinovic, M., Gordon, M., and Schmitz, 2008, Geology of the Lemhi Pass Thorium-Rare Earth District, Idaho and Montana: Evidence for a Buried Paleozoic Alkalic System? [abs.]: SME Annual Meeting 2009 Technical Program, p. 53.

Gillerman, V.S., Fanning, C.M., Link, P.K., Layer, P., and Burmester, R.F., 2008, Newly Discovered Intrusives at the Lemhi Pass Thorium-REE Iron Oxide District, Idaho: Cambrian Syenite and Mystery Ultramafics - Signatures of a Buried Alkaline Complex or Two Systems? [abs.]: Geological Society of America Abstracts with Programs, v. 40:1, p. 51.

Reed, R., and Gillerman, V., 2008, Thorium and Rare Earths in the Lemhi Pass Region, Idaho[abs.]: SME (Society for Mining, Metallurgy, and Exploration, Inc.) Annual Meeting Program, p. 90-91.

Additional Manuscripts in Preparation

Abstract Reprints:

Geology of the Lemhi Pass Thorium-Rare Earth District, Idaho and Montana: Evidence for a Buried Paleozoic Alkalic System?

V. Gillerman1, P. Layer2, M. Jercinovic3, M. Gordon4 and M. Schmitz4;
1Idaho Geological Survey, Boise, ID; 2Geology & Geophysics, Univ. of Alaska, Fairbanks, AK; 3Dept. of Geosciences, Univ. of Massachusetts, Amherst, MA and 4Dept. of Geosciences, Boise State Univ., Boise, ID

The Idaho Geological Survey has been studying the Lemhi Pass District, Idaho and Montana. Base metal and iron mineralization predate thorium-REE veins but are locally coincident. Thorium veins exhibit intense alkali and ferric iron metasomatism and are enriched in middle REE; identifiable hypogene minerals include monazite, allanite and thorite. Mapping discovered a Cambrian (530 Ma) syenite (cut by hematite veins) and a slightly older suite of altered mafic and lamprophyre dikes in proximity to many of the thorite deposits. Nd-rich monazite from the Lucky Horseshoe mine has complex U-Pb zoning, but preliminary results show a younger (recrystallized?) Paleozoic age signature of 300-350 Ma. Lead isotope studies are underway to look at the relationship of the sulfides, thorium veins and intrusives. Regional associations include Paleozoic igneous rocks (with local base metals) intruded along a rifted continental margin, Th-REE deposits at Diamond Creek, a Th-enriched red syenite, and Cretaceous(?) carbonatite replacements. Subsequent structural disruption, the Cretaceous thermal overprint, and lack of subsurface data obscure any buried intrusive-hydrothermal system.

in SME Annual Meeting 2009 Technical Program, p. 53.

NEWLY DISCOVERED INTRUSIVES AT THE LEMHI PASS THORIUM – REE IRON OXIDE DISTRICT, IDAHO: CAMBRIAN SYENITE AND MYSTERY ULTRAMAFICS – SIGNATURES OF A BURIED ALKALINE COMPLEX OR TWO SYSTEMS?

GILLERMAN, Virginia S., Idaho Geological Survey, 322 E. Front St., Ste. 201, Boise, ID 83702, vgillerm@uidaho.edu, FANNING, C. Mark, School of Earth Sciences, Australian National Univ., Canberra, ACT 0200, Australia, LINK, Paul K., Dept. of Geosciences, Idaho State University, Campus Box 8072, Pocatello, ID 83209, LAYER, Paul, Geology and Geophysics, Univ. of Alaska, Fairbanks, PO 755780, Fairbanks, AK 99775, and BURMESTER, Russell F., Geology Dept., Western Washington University, 514 High Street, Bellingham, WA 98225.

Thorium and rare earth element (REE) mineralization in the Lemhi Pass District, Idaho and Montana, is characterized by quartz-thorite-hematite veins and monazite-thorite-apatite-bearing shears and replacements with specularite, biotite and alkali feldspar. REE are unusually enriched in neodymium. Mineralization is hosted in Proterozoic metasediments of the Gunsight/Apple Creek formations (1420 Ma detrital zircons) but has not previously been linked to specific intrusives in the district. New Idaho Geological Survey mapping discovered a small syenite outcrop, locally cut by nonradioactive, specular hematite veins. The syenite (80% feldspar, 63% SiO_2) has thin albite rims on orthoclase; mafics are locally converted to specular hematite. SHRIMP geochronology gives a U-Pb crystallization age on zircon of 529.1 +/- 4.5 Ma, or lower Cambrian. Paleozoic ages are also reported in the literature for granitic plutons further south in the Beaverhead Range, and thorium enrichment has been noted at the Leadore pluton.

A suite of mafic dikes, previously interpreted as Tertiary, include altered pyroxene porphyry lamprophyres. A newly discovered, ultramafic sill (41-45% SiO_2 and 10% MgO with 3% $Na_2O + K_2O$) has possible carbonatitic affiliation (abundant dolomite "phenocrysts" or replacements of olivine phenocrysts; 3% total carbon). The sill contains Ba and Sr minerals found in the thorite veins, suggesting it predates or is contemporaneous with them. At

least one lamprophyre dike is cut by base metal mineralization; many dikes show propylitic alteration. Ages of the mafic rocks are unknown.

Previously reported electron microprobe ages on monazites suggest Th-REE mineralization had a Proterozoic (800-1100 Ma) and a mid-Paleozoic component at the Lucky Horseshoe prospect nearest the sill. A single Re-Os age (1050 Ma) on molybdenite at a copper mine supports Proterozoic mineralization. Non-plateau $^{40}Ar/^{39}Ar$ ages on hydrothermal biotite from the Lucky Horseshoe Th-REE prospect are interpreted to indicate an older (> 200 Ma) component of biotite growth followed by the regional Cretaceous resetting (~140 Ma saddle age). Field relations are consistent with ancient and overprinted mineralization. It could be associated with a buried Precambrian or Cambrian alkaline intrusive complex – or both.

Keywords: Idaho, syenite, carbonatite, thorium, rare earths
Published in 2008, Geological Society of America Abstracts with Programs, v. 40:1, p. 51.

Version 2:CSV		2006-2007 Lemhi Pass Waypoints: VSG					10/30/2007				Samples Taken		Date Sampled	Comments		10/30/2007					
Datum:	NAD27_CONUS			Lemhi Pass Report: APPENDIX A					Virginia Gillerman												
ZoneOffset	0																				
Type	Name	ZoneNum	Easting	Northing	Month#	Day#	Year	Altitude (M	Alt feet	WP											
W	1	12	304922.9	4982260.4	10	4	2006	1909.53	6264	W001			7/18/2006	CQ Middle Stope		with Murray					
W	2	12	304925.2	4982260.2	10	4	2006	1909.29	6264	W002	sample?	photos	7/18/2006	"							
W	3	12	303342.4	4984837.8	10	4	2006	1941.013	6368	W003			7/24/2006	Lucky Horseshoe - Notch Cut - ore, photos with USGS							
W	4	12	304442.1	4980235.3	10	4	2006	2410.613	7908	W004		photos	7/24/2006	Trench #54, Cont Divide							
W	5	12	303935.5	4980366.5	10	4	2006	2302.466	7554	W005	samples	Are these 06Ca??	7/24/2006	Cago Mine, big trench							
W	6	11	723458	4998132.1	10	4	2006	1717.749	5635	W006	Yac, Tour Breccia		7/26/2006	Deep Crk Rd,		Upper Banded Siltite w scapolite					
W	7	11	722175.8	4998743.6	10	4	2006	1679.055	5508	W007			7/26/2006	Biotitite, scapolite bed							
W	8	11	707928.5	5000937.2	10	4	2006	2374.804	7791	W008			7/26/2006	Blacktail Pit, NW corner high bench							
W	9	11	709561.6	5000003.7	10	4	2006	2323.855	7624	W009			7/26/2006	Merle Zone, trenches							
W	10	11	709550.6	5000044.8	10	4	2006	2323.134	7621	W010	samples (WP010), mafic dike		7/26/2006	Merle Zone, trenches							
W	11	11	708015.2	5000922.5	10	4	2006	2393.07	7851	W011			7/26/2006	Blackbird "Boneyard" South Highwall pit							
W	12	11	708081.4	5001030.3	10	4	2006	2405.326	7891	W012			7/26/2006	Blacktail Pit, SE highwall							
W	13	11	708086.7	5001031.2	10	4	2006	2405.086	7890	W013			7/26/2006	"	1st garnet in argillite						
W	14	11	708093	5001055.7	10	4	2006	2407.97	7900	W014			7/26/2006	Blacktail Pit, high wall							
W	15	11	708075.7	5001067.7	10	4	2006	2399.558	7872	W015	probably sampled		7/26/2006	SE Corner, Blacktail pit high wall gt-bi-chld schist							
W	16	11	708641.2	4999863.5	10	4	2006	2175.813	7138	W016	Samples		7/27/2006	Blackbird, 30 ft. west of 7100 portal,							
W	17	11	708646.5	4999867.3	10	4	2006	2176.534	7140	W017	4 Samples		7/27/2006	Blackbird, 7100 portal							
W	18	11	709374.1	4999382.9	10	4	2006	2172.929	7129	W018	Samples W018a, b		7/27/2006	Blackbird, Hawkeye portal 7080' elev.							
W	19	11	710494.9	4996522	10	4	2006	2036.423	6681	W019	Sample W019		7/27/2006	Conicu Tourmaline Breccia							
W	20	12	305469.3	4978841.7	10	4	2006	2362.308	7750	W020	Sample LCHVH-102a	or WP020	7/28/2006	Lemhi Pass - Last Chance Mine trench			Th ore Cu, calcite				
W	21	12	304875.2	4982261	10	4	2006	1883.815	6180	W021	Sample CQ greenstone dike		7/28/2006	Copper Queen lower adit							
W	22	11	576851.2	5087482.8	10	4	2006	543.7473	1783	W022											
W	23	11	576523.6	5087284.8	10	4	2006	702.3635	2304	W023											
W	24	11	576634	5087188.6	10	4	2006	697.5571	2288	W024											
W	25	11	576674.4	5087179.6	10	4	2006	663.4307	2176	W025											
W	26	11	576457	5087092	10	4	2006	672.3228	2205	W026											
W	27	11	576550.5	5087153	10	4	2006	653.8174	2145	W027											
W	28	11	576624.7	5087088.8	10	4	2006	640.5994	2101	W028											
W	29	11	576552.5	5087010.4	10	4	2006	606.9536	1991	W029											
W	30	11	576595.9	5087028.3	10	4	2006	591.5725	1940	W030											
W	31	11	576572.1	5087039.8	10	4	2006	596.1389	1955	W031											
W	32	11	576594.6	5087012.9	10	4	2006	566.5786	1858	W032											
W	33	11	576562.5	5087272.7	10	4	2006	671.3613	2202	W033											
W	34	11	576968	5087240.3	10	4	2006	554.0813	1817	W034											
W	35	12	305050.4	4982337.1	10	4	2006	1980.667	6498	W035	CQ06-20flt, 21A, B	8/23/2006		Copper Queen Greenstone Dike			CQ06-20 float				
W	36	12	304594.7	4981538.8	10	4	2006	2020.802	6629	W036	CQ06-23		Gunsight Fm.	Copper Qn FT Stop 6							
W	37	12	304146.8	4980593.4	10	4	2006	2303.908	7558	W037				Bend in road to Cago							
W	38	12	303443.1	4984530	10	4	2006	1846.564	6058	W038	LH06-21, 22 (dump)			Lucky Horseshoe Lower Adit - Quartzite			LH06-20, oriented at Flume Crk road crossing, alt. qtzt				
W	39	12	303476	4984548.9	10	4	2006	1829.741	6003	W039	LH06-23	A and B, C-E?		Mafic Sill above LH lower adit, N70E, 20N basal contact					Photos 2275,76		
W	40	12	303357.1	4984815.6	10	4	2006	1932.842	6341	W040	LH06-24 through 34 see detailed map			Lucky Horseshoe Mine open cut, close to AML site ID point; Zero pt.					ORE, Alteration		
W	41	12	303335.9	4984868.6	10	4	2006	1964.325	6444	W041	LH06-35		Qtzt, white vns	Lucky Horseshoe, road above cut - weak fsp veins							
W	42	12	303663.6	4984601.8	10	4	2006	1875.403	6152	W042				In Trust, roadcut							
W	43	12	303748.4	4984606	10	4	2006	1915.058	6282	W043	IT06-03a, b; IT06-04, 05			In Trust mine bench		Black Breccia					
W	44	12	303314.9	4984839.8	10	4	2006	1935.726	6350	W044		photos	SC fabric	Lucky Horseshoe, west end							
W	45	12	304853.8	4982282.8	10	4	2006	1883.094	6178	W045	CQ06-52	or CQ06-30	hornfels, sulf	Copper Queen Road - green alt. qtzt with cp, py				get PS			
W	46	12	304743.2	4982582.5	10	4	2006	1892.226	6208	W046	CQ06-53 or CQ06-31		arkose-sericite	CQ road above old tailings dam							
W	47	12	304741.9	4982638.6	10	4	2006	1885.257	6185	W047				Bad WP, Delete							
W	48	12	304744.1	4982642.9	10	4	2006	1870.356	6136	W048				CQ area, arkosic quartzite							
W	49	12	304882.6	4982415.7	10	4	2006	1923.229	6309	W049	CQ06-32 or?			CQ area, quartzite w. mica							
W	50	12	305189.3	4981048.2	10	4	2006	2051.564	6730	W050	WL06-01a, b	brwn vn, wr calc silica	vein, wr	Wonder Lode, 1st adit cut			WL06-02a,b,c next bench up				
W	51	12	305226.5	4981070.4	10	4	2006	2076.558	6812	W051	WL06-3	North Dike - wk alt	Mafic Dike	Wonder Lode, same bench as #2			WL06-04a,b next bench up, Fe; WL06-05 Dike on S switchback, weakly mt				
W	52	12	307312.2	4982973.2	10	4	2006	2251.997	7388	W052	LP06-1 to 5		bleached qtzt	Lemhi Pass, next to bathroom			L-tectonite float				
W	53	12	306133.6	4982547.5	10	4	2006	2287.565	7505	W053	BL06-06a,b		Sandst., cong.	Bluebird Claims							
W	54	12	306012	4982572.9	10	4	2006	2283.72	7492	W054	BL06-01a,b,c,d; BL06-02 Cu veins			Bluebird Shaft dump		whiteqzCu; brownsilica					
W	54x	12	305961	4982482		Jeremy's ?				w054x	BL06-03	BL06-04,5	Pyrox.Porph. +	Bluebird area, intrusives- 05 is hblplag diorite?, 03 is Px Porphyry							
W	55	12	303963.9	4980354.9	10	4	2006	2303.667	7557	W055	CA06-10,11/ CA06-12AtoE Xsect		Vein, WR	Cago Mine Adit/ Trench profile (see map)			also CA06-14,15,16; Russ#207				
W	56	12	308068.2	4979944.7	10	4	2006	2133.996	7001	W056	WP056 sample		Musc. Qtzt.	Frying Pan Creek road							
W	57	12	305306.6	4978952.1	10	4	2006	2418.063	7933	W057	LC06-01a,b,c			East Last Chance Mine prospect							
W	58	12	305436.2	4978887.8	10	4	2006	2376.246	7796	W058	LC06-2a,b,c		vein, wr	East Last Chance Mine trench							
W	59	12	305478.6	4978834.5	10	4	2006	2359.664	7741	W059	LC06-03 a-k		vein, wr profile	E. Last Chance - open cut with fw,hw of vein							
W	60	12	305103.1	4979172	10	4	2006	2323.615	7623	W060	LC06-06,7,8,9,10,11,12,13		Veins	West Last Chance portal - dump samples			12 is ore composite				
W	61	12	307562.7	4983487.2	10	4	2006	2225.08	7300	W061				Lemhi Pass Road, Montana side			qz vein - epid, brown ? In siltite				
W	62	12	305159.3	4983406.5	10	4	2006	1893.188	6211	W062	Sample		Silic. Bxa	Agency Creek Road							
W	63	12	304882.1	4982274.6	10	4	2006	1892.707	6209	W063	CQ06-24, 25, 26/27		Dike, greenstone	Copper Queen Adit 1		bulk sample	#27 is mica, 26 is wallrock				
											CQ06-28, 29a,b,c,d		Hornfels by vein	Copper Queen Adit 2,							
											CQ06-30a,a2,a3 ; -031,32,32a,33		Pyrox. Porph. +	Copper Queen Shaft Dump - variety			sulfide veins cuts porph. And hornfels				PS
											CQ06-34a-c, -38		Cu veins, shears	Copper Queen Adit 3 portal			hm veinlets in 38		34 chlor., gouge		
											CQ06-35a-c, 36, 37a,b		Cu veins, alterat	Copper Queen Stope 2			Veins cut by mylonite				
											CQ06-39a-c		chloritic alt.+	Road above CQ stope 2			intense chlorite				
W	64	12	274939.8	4994702.6	10	4	2006	1761.729	5779	W064	PS06-4	PS06-6 talus to adit	Fault Bxa - late	Pope-Shenon Mine - road by switchback							
W	65	12	275187.9	4994958.7	10	4	2006	1797.778	5898	W065	PS06-1,2,3		veins, argill.	Pope-Shenon Mine - reclaimed adit (#2??)			dump samples				
W	66	12	275276.9	4994941.3	10	4	2006	1836.23	6024	W066	PS06-5a,b		wr, hw, grn. Alt.	Pope-Shenon Mine - uppermost adit			gated				
									Ask Reed	RB211	JA06-01a,b,c,d,e,f,g; JA06-02a,b,c		Syenite	near ridge, west of Divide							
										RB212			Syenite								
W	67	11	726891.4	4984607.6	10	4	2006	2401.961	7880	W067	CAS06-01		QzSerPyCobalt	CAS Property, top of drill road							
W	68	11	726923.3	4984684	10	4	2006	2417.102	7930	W068				CAS Property, DH 2 and 3							
W	69	11	727006.2	4984593	10	4	2006	2372.401	7783	W069	CAS06-02		Siltite	CAS Property, switchback 300' S of Hole 4							
W	70	11	727528.1	4982583.4	10	4	2006	2021.042	6630	W070				No Name Adit							
W	71	11	730842.4	4978007.3	10	4	2006	1622.819	5324	W071			ironstone talus	Iron Creek road		green siltite					
W	72	11	734201.3	4977270	10	4	2006	1506.5	4942	W072	sample		Ore pad for	No Name Adit							
W	73	12	304616.1	4981581.1	10	4	2006	2019.36	6625	W073	DZ-LP1	(wk. alt.)	Gunsight Fm.	Copper Qn FT Stop 6		for detrital zircons					
W	74	12	304589.8	4981545.3	10	4	2006	2016.476	6615	W074	DZ-LP2	fresher	Gunsight Fm.	Copper Qn FT Stop 6		for detrital zircons					
W	75	12	303298	4984740.8	10	4	2006	1920.585	delete/630	W075				Lucky Horseshoe section							
W	76	12	303300.2	4984738.3	10	4	2006	1923.469	6310	W076		survey pt. between powerline pylons		Lucky Horseshoe Survey Marker: Center Sec. 9, T19N, R25E							
W	77	12	303405	4984801.2	10	4	2006	1923.229	6309	W077	DZ-LP3		?	Lucky Horseshoe Adit 2 portal							
W	78	12	303419.8	4984770.5	10	4	2006	1905.925	6253	W078	WP078		ore vein	Lucky Horseshoe, lower bench							
W	79	12	303411.4	4984773.8	10	4	2006	1918.422	6294	W079	WP079a, b		breccia/mylonite	Lucky Horseshoe, lower bench			oriented				
W	80	12	303403.7	4984700.3	10	4	2006	1902.08	6240	W080		boulder of pyroxene porphyry		Lucky Horseshoe		FIND IT again					
W	81	12	303453.5	4984716.5	10	4	2006	1882.613	6176	W081				Lucky Horseshoe, lower road							
W	82	12	303421.5	4984631.8	10	4	2006	1880.45	6169	W082	sample		Qzhmfsp veins	Lucky Horseshoe, lowermost road							
W	83	12	304671.6	4983524.1	10	4	2006	1989.799	6528	W083	BU06-1		variety, ore	Buffalo Mine							
W	84	11	724042.4	5002408.8	10	4	2006	2038.826	6689	W084	photos	tourmaline pod in	Ymg, Augen Gn	Road to Beartrack mine							
W	85	11	719253.1	5001925.1	10	4	2006	1486.313	4876	W085	Sample - geochron		"Ord. Gabbro"	Napias Creek Road							
W	86	11	719709.6	5000277.9	10	4	2006	1501.694	4926	W086	hand sample		"Gabbro"	Deep Creek Rd.							
W	87	12	306102.1	4983917.7	10	4	2006	2048.199	6719	W087	DZ-LP4	Apple Crk?	Siltite-Argill.	Lemhi Pass/Horseshoe Bend Crk. Outcrop			photos				
W	88	12	306554	4981060	10	4	2006	2274.588	7462	W088	sample WP088, JA06-01 samples		Syenite	Large trench, N end, Sec. 23, W of Cont. Divi			Hm veins				
W	89	12	306401.8	4981022	10	4	2006	2267.618	7439	W089			foliated quartzite	Outcrop to w							
W	90	12	306426.2	4980777.9	10	4	2006	2247.19	7372	W090			sanded qtzt.	prospect							
W	91	12	306380.3	4981108.3	10	4	2006	2261.37	7419	W091	small sample		syenite + qtzt.	Prospect Pit (Russ's)		fsp + Fe oxides					
W	92	12	306427.1	4981077.4	10	4	2006	2268.82	7443	W092	sample WP092		syenite, wk, vein	Large prospect on N edge of clearing							
W	93	12	306543.4	4981063.8	10	4	2006	2305.59	7564	W093	sample WP093		syenite, tr. Rad.	Trench, S end of WP 088 trench							
W	94	12	306475.4	4980847.8	10	4	2006	2271.223	7451	W094			quartzite float	Prospect Pit - tiny							
W	95	12	306110.9	4982520	10	4	2006	2291.891	7519	W095			sericitic qtzt.	Bluebell - south of; SW corner of Badger No. 1							
W	96	12	306132.6	4982424.3	10	4	2006	2271.223	7451	W096			sanded qtzt.	Prospect		rare qz-hm vn					
W	97	12	306151.7	4982370.7	10	4	2006	2264.254	7428	W097	WP097		Hornfels - epid.	Large dark outcrop		1 piece syenite float					
W	98	12	306091.4	4982419.4	10	4	2006	2261.13	7418	W098	WP098	Lamprophyre/Tuff?	Biot. Volcanic/in	Prospect, pit, tiny, in gully							
W	99	12	306078	4982326.9	10	4	2006	2222.677	7292	W099	WP099	fresher	Syenite, wk. mt	Prospect Trench/road		same as Jeremy's BL06-05?					
W	100	12	305766.1	4982258.1	10	4	2006	2162.595	7095	W100	WP100	Baked and Qz veinec	Qtzt., qz veins	Brown Outcrop, top		"dry??". Bull Qz veins	pink color				
W	101	12	305733.4	4982380.3	10	4	2006	2226.522	7304	W101	WP101		wk. hornfels, sa	Outcrop, tiny on ridge							
W	102	12	305955.2	4982486.2	10	4	2006	2271.464	7452	W102	sample Por. + wr		Pyrox. Porph.	Trench near S. top of ridge; BL06-03							
W	103	12	315264.8	4953563.2	10	4	2006	1965.767	6449	W103	WP103		Feldspar Porph.	Leadore, mouth of Thompson Gulch							
W	CAS06 2	11	726909.7	4984680.8	10	4	2006	2406.287		CAS06 2											
W	NONAMEA	11	727538.6	4982597.8	10	4	2006	1972.496		NONAMEADIT											
W	104	12	307143.9	4978817.8	8		2007		7144	W104	07WP104	bulk	Diorite - biot rich, bulk sample at pit			S. Frying Pan Creek, MT					
W	105	12	306450.6	4978944	8		2007		7240	W105			Quartzite - gray, few green veinlets								
W	106	12	306696.3	4978582.5	8		2007		7456	W106	07WP106	bulk	SyenoDiorite - large dike, sparse epid, fresh, bulk sample, MT								
W	107	12	307209.3	4978138.5	8		2007		7517	W107	07WP107		Altered Quartzite - black veins, ser.								
W	108	12	307214.8	4978304.9	8		2007		7498	W108			Diabase, mod. Epid.								
W	109	12	305345.2	4981769.4	8		2007		6857	W109	07WP109	several	Copper Prospect #44 Staatz, Ox. Cu veins, Epid-Qz-Fsp?, flat fault,								
W	110	12	305377.5	4981741.2	8		2007		6847	W110			Hematite veins, tan halo								
W	111	12	305855.2	4981808.1	8		2007		6727	W111			Photo fold nose float								
W	112	12	305813.1	4982009.8	8		2007		6671	W112	07WP112		Sheared qtzt, red Fe stain, epid pods, hornfels								
W	113	12	305694.4	4981977.5	8		2007		6567	W113	07WP113	several	Brown Outcrop - hornfels with epid-qz veins, actin., white alteration envelope								
W	114	12	304902.8	4982135.1	8		2007		6252	W114	07CQ-01		South Copper Queen adit - hornfels qtzt with actinolite veins and qz veins								
										Copper Qn	07CQ-02, 07CQ03-09	outcrop; Shaft Dump	Hornfels outcrop behind cabin, cut by qz-epid veins; Dump Samples - por/hnfels, vns								
W	115	12	301066.7	4967738	8		2007		6931	W115			Lemhi Quad - bleached Fe siltstone, on Reese Crk Fault								
W	116	12	300690.3	4967107.1	8		2007		6946	W116	07WP116	several	Iron Mine - Staatz 195; Specular Hematite Vein, Qz								
W	117	12	301321	4969366.9	8		2007		7572	W117	07WP117	several	Claystone/Qtzt - gentle folds, sed. veins								
W	118	12	301739.1	4970182	8		2007		7837	W118	07WP118	?	ThO2 roads								
W	119	12	302326.7	4970507.1	8		2007		7837	W119	07WP119	several	ThO2 Open Pit - recl. Float, high grade ore - pink Kf, qz,								
W	120	12	303476.5	4984549.3	8		2007		6001	W120	07WP120	big, several	Lower Lucky Horseshoe Adit Sill - mafic porphyry, cut by tan vein - feldspar, carb. ??								
										W040	07LH-tan	LH Pit, several	Tan Feldspar zones in argillite below ore zone. "silicified" or feldspathized								
W	121	12	298065.3	4986194.2	8		2007		5469	W121	07WP121		Upper Pattee Creek Workings - sheared phyllite								
W	122	12	265970.1	5032052.6	8		2007		3636	W122	07WP122	Highway Roadcut	White (fsp?) veins cut North Fork Siltite								
W	123	11	718413	5032307.1	8		2007		3990	W123	Shoup area	Hike to NF propspect	Augen Gneiss - North Fork								
W	124	11	718417.4	5032304.3	8		2007		4020	W124		Hike to NF propspects									
W	125	11	718105.2	5032506.5	8		2007		4542	W125	photos		Augen Gneiss cut by pegmatite								
W	126	11	718105.9	5032106	8		2007		4057	W126	07WP126	several at adit	Roberts Prospect - calcite-ilmenite veins, mz?								
W	127	11	718159.6	5032032.1	8		2007		3930	W127	07WP127A, B	2	Roberts South - small outcrop, orangeB, greenA, MZ-rich								
W	128	11	718267.7	5031760.4	8		2007		3533	W128			Parking Area - highway clean up pad								
W	129	12	325189.4	4947433.5	8		2007		6665	W129	07WP129	Leadore Pluton - bulk	Hawley Creek Canyon - oc, pink granite, wk.chlorite								
W	130	12	340133.6	4917802.2	8		2007		7586	W130	07WP130	Willow Creek	Nicholia Ranch - Willow Creek - stream cobbles - pink syenite, granite								
W	131	12	340136.3	4917807.5	8		2007		7590	W131		Willow Creek									

THIN SECTION NOTES			APPENDIX B	Lemhi Pass Project, Idaho			
V.S. Gillerman, May 2007			*Dec 30, 2008 version*				
Property	**Sample #**	**PS, TS Lab#**	**Field Name**	**Mineralogy**	**Alteration / Mineralization**	**Comments**	
Wonder Lode							
	WL06-01A						
	WL06-01B						
	WL06-02A						
	WL06-02B						
	WL06-02C						
ts-f	WL06-03A	syx-006	Dike - Px?Amph Por.	Brown Amph megacryst, phenos	More altered, green; faint Kf stain		
ts	WL06-05	syx-007	Dike - fg				
ts-c	07Wr	VOV-004	Wonder Th vein	lue-stained Mg-calcite?, opaques; late veins pink-sta	Coarse mosaic carb. Cut by opaques that replace twin lamella	pink-stained calcite cuts opaques in crackle bxa.	
Copper Queen							
ps	CQ06-35B	TSX-009	Quartz Vein-deformed	Qz-Musc10%-(fsp)-bornite1%	Sutured Qz; Microcline, Local Kf; Strained, no hm	GET STAINED -Kf	
ps	CQ06-35C	TSX-010	Quartz Vein - cataclastite	Qz-Bornite5% - Fsp?	Qz suture/gran./Bornite (liquid?), Secondary Ox. Cu	Mylonitized/sheared QzBn vein; late Cucarb.	
ps, ts-f	CQ06-37A	TSX-011, TSY-006	Meta Siltstone- stylolites	Qz-muscovite-Kf-Carb./Vn-strainedQz-Carb	Qz-Calcite Vein has K-feldspar halo?; ? Hm,Th??	Stope 2 talus	
ps	CQ06-37B	TSX-012	Hornfels	Epidote-Qz-Kf-Mica-(Sphene)	Qz vein, Epidote replacing Kf qz musc wr??	Stope 2 talus	
ps	CQ-06A	swx-001	Greenstone Dike	plag-chl-grn amph?-Epid-mica-Calcite	Propylitic - strong, opaq. 10%	well altered basaltic dike	
ps	CQ-06C	swx-002	Musc. Quartzite - foliated	Qz-Musc. / Fsp	Foliated, Microcline vein cut by qz-calcite gash vns	deformed	
ts-f	CQ-06A	swx-014	Greenstone		Stained - no Kf in rock. Lots opaq., epid.	uncovered section	
ts-f	CQ-06C	swx-015	Micaceous Quartzite	Cut by vein of Qz-microcline, pale pink	intense Kf stain; late carbonate gash vns; albite ??	uncovered section	Yes:
ts	CQ06-21	syx-010	Greenstone Dike		Propylitic - strong; vesicles to calcite-epid	Dike above CQ workings	
ts	CQ06-24A	syx-011	Greenstone-carb. Alt.	fsp-chl-epid-?-mica/ qz-calcite	g to calcite+qz; musc-chlor-py; Propylitic - strong/Late carb. (	WOW-relook	
ps	CQ06-25A1	syx-012	Greenstone - dump	calcite-epid-py	Propylitic - strong, diss. Sulfides	RELOOK	
ts	CQ06-25A2	syx-013			epidote	Relook	
ps	CQ06-30A1	syx-014	Pyroxene Porphyry - CQ Shaf	Px-Brn. Amph-Oliv?/Trem-epid-calcite	Propylitic (Trem, chl, ep) - weak, pyrite abund.	relook	Yes:
ts-f	CQ06-30A2	syx-015	Pyroxene Porphyry	as above	Cut by Qz-cp-gn-po vein	relook	
	CQ06-30B	separate	Pyroxene Porphyry	lots of pyrite crystals (noncubic) in T1 fraction			
ts-f ??	CQ06-24A	UCS-009				from syx-011	
ts-f	CQ06-35B	UCS-010				from tsx-009	
ts	07ABS	UOS-8	Carbonate Vein-AgencyCrk	Carbonate-Fsp-opaq	e Opaques; microcline twins, late clay/mica; ? Acc. Apat, allar	Agency Creek	
ps	CQ06-28	VGG-6	Quartz-Bornite Vein	Vn: Qz-bn-FeCuOx; Env: Fsp in Musc Qtzt	Need Stain/SEM to confirm narrow K alt	detrital? Zircons; high strain	
ts-f	CQ06-28wr	VGG-7	Quartzite - foliated	Qz-Musc-Kf-(Opaq)-Zirc	Wallrock, with more Kf near vein	hint of potassic alt by vein, scan ts	
ps	CQ06-38	VGG-8	Quartzite - foliated	Qz-epid?_Musc-Hm-Fsp	Sent to UI for xray; musc more common by vein	Complex. Qz-epid may be early, cut by spec vn.	
Lucky Horseshoe							
ts-f	LH06-21	VOV-001	Metasiltstone-altered (low ad	Recry. Detrital Qz, Fsp, Musc. And shreddy; carbonat	Weak Potassic; strong foliation/stylolitic; cut by calcite vn.	Accessory apatite, green tour.; Kf rims on musc.	
ts-f	LH06-22	VOV-002	Laminated Siltstone (low adit	Detrital Qz, Green Biot?, musc., opaques, untwin Fsp	Accessory apat., zirc., sphene, or allanite,	Lots of heavy minerals	
ts-f	LH06-23A	syx-008	Dike- Oliv. Porph.; UM?	Oliv. Xxxxx, Mt in field; Carbonate	Faint Kf stain	Get Polish Sec/Geochem	
ts-f	LH06-23B	syx-009	Sill: Oliv.-Px Porph.	Oliv-px-Fsp-Bi-Dolomite?-Barite-talc?	Apatite?, Trem-Talc alteration; Faint Kf stain	fresher, need Xray, SEM	
ts-c	LH06-23D	VOV-003	Sill: with carbonate vein	Stained blue phenos (magnesite); veins also Mg,	or serpentine or clay alt. near carbonate veins. Minor red stain on late calcite.		
ps, ts-f	LH06-24A	TTT-010, TSY-010	Breccia:	Fsp (2 types), GreenMica, big MZ	Wk Kf; MZ-AP vein cut by shear Qz-Fl	WOW: Take to Umass; clasts=syenite?	Yes:
ps	LH06-24A2	UOS-14	Ore Breccia	Fsp Clasts-Mica(grn,c)-Opaq-MZ-Apat-Fl	Cataclastic; Fsp in Clasts, Mz in clasts, shears,	Mylonitic WOW section take photos	WSU
ps	LH06-24B	TTT-011	Black Breccia	SpecHm-Fsp-Qz?-Ap-MZ	minor Mz vein	Boudins, late mylonite	
ps, ts-f	LH06-25	TTT-012, TSY-011	Ore Breccia	Fsp-Mica-Ap-Mz-Hm	Mod. Coarse Kf in clasts, fsp replacements	Need imaging; Umass	
ps	LH06-25b	UOS-15	Ore Breccia	Fsp Clasts-Mica(grn, brwn)-MZ-Opaq	more retrograded, large MZ	Syenite Clasts??	
ps	LH06-26	TTT-013	Cataclasite	Qz?-Fsp-Mica	acc. Zircon, sphene?		
ps, ts-f	LH06-27	TTT-014, TSY-012	Ore- Breccia	Kf/Ab-bi-Hm-mica	Strong coarse Kf, tiny MZ,	Fsp replacements of Kf clasts	
ts-orient	LH06-28o	TSY-013				oriented	
ps	LH06-29	TTT-015	Layered Black Breccia	Fsp agg. Clasts-brn biot-apat-Opaq-Allanite	Allanite>>Mz; rotated fsp clasts; qz clsts.	Rare Qz deformed	
ps, ts-f	LH06-30	TTT-016, TSY-014	Cataclasite Ore	Fsp-Apat clasts in brwn biot-MZ-Hm	Mod. Kf; PHOTOS; 45% fsp, coarse allanite lots MZ		
ps, ts-f	LH06-31	TTT-017, TSY-015	Cataclasite Ore	Brwn Biot-Apat-Fsp-MZ-Hm-Grn Bi	Wk Kf; Cut by late brittle Qz vein 2-4mm normal to fol.	some green biotite (retro?)	
ps, ts-f	LH06-32	TTT-018, TSY-016	Siltite - cut by tan veins	Feldspar-Biot-Opaq rhomb	Veins are areas w/ no mica; local K, Na?Weak Kf stain	veins merge to WR, Wk Kf	geoc
ps, ts-f	LH06-33	TTT-019, TSY-017	Tan Veins cut cataclasite	Kf-Ab-Musc.-Biot	Mod. Kf stain, Potassic, sodic; albite twins	Fold Nose? In opaques, sheared	geoc
ps	LH-06A1	swx-006	spec. schist/breccia	Biot-MZ-Kf-allanite?; Xeno??	Abundant Monazite, K, Opaq.	WOW: Take to Umass; find rock	
ps	LH06-A2	swx-007	spec. schist/breccia	Kfeldspar-Bi-MZ-Apat-Allanite-	Orth98 +Albite, MZ veins cut fabric/along	Probed 8/07 Biot, Fsp, Apat	Yes:
ts-f	LH06-A1	swx-017	spec. schist	Kfeldspar abundant	Potassic, plag, microcline in clasts		
ps	LH06-23Bp	UCS-006	UM Sill- Carbonate Alt?Ol? - F	Oliv??-Px Phenos-Biot/Amph? Fsp-carb matrix	Magnesite repl Ol?; 25% Carbonate; barite?	Bizarre: Primary/Sec.? Carb.,	Yes:
ps	04LH-E	TTT-009	Spec. Schist Cataclasite	Fsp clasts-brwn biot-MZ-grn mica	Very fresh; lots of coarse MZ	Photos	give
ps	04LH-C1	TTT-008	Spec. Schist Cataclasite	Hm-Biot-Fsp-MZ shear	Possible clast of MZ crystals in biot shear	Photos	Phot
ps	07LHtan	UOS-13	Feldspar lens	Qz-Fsp mosaic, Hm crackle vns	20% Hm, at least 20% Fsp. Albite twins, recrystallized		
	07WP120a,b	UJK-001,002	Mafic/UM Sill	Px-Amph-Fsp-Carbonate(Ol?), carb veins	Oliv to Magnesite, late Dolomite	Fe-Magnesite after Oliv?, Amph	Yes:
ts	07rLHB	UOS-007	Ultramafic Boulder	Px-Amph-Opaq.-plag-epid-chl-Olpseudos	Coarse Mafic Porph./gabbro; well-altered.	FLOAT	
ts-f	06RL487	UOS-16	LP Fault Z. in Qtzt.- shear	Qz-musc.-biot?-Mz or zirc??-rutile?	Detrital heavies or intro by shear Zone; no Kf stain	Qz vein, minor mica shears.	
Cago							
ps	CA06-10A	TSX-007	Quartz Vein/Breccia	Qz-Opaques(HmTh)-Apatite	Waxy look in HS; Multgen Qz; rhombs	Get Stained	

ps	CA06-10B	TSX-008	Quartz Vein	Qz(2 generations)-Opaques	Hm-Thorite(?) rhombs; Ore on Dump	Get Stained; Map; Undul. Extinct.	
ps	CA06-12A1	TSX-002	Silic. Siltstone: Cago FW	Qz-Opaques-Kf-Carb.	25% opaques, patchy Kf-apatite?	Vein Footwall, qz veins; multigen qz strained	
ps	CA06-12A2	TSX-003	Silic. Siltstone - vein	Qz-Kf-Hm(opaq)-Carb.	Qz-hm Veins, Kf alteration	probe/stains; photos	
ps, ts-f	CA06-12C1	TSX-004, TSY-001	Muddy Siltstone - CagoHW	Qz-Musc-Opaques-Kf	Qz-Kf veins; late shears; Hm	Mod. Kf stain	
ps, ts-f	CA06-12D	TSX-005, TSY-002	Siltstone- blocky, white alt. H	Qz-Kf-Carb.-Opaques- Apat??	White Alt. HW: Silic.?/Kf alt. Qz (mosaic), fsp detrital plag	Mod. Kf stain	imag
ps, ts-f	CA06-12E	TSX-006, TSY-003	Muddy Siltstone- outer HW	Qz-Mica-Opaques	very little Kf; detrital text.	acc. Tourmaline?	
ps	CA- 06A	swx-003	Quartz Vein	Qz-Goethite(Mt?)-Hm-Fl	Latw Qz+fl after Mt	Latticework, 2 generations Qz	Need
ps	CA-06B1	swx-004	Quartzite - Hm vns	OrthoclaseKf-Albite-opaques	Orthoclase vein +Ab wr?, rutile, Hm veins	2 generations feldspar	Yes:
ts-f	CA-06B2	swx-005	Quartzite/Siltite - clast suppo	Qz-Kf-Mica-Hm	potassic?? Yellow Kf stain-pervasive; Hm vns	dehydration reactions: Kf env on Hm vns	
ts-f	CA-06B1	swx-016	Quartzite - Hm vns	Kf-qz-hm	potassic envelope .5-1" on vn, outer Kf vnlts	strong yellow. Uncovered section	
ts-f	CA06-12A2	UCS-007	Silic. Siltstone - vein	abundant Kf from stain		from tsx-003	
ts-f	CA06-10A	UCS-008	Quartz Vein/Breccia	moderate Kf stain		from tsx-007	
Last Chance							
ps	LC06-06	TTT-001	Quartz Vein	Quartz-2 gen, allanite?	Recry. Mosaic, euhedral overgrowths	West Portal Dump, try CL	
ps	LC06-09	TTT-002	Quartz Vein	Qz-Kf? Or barite??	a few opaques	late yellow barite veins on dump	
ps	LC06-10	TTT-003					
ts-f	LC06-03A	TSY-007	Footwall Siltstone	Qz(detrital)-mica-opaq	Metased textures; fg musc - c to pale tan	tr. Kf stain	Tren
ts-f	LC06-03B	TSY-008	Recryst. Siltstone/vns	Qz-mica-Kf-opaq	Strong recrystallization, tr. Potassic; Qz vns-Kf center	wk. Kf stain, geochem	Tren
ps, ts-f	LC06-03D	TTT-004, TSY-009	Qz. Veins/Siltstone	Qz-Kf-mica-opaques	Strong potassic Wall rock alt., mica to Kf	Strong Kf stain, Qz Vein stockwork	Tren
ps	LC06-03E1	TTT-005	Pink Quartz vein-breccia	Qz-CuOx?-fl?-ap? (ba?)	brecciated, strained, late vugs, check HS for Cu	8800 ppm Ba; 1600 ppm Th & Cu	Tren
ps	LC06-03F	TTT-006	Quartz Vein - "HOT"	Qz-opaques	Sheared	check for Kf	Tren
ps	LC06-03G	TTT-007	Limonitic Quartz Vein	Qz-multigenerations, opaq.	Shear Zone with opaques	"Dirty" quartz; no mz seen	Tren
Other Copper Veins							
ps	07WP109a	UOS-17	Pros. #44 - Cu Vein, mylonite	Qz-fsp-microcline-opaq-chl/clay	Strong mylonitization. Shearing, bxa,	check to see if spec. hm	
ps	07WP109b	UOS-18	Shear Zone: Silic. Mylonite	Qzt. Cut by qz-opaq vein, grundge	strong shearing, silicification. Some late calcite	late brittle fx normal to vein,	
ts-f	07WP109w	UOS-19	Prospect #44 - Hornfels	Qtzt with epidote(?), tr. Mica, apat, sphene:	intensely recrystallized, no Kf (stained)	lots of apatite.	
	1189		South of district	chalcopyrite	pure cp vein no thin section.		
ts-f	PS06-05a	VOV-009	Pope Shennon wall rock	Qz-musc.-grn?amph?mica?	No fabric, micaceous qtzt, 5% green hornfels	cut by qz vn highly sutured bound.	
ps	P08PS-1b	VOV-010	Pope Shennon Cu vein	Meta Qtzt and Cu vein	own Hbl?? In wall rock absent near vein; chlorite/act? And mus	Chalcopyrite-qz Vein recrystallized; late calcite	
Other Thorium Veins							
ps	07WP119w	UOS-20	ThO2 Pit - Qz vein, wall rock	Qz-Opaq-Fsp vein in micaceous quartzite	Musc. Destroyed in vein envelope, Sec. fsp growing	Euhedral Qz ghosts; rutile; NOT Deformed.	Geoc
ps	07WP119v	UOS-21	ThO2 Vein				
ts	CACTr2	VGG-9	CagoContact - dupl.	Qz- with minor Fsp, Opaq, Apat, MZ	Opaq rhombs, crackle bxa and high strain	could stain slab, photo textures	
ts-f	BKBRZa	VGG-10	Black Bear	Qz-Kf-Ab-Apat-Opaq	Altered Wallrock; intense K (Na albite twins) alt. P 6%	musc to KF to hm interstitial; fine, messy	
ps	WSZ-DC4	VGG-11	Diam. Crk Vein	Qz-Fsp-Biot-Opaq-Apat-(MZ)-Fl-rut?	Na-Fsp(>5%tot) late Fluorite, mg mz	recry Qz vn/replacing qtzt?, brown biot	
ps	08DC-2b	VOV-005	White Alteration Zone (float)	ıssive Feldspar (alkali); opaq., rare musc. In gash vn	ns/pericline or recryst. Alterationl cut by vein of coarse hematite or rutile		
ts	08DC-4a	VOV-006	Mica-rich Radioactive "vein"	RedBrwn opaq., Qz, Muscovite	coarse mica, acc. MZ on diffuse quartz vn., minor calcite, apat	No hint of igneous texture. Very Rad.	
BlackBird							
ps	Yac-06A	swx-008	Siltite with Scapolite	Qz-Scapolite-Biot(20%, brwn)	Fresh rock	Minimal Foliation	Yes:
ps	Yac-06B	swx-009	Biotite Siltite	Qz-Biot-Musc-(Zr)	local silicification	Weak Foliation	
ps	He-06A1	swx-010	Ore Schist, layered	Qz-sulf-chl-biot-cc	Cobaltite-Cp-motheatern ? Marcasite?	Hawkeye Lode; good fabric	
ps	He-06A2	swx-011	Quartzite - ore	WR: qtzt but by Vns:Qz-Sulf-biot(gn/bn)	Micas by Coblt are green mica/chlor	tr. Late qz-calcite-cp	Yes:
ps	He-06B	swx-012	Mica Quartzite	Qz-Biot (brwn)	Qz-Musc vein, chl; Opaq. And ??	Metamorphic look cut by Qz-musc-vn	
ps	BZ-06A1	swx-013	Biotite-chloritoid Siltite	Biot-Qz-Chloritoid-Garnet	small gt; huge porphyroblasts chld.	Chloritoid is very Fe-rich; in meta BIFs	Yes:
ts-f	Yac-06A	swx-018	Siltite with Scapolite	stain indicates only very minor Kf			
ts-f	Yac-06B	swx-019	Biotite Siltite	stain indicates only very minor Kf			
ts	R05-04-49	no cover slip	Chloritoid-Gt-Biot Schist	Qz-Biot-Gt-Chld (blue porphyroblast)-(Zirc)	retrograde chlorite rims, zircons; strong foliation; qz vns	RAM	
ts	R99-3	opx-2	Biotitite w. Qz	Biot-Quartz	Is some of Qz feldspar.	RAM	
ts	R99-5	opx-3	Biotitite	foliated biotite - 2% qz	Weird; no hint of igneous texture	RAM	
ps	RMet1	opx-4	Biot Siltite/ Gt-Biot Schist	Layered: Qz-biot/Gt-Qz-Biot-musc	Chld to Biot-musc-qz, gt incl rotated?	RAM	Yes:
ps	RMet2	opx-5	Biotite Quartzite w vein	Qz-Biot-Musc with Qz-musc-Cp vein	relook?	RAM	
ps	sccg1	UCS-1	Garnet Amphibolite	Amphibole-Gt (isot.)-Plag-Qz-(Op)	Bands with Qz, gt some rim plag, gt cores inclusions	Salmon Canyon Cu; late retro vnlets	
ps	btg1	UCS-2	Garnet-Biotite Schist	Qz-biotite25% (brwn)-Gt20%	lusions of qz, foliation thru gt; few opaq; thin retrograded rims	Blacktail Pit	
ps	N34 VSG9-05		Ore - Sunshine Lode	Qz-Biotite-MZ-Chl-Sulf	Cobaltite, Monazite; bxa vein text.	Probed MZ; from Stockpile/J.Slack	Yes:
Miscellaneous Intrusives and other Veins							
ps	IT06-04	TSX-001	In Trust Ore				
ts-f	BL06-02A	TSY-004	Altered Siltite, Cu veins				
ts-f	BL06-02B	TSY-005	Siltite, Cu veins				

ts	BL06-03	syx-004	Pyroxene Porphyry (Lamp.)	ed brwn Amph-Px-(Oliv?)toChl-talc?-Trem-Fsp matri	Semi-fresh; weak propylitic, apatite	Pseudomorph Oliv Phenos	
PS	BL06-03p	UCS-005	Px Porph -Lamprophyre	Px-Brown Amph-Oliv Porph + Kf? Matrix	Oliv to Trem+Serp, chlorite,talc?; ep.	WOW. 2 pyroxenes?? fresher	same
ps	BL06-05	syx-005	Syenite - w/biot	Feldspar(turbid) - Remnant Biot- Hm	Less Altered	alignment of tabular fsp xstals	Yes:
ps	BL06-05	syx-017	Syenite -	Feldspar-Biot(10%)-Hm; 10% dark crud	Less Altered, fsp. Aligned	flow foliation?	
ts-f	06CT13a	TSY-018	Mudstone	Qz-mud	No yellow stain, no Kf	vfg mudstone	
ts-f	06CT13b	TSY-019	Argill. Siltstone	Quartz-Mica25%- (chlorite)	Trace chlorite, pyrite?; no Kf stain visible	Detrital textures	
ps	06CTCArr	TSX-015	Quartz-Th-Hm Vein	Qz-Hm-Th-MZ-Apat	2 types of opaque veins; weak potassic	Crackle Veins/Sent to Umass; see dupl	UMA
ps	06CT13d	TSX-014	Siltite with Qz-Hm vein	Kf-Hm(30%)-(Th?)-Qz-Biot late	Strong Potassic-mosaic microcline; probe/chem	late pale brwn mica?	
ps	06B3r	TSX-013	Quartzite/ Qz-Hm Vn, Buffalo	Qz-Hm35%-Cp-(Apat)-(Fl)	Chalcopyrite-Hm in same vein, check for F	Deformed vein, crushed; xray	
	JA-6-01A		Syenite			Mineral Sep. Shrimp Date U-Pb	
ps	JA06-01C	syx-001	Syenite	Feldspar(80%)-Opaque(15%)	Orthoclase with Ab rims, Cut by Qz-Hm veins	Probed Fsp, oxide	Yes:
ps	JA06-01D	syx-002	see below?				
ts-f	JA06-02C	syx-003	Syenite -	Abund. K-fsp-opaq-(qz); 80% turbid Fsp	Hm, replaces mafic? Only 5%qz interstit	euhedral zircon	
ps	JA06-01D	syx-016					
ps	JA06-01B	TSX-016	Syenite	Fsp(70%)-Opaq.	big feldspars	do relook?	
ps	JA06-01D	syx-002*	Syenite-Hm vein	Kf(70%)-Opaques(25%)-(plag)-Qz-Fl?	Qz(unstrain)-Hm vein; Plag rims Kf; check fl, zirc	Photogenic, probe?	
ts	CQD	OPX-1	Greenstone Dike				
ps	06WP099	UCS-003	Syenite	Kf(85%)Plag rims-Bi (brown)-opaq-fl?	fresher; Bluebird area;green needles apat?	geochem	
ts-f	06WP099k	UCS-004	Syenite	as above, virt. No quartz	Mod. Kf stain esp. in cores		
ps	BL06-03p	UCS-005	Px Porph -Lamprophyre	Px-Brown Amph-Oliv Porph + Kf? Matrix	Oliv to Trem+Serp, chlorite,talc?; ep.	WOW. 2 pyroxenes?? fresher	same
ps	07WP102	UOS-1	Pyroxene Porphyry	Px-Brown Amph-Oliv?psuedoPhenos	Oliv to Trem. Lozenges,Alt. Matrix Fsp, epid, chl	prob. same loc BL06-03	phot
ts-f	07WP106	UOS-2	Diorite/Monzonite?	Fsp(AbKf)-Px,Biot,graphic granite-Apat	Strong Alt: chlorite-epid, apatite-vugs, 5% opaq,	CRUSH for zircons, probe; Low Qz-interstit	
ts-f	07SHD	UOS-4	Mafic Dike - Px Porph	Px, brown amph, Ol pseudos, fsp matrix	propylitic; Oliv to Trem; Ampfresh, carb.epid	yellow epid, weak Kf	
ps	07-77d	UOS-5	Dike loc. 77 - Px Porph	Pseudo?, Brn Amph, Px phenos; sphene?	chlorite-epid-carbonate; allanite???	Mg-rich, next to breccia pipe	
ts	07-77di	UOS-6	Dike with inclusions	1 incl may be syenitic, also quartzite	brown carbonate in vugs?		
ps	07-77bp	UOS-9	Breccia Pipe - Carbonate	Calcite, Large Brown Amph, small tan amph, in calcit	Opaque - mt or ilm?		
ps	07-77bp2	UOS-10	Breccia Pipe - Carbonate				
ts-f	07FPr	VGG-4	Mafic Dike - Px Porph	px phenos amph rims, Ol(?)-Amph-Fsp	ly altered, px fresh, ol to talc-trem, Kf rims on plag Mod. Kf st	3%Na, 2%K, 3800 ppm Ba	
ts	07PCLr	VGG-5	Mica UM Lamprophyre - alt.	Biot(brwn)-Ol(talcFeOx)-Px-Opaq-Calc	highly altered-propylitic	mary Biot. -Px-Ol phenos; 1400ppm Cr, 22% MgO	
Regional Samples							
ps	07WP129	UOS-3	Leadore Pluton - pink granite	Kf-perthite-25%qz-granophy-Opaq-mica	20% myrm (Kf-qz), zircon, opaq. Sauceritizzation	granophyric Kf+Qz late intergrow; late ser.	
ts-f	08BC1-2	VOU-1	Bull Canyon Stock (mg)	Fsp(altKf?)-Qz-Hematite-MZ-sericite	1% Monazite, euhed.; hm in fsp/intergrown with sericite	WOW. Igneous MZ, graphic qz-fsp	shou
ps	08BC1-2a	VSP-001	Bull Canyon Stock - purple	Hm-altered Granite; brown sphene?	FSP to Hm + Musc.; Zoned sphene altering?		Need
ps	08BC1-2b	VSP-002	Bull Canyon Stock - purple	Hm-altered Granite; brown sphene?	Monazite or sphene or both??		
ps	08BC-4	VOV-008	Bull Canyon Stock-pink/purpl	Pink: 1-alk.fsp, qz, ZircMZ?; Purple: Qz, Fsp, Hm	spars altering to opaq + Musc.; Matrix to sericite? Check Mz again		
ts	08Y-3	VOV-007	Yearian Vein/Peg?	Quartz, opaques	Red brown opaq., fractured qz. Check chem - dead?		
ps	07WP126a	UOS-11	Roberts adit - Carb Bxa	Calcite (vcg)-Trem-Opaq-tr. Mica, Mz	Calc-silicate Carbonatite	Opaq. May be ilmenite (lit)	
ps	07WP126b	UOS-12	Roberts	Calcite (vcg)-TremAct-Opaq- Barite??	Calc-silicate Carbonatite	NO deformation - rosettes of amph.	
ps	07WP127A	UJK-003	Roberts South - Carbonatite	Calcite-Amph-MZ-Apat	Abund. Monazite		Yes:
ps	07WP127B	UJK-004	Roberts South Deposit	Calcite-Amph-MZ-Apat	Abund. Monazite	geochem	
ps	01LB-1	VGG-12	Lee Buck - Carbonatite	Calcite-TremAct-Apat-Biot-Allan-Opaq	Calc-silicate Carbonatite	No Hint of metamorphic fabric, Hydrothermal	
ps	01LB-2	VGG-13	Lee Buck - Carbonatite				
ps	07WP127A2	VGG-14	Roberts South - Carbonatite	Calcite-Act(bluegrn)-Allan-MZ-Apat	Banded and altered; supergene; Act retro on Trem?	Apat, Mz cores rimmed by Allanite	
ps	07WP127A3	VGG-15	Roberts South - Carbonatite				WSU
	DC		Diamond Crk PC Granite				
Other Areas							
ts	08MPc-1a	VGG-001	Mtn. Pass Carbonatite	Calcite-bastnaesite-barite	Barite Phenos with bast.rims/interstitial;vcg	WOW. Had intrusive contact in field	
ts	08MPc-1b	VGG-002	Mtn. Pass Carbonatite	Calcite-bastnaesite-barite	More Fe stain; brecciated, acc. Opaq.		
ts-f	08MPs-1	VGG-003	Mtn. Pass Syenite	Kf(microcline)-Amph(blue)-Qz-Opaq.	about 2% opaq., qz interstitial, fsp - vcg	Perthite; amph blue-brwn pleo. Alkali Amph.?	Fres
Older Thin Sections							
Box B	**2001**		**Name**	**Mineralogy**	**Alteration/Mineralization**	**Comments**	**Prob**
ts-f	LH-4a	kcv-1	Black Breccia	Qz?-Kf-Biot-allanite-Apat-Mz	Potassic(microcline), 25% Monazite	Schistose Qtzt, sutured; Strong Kstain	GET
OTS	LH-4B	kcv-2	Black Breccia	Qtzt-Mica; Fsp-Biot-Hm-allanite	vein MZ, allanite in grn mica; multiple Bxas	relook	
ts-f	Lh-5	kcv-3	Quartzite-Host Rock	Qz-tr. Biot, (Kf), zircon, albite?	Strained, silicified, very little Kf		
ts-f	LH-7	kcv-4	Tan Rock, bx'd	Qz-Kf veins- Albite?-Allanite	Weak K, mica, silicifed veins	10-15% Kf stain, Hi Na Geochem	GET
ps	LH-8a	kcv-5	Specularite	Spec Hm-Biot-Apat-Mz		Nice Pressure Shadows, struct.	Yes:
OTS	LH-8b	kcv-6	Specularite				
ts-f	LH-9	kcv-7	Siltite	Qz-Mica-Apat-Kf-(Albite?)	Sutured qz, crenulated mica, weak potassic?	Very little Kf, Colorless Musc/Biot	GET
ts	LH-11a	kcv-8	Siltite/Qztite, black vns	Qz-Hm, acc. Zircon, Mz	Stylolites? Musc., detrital? Mz??		

ps	LH-12	kcv-9	Specularite Schist	Hm-Biot-Mz-Th-Apat	Sent to Umass, about 25% monazite	Try Grain Mount to find Monazite	Yes:
OTS	CQ-1	kcv-10	Quartzite, Cu vein	ED:Qz-Mica-Ep?-Apat;VN:Qz-Chl-Epid-Trem?-late Ca	RELOOK; Deformed Qz double extinct+Opaq	Vn center: Epid?+Trem?Late Calcite	
Box B							
	LH-12c2*	LAW-2	Spec. Schist	Hm-Mz-Biot-Apat-Allanite			Yes:
ts	LH-12a	unc	Spec. Schist	Hm-Biot-Mz (lots)-Apat	Apatite boudins	Very Schistose, pressure shadows	TO T
ts	LH-12b	unc	Spec. Schist	Hm-Biot-Mz	Section too thin		white
ts	LH-4b	unc	Black Breccia	Kf-Biot-Allanite	Kink lamellae in feldspars		TO T
	LH-12c1*	unc	to Brent Miller?	Hm-Mz-Apat		Section too thin, biot ground out	
Box C	**2001**						
ps	LH-12c1*	LAW-1	Spec. Schist	Hm-Biot-Mz-Th	Biot-MZ bands; late mica pullaparts	Mz growing on Apat?	also
ps	LH-12c2	LAW-2	Spec. Schist	Hm-Biot-Mz-Allanite-Th	lots small MZ; veins cut bxa also	photos 6-15-01, LPTS 2	Yes:
ps	LH-8c	LAW-3	Specularite	Hm-Allanite-Chlor-MZ	90% Hematite; chlorite alteration	Photos, check for allanite	Uma
ps	LH-4ac	LAW-4	Breccia/Cataclasite	Qz-Kf-Biot-Th-Mz-(Allanite)	rounded clasts, sutured Qz; pale Biot	check for apat., zircon	
ps	LH-4ac	LAW-5	Breccia/Shear Zone	Qz-Fsp-green mica	Pale green Biot	Pressure Solution	Prob
ps	LH-4bc	LAW-6	Quartzite- cataclasite	Qz-Hm-green biot/chl-allanite-Mz	lineated qz?, colorless	Show to CJ	Prob
Box D	**LP 6-03**						
ps	LH-12	OHI-001	Specularite Schist	Hm-Mz-brown Biot	HOT; green biotite	Intact Monazite layer	Send
ps	LH-12d	OHI-002	Specularite Schist	Hm-Biot	Supergene alt., less Mz		
ps	LH01-1a	OHI-003	Breccia	Biot-Apat--Hm-Mz-Kf (tan areas)	Retrograde mica, lots Mz	To Tony Mariano(2007)	Yes:
ps	LH01-1b	OHI-004	Breccia/Shear	Qz-Kf-Biot-Mz-Hm	Hm-Mz intergrown, to green mica	send to MJJ	Prob
ps	CA01-1a(s)	OHI-005	Quartzite - deformed	Qz-Hm veins Th; check for Mz	Hm Vein, Thorite?; clay centerline to vein	s= small piece	
ps	CA01-1a(L)	OHI-006	Quartzite- strained	Qz-Kf-Hm; zoned qz	Brown Rhomps-Rutile, thorite, Mz?	l=large piece; crossing vns?? Deformed	Show
ps	CQ-2a	QHQ-1	Quartzite - sutured	Qz-Pyrox. Vein	Bn-Cp with carbonate-qz	Carbonate overprint?	
ps	CQ-2b	QHQ-2	Quartzite/Hornfels	Qz-Pyrox.-opaq-Fsp?	Bn-Py-Moly, Pyrox to CcFeOxQz,	retrograde?, acc. Zircon	Get
Box E							
ps	04LH-b	QDG-001	Specularite Breccia	Hm-Fsp-MZ-Musc-Apat	cataclasite- Fsp broken; Bi-MZ clast?	kinked musc grains/mylonite; get photos	
ts-f	04LH-b	QDG-001	Breccia	Allanite?	feldspar		
ps	04LH-C1	QDG-002	Spec. Schist/Breccia	Hm-Mz-Musc-Fsp-Apat-Qz?	Some Musc repl Fsp, lat quartz veinlet?	clast = Fsp aggreg.,	
ps	04LH-C1	QDG-003	Specularite Breccia	same as QDG-002		Sent to Umass	
ps	04LH-C2	QDG-004	Umass			Umass	
ps	04LH-C2	QDG-005	Breccia				
ps	04LH-E	QDG-006	Umass			Umass	
	04LH-E	QDG-007	Aleinikoff			Aleinikoff	
ps	04LH-F	QDG-008					Tony
ts-f	04LH-F	QDG-008	Breccia		Potassic		
Other (extras)							

APPENDIX C1 - Representative Mineral Compositions, Formulas and End-Members: Blackbird Mining District Samples
Determined by Electron Microprobe, Washington State University

Sample	RMet1, pt. E3	RAM deposit		Sample	BZ-06A1, ptE1	
Wt. % Oxides	Garnet Core	Garnet - Int.	Garnet Rim	Garnet Core	Garnet - In	Garnet Rim
SiO2	35.36	35.84	35.4	34.55	34.87	35.18
TiO2	0.06	0.19	0.06	0.04	0.06	0.03
Al2O3	19.77	19.84	20.16	19.43	20.2	19.94
FeO t	32.41	32.82	33.57	37.06	38.49	39.36
MnO	2.58	2.04	0.83	2.55	1.92	1.28
MgO	0.26	0.33	0.71	0.37	0.47	0.46
CaO	6.42	7.02	6.59	1.56	1.81	1.51
Na2O	0	0	0	0.01	0.04	0.04
K2O	0	0.01	0	0	0.01	0
F, Cl zero						
Total	96.86	98.08	97.32	95.57	97.87	97.81
	Cations					
Si	2.982	2.982	2.962	2.985	2.946	2.973
Ti	0.004	0.012	0.004	0.003	0.004	0.002
Al -IV						
Al-VI	1.964	1.945	1.988	1.979	2.011	1.986
Fe	2.286	2.284	2.348	2.678	2.72	2.782
Mn	0.184	0.144	0.058	0.186	0.138	0.092
Mg	0.033	0.04	0.089	0.047	0.059	0.058
Ca	0.58	0.625	0.591	0.144	0.164	0.137
Na	0	0	0	0.002	0.006	0.007
K	0	0.002	0	0	0.001	0
Formula Total	20.032	20.034	20.04	20.024	20.048	20.036
Fe/(Fe+Mg)	0.99	0.98	0.96	0.98	0.98	0.98

APPENDIX C1 - Representative Mineral Compositions, Formulas and End-Members: Blackbird Mining District Samples

MICAS line	SiO2	Al2O3	TiO2	FeO	MnO	MgO	CaO	Na2O	K2O	F	Cl	PROBE SUM	Fe3+	Fe2+	%Fe3+	corr F,Cl	H2O	Total
Average, Yac-06A, biotite good analy	32.82	16.39	2.72	23.77	0.30	5.97	0.00	0.04	9.59	0.24	0.65	92.23	13.22	11.89	0.50	-0.25	3.51	97.07
Average, RMet1, biotite good analyse	31.71	16.90	2.10	26.75	0.04	4.39	0.00	0.13	9.35	0.25	0.42	91.85	14.88	13.38	0.50	-0.20	3.51	96.86
Average, BZ-06A1, biotite good anal.	30.29	17.30	1.38	29.58	0.04	2.32	0.01	0.06	9.25	0.13	0.78	90.90	16.44	14.79	0.50	-0.23	3.38	95.94
Average, He-06A, biotite brown to gre	31.03	17.13	0.70	28.28	0.03	4.33	0.00	0.07	9.38	0.32	0.78	91.74	15.72	14.14	0.50	-0.31	3.34	96.66
Average (2)Muscovite RMet1	45.07	33.57	0.26	2.64	0.00	0.62	0.00	0.49	10.44	0.31	0.00	93.28	1.47	1.32	0.50	-0.13	4.23	97.66

formula based on 24 O,OH,F,Cl

Si	Al	SiAl -8	Ti	Fe3+	Fe2+	Mn	Mg	Sum Y	Ca	Na	K	F	Cl	H	Sum cation	(OH, F,Cl)	
5.20	3.06	0.26	0.32	1.58	1.57	0.04	1.41	5.18	0.00	0.01	1.94	0.12	0.17	3.70	15.13	4.00	Average, Yac-06A, biotite good analyses
5.09	3.20	0.29	0.25	1.80	1.79	0.01	1.05	5.18	0.00	0.04	1.91	0.13	0.11	3.76	15.14	4.00	Average, RMet1, biotite good analyses
4.99	3.36	0.34	0.17	2.04	2.04	0.01	0.57	5.16	0.00	0.02	1.94	0.07	0.22	3.72	15.13	4.00	Average, BZ-06A1, biotite good anal.
5.04	3.28	0.32	0.09	1.92	1.92	0.00	1.05	5.29	0.00	0.02	1.94	0.17	0.22	3.62	15.26	4.00	Average, He-06A, biotite brown to green
6.17	5.42	3.59	0.03	0.15	0.15	0.00	0.13	4.04	0.00	0.13	1.82	0.13	0.00	3.86	14.00	4.00	

Determined by Electron Microprobe, Washington State University

Sample Average	**Yac-06A,**	**RMet1, biotite**	**BZ-06A1, biotite**	**He-06A, biotite**	**RMet1, Muscovite**
Wt. % Oxides - Averages	Biotite	Biotite	Biotite	Biot. brown/grn	Muscovite
SiO2	32.82	31.71	30.29	31.03	45.07
Al2O3	16.39	16.90	17.30	17.13	33.57
TiO2	2.72	2.10	1.38	0.70	0.26
FeO if 50% Fe+2	11.89	13.38	14.79	14.14	1.32
Fe2O3 calc at 50%	13.22	14.88	16.44	15.72	1.47
MnO	0.30	0.04	0.04	0.03	0.00
MgO	5.97	4.39	2.32	4.33	0.62
CaO	0.00	0.00	0.01	0.00	0.00
Na2O	0.04	0.13	0.06	0.07	0.49
K2O	9.59	9.35	9.25	9.38	10.44
F	0.24	0.25	0.13	0.32	0.31
Cl	0.65	0.42	0.78	0.78	0.00
(H2O)	3.51	3.51	3.38	3.34	4.23
TOTAL - w/ corrections	97.07	96.86	95.94	96.66	97.66

APPENDIX C1: Other Minerals at Blackbird

	SiO2	Al2O3	TiO2	FeO	MnO	MgO	CaO	Na2O	K2O	F	Cl	PROBE SUM	Fe3+	Fe2+	%Fe3+	corr F,Cl	H2O	Total
Average, BZ-06A1, Chloritoid (6)	21.01	38.96	0.01	26.06	0.10	0.58	0.01	0.01	0.01	0.02	0.00	86.77	0.00	26.06	0.00	-0.01	6.68	93.45
Average, Yac-06A, Scapolite (4)	50.61	22.93	2.48	1.95	0.17	0.00	10.25	7.50	0.69	0.07	2.17	98.30	0.00	1.95	0.00	-0.52	0.39	98.69

using anorthite as Si std - structure works out a little better

formula based on 24 O,OH,F,Cl

	Si	Al	Ti	Fe3+	Fe2+	Mn	Mg	Sum Y	Ca	Na	K	F	Cl	H	Sum cation	(OH, F,Cl)	
Average, BZ-06A1, Chloritoid (6)	1.89	4.12	0.00	0.00	1.96	0.01	0.08	2.04	0.00	0.00	0.00	0.01	0.00	4.00	8.05	4.01	Average, BZ-06A1, Chloritoid (6)

formula based on 12 (Si,Al)

	Si	Al	Ti	Fe3+	Fe2+	Mn	Mg	Ca	Na	K	F	Cl	H	Sum cation	(OH, F,Cl)
Average, Yac-06A, Scapolite (4)	7.82	4.18	0.34	0.00	0.29	0.03	0.00	1.70	2.26	0.14	0.04	0.57	0.40	16.75	1.00

Yac samples from exposure on Deep Creek road of unmineralized Apple Creek Formation with visible scapolite ovals, Waypoint 7.

BZ sample is from the Blacktail Zone, exposed in th or Blacktail Pit, W015
HE is from the Hawkeye 7080' portal, underground. (Waypoint 18)
R Met1 is from the RAM Deposit, drill core from Metallurgical Hole 1. (get depth and location from Formation)

APPENDIX C2: Microprobe Analyses, Lemhi Pass Silicates

Amphiboles	Line	SiO_2	Al_2O_3	TiO_2	FeO	MnO	MgO	CaO	Na_2O	K_2O	F	Cl	PROBE SUM	Fe^{3+}	Fe^{2+}	%Fe^{3+}	corr F,Cl	H_2O	Total
Average, CQ06-30A1, Amphibole, red brown (12)		35.63	13.13	5.70	10.89	0.12	11.92	11.95	2.12	1.35	0.33	0.05	93.03	7.26	4.35	0.60	-0.15	1.76	95.53
Average, CQ06-30A1, brown Amph, (12) rerun, but F not working		38.45	13.43	5.78	11.15	0.13	12.20	12.05	2.20	1.36	0.00	0.06	96.81	0.00	11.15	0.00	-0.01	1.98	98.78
Average, CQ06-30A1, Colorless Amph (10) - alteration replacing olivine?		55.50	0.95	0.02	7.85	0.23	19.22	12.85	0.22	0.04	0.00	0.01	96.90	2.18	5.89	0.25	0.00	2.12	99.24

										B site				A site							
	Si	Al	SiAl -8	Ti	Fe^{3+}	Fe^{2+}	Mn	Mg	leftover from C	Ca	B Na	Tot Na	A Na	K	A total	H	F	Cl	Sum cation	(OH, F,Cl)	
Average, CQ06-30A1, Amphibole, red brown (12)	5.519	2.397	-0.084	0.663	0.847	0.564	0.016	2.752	-0.241	1.984	0.016	0.637	0.621	0.266	0.888	1.823	0.163	0.014	15.647	2.000	Average, CQ06-30A1, Amphibole, red brown (12)
Average, CQ06-30A1, brown Amph, (12) rerun, but F not working	5.784	2.382	0.166	0.654	0.000	1.404	0.017	2.735	-0.024	1.943	0.054	0.642	0.588	0.262	0.850	1.985	0.000	0.015	15.823	2.000	
Average, CQ06-30A1, Colorless Amph (10) - alteration replacing olivine?	7.834	0.158	-0.008	0.002	0.232	0.696	0.027	4.042	-0.009	1.944	0.047	0.061	0.014	0.007	0.021	1.997	0.000	0.003	15.003	2.000	

APPENDIX C2: Microprobe Analyses, Lemhi Pass Silicates

Representative Mineral Compositions: Lucky Horseshoe Mine, Lemhi Pass District

BIOTITES	line	SiO2	Al2O3	TiO2	FeO	MnO	MgO	CaO	Na2O	K2O	F	Cl	PROBE SUM	Fe3+	Fe2+	%Fe3+	corr F,Cl	H2O	Total
Lucky Horseshoe Th-REE deposit																			
Average, LH-12c, biotite brown (18)	Th ore	38.19	11.24	0.19	9.88	0.10	19.64	0.02	0.03	10.24	4.03	0.02	91.87	5.50	4.94	0.50	-1.70	1.98	94.41
Average, LH-12c2, Mica, green (6)	Th ore	38.23	11.11	0.12	10.05	0.11	19.97	0.12	0.05	10.28	4.84	0.02	92.86	5.59	5.02	0.50	-2.04	1.61	95.03
Average, LH01-1a, Biotite, green/brown (11)		41.67	11.72	0.28	11.06	0.10	19.31	0.05	0.05	10.47	NA	0.03	94.73	6.15	5.53	0.50	-0.01	4.13	99.47
Un 118 LH-8a, Biotite-dark brown, C5	252	41.41	12.44	0.49	11.13	0.09	19.51	0.00	0.02	10.25	NA	0.01	95.35	6.19	5.56	0.50			
Syenite																			
Average, BL06-05, biotite, brown (15)	Syenite	32.25	11.24	1.96	32.02	0.78	1.18	0.28	0.03	8.68	0.90	0.53	89.36	17.81	16.01	0.50	-0.50	2.96	94.11

formula based on 24 O,OH,F,Cl

BIOTITES	Si	Al	SiAl -8	Ti	Fe3+	Fe2+	Mn	Mg	Sum Y	Ca	Na	K	F	Cl	H	Sum cation	(OH, F,Cl)	
Average, LH-12c, biotite brown (18)	5.88	2.04	-0.08	0.02	0.64	0.64	0.01	4.51	5.74	0.00	0.01	2.01	1.96	0.01	2.03	15.77	4.00	Average, LH-12c, biotite brown (18 good pts)
Average, LH-12c2, Mica, green (6)	5.87	2.01	-0.12	0.01	0.65	0.64	0.01	4.57	5.76	0.02	0.02	2.01	2.35	0.01	1.64	15.81	4.00	Average, LH-12c2, Mica, green (6)
Average, LH01-1a, Biotite, green/brown (11)	6.04	2.00	0.05	0.03	0.67	0.67	0.01	4.17	5.60	0.01	0.01	1.94	0.00	0.01	3.99	15.56	4.00	
Average, BL06-05, biotite, brown (15)	5.49	2.26	-0.25	0.25	2.28	2.28	0.11	0.30	4.98	0.05	0.01	1.89	0.48	0.15	3.36	14.93	4.00	Average, BL06-05, biotite, brown

	Biotites				Amphiboles	
	Syenite	**Th ore**	**Th ore**	**Th ore**	**Px Porphyry Phenos**	
Sample (Averages)	BL06-05	LH-12c	LH-12c2	LH01-1a	CQ06-30A1	CQ06-30A1
biotite:	brown	brown	green	gn/brwn	red brown	clear -alt.
Wt. % Oxides						
SiO2	32.25	38.19	38.23	41.67	35.63	55.50
Al2O3	11.24	11.24	11.11	11.72	13.13	0.95
TiO2	1.96	0.19	0.12	0.28	5.70	0.02
FeO if 50% Fe+2	16.01	4.94	5.02	5.53	4.35	5.89
Fe2O3 calc at 50%	17.81	5.50	5.59	6.15	7.26	2.18
MnO	0.78	0.10	0.11	0.10	0.12	0.23
MgO	1.18	19.64	19.97	19.31	11.92	19.22
CaO	0.28	0.02	0.12	0.05	11.95	12.85
Na2O	0.03	0.03	0.05	0.05	2.12	0.22
K2O	8.68	10.24	10.28	10.47	1.35	0.04
F	0.90	4.03	4.84	NA	0.33	0.00
Cl	0.53	0.02	0.02	0.03	0.05	0.01
(H2O)	2.96	1.98	1.61	4.13	1.76	2.12
TOTAL - w/ corrections	94.11	94.41	95.03	99.47	95.53	99.24

Feldspars	Line Numb	Na2O Oxide	Al2O3 Oxi	Fe2O3 Oxi	K2O Oxide	CaO Oxide	SiO2 Oxide P	BaO Oxide Percer	Oxide Totals	Na Formul	Al Formula	Fe Formula	K Formula	Ca Formul	Si Formula	Ba Formul	Formula Totals	
Syenite																		
Average of 5 cores (BL06-05)		0.45	19.04	0.06	16.20	0.01	63.28	0.21	99.24	0.041	1.049	0.002	0.966	0.001	2.958	0.004	13.020	Average Core, BL06-05
Average of 5 rims (BL06-05)		11.24	20.58	0.10	0.41	0.22	67.08	0.01	99.65	0.957	1.066	0.003	0.024	0.010	2.948	0.000	13.008	Average Rim, BL06-05

label	Line Numb	Na2O Oxide	Al2O3 Oxi	FeO Oxide	K2O Oxide	CaO Oxide	SiO2 Oxide P	Oxide Totals	Na Formula At	Al Formula	Fe Formula	K Formula	Ca Formul	Si Formula	Totals
Un 79 JA06-01C, Feldspar Trav., rim, pt. B1	197	7.72	19.57	-0.01	5.91	0.00	66.66	99.85	0.668	1.030	0.000	0.336	0.000	2.976	13.011
Un 80 JA06-01C, Feldspar Trav., rim/core, pt. B2	198	0.35	18.71	0.01	16.37	-0.01	62.53	97.95	0.032	1.044	0.000	0.989	0.000	2.962	13.027
Un 81 JA06-01C, Feldspar Trav., core, pt. B3	199	0.38	19.08	0.11	16.53	-0.02	63.49	99.57	0.034	1.048	0.004	0.983	-0.001	2.958	13.026
Un 82 JA06-01C, Feldspar Trav., core middle, pt. B4	200	0.75	18.59	0.63	16.04	0.00	63.60	99.61	0.067	1.022	0.024	0.954	0.000	2.966	13.034
Un 83 JA06-01C, Feldspar Trav., core, pt. B5	201	0.39	18.94	0.03	16.76	0.00	64.44	100.55	0.035	1.030	0.001	0.986	0.000	2.972	13.023
Un 84 JA06-01C, Feldspar Trav., rim/core, pt. B6	202	11.76	19.76	0.01	0.12	0.05	67.51	99.21	1.005	1.026	0.001	0.007	0.003	2.976	13.017
Un 85 JA06-01C, Feldspar Trav., rim, pt. B7	203	9.73	19.84	0.03	3.06	0.02	67.70	100.38	0.830	1.028	0.001	0.172	0.001	2.977	13.009
Copper Veins															
Average CQ-06C, swx-2, Vein Feldspar (12)		0.39	19.02	0.01	16.20	0.00	64.17	99.79	0.03	1.039	0.000	0.958	0.000	2.973	13.004
Copper Qn vein cuts qtzt.															
label	Line Numb	Na2O Oxide	Al2O3 Oxi	FeO Oxide	K2O Oxide	CaO Oxide	SiO2 Oxide P	Oxide Totals	Na Formula At	Al Formula	Fe Formula	K Formula	Ca Formul	Si Formula	Totals
Thorium Veins															
Average, CA06-B1, swx-4, orangy Feldspar, pts. A,C,D,E,H		0.34	18.87	0.09	16.36	-0.03	64.52	100.14	**0.03**	**1.027**	**0.003**	**0.964**	**-0.001**	**2.980**	**13.004**
Average, CA06-B1, swx-4, Na-rich feldspar by brown rhombs, loc. (		10.93	20.62	0.03	0.13	0.06	70.91	102.67	0.90	1.028	0.001	0.007	0.003	3.001	12.937
Un 148 LH01-1a pt 1 of 2, Orange Patch, G1, un 148	283	0.17	18.89	0.03	16.11	-0.02	66.34	101.47	0.02	1.009	0.001	0.932	-0.001	3.008	12.962
Average LH01-1a, Orange Feldspar (3) late??		9.87	20.39	0.17	0.16	0.08	70.50	101.18	0.82	1.028	0.006	0.009	0.004	3.017	12.883

Feldspars	Line Numb	Na2O Oxide	Al2O3 Oxi	Fe2O3 Oxi	K2O Oxide	CaO Oxide	SiO2 Oxide P	BaO Oxide Percer	Oxide Totals

Feldspars	Cores	Rims		Orangy	clearer/outer?
Sample Number	BL06-05	BL06-05		CA06-B1	CA06-B1
Wt. % Oxides	syenite			Cago Th ve	Envelope?
SiO2	63.28	67.08		64.52	70.91
Al2O3	19.04	20.58		18.87	20.62
Fe2O3	0.06	0.10	as FeO	0.09	0.03
CaO	0.01	0.22		-0.03	0.06
Na2O	0.45	11.24		0.34	10.93
K2O	16.20	0.41		16.36	0.13
BaO	0.21	0.01		na	na
Total	99.24	99.65		100.14	102.67

Weight Percent Oxide on Grain Traverse	**Na2O**	**K2O**
Un 79 JA06-01C, Feldspar Trav., rim, pt. B1	7.72	5.91
Un 80 JA06-01C, Feldspar Trav., rim/core, pt. B2	0.35	16.37
Un 81 JA06-01C, Feldspar Trav., core, pt. B3	0.38	16.53
Un 82 JA06-01C, Feldspar Trav., core middle, pt. B4	0.75	16.04
Un 83 JA06-01C, Feldspar Trav., core, pt. B5	0.39	16.76
Un 84 JA06-01C, Feldspar Trav., rim/core, pt. B6	11.76	0.12
Un 85 JA06-01C, Feldspar Trav., rim, pt. B7	9.73	3.06

APPENDIX C2: Microprobe Analyses, Lemhi Pass Silicates

Muscovite	line	SiO2	Al2O3	TiO2	FeO	MnO	MgO	CaO	Na2O	K2O	F	Cl	PROBE SUM	Fe3+	Fe2+	%Fe3+	corr F,Cl	H2O	Total
Average, CQ-06C, swx-2, Mica in host rock (8)		46.97	29.51	0.57	3.84	0.05	2.14	-0.01	0.19	10.58	0.00	0.00	93.84	2.13	1.92	0.50	0.00	4.39	98.45
Average, LH01-1a, Sericite Vein, late (3)		47.51	32.79	0.71	3.84	0.01	1.12	0.01	0.11	9.31	0.00	0.02	95.42	2.13	1.92	0.50	0.00	4.51	100.15

formula based on 24 O,OH,F,Cl

Muscovite	Si	Al	SiAl -8	Ti	Fe3+	Fe2+	Mn	Mg	Sum Y	Ca	Na	K	F	Cl	H	Sum cation	(OH, F,Cl)
Average, CQ-06C, swx-2, Mica in host rock (8)	6.412	4.750	3.161	0.058	0.219	0.219	0.005	0.436	4.100	-0.001	0.050	1.844	0	0.000775	3.999225	13.99216	4
Average, LH01-1a, Sericite Vein, late (3)	6.303	5.129	3.432	0.071	0.213	0.213	0.001	0.222	4.152	0.001	0.029	1.577	0	0.004209	3.995791	13.75801	4

APPENDIX C2: **Microprobe Analyses, Lemhi Pass Silicates**

Pyroxenes	Line Nu	F Oxide Pe	Na2O Oxic	MgO Oxide	Al2O3 Oxi	FeO Oxide	MnO Oxide	TiO2 Oxide	K2O Oxide	CaO Oxide	SiO2 Oxide	Cl Oxide P	Oxide Tota	F Formula	Na Formul	Mg Formul	Al Formula	Fe Formula	Mn Formul	Ti Formula	K Formula	Ca Formul	Si Formula	Cl Formula	Totals
Average, CQ06-30A1, Pyroxene-c (10)		0.11	0.55	14.49	5.46	5.26	0.11	1.07	0.01	21.76	46.09	0.00	94.86	0.01	0.04	0.85	0.25	0.17	0.00	0.03	0.00	0.91	1.80	0.00	10.08

Appendix C3: LP Monazite	Y2O3 Oxi	La2O3 Ox	Ce2O3 Oxi	Pr2O3 O	Nd2O3 O	Sm2O3 O	Eu	Gd2O3	ThO2	UO2 Oxi	PbO Oxi	CaO Oxi	SiO2 Oxi	Al2O3 O	P2O5 Ox	Oxide Totals
Sample																
LH12c2 Average (27 points)	0.88	3.40	16.19	5.44	34.94	5.01	NA	1.43	0.63	0.09	0.08	0.31	0.32	0.05	29.29	98.05
LH06-24A Average (14 points)	0.62	2.77	15.16	5.50	36.59	5.08	NA	1.32	0.56	0.09	0.17	0.15	0.35	0.08	29.13	97.57
LH-8a Average (12 points)	0.44	3.44	16.25	5.50	36.38	4.77	NA	1.40	0.49	0.09	0.15	0.31	0.22	0.01	29.49	98.94
LH-12, kcv-9 Average (18 points)	0.81	3.63	16.67	5.58	35.17	4.89	NA	1.52	0.52	0.09	0.18	0.16	0.16	0.01	29.49	98.90
Sunshine Lode VSG92005 Aver. (12 points)	1.09	13.89	31.39	4.23	12.86	2.40	NA	2.14	0.26	0.22	0.17	0.08	0.34	0.24	29.87	99.19
07WP127B Roberts S Average (14 points)	0.03	25.18	32.87	4.10	6.71	0.30	NA	0.58	0.65	0.11	0.09	0.09	-0.01	-0.01	30.49	101.17

APPENDIX C3 - Lemhi Pass Monazite Analyses - Averages to Plot

LH12c2, LH-6-24A, LH-8a, and LH-12 are all from the Lucky Horseshoe mine, Lemhi Pass District
Sunshine Lode VSG92005 is from Blackbird District
07WP127B is from Roberts South carbonatite near North Fork/Shoup, Idaho

Appendix C3b: Monazites	Line Numbe	SiO2 Oxi	Sm2O3	Nd2O3 Ox	Ce2O3	La2O3	CaO Oxi	ThO2 O	Y2O3 Ox	Pr2O3	Gd2O3	UO2 O	PbO Oxid	Al2O3 Ox	P2O5 Oxi	Oxide Totals	Si Form	Sm Form	Nd Formu	Ce Form	La Formu	Ca Form	Th Form	Y Formu	Pr Form	Gd Form	U Formu	Pb For	Al Form	P Form	Formula Totals
Un 15 LH12c2-A MZcore	1624	0.14	5.10	34.80	16.13	3.61	0.24	0.33	1.05	5.46	1.47	0.10	0.05	-0.01	29.63	98.08	0.005	0.070	0.497	0.236	0.053	0.010	0.003	0.022	0.080	0.019	0.001	0.001	-0.001	1.002	5.999
Un 16 LH12c2-A MZswRim	1625	0.24	4.78	35.49	17.05	3.76	0.12	0.41	0.57	5.79	1.26	0.07	-0.03	0.02	29.67	99.20	0.009	0.065	0.503	0.248	0.055	0.005	0.004	0.012	0.084	0.017	0.001	0.000	0.001	0.997	5.999
Un 17 LH12c2-A MZseRim	1626	0.21	4.68	35.72	16.84	3.70	0.18	0.56	0.66	5.56	1.26	0.12	0.06	-0.01	29.15	98.71	0.008	0.065	0.512	0.247	0.055	0.008	0.005	0.014	0.081	0.017	0.001	0.001	0.000	0.990	6.004
Un 18 LH12c2-A2 MZCore	1627	0.29	4.97	34.95	16.15	3.58	0.11	0.61	1.07	5.35	1.43	0.08	0.04	0.01	29.39	98.02	0.012	0.069	0.500	0.237	0.053	0.005	0.006	0.023	0.078	0.019	0.001	0.000	0.000	0.997	5.998
Un 19 LH12c2-A2 MZint	1628	0.18	5.26	35.38	16.65	3.59	0.07	0.58	0.75	5.68	1.38	0.12	0.05	-0.02	29.63	99.29	0.007	0.072	0.502	0.242	0.053	0.003	0.005	0.016	0.082	0.018	0.001	0.001	-0.001	0.997	5.999
Un 20 LH12c2-A2 MZswRim	1629	0.14	4.87	35.31	17.19	3.81	0.11	0.45	0.64	5.43	1.31	0.07	0.09	-0.01	29.50	98.91	0.006	0.067	0.504	0.251	0.056	0.005	0.004	0.014	0.079	0.017	0.001	0.001	-0.001	0.997	6.000
Un 22 LH12c2-A3 MZwRim	1631	0.28	5.06	34.44	15.98	3.45	0.26	0.68	1.25	5.60	1.49	0.14	0.02	0.00	29.39	98.04	0.011	0.070	0.492	0.234	0.051	0.011	0.006	0.027	0.082	0.020	0.001	0.000	0.000	0.996	6.001
Un 23 LH12c2-A3 MZswRim	1632	0.19	5.21	36.48	15.24	3.10	0.07	0.81	0.74	5.42	1.49	0.12	0.05	0.02	29.06	97.99	0.007	0.073	0.526	0.225	0.046	0.003	0.007	0.016	0.080	0.020	0.001	0.001	0.001	0.994	6.000
Un 24 LH12c2-B MZcore	1633	0.38	4.70	35.60	17.22	3.64	0.10	0.54	0.62	5.57	1.15	0.05	0.13	0.05	29.29	99.04	0.015	0.065	0.507	0.251	0.053	0.004	0.005	0.013	0.081	0.015	0.000	0.001	0.002	0.989	6.003
Un 25 LH12c2-B1 MZsRim	1634	0.10	4.71	35.30	17.19	3.60	0.10	0.40	0.73	5.62	1.26	0.11	0.16	0.00	29.15	98.44	0.004	0.065	0.508	0.253	0.054	0.004	0.004	0.016	0.082	0.017	0.001	0.002	0.000	0.994	6.003
Un 26 LH12c2-B2 MZCore	1635	0.13	4.58	34.83	17.69	3.86	0.20	0.37	0.69	5.63	1.14	0.08	0.16	0.01	29.36	98.70	0.005	0.063	0.498	0.259	0.057	0.009	0.003	0.015	0.082	0.015	0.001	0.002	0.000	0.995	6.004
Un 27 LH12c2-B2 MZ Erim	1636	0.17	4.97	34.74	16.01	3.29	0.22	0.45	0.90	5.29	1.41	0.05	0.06	0.02	31.65	99.23	0.007	0.066	0.477	0.226	0.047	0.009	0.004	0.018	0.074	0.018	0.000	0.001	0.001	1.031	5.979
Un 28 LH12c2-B2 MZ Wrim	1637	0.07	4.23	35.29	18.27	3.98	0.23	0.21	0.50	5.76	0.93	0.09	0.20	0.01	29.22	98.97	0.003	0.058	0.505	0.268	0.059	0.010	0.002	0.011	0.084	0.012	0.001	0.002	0.000	0.992	6.008
Un 29 LH12c2-B2 MZ Nrim	1638	0.28	4.88	34.16	16.71	3.46	0.12	0.31	0.90	5.42	1.32	0.12	0.10	0.03	29.52	97.32	0.011	0.068	0.490	0.246	0.051	0.005	0.003	0.019	0.079	0.018	0.001	0.001	0.001	1.003	5.995
Un 30 LH12c2-C1 MZ core	1639	0.25	5.27	35.25	16.35	3.34	0.13	0.50	1.05	5.45	1.43	0.09	0.04	-0.01	29.26	98.39	0.010	0.073	0.505	0.240	0.049	0.006	0.005	0.022	0.080	0.019	0.001	0.000	0.000	0.993	6.002
Un 31 LH12c2-C1 MZ NE rim	1640	1.74	4.92	34.85	15.48	3.23	0.11	1.10	0.78	5.16	1.46	0.11	0.20	0.51	30.69	100.33	0.066	0.064	0.471	0.214	0.045	0.005	0.009	0.016	0.071	0.018	0.001	0.002	0.023	0.983	5.988
Un 32 LH12c2-C2 MZ int	1641	0.34	4.85	34.24	15.95	3.41	0.34	0.60	0.91	5.39	1.39	0.07	0.03	0.05	28.53	96.10	0.014	0.068	0.501	0.239	0.051	0.015	0.006	0.020	0.080	0.019	0.001	0.000	0.002	0.989	6.006
Un 34 LH12c2-C2 MZ SWint	1643	1.20	4.58	34.31	16.51	3.66	0.11	0.49	0.54	5.53	1.25	0.06	0.05	0.30	27.96	96.52	0.049	0.064	0.498	0.246	0.055	0.005	0.005	0.012	0.082	0.017	0.001	0.000	0.014	0.962	6.009
Un 36 LH12c2-D1 MZ Core	1645	0.12	5.36	35.18	15.35	2.99	0.24	0.71	1.02	5.35	1.54	0.02	0.02	0.02	29.38	97.30	0.005	0.074	0.506	0.226	0.044	0.010	0.007	0.022	0.079	0.021	0.000	0.000	0.001	1.002	5.998
Un 37 LH12c2-D1 MZ Wint	1646	0.13	5.54	35.89	15.39	3.07	0.12	0.44	1.11	5.40	1.70	0.10	0.10	0.02	29.52	98.53	0.005	0.076	0.512	0.225	0.045	0.005	0.004	0.024	0.079	0.023	0.001	0.001	0.001	0.999	6.000
Un 38 LH12c2-D1 MZ Erim	1647	0.19	5.73	35.36	14.92	2.95	0.27	0.37	1.17	5.35	1.87	0.09	0.04	-0.01	29.57	97.87	0.007	0.079	0.505	0.219	0.043	0.012	0.003	0.025	0.078	0.025	0.001	0.000	0.000	1.002	5.999
Un 40 LH12c2-D1 MZ SWrim	1649	1.13	5.08	34.20	15.23	3.17	0.26	1.53	0.92	5.22	1.54	0.10	0.10	0.28	27.89	96.64	0.046	0.071	0.497	0.227	0.048	0.011	0.014	0.020	0.077	0.021	0.001	0.001	0.014	0.961	6.010
Un 41 LH12c2-D1 MZ Wrim	1650	0.19	5.32	35.16	15.61	2.90	0.16	0.61	1.17	5.43	1.59	0.11	0.11	0.00	29.22	97.58	0.008	0.074	0.506	0.230	0.043	0.007	0.006	0.025	0.080	0.021	0.001	0.001	0.000	0.997	6.000
Un 42 LH12c2-D1 MZ Nint	1651	0.10	4.78	32.96	15.17	3.09	3.25	0.44	0.90	5.13	1.44	0.13	0.17	0.01	27.69	95.26	0.004	0.068	0.485	0.229	0.047	0.144	0.004	0.020	0.077	0.020	0.001	0.002	0.000	0.967	6.068
Un 43 LH12c2-D2 MZ core	1652	0.20	5.40	34.15	15.23	3.08	0.40	1.33	1.14	5.30	1.75	0.09	0.04	0.04	29.49	97.64	0.008	0.075	0.489	0.223	0.046	0.017	0.012	0.024	0.077	0.023	0.001	0.000	0.002	1.001	5.998
Un 44 LH12c2-D2 MZ Erim	1653	0.16	5.30	35.05	16.05	3.20	0.30	0.61	1.14	5.40	1.59	0.12	0.09	0.00	29.23	98.24	0.007	0.073	0.503	0.236	0.047	0.013	0.006	0.024	0.079	0.021	0.001	0.001	0.000	0.994	6.005
Un 46 LH12c2-D2 MZ NWint	1655	0.15	5.09	34.23	15.54	3.33	0.43	1.45	0.93	5.26	1.64	0.06	0.03	0.01	28.93	97.08	0.006	0.071	0.497	0.231	0.050	0.019	0.013	0.020	0.078	0.022	0.001	0.000	0.000	0.995	6.003
LH12c2 Average (27 points)		**0.32**	**5.01**	**34.94**	**16.19**	**3.40**	**0.31**	**0.63**	**0.88**	**5.44**	**1.43**	**0.09**	**0.08**	**0.05**	**29.29**	**98.05**	**0.01**	**0.07**	**0.50**	**0.24**	**0.05**	**0.01**	**0.01**	**0.02**	**0.08**	**0.02**	**0.00**	**0.00**	**0.00**	**0.99**	**6.00**
Std Dev LH12c2		*0.38*	*0.33*	*0.69*	*0.85*	*0.30*	*0.59*	*0.34*	*0.21*	*0.17*	*0.20*	*0.03*	*0.06*	*0.12*	*0.75*	*1.09*	*0.01*	*0.00*	*0.01*	*0.01*	*0.00*	*0.03*	*0.00*	*0.00*	*0.00*	*0.00*	*0.00*	*0.00*	*0.01*	*0.01*	*0.01*
Un 47 LH06-24A-A red unk.	1656	1.21	5.15	36.38	14.90	2.64	0.17	0.56	0.79	5.43	1.33	0.12	0.05	0.43	29.03	98.18	0.048	0.070	0.514	0.216	0.038	0.007	0.005	0.017	0.078	0.017	0.001	0.000	0.020	0.972	6.003
Un 48 LH06-24A-A1 MZ int	1657	0.24	5.14	36.27	14.24	2.45	0.11	0.47	0.68	5.27	1.37	0.05	0.24	0.01	28.60	95.14	0.010	0.073	0.535	0.215	0.037	0.005	0.004	0.015	0.079	0.019	0.000	0.003	0.001	1.000	5.997
Un 49 LH06-24A-A1 MZ Srim	1658	0.38	5.07	37.69	15.18	2.65	0.11	0.46	0.54	5.55	1.32	0.14	0.29	0.13	28.79	98.31	0.016	0.070	0.543	0.224	0.039	0.005	0.004	0.012	0.082	0.018	0.001	0.003	0.006	0.983	6.007
Un 50 LH06-24A-A1 Red Opaque	1659	1.47	4.93	35.36	15.24	2.78	0.18	0.77	0.62	5.35	1.35	0.05	0.16	0.52	29.01	97.79	0.058	0.067	0.498	0.220	0.040	0.007	0.007	0.013	0.077	0.018	0.000	0.002	0.024	0.969	6.002
Un 51 LH06-24A A2 MZor apat	1660	0.19	5.31	36.94	15.14	2.69	0.06	0.66	0.67	5.51	1.45	0.08	0.20	0.00	29.03	97.92	0.008	0.074	0.534	0.224	0.040	0.003	0.006	0.014	0.081	0.019	0.001	0.002	0.000	0.994	6.001
Un 52 LH06-24A B1 MZ core	1661	0.08	5.04	37.07	15.36	2.80	0.05	0.36	0.77	5.63	1.40	0.09	0.36	-0.02	29.66	98.64	0.003	0.069	0.529	0.225	0.041	0.002	0.003	0.016	0.082	0.018	0.001	0.004	-0.001	1.004	5.997
Un 53 LH06-24A B1 MZ Ecore	1662	0.17	5.35	36.33	14.85	2.40	0.11	0.41	1.04	5.49	1.55	0.10	0.26	-0.02	28.92	96.96	0.007	0.075	0.528	0.221	0.036	0.005	0.004	0.023	0.081	0.021	0.001	0.003	-0.001	0.997	6.001
Un 54 LH06-24A B1 MZ Eint	1663	0.16	5.31	37.18	14.61	2.49	0.10	0.29	0.93	5.45	1.47	0.05	0.26	0.02	29.49	97.81	0.006	0.073	0.533	0.215	0.037	0.004	0.003	0.020	0.080	0.020	0.000	0.003	0.001	1.003	5.997
Un 57 LH06-24A C1 MZcore	1666	0.10	4.98	35.86	15.79	3.00	0.37	0.67	0.54	5.69	1.20	0.11	0.27	-0.02	29.33	97.89	0.004	0.069	0.516	0.233	0.045	0.016	0.006	0.012	0.083	0.016	0.001	0.003	-0.001	1.000	6.003
Un 58 LH06-24A C1 MZrim	1667	0.24	4.70	35.02	16.63	3.33	0.24	0.84	0.44	5.68	1.17	0.13	0.09	0.02	29.39	97.92	0.010	0.065	0.502	0.244	0.049	0.010	0.008	0.009	0.083	0.016	0.001	0.001	0.001	0.999	5.998
Un 59 LH06-24A D1 MZint	1668	0.12	4.81	36.24	16.16	3.46	0.11	0.35	0.41	5.52	1.12	0.08	0.03	0.00	29.49	97.91	0.005	0.067	0.520	0.238	0.051	0.005	0.003	0.009	0.081	0.015	0.001	0.000	0.000	1.003	5.997
Un 60 LH06-24A D1 MZrimmy	1669	0.16	4.89	36.71	15.25	2.87	0.29	1.20	0.43	5.56	1.15	0.09	0.07	0.01	29.01	97.68	0.006	0.068	0.531	0.226	0.043	0.013	0.011	0.009	0.082	0.015	0.001	0.001	0.000	0.995	6.002
Un 63 LH06-24A D3 MZint	1672	0.15	5.23	38.29	14.42	2.60	0.08	0.33	0.31	5.51	1.22	0.08	0.14	0.02	29.03	97.41	0.006	0.073	0.555	0.214	0.039	0.003	0.003	0.007	0.081	0.016	0.001	0.002	0.001	0.998	6.000
Un 64 LH06-24A D3 MZrim	1673	0.20	5.14	36.86	14.46	2.68	0.10	0.51	0.52	5.42	1.33	0.07	0.00	0.02	29.05	96.35	0.008	0.072	0.537	0.216	0.040	0.004	0.005	0.011	0.080	0.018	0.001	0.000	0.001	1.002	5.995
LH06-24A Average (14 points)		**0.35**	**5.08**	**36.59**	**15.16**	**2.77**	**0.15**	**0.56**	**0.62**	**5.50**	**1.32**	**0.09**	**0.17**	**0.08**	**29.13**	**97.57**	**0.01**	**0.07**	**0.53**	**0.22**	**0.04**	**0.01**	**0.01**	**0.01**	**0.08**	**0.02**	**0.00**	**0.00**	**0.00**	**0.99**	**6.00**
Std Dev LH06-24A		*0.41*	*0.19*	*0.83*	*0.65*	*0.30*	*0.09*	*0.24*	*0.20*	*0.11*	*0.12*	*0.03*	*0.11*	*0.17*	*0.29*	*0.86*	*0.02*	*0.00*	*0.01*	*0.01*	*0.00*	*0.00*	*0.00*	*0.00*	*0.00*	*0.00*	*0.00*	*0.00*	*0.01*	*0.01*	*0.00*
Un 67 LH-8a - A1 MZrim	1680	0.14	3.59	34.39	19.29	4.31	0.45	0.37	0.30	6.11	0.84	0.10	0.04	0.01	29.45	99.38	0.006	0.049	0.489	0.281	0.063	0.019	0.003	0.006	0.089	0.011	0.001	0.000	0.000	0.992	6.009
Un 70 LH-8a - A2 MZ Sint	1683	0.17	4.87	38.45	15.37	3.08	0.20	0.37	0.36	5.45	1.29	0.10	0.31	0.01	29.71	99.73	0.007	0.066	0.544	0.223	0.045	0.009	0.003	0.008	0.079	0.017	0.001	0.003	0.000	0.997	6.002
Un 72 LH-8a - B1 MZ int	1685	0.51	4.56	34.13	16.88	3.30	0.24	0.42	0.54	5.82	1.17	0.12	0.12	0.17	29.13	97.12	0.021	0.063	0.490	0.249	0.049	0.010	0.004	0.012	0.085	0.016	0.001	0.001	0.008	0.992	6.001
Un 74 LH-8a - B3 MZ core	1687	0.15	6.12	37.46	13.80	3.02	0.03	0.55	0.55	4.93	2.25	0.06	0.21	0.00	30.01	99.15	0.006	0.084	0.530	0.200	0.044	0.001	0.005	0.012	0.071	0.030	0.001	0.002	0.000	1.007	5.993
Un 75 LH-8a - B3 MZ NErim	1688	0.15	5.52	37.06	15.43	3.34	0.02	0.51	0.52	5.25	1.70	0.11	0.25	-0.01	31.32	101.16	0.006	0.073	0.509	0.217	0.047	0.001	0.004	0.011	0.074	0.022	0.001	0.002	0.000	1.019	5.985
Un 76 LH-8a - B3 MZ Nrim	1689	0.21	6.16	37.44	13.48	2.78	0.23	0.30	0.92	4.96	2.33	0.15	0.31	0.01	28.21	97.47	0.009	0.087	0.549	0.203	0.042	0.010	0.003	0.020	0.074	0.032	0.001	0.003	0.000	0.980	6.013
Un 77 LH-8a - C1 MZ core	1690	0.31	4.58	35.34	16.72	3.55	0.99	0.73	0.39	5.42	1.20	0.10	0.09	-0.01	28.63	98.05	0.013	0.064	0.510	0.247	0.053	0.043	0.007	0.008	0.080	0.016	0.001	0.001	0.000	0.980	6.022
Un 78 LH-8a - C1 MZ Srim	1691	0.17	4.27	35.92	17.56	3.62	0.21	0.52	0.34	5.74	1.08	0.08	0.17	0.01	29.77	99.47	0.007	0.058	0.508	0.255	0.053	0.009	0.005	0.007	0.083	0.014	0.001	0.002	0.000	0.999	6.000
Un 79 LH-8a - C2 MZ Core	1692	0.20	4.26	35.72	17.30	3.67	0.19	0.54	0.40	5.82	1.16	0.10	0.00	0.00	29.62	98.96	0.008	0.058	0.508	0.252	0.054	0.008	0.005	0.008	0.084	0.015	0.001	0.000	0.000	0.998	6.000
Un 80 LH-8a - C2 MZ Wrim	1693	0.14	3.65	34.29	18.42	4.44	0.79	0.28	0.21	5.93	0.93	0.05	0.09	0.00	29.64	98.86	0.006	0.050	0.486	0.268	0.065	0.034	0.003	0.004	0.086	0.012	0.000	0.001	0.000	0.996	6.011
Un 81 LH-8a - D1 MZ core	1694	0.26	5.32	40.91	13.61	2.54	0.02	0.69	0.36	5.18	1.61	0.06	0.09	0.00	29.26	99.91	0.010	0.073	0.583	0.199	0.037	0.001	0.006	0.008	0.075	0.021	0.001	0.001	0.000	0.988	6.003
Un 82 LH-8a - D1 MZ Wrim	1695	0.23	4.32	35.45	17.11	3.68	0.37	0.55	0.40	5.38	1.18	0.09	0.12	0.01	29.12	97.98	0.009	0.060	0.510	0.252	0.055	0.016	0.005	0.009	0.079	0.016	0.001	0.001	0.001	0.993	6.005
LH-8a Average (12 points)		**0.22**	**4.77**	**36.38**	**16.25**	**3.44**	**0.31**	**0.49**	**0.44**	**5.50**	**1.40**	**0.09**	**0.15**	**0.01**	**29.49**	**98.94**	**0.01**	**0.07**	**0.52**	**0.24**	**0.05**	**0.01**	**0.00**	**0.01**	**0.08**	**0.02**	**0.00**	**0.00**	**0.00**	**0.99**	**6.00**
Std Dev LH-8a Average		*0.10*	*0.82*	*1.83*	*1.83*	*0.54*	*0.29*	*0.14*	*0.17*	*0.37*	*0.46*	*0.03*	*0.10*	*0.05*	*0.73*	*1.09*	*0.00*	*0.01*	*0.03*	*0.03*	*0.01*	*0.01*	*0.00*	*0.00*	*0.01*	*0.01*	*0.00*	*0.00*	*0.00*	*0.01*	*0.01*
Un 83 VSG-9-2005, N34 Sunshine test	1696	0.00	2.28	13.01	31.74	13.92	0.06	0.23	1.10	4.28	2.20	0.20	0.05	0.04	30.10	99.21	0.000	0.031	0.183	0.457	0.202	0.003	0.002	0.023	0.061	0.029	0.002	0.001	0.002	1.003	5.998
Un 84 VSG92005, Sunshine B1 MZint	1697	0.03	2.37	12.64	31.83	14.30	0.04	0.07	1.04	4.24	2.29	0.15	0.13	-0.03	30.11	99.20	0.001	0.032	0.178	0.459	0.208	0.002	0.001	0.022	0.061	0.030	0.001	0.001	-0.001	1.004	5.997
Un 85 VSG92005, Sunshine B1 MZrim	1698	0.03	2.46	13.16	31.71	14.22	0.05	0.12	1.08	4.37	2.18	0.13	0.06	0.01	30.32	99.89	0.001	0.033	0.184	0.454	0.205	0.002	0.001	0.023	0.062	0.028	0.001	0.001	0.000	1.003	5.998
Un 86 VSG92005, Sunshine B2 MZint	1699	1.65	2.21	12.84	30.55	13.61	0.06	0.13	1.01	4.05	1.91	0.13	0.12	1.31	29.03	98.61	0.064	0.029	0.177	0.432	0.194	0.002	0.001	0.021	0.057	0.025	0.001	0.001	0.059	0.949	6.013
Un 87 VSG92005,Sunsh B2 MZ rim	1700	0.02	2.42	12.83	31.85	14.22	0.03	0.05	1.04	4.28	2.15	0.20	0.15	-0.02	30.12	99.37	0.001	0.033	0.180	0.459	0.206	0.001	0.000	0.022	0.061	0.028	0.002	0.002	-0.001	1.003	5.998
Un 88 VSG92005,Sunsh C1 MZint	1701	0.02	2.49	12.94	31.52	14.56	0.12	0.40	1.05	4.22	2.04	0.24	0.09	0.01	30.48	100.19	0.001	0.033	0.180	0.449	0.209	0.005	0.004	0.022	0.060	0.026	0.002	0.001	0.001	1.005	5.997
Un 90 VSG92005,Sunsh C1 MZint2	1711	0.03	2.41	12.93	31.94	14.22	0.10	0.39	1.09	4.20	1.95	0.36	0.26	0.00	29.79	99.68	0.001	0.033	0.182	0.462	0.207	0.004	0.004	0.023	0.060	0.026	0.003	0.003	0.000	0.995	6.003
Un 91 VSG92005,Sunsh C1 MZ	1712	0.01	2.53	12.83	31.06	13.77	0.14	0.50	1.12	4.22	2.15	0.24	0.30	0.04	29.68	98.62	0.000	0.035	0.182	0.452	0.202	0.006	0.005	0.024	0.061	0.028	0.002	0.003	0.002	0.999	6.001
Un 92 VSG92005,Sunsh D1 MZint	1713	0.01	2.50	12.74	31.24	13.51	0.13	0.50	1.30	4.22	2.18	0.33	0.13	-0.01	30.24	99.03	0.001	0.034	0.179	0.450	0.196	0.005	0.004	0.027	0.060	0.028	0.003	0.001	0.000	1.006	5.995
Un 93 VSG92005,Sunsh D1 MZtip	1714	0.00	2.47	12.83	31.32	13.52	0.10	0.32	1.35	4.31	2.32	0.23	0.24	-0.02	30.03	99.04	0.000	0.034	0.181	0.452	0.197	0.004	0.003	0.028	0.062	0.030	0.002	0.003	-0.001	1.003	5.999
Un 94 VSG92005,Sunsh D1 MZSrim	1715	2.23	2.29	12.41	30.40	13.19	0.06	0.27	0.84	4.02	2.00	0.24	0.26	1.63	28.29	98.13	0.086	0.031	0.172	0.431	0.188	0.002	0.002	0.017	0.057	0.026	0.002	0.003	0.075	0.928	6.020
Un 96 VSG92005,Sunsh E1 MZ	1717	0.03	2.41	13.10	31.53	13.64	0.05	0.17	1.11	4.31	2.29	0.23	0.22	-0.04	30.28	99.33	0.001	0.033	0.184	0.453	0.198	0.002	0.002	0.023	0.062	0.030	0.002	0.002	-0.002	1.007	5.996
Sunshine Lode VSG92005 Aver. (12 points)		**0.34**	**2.40**	**12.86**	**31.39**	**13.89**	**0.08**	**0.26**	**1.09**	**4.23**	**2.14**	**0.22**	**0.17**	**0.24**	**29.87**	**99.19**	**0.01**	**0.03**	**0.18**	**0.45**	**0.20**	**0.00**	**0.00**	**0.02**	**0.06**	**0.03**	**0.00**	**0.00**	**0.01**	**0.99**	**6.00**
Std Dev Sunshine Lode		*0.73*	*0.10*	*0.19*	*0.48*	*0.39*	*0.04*	*0.15*	*0.13*	*0.10*	*0.13*	*0.07*	*0.08*	*0.55*	*0.60*	*0.55*	*0.03*	*0.00*	*0.00*	*0.01*	*0.01*	*0.00*	*0.00*	*0.00*	*0.00*	*0.00*	*0.00*	*0.00*	*0.03*	*0.02*	*0.01*
Un 100 07WP127B A1 MZint	1721	-0.03	0.39	6.60	33.09	24.91	0.06	0.58	-0.02	3.90	0.67	0.14	0.06	0.01	30.87	101.23	-0.001	0.005	0.091	0.467	0.354	0.003	0.005	0.000	0.055	0.009	0.001	0.001	0.000	1.007	5.995
Un 101 07WP127B A1 MZint2	1722	-0.02	0.26	6.30	32.81	25.50	0.06	0.71	0.00	3.99	0.66	0.14	0.10	0.01	30.61	101.14	-0.001	0.004	0.087	0.465	0.364	0.003	0.006	0.000	0.056	0.009	0.001	0.001	0.001	1.002	5.997
Un 102 07WP127B A2 MZ	1723	0.02	0.48	7.15	32.23	24.55	0.15	0.74	0.11	4.11	0.67	0.12	0.11	-0.02	30.44	100.85	0.001	0.006	0.099	0.458	0.351	0.006	0.007	0.002	0.058	0.009	0.001	0.001	-0.001	1.000	5.999
Un 103 07WP127B A3 MZ	1724	-0.04	0.36	6.32	33.17	24.95	0.08	0.88	0.03	4.03	0.51	0.10	0.04	-0.02	30.66	101.07	-0.001	0.005	0.087	0.470	0.356	0.004	0.008	0.001	0.057	0.007	0.001	0.000	-0.001	1.004	5.996
Un 104 07WP127B A4 MZ	1725	-0.02	0.19	6.98	33.33	24.40	0.07	0.59	0.05	4.13	0.53	0.09	0.03	-0.02	30.56	100.92	-0.001	0.003	0.097	0.473	0.349	0.003	0.005	0.001	0.058	0.007	0.001	0.000	-0.001	1.003	5.998
Un 105 07WP127B A5 MZcore	1726	-0.01	0.13	6.09	32.25	27.44	0.02	0.16	0.00	4.14	0.53	0.07	0.05	-0.03	30.57	101.42	0.000	0.002	0.084	0.456	0.391	0.001	0.001	0.000	0.058	0.007	0.001	0.000	-0.001	1.000	6.000
Un 106 07WP127B A5 MZrim	1727	0.00	0.27	6.47	32.86	26.05	0.05	0.28	-0.03	4.14	0.46	0.13	0.11	-0.01	30.82	101.61	0.000	0.004	0.089	0.463	0.369	0.002	0.002	-0.001	0.058	0.006	0.001	0.001	0.000	1.003	5.998
Un 109 07WP127B B2 MZint	1730	-0.03	0.33	6.89	33.05	24.92	0.05	0.65	0.02	4.25	0.70	0.13	0.21	0.00	30.31	101.48	-0.001	0.004	0.096	0.470	0.357	0.002	0.006	0.000	0.060	0.009	0.001	0.002	0.000	0.996	6.002
Un 110 07WP127B B2 MZrim	1731	-0.03	0.29	7.11	33.50	24.70	0.04	0.66	0.00	4.10	0.50	0.09	0.18	-0.02	30.60	101.73	-0.001	0.004	0.098	0.473	0.352	0.002	0.006	0.000	0.058	0.006	0.001	0.002	-0.001	1.000	5.999
Un 111 07WP127B C1 MZrim	1732	0.05	0.24	6.60	32.92	25.14	0.17	0.87	0.07	4.13	0.49	0.09	0.15	-0.03	30.76	101.67	0.002	0.003	0.091	0.463	0.357	0.007	0.008	0.002	0.058	0.006	0.001	0.001	-0.001	1.001	5.999
Un 112 07WP127B C2 MZcore	1733	-0.02	0.24	6.60	32.65	25.53	0.04	0.75	0.02	4.13	0.55	0.15	0.11	0.00	30.27	101.02	-0.001	0.003	0.092	0.465	0.366	0.002	0.007	0.000	0.059	0.007	0.001	0.001	0.000	0.997	6.000
Un 114 07WP127B C4 MZ	1735	0.00	0.30	6.63	32.79	25.08	0.07	0.83	0.04	4.29	0.45	0.06	0.07	-0.02	29.71	100.29	0.000	0.004	0.093	0.473	0.364	0.003	0.007	0.001	0.062	0.006	0.000	0.001	-0.001	0.991	6.005
Un 117 07WP127B D3 MZ	1738	-0.03	0.29	7.30	33.04	24.62	0.07	0.65	0.01	4.07	0.68	0.09	0.06	-0.02	30.38	101.21	-0.001	0.004	0.101	0.470	0.353	0.003	0.006	0.000	0.058	0.009	0.001	0.001	-0.001	0.999	6.000
Un 118 07WP127B E1 MZ	1739	0.06	0.38	6.89	32.47	24.71	0.26	0.74	0.13	3.99	0.72	0.12	0.04	-0.01	30.26	100.76	0.002	0.005	0.096	0.462	0.354	0.011	0.007	0.003	0.057	0.009	0.001	0.000	-0.001	0.996	6.003
07WP127B Roberts S Average (14 points)		**-0.01**	**0.30**	**6.71**	**32.87**	**25.18**	**0.09**	**0.65**	**0.03**	**4.10**	**0.58**	**0.11**	**0.09**	**-0.01**	**30.49**	**101.17**	**0.00**	**0.00**	**0.09**	**0.47**	**0.36**	**0.00**	**0.01**	**0.00**	**0.06**	**0.01**	**0.00**	**0.00**	**0.00**	**1.00**	**6.00**
Std Dev 07WP127B		*0.03*	*0.09*	*0.34*	*0.36*	*0.76*	*0.06*	*0.20*	*0.05*	*0.10*	*0.09*	*0.03*	*0.05*	*0.01*	*0.29*	*0.38*	*0.00*	*0.00*	*0.00*	*0.01*	*0.01*	*0.00*	*0.00*	*0.00*	*0.00*	*0.00*	*0.00*	*0.00*	*0.00*	*0.00*	*0.00*
Un 119 LH-12, KCV9-A MZint	1740	0.11	5.05	35.31	16.79	3.75	0.10	0.29	0.96	5.69	1.57	0.10	0.14	0.00	29.81	99.67	0.004	0.069	0.499	0.243	0.055	0.004	0.003	0.020	0.082	0.021	0.001	0.001	0.000	0.998	6.000
Un 120 LH-12, KCV9-A1 MZint	1741	0.07	4.80	35.38	17.12	3.71	0.06	0.19	0.77	5.53	1.39	0.13	0.14	0.00	29.57	98.83	0.003	0.066	0.505	0.250	0.055	0.003	0.002	0.016	0.080	0.018	0.001	0.001	0.000	1.000	6.000
Un 121 LH-12, KCV9-A2 MZcore	1742	0.04	4.85	35.48	16.95	3.67	0.04	0.24	0.67	5.78	1.33	0.11	0.16	0.02	29.82	99.18	0.002	0.066	0.503	0.247	0.054	0.002	0.002	0.014	0.084	0.018	0.001	0.002	0.001	1.003	5.998
Un 122 LH-12, KCV9-A2 MZint	1743	0.10	5.19	35.67	16.23	3.44	0.04	0.33	0.77	5.55	1.69	0.07	0.20	0.01	29.61	98.90	0.004	0.071	0.508	0.237	0.051	0.002	0.003	0.016	0.081	0.022	0.001	0.002	0.001	1.000	5.999
Un 123 LH-12, KCV9-A2 MZrim	1744	0.10	5.13	36.20	15.85	3.22	0.11	0.29	0.94	5.45	1.73	0.00	0.29	0.00	29.15	98.47	0.004	0.071	0.520	0.234	0.048	0.005	0.003	0.020	0.080	0.023	0.000	0.003	0.000	0.994	6.005
Un 124 LH-12, KCV9-A2 MZWrim	1745	0.31	4.89	35.10	16.95	3.74	0.07	0.53	0.59	5.73	1.44	0.07	0.14	0.11	29.82	99.51	0.012	0.067	0.495	0.245	0.054	0.003	0.005	0.012	0.082	0.019	0.001	0.001	0.005	0.996	5.998
Un 125 LH-12, KCV9-A3 MZint	1746	0.11	4.74	34.76	16.80	3.69	0.49	0.39	0.80	5.67	1.47	0.02	0.24	0.01	29.80	98.98	0.004	0.065	0.492	0.244	0.054	0.021	0.004	0.017	0.082	0.019	0.000	0.003	0.000	1.000	6.005
Un 126 LH-12, KCV9-A3 MZtip	1747	0.20	4.69	35.86	17.19	3.72	0.66	0.56	0.64	5.58	1.39	0.04	0.17	0.02	29.10	99.81	0.008	0.064	0.510	0.251	0.055	0.028	0.005	0.013	0.081	0.018	0.000	0.002	0.001	0.981	6.018
Un 127 LH-12, KCV9-B1 MZcore	1748	0.26	4.68	35.42	16.99	3.55	0.04	0.57	0.79	5.77	1.34	0.09	0.06	-0.01	29.13	98.65	0.010	0.065	0.508	0.250	0.052	0.002	0.005	0.017	0.084	0.018	0.001	0.001	-0.001	0.990	6.002
Un 128 LH-12, KCV9-B1 MZint	1749	0.12	5.12	35.02	15.35	3.26	0.24	0.60	0.93	5.44	1.64	0.14	0.10	0.00	29.63	97.58	0.005	0.071	0.502	0.225	0.048	0.010	0.005	0.020	0.079	0.022	0.001	0.001	0.000	1.006	5.996
Un 129 LH-12, KCV9-B1 MZrim	1750	0.17	4.34	33.99	18.05	4.21	0.15	0.57	0.63	5.75	1.27	0.12	0.14	0.02	29.17	98.59	0.007	0.060	0.487	0.265	0.062	0.006	0.005	0.013	0.084	0.017	0.001	0.002	0.001	0.992	6.004
Un 130 LH-12, KCV9-B1 MZNrim	1751	0.18	4.93	35.43	16.36	3.58	0.10	0.90	0.95	5.42	1.63	0.09	0.29	-0.02	29.53	99.35	0.007	0.068	0.504	0.238	0.053	0.004	0.008	0.020	0.079	0.021	0.001	0.003	-0.001	0.995	6.000
Un 131 LH-12, KCV9-B1 MZErim	1752	0.21	4.83	35.25	16.79	3.67	0.10	0.67	0.87	5.53	1.53	0.12	0.09	0.01	29.13	98.79	0.008	0.067	0.505	0.247	0.054	0.004	0.006	0.019	0.081	0.020	0.001	0.001	0.000	0.990	6.004
Un 134 LH-12, KCV9-D1 MZcore	1755	0.28	4.98	34.49	16.55	3.73	0.26	0.66	1.14	5.47	1.59	0.10	0.15	0.00	29.20	98.60	0.011	0.069	0.493	0.243	0.055	0.011	0.006	0.024	0.080	0.021	0.001	0.002	0.000	0.990	6.005
Un 135 LH-12, KCV9-D1 MZrim	1756	0.31	4.64	33.85	16.89	3.77	0.09	1.35	0.70	5.46	1.50	0.13	0.34	-0.02	29.60	98.61	0.012	0.064	0.482	0.247	0.055	0.004	0.012	0.015	0.079	0.020	0.001	0.004	-0.001	1.000	5.994
Un 136 LH-12, KCV9-D2 MZcore	1757	0.13	5.12	35.68	16.23	3.57	0.09	0.48	0.94	5.42	1.64	0.08	0.27	0.02	29.26	98.94	0.005	0.071	0.511	0.238	0.053	0.004	0.004	0.020	0.079	0.022	0.001	0.003	0.001	0.993	6.004
Un 137 LH-12, KCV9-D2 MZrim	1758	0.09	5.18	35.11	16.44	3.61	0.08	0.35	0.71	5.59	1.70	0.13	0.17	-0.02	29.89	99.05	0.003	0.071	0.498	0.239	0.053	0.004	0.003	0.015	0.081	0.022	0.001	0.002	-0.001	1.005	5.996
Un 139 LH-12, KCV9-E1 MZrim	1760	0.16	4.92	35.12	16.59	3.53	0.12	0.43	0.81	5.66	1.54	0.10	0.11	0.00	29.68	98.76	0.006	0.067	0.499	0.242	0.052	0.005	0.004	0.017	0.082	0.020	0.001	0.001	0.000	1.001	5.998
LH-12, kcv-9 Average (18 points)		**0.16**	**4.89**	**35.17**	**16.67**	**3.63**	**0.16**	**0.52**	**0.81**	**5.58**	**1.52**	**0.09**	**0.18**	**0.01**	**29.49**	**98.90**	**0.01**	**0.07**	**0.50**	**0.24**	**0.05**	**0.01**	**0.00**	**0.02**	**0.08**	**0.02**	**0.00**	**0.00**	**0.00**	**1.00**	**6.00**
Std Dev LH-12		*0.08*	*0.22*	*0.58*	*0.56*	*0.21*	*0.16*	*0.27*	*0.14*	*0.12*	*0.14*	*0.04*	*0.08*	*0.03*	*0.28*	*0.49*	*0.00*	*0.00*	*0.01*	*0.01*	*0.00*	*0.01*	*0.00*	*0.00*	*0.00*	*0.00*	*0.00*	*0.00*	*0.00*	*0.01*	*0.01*

AVERAGES:

	Line Numbe	SiO2 Oxi	Sm2O3 O	Nd2O3 Oxi	Ce2O3 O	La2O3 O	CaO Oxi	ThO2 Ox	Y2O3 Oxi	Pr2O3 O	Gd2O3 O	UO2 Ox	PbO Oxid	Al2O3 Ox	P2O5 Oxid	Oxide Totals	Si Form	Sm Form	Nd Form	Ce Form	La Formu	Ca Formu	Th Form	Y Formu	Pr Form	Gd Form	U Formu	Pb Form	Al Form	P Form	Formula Totals
LH12c2 Average (27 points)		0.32	5.01	34.94	16.19	3.40	0.31	0.63	0.88	5.44	1.43	0.09	0.08	0.05	29.29	98.05	0.01	0.07	0.50	0.24	0.05	0.01	0.01	0.02	0.08	0.02	0.00	0.00	0.00	0.99	6.00
LH06-24A Average (14 points)		0.35	5.08	36.59	15.16	2.77	0.15	0.56	0.62	5.50	1.32	0.09	0.17	0.08	29.13	97.57	0.01	0.07	0.53	0.22	0.04	0.01	0.01	0.01	0.08	0.02	0.00	0.00	0.00	0.99	6.00
LH-8a Average (12 points)		0.22	4.77	36.38	16.25	3.44	0.31	0.49	0.44	5.50	1.40	0.09	0.15	0.01	29.49	98.94	0.009	0.066	0.518	0.237	0.051	0.013	0.004	0.009	0.080	0.018	0.001	0.001	0.001	0.995	6.004
LH-12, kcv-9 Average (18 points)		0.16	4.89	35.17	16.67	3.63	0.16	0.52	0.81	5.58	1.52	0.09	0.18	0.01	29.49	98.90	0.007	0.067	0.501	0.244	0.053	0.007	0.005	0.017	0.081	0.020	0.001	0.002	0.000	0.996	6.001
Sunshine Lode VSG92005 Aver. (12 points)		0.34	2.40	12.86	31.39	13.89	0.08	0.26	1.09	4.23	2.14	0.22	0.17	0.24	29.87	99.19	0.01	0.03	0.18	0.45	0.20	0.00	0.00	0.02	0.06	0.03	0.00	0.00	0.01	0.99	6.00
07WP127B Roberts S Average (14 points)		-0.01	0.30	6.71	32.87	25.18	0.09	0.65	0.03	4.10	0.58	0.11	0.09	-0.01	30.49	101.17	0.000	0.004	0.093	0.466	0.360	0.004	0.006	0.001	0.058	0.007	0.001	0.001	-0.001	1.000	5.999

	Y2O3 Oxide	La2O3 O	Ce2O3 O	Pr2O3 Oxi	Nd2O3 O	Sm2O3 O	Eu	Gd2O3 O	ThO2 Oxi	UO2 Oxi	PbO Oxi	CaO Ox	SiO2 Oxi	Al2O3 Ox	P2O5 Oxid	Oxide Totals
LH12c2 Average (27 points)	0.88	3.40	16.19	5.44	34.94	5.01	NA	1.43	0.63	0.09	0.08	0.31	0.32	0.05	29.29	98.05
LH06-24A Average (14 points)	0.62	2.77	15.16	5.50	36.59	5.08	NA	1.32	0.56	0.09	0.17	0.15	0.35	0.08	29.13	97.57
LH-8a Average (12 points)	0.44	3.44	16.25	5.50	36.38	4.77	NA	1.40	0.49	0.09	0.15	0.31	0.22	0.01	29.49	98.94
LH-12, kcv-9 Average (18 points)	0.81	3.63	16.67	5.58	35.17	4.89	NA	1.52	0.52	0.09	0.18	0.16	0.16	0.01	29.49	98.90
Sunshine Lode VSG92005 Aver. (12 poin	1.09	13.89	31.39	4.23	12.86	2.40	NA	2.14	0.26	0.22	0.17	0.08	0.34	0.24	29.87	99.19
07WP127B Roberts S Average (14 point	0.03	25.18	32.87	4.10	6.71	0.30	NA	0.58	0.65	0.11	0.09	0.09	-0.01	-0.01	30.49	101.17

APPENDIX C4 - Lemhi Carbonates	Line	MgO Ox	FeO Oxi	MnO Ox	CaO Oxi	BaO Oxi	SrO Oxi	SiO2 Oxi	Ce2O3 O	Oxide Tot	Mg For	Fe Form	Mn For	Ca For	Ba For	Sr Form	Si Form	Ce Form	Formula Totals
Un 6 07WP127B C1 carbonate- *Roberts South*	38	11.02	4.18	1.58	37.83	0.04	0.17	-0.01	0.09	100.10	0.266	0.057	0.022	0.656	0.000	0.002	0.000	0.001	5.001
Un 7 07WP127B C3 carbonate-	39	17.54	6.16	1.86	27.72	-0.03	0.34	-0.03	0.03	99.80	0.415	0.082	0.025	0.472	0.000	0.003	0.000	0.000	4.999
Un 8 07WP127B C4 clear carb	40	17.28	6.39	1.53	28.01	-0.03	0.32	-0.01	0.08	99.74	0.410	0.085	0.021	0.477	0.000	0.003	0.000	0.000	4.998
Un 9 07WP127B C1 clear carb	41	5.77	2.79	1.68	44.54	0.05	0.20	0.00	-0.03	99.60	0.142	0.038	0.023	0.787	0.000	0.002	0.000	0.000	4.996
Un 10 07WP127B C5 MZ?	42	-0.03	-0.42	-0.05	0.06	-13.59	0.09	0.02	35.85	73.34	-0.001	-0.007	-0.001	0.001	-0.103	0.001	0.000	0.255	4.509
Un 11 07WP127B A5 clear carb	43	0.06	0.90	2.42	54.40	0.05	0.05	-0.01	0.00	101.16	0.001	0.013	0.034	0.975	0.000	0.001	0.000	0.000	5.012
Un 12 07WP127B A5 dusty carb	44	17.43	6.56	1.57	27.76	0.02	0.28	-0.02	0.03	99.80	0.413	0.087	0.021	0.473	0.000	0.003	0.000	0.000	4.998
Un 13 07WP127B A6 dusty carb	45	0.37	0.44	1.13	53.25	0.01	0.10	-0.01	0.15	99.43	0.009	0.006	0.016	0.955	0.000	0.001	0.000	0.001	4.994
Un 14 07WP127B B5 dusty carb	46	1.12	0.93	1.07	51.92	-0.05	0.13	0.42	0.05	99.76	0.028	0.013	0.015	0.924	0.000	0.001	0.007	0.000	4.991
Un 15 07WP127B B6 dusty carb	47	0.45	1.40	0.90	51.60	0.03	0.09	1.85	0.03	100.63	0.011	0.019	0.013	0.908	0.000	0.001	0.030	0.000	4.976
Un 16 07WP127B B7 big clear carb	48	17.02	6.11	1.97	28.21	-0.09	0.22	-0.05	0.00	99.60	0.404	0.081	0.027	0.481	-0.001	0.002	-0.001	0.000	4.997
Un 17 07WP127B B8 clear pink?carb	49	17.02	6.04	1.68	28.26	0.00	0.18	-0.03	0.11	99.50	0.404	0.080	0.023	0.482	0.000	0.002	0.000	0.001	4.995
Un 18 07WP127B B9 small Ce min	50	-0.06	-0.23	0.07	0.31	-12.86	-0.02	0.14	35.54	73.78	-0.002	-0.004	0.001	0.006	-0.098	0.000	0.003	0.254	4.515
Un 19 07WP127B B10 dusty carb	51	16.70	6.59	1.66	27.79	0.05	0.19	-0.04	0.04	99.21	0.397	0.088	0.022	0.475	0.000	0.002	-0.001	0.000	4.993
Un 20 07WP127B F1 dusty carb	52	0.28	0.69	1.52	52.40	-0.01	0.18	0.17	0.06	99.32	0.007	0.010	0.022	0.940	0.000	0.002	0.003	0.000	4.990
Un 21 07WP127B F2 clear carb	53	15.97	7.72	1.76	27.66	-0.05	0.59	-0.06	0.03	99.47	0.383	0.104	0.024	0.476	0.000	0.006	-0.001	0.000	4.996
Un 22 07WP127B F2 big clear carb	54	16.38	6.96	2.09	27.71	0.02	0.39	-0.07	0.04	99.48	0.391	0.093	0.028	0.475	0.000	0.004	-0.001	0.000	4.996
Un 23 07WP127B F3 big clear carb	55	16.81	6.77	1.71	27.89	0.05	0.36	-0.05	0.14	99.68	0.400	0.090	0.023	0.477	0.000	0.003	-0.001	0.001	4.997
Un 24 07WP127B F4 semi clear carb	56	14.05	5.93	2.02	32.31	0.00	0.35	0.00	0.13	100.22	0.337	0.080	0.027	0.557	0.000	0.003	0.000	0.001	5.002
Un 29 07WP120b A3 unk clear rim *LH sill*	61	30.07	19.20	0.47	1.89	-0.01	0.00	1.71	0.04	100.92	0.684	0.245	0.006	0.031	0.000	0.000	0.026	0.000	4.983
Un 31 07WP120b B1a unk dusty rim	63	28.08	15.37	0.33	0.76	0.04	0.05	6.60	-0.01	100.71	0.615	0.189	0.004	0.012	0.000	0.000	0.097	0.000	4.910
Un 36 07WP120b C1 Carbonate Vein	68	17.49	6.31	0.37	28.88	0.11	0.30	-0.02	-0.05	99.72	0.413	0.084	0.005	0.490	0.001	0.003	0.000	0.000	4.998
Un 37 07WP120b C2 Carbonate Vein	69	17.21	6.23	0.34	29.67	-0.02	0.31	-0.05	-0.04	99.90	0.407	0.083	0.005	0.504	0.000	0.003	-0.001	0.000	5.000
Un 38 07WP120b C3 Carbonate Vug Xstal	70	18.42	4.83	0.62	29.09	-0.01	0.04	0.05	-0.05	99.72	0.432	0.063	0.008	0.490	0.000	0.000	0.001	0.000	4.997
Un 39 07WP120b C4 Carbonate Vug Xstal	71	18.06	5.38	0.55	28.82	0.02	0.10	-0.01	0.04	99.56	0.425	0.071	0.007	0.487	0.000	0.001	0.000	0.000	4.996
Un 40 07WP120b C5 later Carbonate Vug fill	72	18.35	5.34	0.58	28.14	0.04	0.11	-0.02	-0.08	99.25	0.431	0.071	0.008	0.476	0.000	0.001	0.000	0.000	4.993
Un 41 07WP120b C6 innermost Carbonate Vug fi	73	18.11	5.21	0.74	29.38	-0.01	0.09	-0.01	0.00	100.00	0.425	0.069	0.010	0.496	0.000	0.001	0.000	0.000	5.000
Un 42 LH06-23B A1 unk gray *LH sill*	74	31.50	18.04	0.26	1.14	-0.02	0.01	2.28	0.00	101.24	0.707	0.227	0.003	0.018	0.000	0.000	0.034	0.000	4.978
Un 43 LH06-23B A1a unk gray	75	31.19	18.37	0.47	0.58	0.02	-0.01	0.14	0.00	98.77	0.718	0.237	0.006	0.010	0.000	0.000	0.002	0.000	4.986
Un 45 LH06-23B B1 unk gray rhomb	77	29.88	19.51	0.48	1.48	0.07	0.07	1.06	-0.07	100.03	0.686	0.251	0.006	0.024	0.000	0.001	0.016	0.000	4.984
Un 46 LH06-23B B1a unk gray rhomb	78	29.07	16.69	0.65	4.41	0.03	0.04	1.30	-0.09	99.92	0.664	0.214	0.008	0.072	0.000	0.000	0.020	0.000	4.980
Un 47 LH06-23B B1b unk gray rhomb tip	79	16.44	5.24	0.75	29.99	0.04	0.29	0.22	0.00	99.39	0.389	0.070	0.010	0.510	0.000	0.003	0.004	0.000	4.991
Un 48 LH06-23B C1 unk gray replace	80	17.06	4.99	0.05	24.84	0.08	0.38	8.23	0.08	103.75	0.374	0.061	0.001	0.391	0.000	0.003	0.121	0.000	4.915
Un 50 LH06-23B D1 Vug carb	82	23.15	28.24	0.55	2.95	-0.02	0.02	0.00	0.03	100.06	0.559	0.383	0.008	0.051	0.000	0.000	0.000	0.000	5.001
Un 53 LH06-23B E1 Unk gray clear	85	29.27	19.22	0.24	0.37	0.01	0.05	4.69	0.10	102.07	0.651	0.240	0.003	0.006	0.000	0.000	0.070	0.001	4.950
Un 54 LH06-23B F1 Unk gray clear	86	31.64	11.94	0.24	6.00	0.12	0.04	1.98	-0.01	100.65	0.705	0.149	0.003	0.096	0.001	0.000	0.030	0.000	4.977
Un 55 LH06-23B F2 Carb vein	87	17.05	5.19	0.72	29.36	0.04	0.40	-0.01	-0.08	99.19	0.403	0.069	0.010	0.499	0.000	0.004	0.000	0.000	4.992

Analyses include CO2 in the oxide weight percent (by stoichiometry) and the structural formula

APPENDIX D1 - Sample Locations - SHRIMP Detrital Zircon and Syenite Samples at Lemhi Pass

Sample No.	Lithology	Waypoint	NAD 27 Zone (NAD 27)	Easting (m)	Northing (m)	Comments	
DZ-LP1	Quartzite - wk. rust; not analysed	73	12	304616	4981581	Gunsight Fm. ?	Copper Qn FT Stop 6 (wk. alt.)
DZ-LP2	Quartzite - fresher	74	12	304590	4981545	Gunsight Fm. ?	Copper Qn FT Stop 6 fresher
DZ-LP3	Silicified arg. Siltite?	77	12	303405	4984801	Apple Creek/Gunsight???	Lucky Horseshoe Adit 2 portal
DZ-LP4	Argill.-Siltite; not analysed	87	12	306102	4983918	Siltite-Argill.	Lemhi Pass/Horseshoe Bend Crk. Outcrop
JA06-01	Syenite - fresh feldspars	88	12	306554	4981060	Large trench, N end, Sec. 23, W of Cont. Divide road cut by sparse quartz-specular hematite veins	

DZ samples collected by Virginia Gillerman, 2006
JA sample collected by Jeremy Alexander, 2006

<u>Description</u>

DZ-LP-2	Quartzite-gray, planar laminated. Gunsight Fm. (Lund)	
DZ-LP-3	Quartzite-silicified, veined, LuckyHorseshoe Adit. AppleCrk?? Or Gunsight??	
JA-06-01	"Syenite" Intrusive-abund.FeOx, K-feldspar alteration	alkali feldspars fresh

APPENDIX D2: LEMHI PASS SAMPLE JA06-1 : SYENITE WITH ZIRCONS

JA06-1

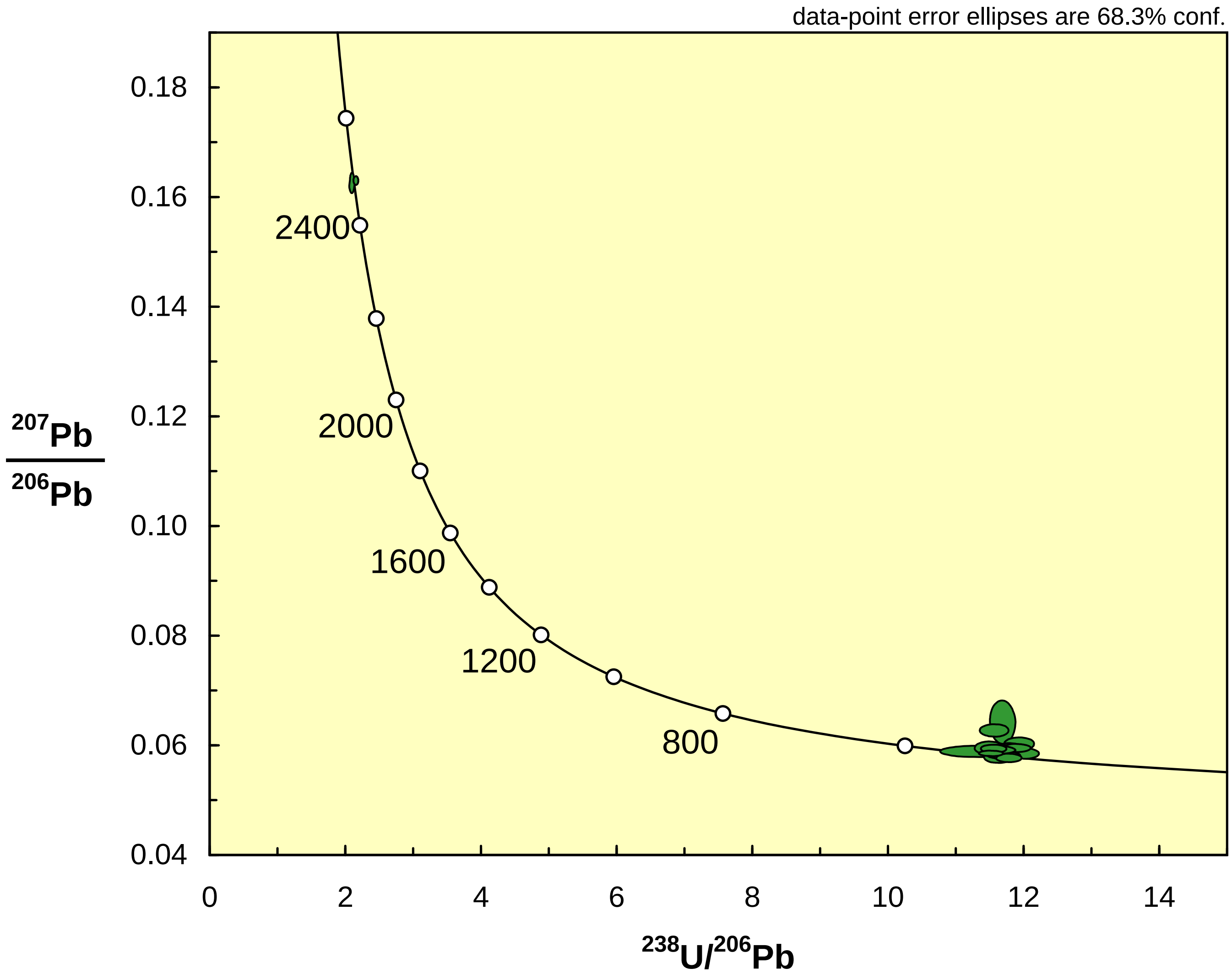
data-point error ellipses are 68.3% conf.
2400
2000
1600
1200
800
0.18
0.16
0.14
0.12
0.10
0.08
0.06
0.04
0
2
4
6
8
10
12
14
207Pb/206Pb
238U/206Pb

JA06-1

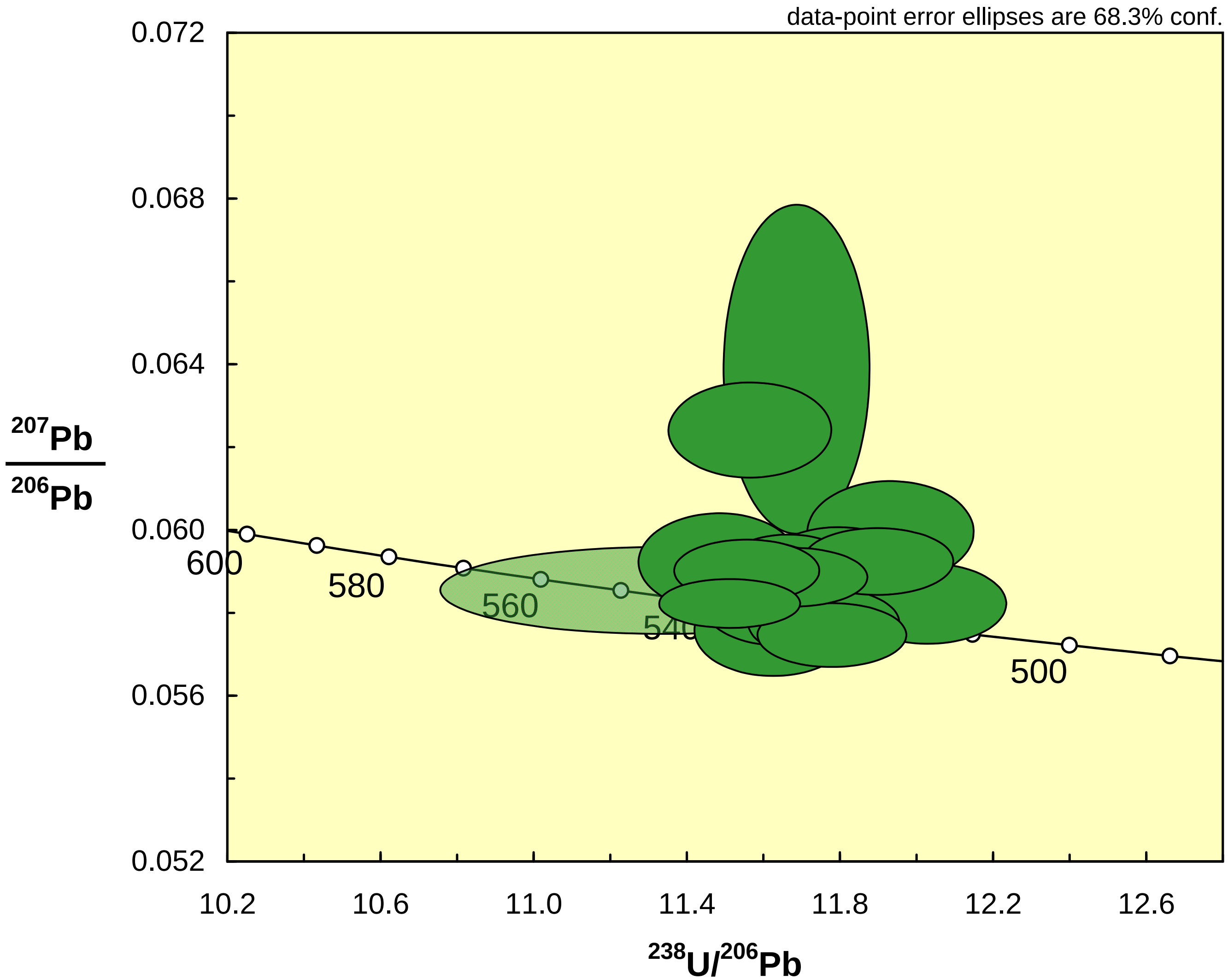

data-point error ellipses are 68.3% conf.
0.072
0.068
0.064
0.060
0.056
0.052
$^{207}Pb/^{206}Pb$
600
580
560
540
500
10.2
10.6
11.0
11.4
11.8
12.2
12.6
$^{238}U/^{206}Pb$

JA06-1

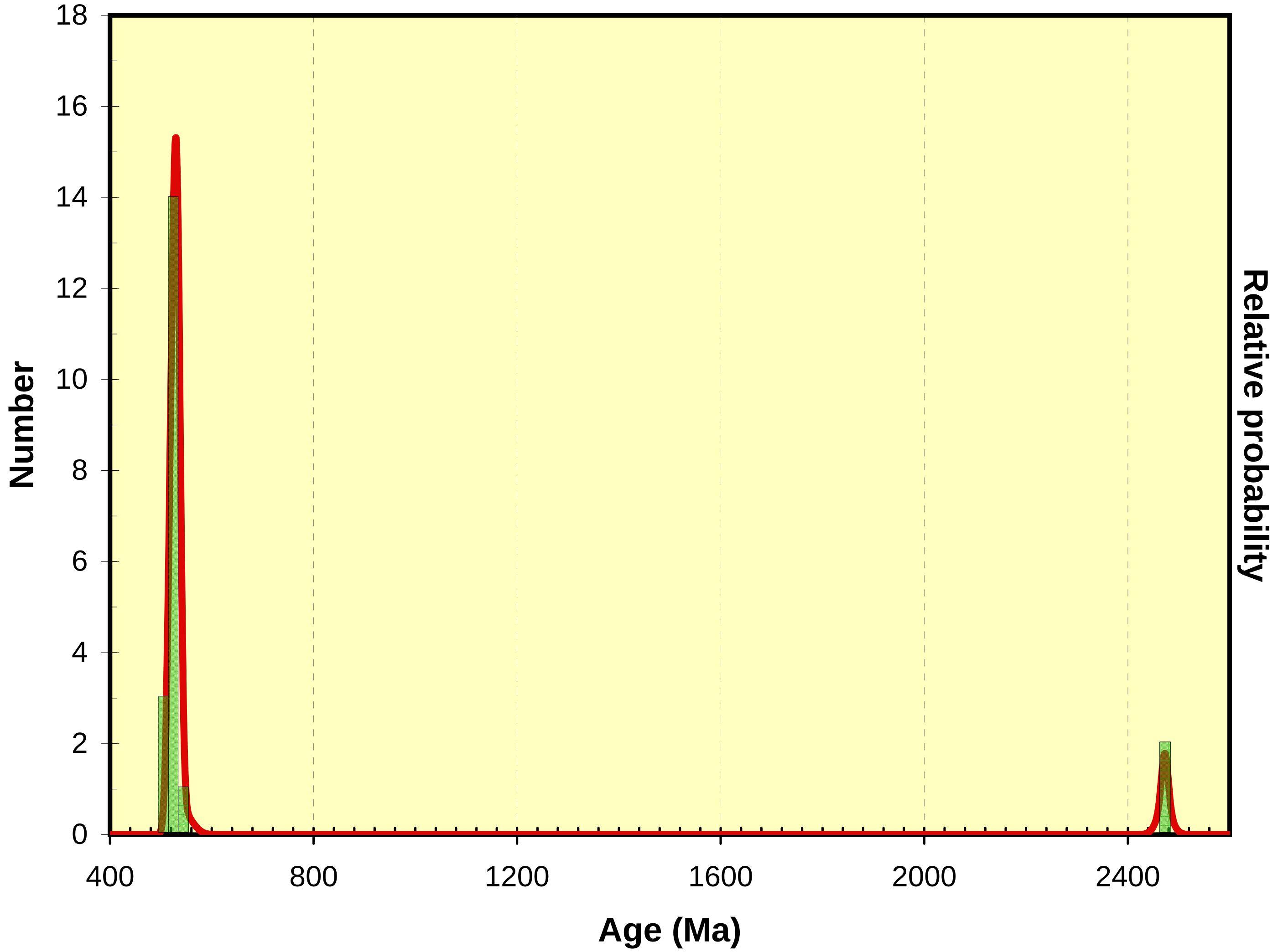

18
16
14
12
10
8
6
4
2
0
Number
Relative probability
400
800
1200
1600
2000
2400
Age (Ma)

JA06-1

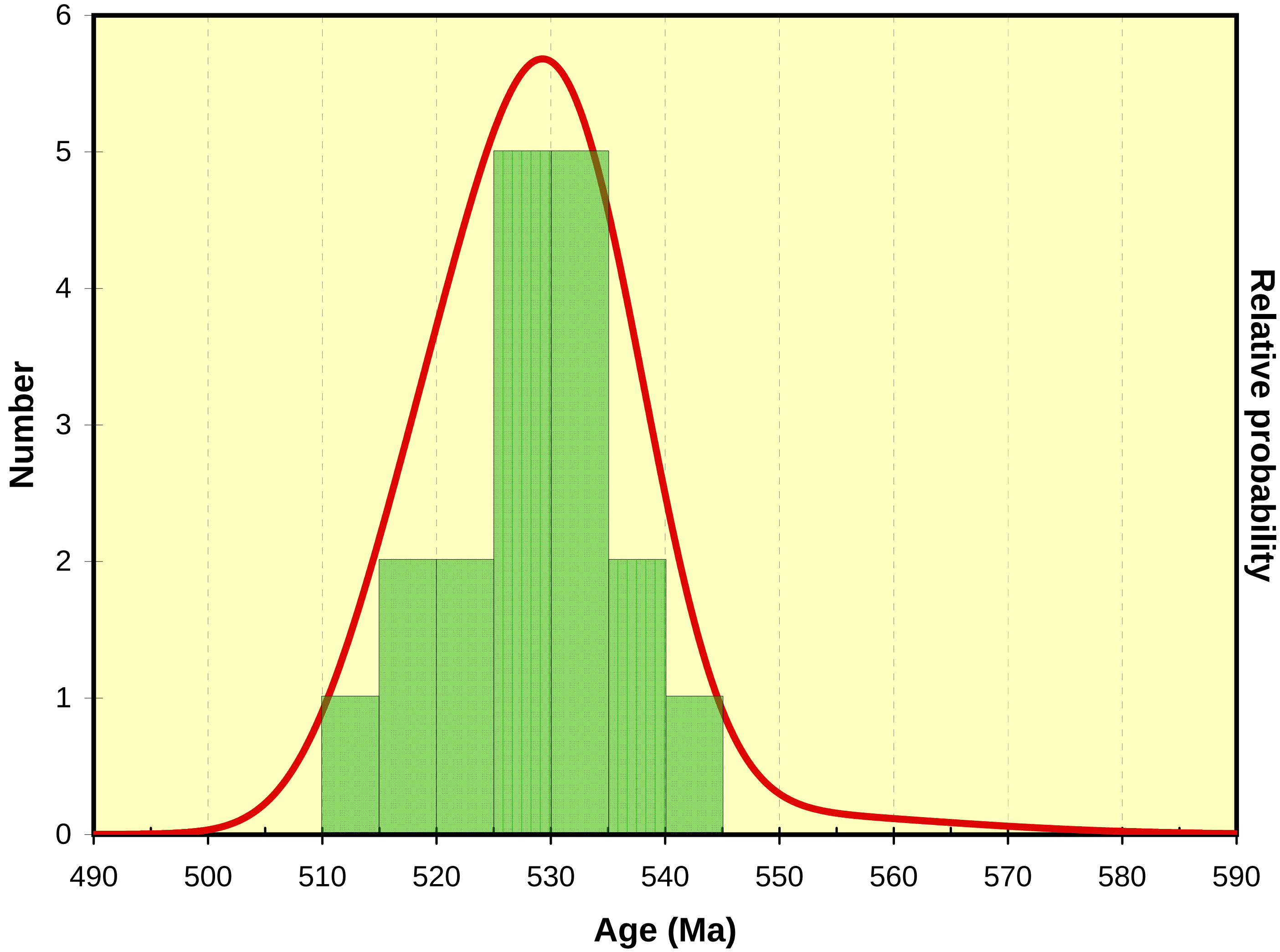

Number
Relative probability
Age (Ma)
0
1
2
3
4
5
6
490
500
510
520
530
540
550
560
570
580
590

JA06-1

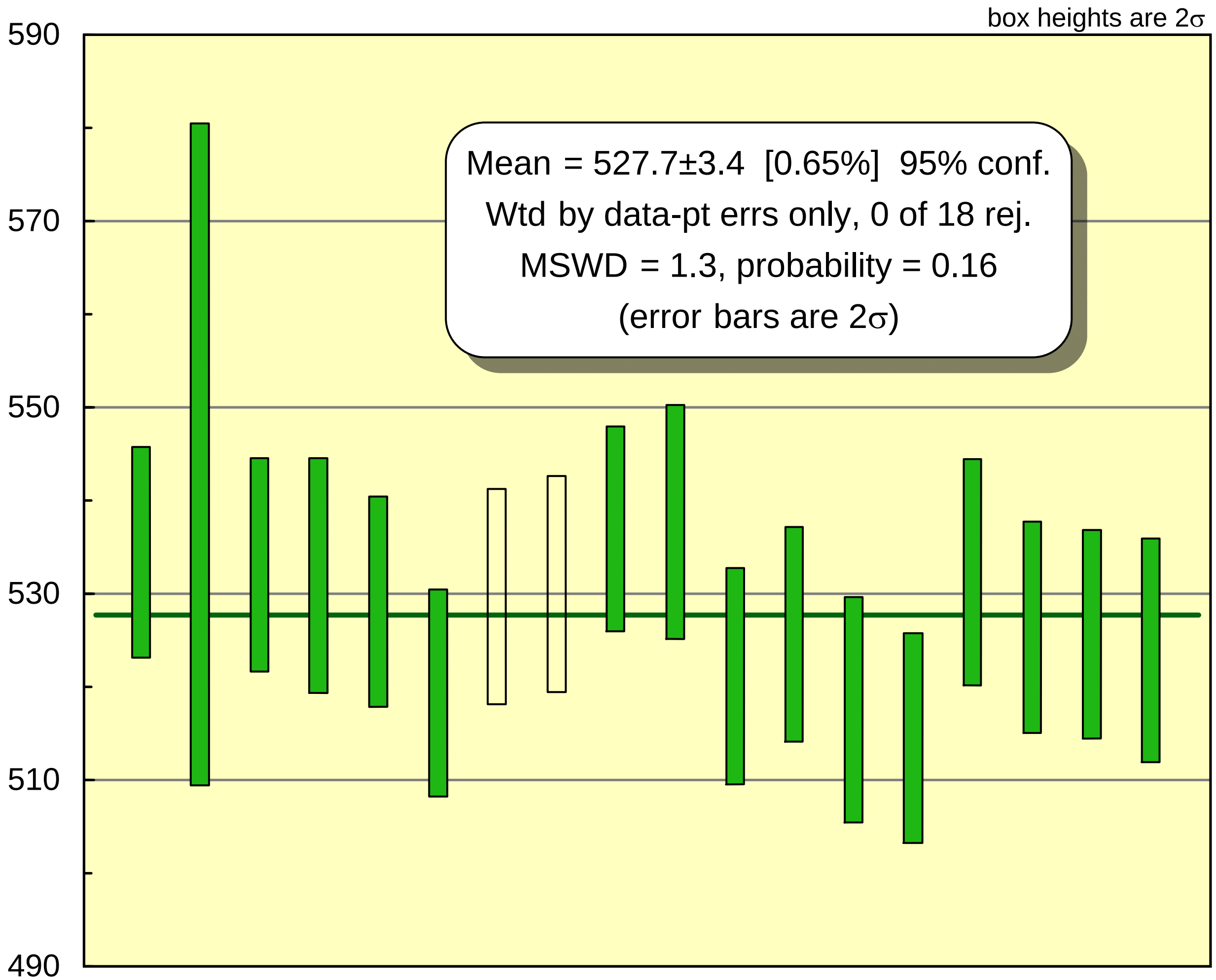

box heights are 2σ
590
570
550
530
510
490
Mean = 527.7±3.4 [0.65%] 95% conf.
Wtd by data-pt errs only, 0 of 18 rej.
MSWD = 1.3, probability = 0.16
(error bars are 2σ)

JA06-1

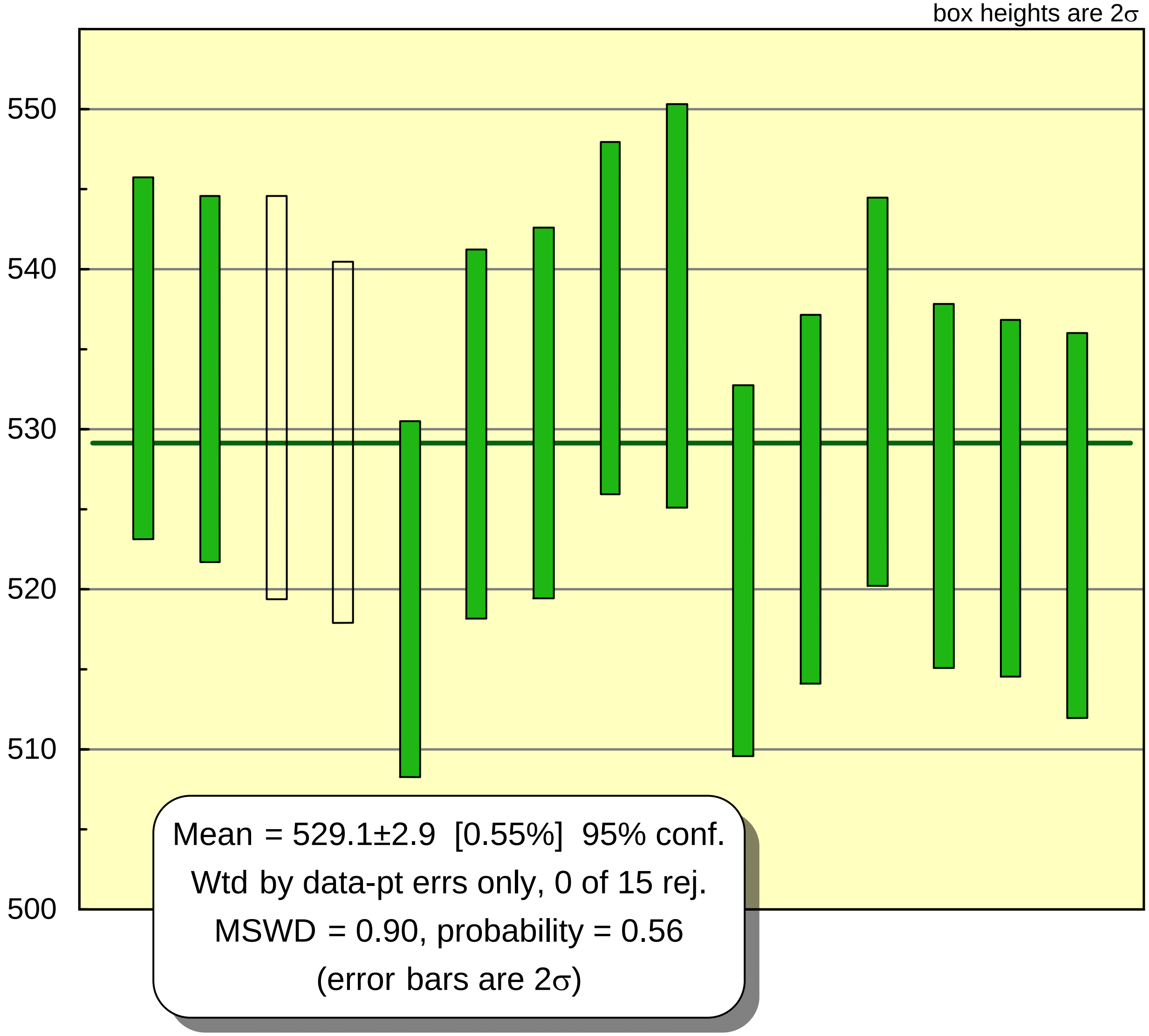
box heights are 2σ
550
540
530
520
510
500
Mean = 529.1±2.9 [0.55%] 95% conf.
Wtd by data-pt errs only, 0 of 15 rej.
MSWD = 0.90, probability = 0.56
(error bars are 2σ)

Table *xyz*. Summary of SHRIMP U-Pb zircon results for sample JA061.

Grain. spot	U (ppm)	Th (ppm)	Th/U	$^{206}Pb^*$ (ppm)	$^{204}Pb/^{206}Pb$	f_{206} %	Total Ratios $^{238}U/^{206}Pb$	±	$^{207}Pb/^{206}Pb$	±	Radiogenic Ratios $^{206}Pb/^{238}U$	±	$^{207}Pb/^{235}U$	±	$^{207}Pb/^{206}Pb$	±	ρ	Age (Ma) $^{206}Pb/^{238}U$	±	$^{207}Pb/^{206}Pb$	±	% Disc
1.1	506	485	0.96	38	0.000064	0.10	11.557	0.125	0.0590	0.0005	0.0864	0.0010						534	6			
2.1	329	290	0.88	25	0.000009	0.01	11.334	0.378	0.0585	0.0007	0.0882	0.0030						545	18			
3.1	512	440	0.86	38	-	0.08	11.589	0.127	0.0587	0.0006	0.0862	0.0010						533	6			
4.1	135	53	0.39	55	0.000071	0.10	2.110	0.026	0.1624	0.0013	0.4735	0.0057	10.545	0.155	0.1615	0.0013	0.825	2499	25	2472	14	-1
5.1	263	241	0.92	20	0.000457	0.53	11.563	0.140	0.0624	0.0008	0.0860	0.0011						532	6			
6.1	664	710	1.07	49	0.000008	0.10	11.677	0.127	0.0588	0.0005	0.0856	0.0009						529	6			
7.1	505	490	0.97	36	0.000082	0.18	11.897	0.130	0.0592	0.0005	0.0839	0.0009						519	6			
8.1	427	344	0.81	31	0.000103	0.10	11.665	0.129	0.0588	0.0007	0.0856	0.0010						530	6			
9.1	405	430	1.06	30	0.000042	0.01	11.645	0.130	0.0581	0.0006	0.0859	0.0010						531	6			
10.1	995	1440	1.45	74	0.000034	<0.01	11.513	0.121	0.0582	0.0004	0.0869	0.0009						537	6			
11.1	218	206	0.94	16	0.000136	0.12	11.482	0.137	0.0592	0.0008	0.0870	0.0011						538	6			
12.1	344	243	0.71	25	0.000042	0.10	11.864	0.135	0.0586	0.0006	0.0842	0.0010						521	6			
13.1	325	142	0.44	128	0.000098	0.14	2.178	0.024	0.1629	0.0005	0.4584	0.0050	10.217	0.119	0.1616	0.0006	0.943	2433	22	2473	7	2
14.1	1068	1633	1.53	78	0.000565	0.73	11.685	0.125	0.0639	0.0026	0.0850	0.0010						526	6			
15.1	298	255	0.86	21	0.000041	0.28	11.929	0.142	0.0599	0.0008	0.0836	0.0010						518	6			
16.1	614	774	1.26	44	0.000038	0.07	12.027	0.135	0.0582	0.0006	0.0831	0.0009						515	6			
17.1	339	301	0.89	25	-	<0.01	11.624	0.135	0.0575	0.0007	0.0861	0.0010						532	6			
17.2	591	549	0.93	43	-	<0.01	11.755	0.130	0.0577	0.0006	0.0851	0.0010						526	6			
18.1	709	581	0.82	52	0.000041	<0.01	11.777	0.128	0.0574	0.0005	0.0850	0.0009						526	6			
19.1	333	280	0.84	24	-	0.13	11.794	0.138	0.0589	0.0008	0.0847	0.0010						524	6			

Notes :

1. Uncertainties given at the one σ level.
2. Error in Temora reference zircon calibration was 0.65% for the analytical session.
   (not included in above errors but required when comparing $^{206}Pb/^{238}U$ data from different mounts).
3. f_{206} % denotes the percentage of ^{206}Pb that is common Pb.
4. For areas older than ~800 Ma correction for common Pb made using the measured $^{204}Pb/^{206}Pb$ ratio.
5. For areas younger than ~800 Ma correction for common Pb made using the measured $^{238}U/^{206}Pb$ and $^{207}Pb/^{206}Pb$ ratios
   following Tera and Wasserburg (1972) as outlined in Williams (1998).
6. For % Disc, 0% denotes a concordant analysis.

Age	± no std		**± include std**
529.1	2.9	0.85	**4.5**

Grain. spot	Preferred Age (Ma)	±	% Disc	Total Ratios $^{238}U/^{206}Pb$	±	$^{207}Pb/^{206}Pb$	±	Radiogenic Ratios $^{207}Pb/^{235}U$	±	$^{206}Pb/^{238}U$	±	ρ	$^{207}Pb/^{206}Pb$	±
1.1	534	6		11.557	0.125	0.0590	0.0005			0.0864	0.0010			
2.1	545	18		11.334	0.378	0.0585	0.0007			0.0882	0.0030			
3.1	533	6		11.589	0.127	0.0587	0.0006			0.0862	0.0010			
5.1	532	6		11.563	0.140	0.0624	0.0008			0.0860	0.0011			
6.1	529	6		11.677	0.127	0.0588	0.0005			0.0856	0.0009			
7.1	519	6		11.897	0.130	0.0592	0.0005			0.0839	0.0009			
8.1	530	6		11.665	0.129	0.0588	0.0007			0.0856	0.0010			
9.1	531	6		11.645	0.130	0.0581	0.0006			0.0859	0.0010			
10.1	537	6		11.513	0.121	0.0582	0.0004			0.0869	0.0009			
11.1	538	6		11.482	0.137	0.0592	0.0008			0.0870	0.0011			
12.1	521	6		11.864	0.135	0.0586	0.0006			0.0842	0.0010			
14.1	526	6		11.685	0.125	0.0639	0.0026			0.0850	0.0010			
15.1	518	6		11.929	0.142	0.0599	0.0008			0.0836	0.0010			
16.1	515	6		12.027	0.135	0.0582	0.0006			0.0831	0.0009			
17.1	532	6		11.624	0.135	0.0575	0.0007			0.0861	0.0010			
17.2	526	6		11.755	0.130	0.0577	0.0006			0.0851	0.0010			
18.1	526	6		11.777	0.128	0.0574	0.0005			0.0850	0.0009			
19.1	524	6		11.794	0.138	0.0589	0.0008			0.0847	0.0010			
4.1	2472	14	-1	2.110	0.026	0.1624	0.0013	10.545	0.155	0.4735	0.0057	0.825	0.1615	0.0013
13.1	2473	7	2	2.178	0.024	0.1629	0.0005	10.217	0.119	0.4584	0.0050	0.943	0.1616	0.0006

Notes :

APPENDIX D3: Sample DZ_LP_2   SHRIMP DATA
Detrital Zircon in Proterozoic Quartzite

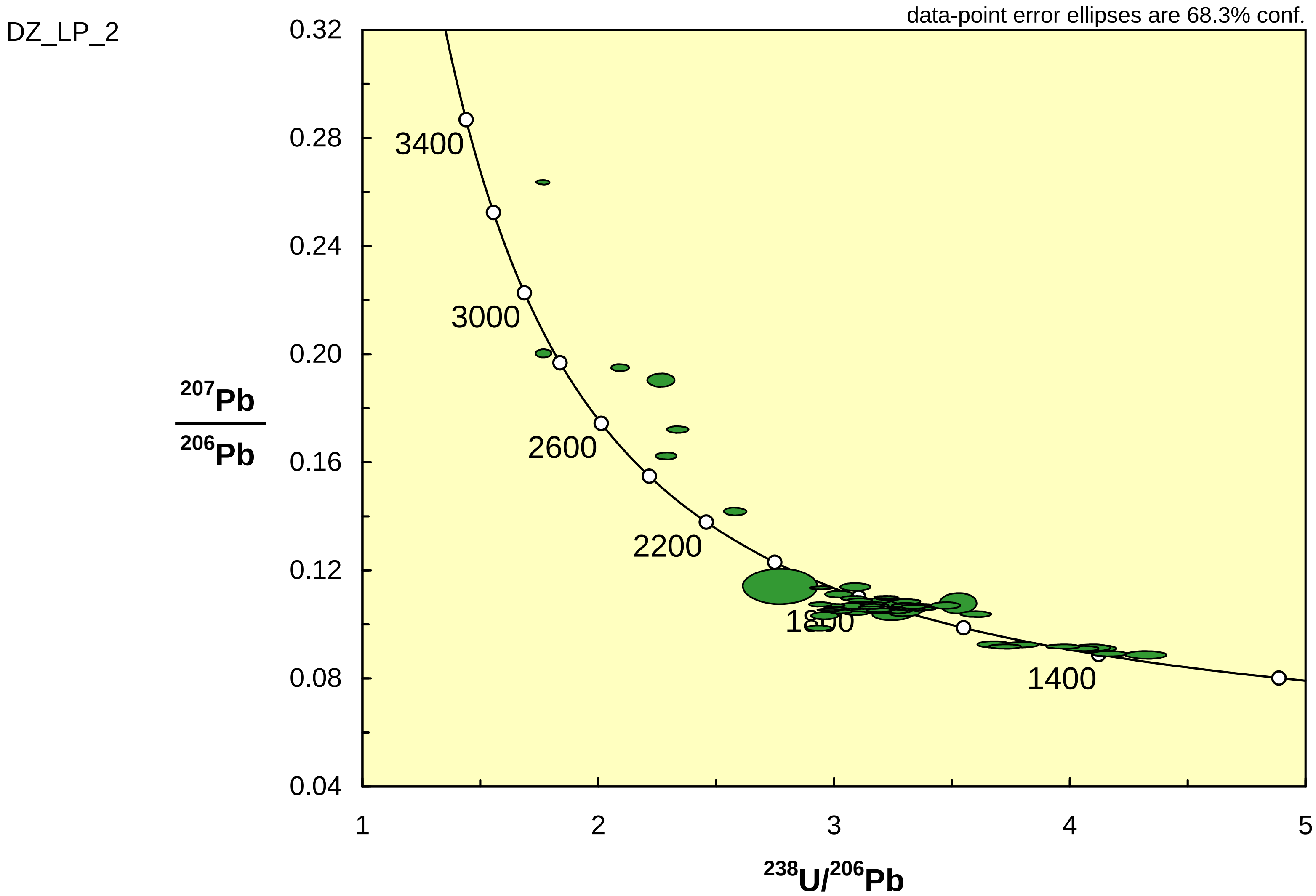
DZ_LP_2
data-point error ellipses are 68.3% conf.
0.32
0.28
0.24
0.20
0.16
0.12
0.08
0.04
3400
3000
2600
2200
1800
1400
$^{207}Pb/^{206}Pb$
1
2
3
4
5
$^{238}U/^{206}Pb$

DZ_LP_2

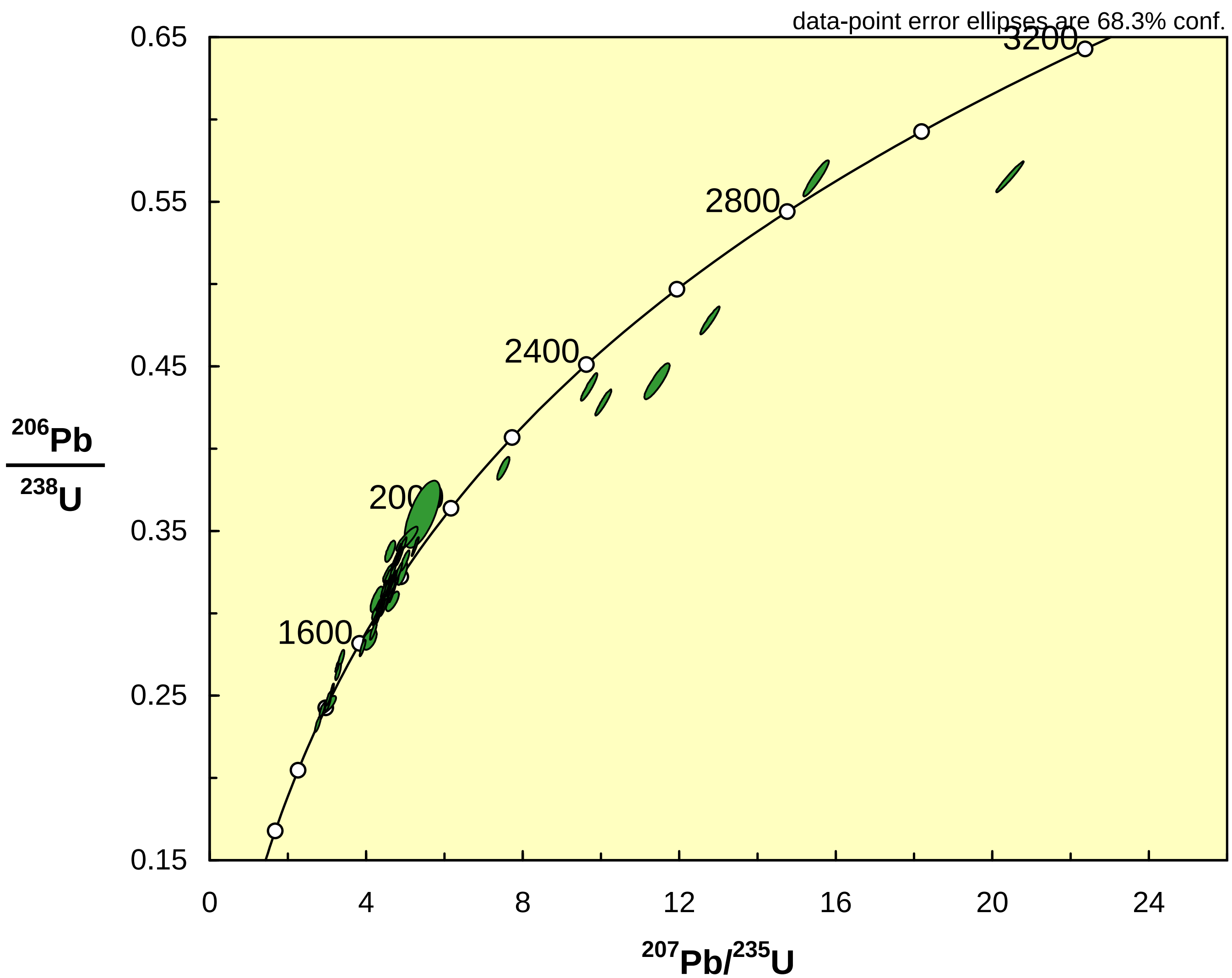
data-point error ellipses are 68.3% conf.
0.65
0.55
0.45
0.35
0.25
0.15
3200
2800
2400
2000
1600
0
4
8
12
16
20
24
$^{206}Pb/^{238}U$
$^{207}Pb/^{235}U$

DZ_LP_2

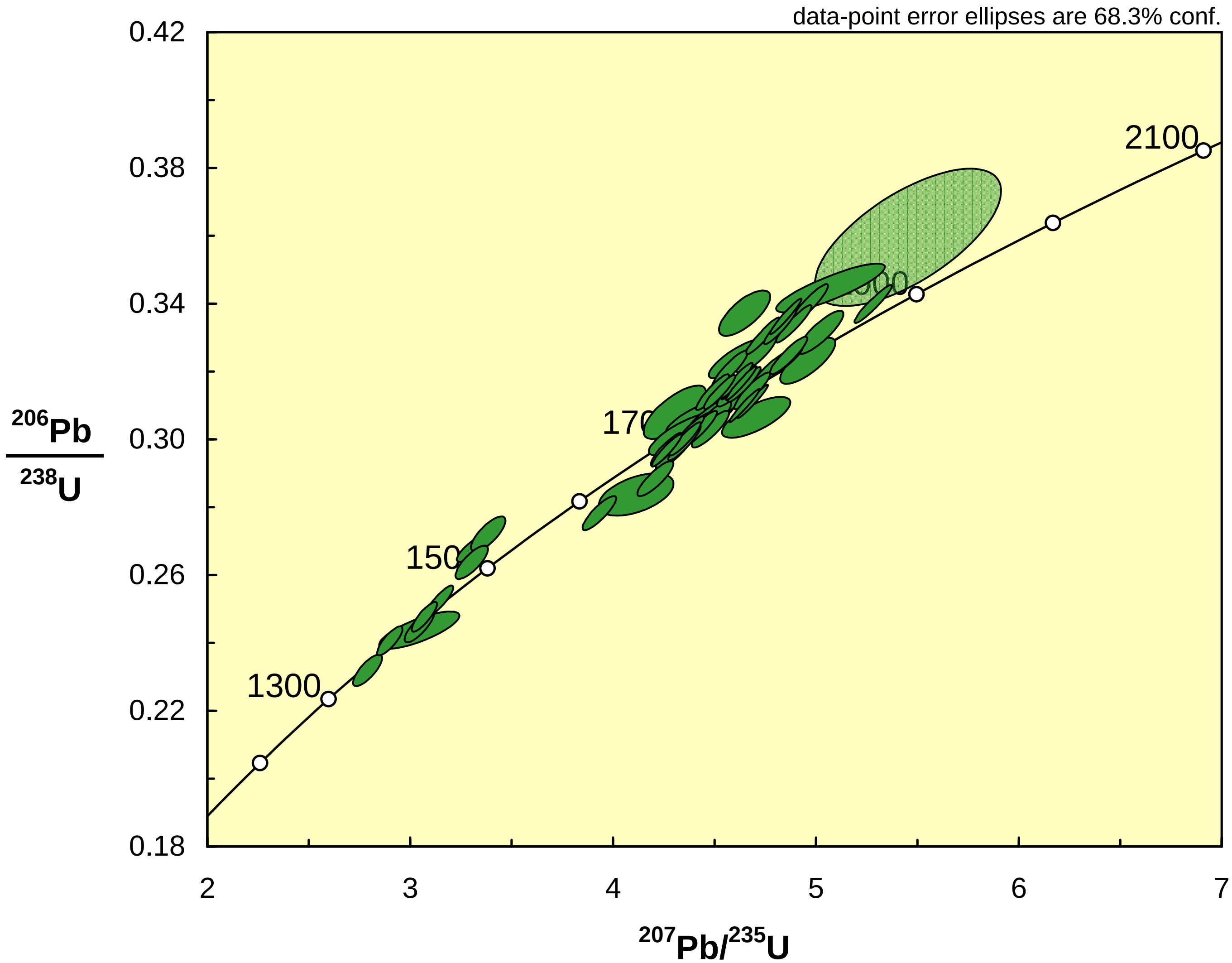

data-point error ellipses are 68.3% conf.
0.42
0.38
0.34
0.30
0.26
0.22
0.18
2100
1300
2
3
4
5
6
7
206Pb/238U
207Pb/235U

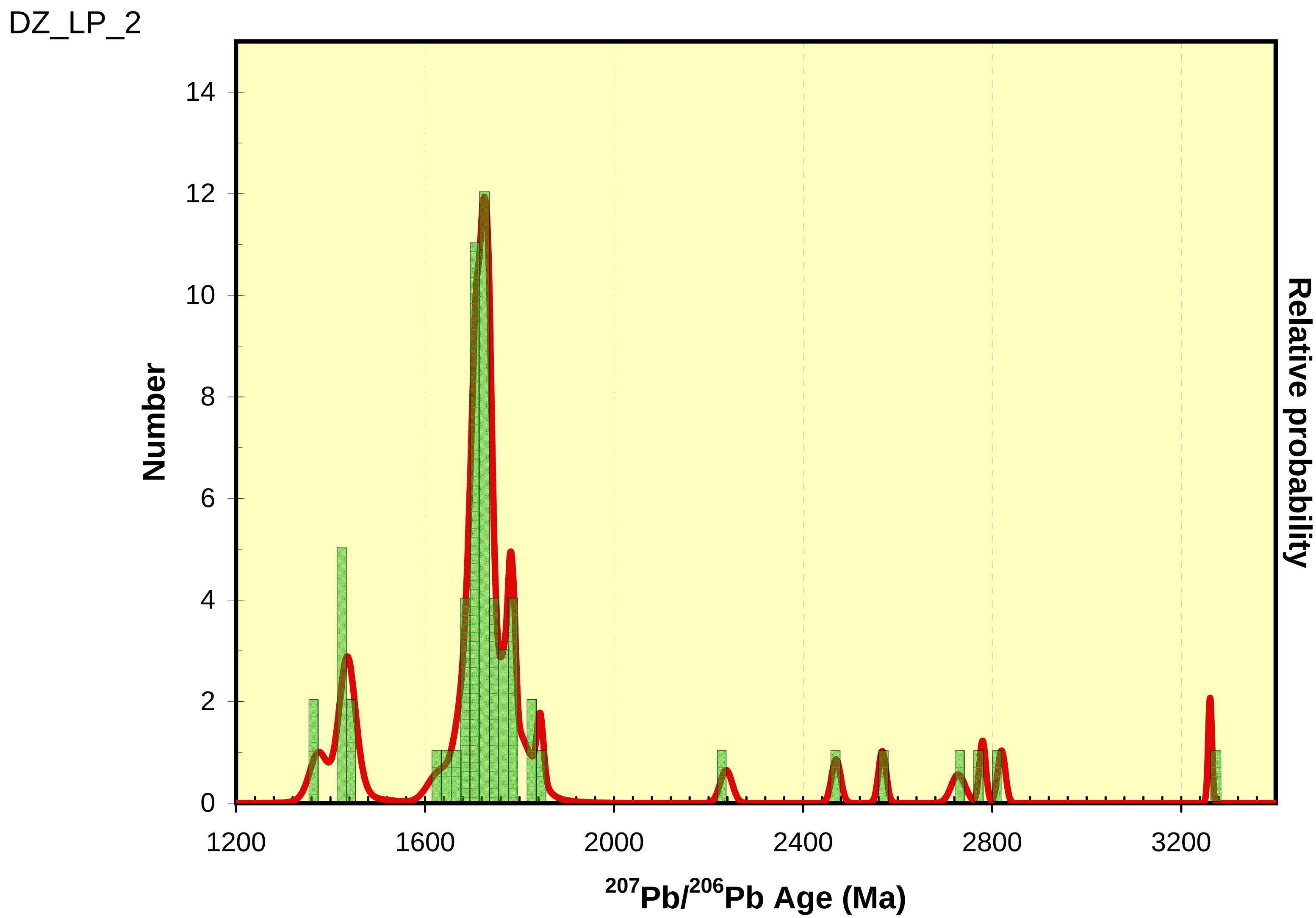

DZ_LP_2
Number
Relative probability
0
2
4
6
8
10
12
14
1200
1600
2000
2400
2800
3200
$^{207}Pb/^{206}Pb$ Age (Ma)

DZ_LP_2

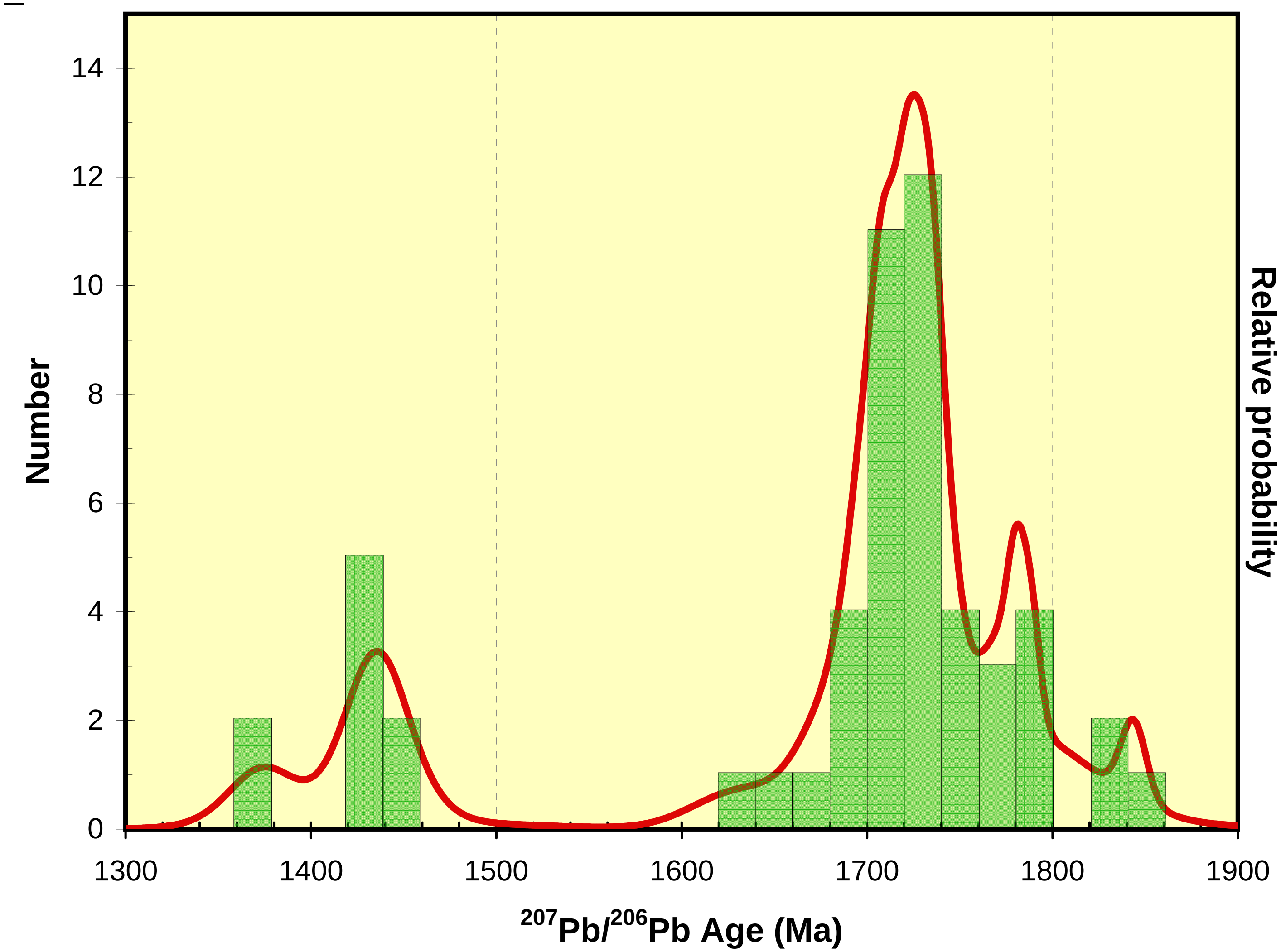

Number
Relative probability
0
2
4
6
8
10
12
14
1300
1400
1500
1600
1700
1800
1900
^{207}Pb/^{206}Pb Age (Ma)

DZ_LP_2

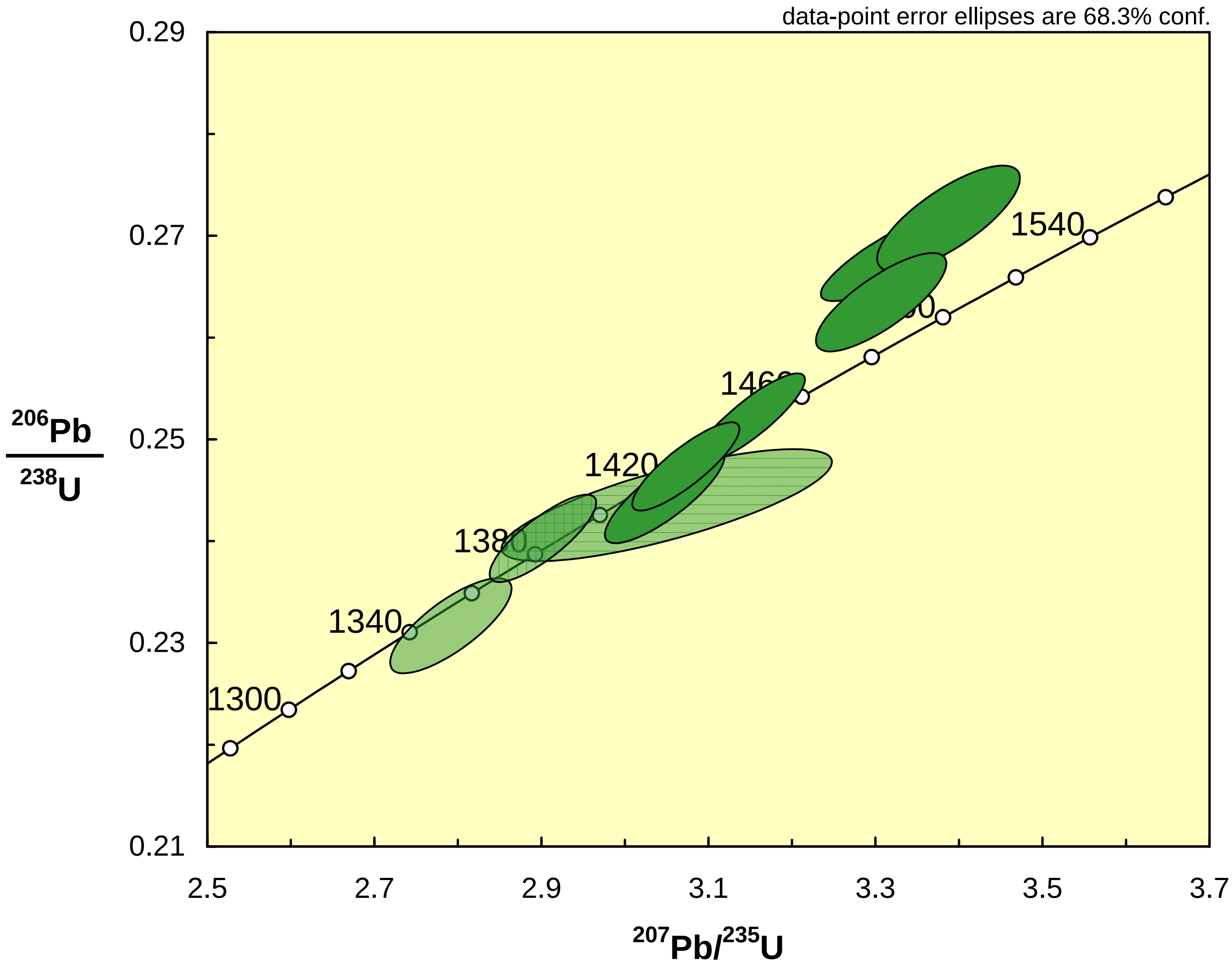
data-point error ellipses are 68.3% conf.
0.29
0.27
0.25
0.23
0.21
^{206}Pb / ^{238}U
1540
1460
1420
1380
1340
1300
2.5
2.7
2.9
3.1
3.3
3.5
3.7
$^{207}Pb/^{235}U$

Table *xyz*. Summary of SHRIMP U-Pb zircon results for sample DZ-LP-2.

							Total Ratios				Radiogenic Ratios							Age (Ma)				
Grain. spot	U (ppm)	Th (ppm)	Th/U	$^{206}Pb^*$ (ppm)	$^{204}Pb/^{206}Pb$	f_{206} %	$^{238}U/^{206}Pb$	±	$^{207}Pb/^{206}Pb$	±	$^{206}Pb/^{238}U$	±	$^{207}Pb/^{235}U$	±	$^{207}Pb/^{206}Pb$	±	ρ	$^{206}Pb/^{238}U$	±	$^{207}Pb/^{206}Pb$	±	% Disc
1.1	194	50	0.26	54	0.000092	0.14	3.071	0.037	0.1061	0.0007	0.3252	0.0039	4.703	0.069	0.1049	0.0009	0.825	1815	19	1712	15	-6
2.1	233	69	0.29	54	0.000110	0.18	3.720	0.044	0.0912	0.0006	0.2685	0.0033	3.336	0.068	0.0901	0.0011	0.855	1533	17	1428	22	-7
3.1	538	253	0.47	139	0.000012	0.02	3.315	0.036	0.1052	0.0004	0.3016	0.0033	4.369	0.050	0.1051	0.0004	0.938	1699	16	1716	7	1
4.1	129	61	0.48	37	0.000191	0.30	2.959	0.038	0.1026	0.0010	0.3369	0.0044	4.645	0.083	0.1000	0.0012	0.725	1872	21	1624	23	-15
5.1	458	101	0.22	117	0.000084	0.13	3.366	0.037	0.1054	0.0004	0.2967	0.0032	4.264	0.051	0.1042	0.0005	0.906	1675	16	1701	9	2
6.1	1512	73	0.05	433	0.000014	0.02	3.002	0.031	0.1052	0.0004	0.3331	0.0035	4.821	0.054	0.1050	0.0004	0.928	1853	17	1714	8	-8
7.1	507	138	0.27	141	0.000130	0.21	3.090	0.035	0.1037	0.0005	0.3234	0.0038	4.606	0.091	0.1033	0.0013	0.815	1806	18	1684	23	-7
8.1	177	94	0.53	73	0.000018	0.02	2.094	0.025	0.1946	0.0008	0.4773	0.0057	12.795	0.162	0.1944	0.0008	0.946	2516	25	2780	7	10
9.1	320	100	0.31	83	0.000029	0.05	3.301	0.037	0.1064	0.0005	0.3028	0.0034	4.426	0.054	0.1060	0.0005	0.913	1705	17	1732	9	2
10.1	456	271	0.59	117	0.000040	0.06	3.333	0.036	0.1059	0.0004	0.2998	0.0033	4.354	0.051	0.1053	0.0005	0.924	1690	16	1720	8	2
11.1	73	33	0.45	18	0.000149	0.23	3.521	0.052	0.1073	0.0025	0.2833	0.0042	4.114	0.120	0.1053	0.0026	0.505	1608	21	1719	46	6
12.1	139	81	0.58	29	0.000027	0.04	4.090	0.052	0.0908	0.0008	0.2444	0.0031	3.047	0.047	0.0904	0.0008	0.818	1409	16	1435	17	2
13.1	386	128	0.33	102	0.000051	0.08	3.269	0.038	0.1046	0.0005	0.3060	0.0037	4.433	0.112	0.1050	0.0019	0.748	1721	18	1715	33	0
14.1	218	117	0.54	45	0.000066	0.11	4.160	0.049	0.0886	0.0006	0.2401	0.0028	2.902	0.042	0.0877	0.0007	0.818	1387	15	1375	16	-1
15.1	237	170	0.72	50	0.000018	0.03	4.044	0.047	0.0904	0.0006	0.2472	0.0029	3.072	0.042	0.0901	0.0006	0.852	1424	15	1429	14	0
16.1	269	346	1.29	58	0.000031	0.05	3.966	0.046	0.0911	0.0006	0.2520	0.0029	3.151	0.042	0.0907	0.0006	0.863	1449	15	1440	13	-1
17.1	385	88	0.23	99	0.000032	0.05	3.348	0.038	0.1061	0.0005	0.2985	0.0034	4.349	0.053	0.1057	0.0005	0.923	1684	17	1726	9	2
18.1	173	186	1.08	63	0.000049	0.07	2.338	0.029	0.1716	0.0008	0.4273	0.0054	10.077	0.136	0.1710	0.0008	0.933	2294	24	2568	8	11
19.1	763	622	0.82	206	0.000007	0.01	3.188	0.034	0.1047	0.0004	0.3136	0.0033	4.522	0.051	0.1046	0.0004	0.932	1758	16	1707	8	-3
20.1	131	52	0.40	34	0.000111	0.18	3.319	0.042	0.1050	0.0010	0.3012	0.0041	4.338	0.107	0.1045	0.0016	0.814	1697	20	1705	29	0
21.1	1915	196	0.10	549	0.000014	0.02	2.995	0.033	0.1064	0.0005	0.3338	0.0036	4.887	0.057	0.1062	0.0005	0.931	1857	18	1735	8	-7
22.1	46	12	0.26	14	0.000262	0.41	2.772	0.104	0.1135	0.0043	0.3593	0.0134	5.447	0.303	0.1100	0.0045	0.673	1979	64	1799	75	-10
23.1	235	108	0.46	60	0.000057	0.09	3.372	0.041	0.1061	0.0006	0.2963	0.0036	4.302	0.060	0.1053	0.0007	0.878	1673	18	1720	12	3
24.1	433	195	0.45	114	0.000019	0.03	3.254	0.036	0.1040	0.0005	0.3081	0.0036	4.511	0.089	0.1062	0.0012	0.884	1731	18	1735	20	0
25.1	231	66	0.29	60	0.000034	0.05	3.303	0.039	0.1077	0.0006	0.3026	0.0036	4.476	0.061	0.1073	0.0007	0.868	1704	18	1754	12	3
26.1	283	92	0.33	79	0.000020	0.03	3.082	0.035	0.1090	0.0006	0.3244	0.0037	4.863	0.061	0.1087	0.0006	0.908	1811	18	1778	10	-2
27.1	123	85	0.70	26	0.000320	0.53	4.111	0.055	0.0905	0.0009	0.2434	0.0037	3.050	0.130	0.0909	0.0030	0.770	1404	19	1444	62	3
28.1	181	43	0.24	47	0.000120	0.19	3.296	0.042	0.1036	0.0008	0.3061	0.0040	4.703	0.111	0.1114	0.0019	0.730	1722	20	1823	30	6
29.1	381	283	0.74	185	0.000084	0.10	1.769	0.019	0.2633	0.0006	0.5648	0.0062	20.432	0.231	0.2624	0.0007	0.974	2886	26	3261	4	11
30.1	373	123	0.33	100	0.000035	0.06	3.188	0.036	0.1043	0.0005	0.3135	0.0035	4.488	0.055	0.1038	0.0005	0.910	1758	17	1694	9	-4
31.1	573	113	0.20	156	0.000014	0.02	3.157	0.034	0.1058	0.0004	0.3167	0.0034	4.610	0.053	0.1056	0.0004	0.936	1774	17	1724	7	-3
32.1	466	104	0.22	136	0.000065	0.10	2.940	0.032	0.1069	0.0005	0.3398	0.0037	4.965	0.060	0.1060	0.0005	0.913	1886	18	1731	9	-9
33.1	1221	433	0.35	326	0.000006	0.01	3.218	0.034	0.1094	0.0003	0.3107	0.0032	4.684	0.050	0.1093	0.0003	0.969	1744	16	1788	5	2
34.1	93	37	0.40	26	0.000153	0.24	3.089	0.043	0.1134	0.0010	0.3229	0.0045	4.956	0.090	0.1113	0.0013	0.767	1804	22	1821	21	1
35.1	499	167	0.34	135	0.000019	0.03	3.165	0.034	0.1069	0.0004	0.3159	0.0034	4.646	0.054	0.1067	0.0004	0.933	1770	17	1743	8	-2
36.1	249	170	0.68	94	0.000139	0.19	2.267	0.038	0.1901	0.0016	0.4404	0.0073	11.439	0.215	0.1884	0.0017	0.881	2352	33	2728	15	14
37.1	858	246	0.29	219	0.000056	0.09	3.372	0.036	0.1051	0.0003	0.2963	0.0031	4.264	0.048	0.1044	0.0004	0.941	1673	16	1703	7	2
38.1	207	47	0.23	69	0.000031	0.05	2.582	0.031	0.1412	0.0010	0.3871	0.0047	7.516	0.106	0.1408	0.0010	0.852	2110	22	2237	13	6
39.1	562	199	0.35	164	0.000024	0.04	2.944	0.032	0.1131	0.0004	0.3396	0.0037	5.278	0.060	0.1127	0.0004	0.945	1885	18	1844	7	-2
40.1	991	509	0.51	269	0.000032	0.05	3.160	0.033	0.1066	0.0003	0.3163	0.0033	4.630	0.050	0.1062	0.0003	0.962	1772	16	1735	5	-2
41.1	723	270	0.37	197	0.000029	0.05	3.153	0.033	0.1058	0.0003	0.3170	0.0034	4.609	0.051	0.1054	0.0004	0.949	1775	16	1722	6	-3
42.1	49	45	0.92	13	0.000126	0.20	3.244	0.055	0.1032	0.0014	0.3076	0.0053	4.304	0.100	0.1015	0.0016	0.733	1729	26	1651	29	-5
43.1	964	57	0.06	278	0.000007	0.01	2.976	0.031	0.1047	0.0003	0.3360	0.0035	4.848	0.052	0.1046	0.0003	0.965	1867	17	1708	5	-9
44.1	262	109	0.42	71	0.000046	0.07	3.174	0.037	0.1066	0.0006	0.3148	0.0036	4.600	0.060	0.1060	0.0006	0.885	1764	18	1731	11	-2
45.1	1136	388	0.34	302	0.000006	0.01	3.229	0.033	0.1089	0.0003	0.3096	0.0032	4.647	0.050	0.1088	0.0003	0.971	1739	16	1780	5	2
46.1	114	61	0.53	23	0.000043	0.07	4.316	0.058	0.0881	0.0009	0.2315	0.0031	2.792	0.048	0.0875	0.0010	0.775	1342	16	1371	21	2
47.1	145	51	0.35	41	0.000047	0.07	3.018	0.038	0.1105	0.0008	0.3312	0.0042	5.018	0.075	0.1099	0.0009	0.855	1844	20	1798	14	-3
48.1	194	134	0.69	44	0.000066	0.11	3.793	0.046	0.0919	0.0007	0.2634	0.0032	3.306	0.051	0.0910	0.0009	0.787	1507	16	1447	18	-4
49.1	165	87	0.53	38	0.000116	0.19	3.674	0.046	0.0920	0.0008	0.2717	0.0034	3.385	0.056	0.0904	0.0010	0.759	1549	17	1434	21	-8
50.1	377	270	0.72	104	0.000060	0.09	3.118	0.035	0.1043	0.0005	0.3204	0.0036	4.573	0.057	0.1035	0.0006	0.898	1792	17	1688	10	-6
51.1	236	74	0.31	62	0.000035	0.06	3.271	0.038	0.1070	0.0007	0.3055	0.0036	4.486	0.062	0.1065	0.0008	0.850	1719	18	1740	13	1
52.1	187	192	1.0	55	0.000027	0.04	2.934	0.036	0.0981	0.0006	0.3443	0.0048	5.069	0.175	0.1068	0.0025	0.860	1908	23	1745	43	-9
53.1	224	75	0.34	58	0.000068	0.11	3.305	0.039	0.1064	0.0006	0.3023	0.0036	4.398	0.060	0.1055	0.0007	0.861	1703	18	1723	13	1
54.1	219	92	0.42	52	0.000035	0.06	3.598	0.043	0.1032	0.0007	0.2778	0.0033	3.934	0.054	0.1027	0.0007	0.869	1580	17	1673	13	6
55.1	128	77	0.60	48	0.000041	0.06	2.288	0.029	0.1619	0.0009	0.4367	0.0056	9.716	0.136	0.1614	0.0009	0.914	2336	25	2470	10	5
56.1	127	15	0.12	62	0.000056	0.08	1.772	0.023	0.1999	0.0009	0.5639	0.0072	15.491	0.213	0.1992	0.0010	0.934	2883	30	2820	8	-2
57.1	278	61	0.22	69	0.000037	0.06	3.470	0.041	0.1064	0.0007	0.2880	0.0034	4.205	0.058	0.1059	0.0008	0.847	1631	17	1730	13	6
58.1	371	96	0.26	102	0.000029	0.05	3.109	0.035	0.1083	0.0005	0.3218	0.0037	4.812	0.077	0.1085	0.0008	0.910	1798	18	1774	13	-1
59.1	550	129	0.23	156	0.000012	0.02	3.027	0.033	0.1042	0.0004	0.3303	0.0036	4.738	0.055	0.1040	0.0004	0.938	1840	17	1697	7	-8
60.1	334	114	0.34	90	0.000007	0.01	3.185	0.036	0.1083	0.0005	0.3139	0.0035	4.683	0.058	0.1082	0.0005	0.912	1760	17	1769	9	1

Notes :

1. Uncertainties given at the one σ level.
2. Error in Temora reference zircon calibration was 0.69% for the analytical session.
   (not included in above errors but required when comparing $^{206}Pb/^{238}U$ data from different mounts).
3. f_{206} % denotes the percentage of ^{206}Pb that is common Pb.
4. Correction for common Pb made using the measured $^{204}Pb/^{206}Pb$ ratio.
5. For % Disc, 0% denotes a concordant analysis.

	Age (Ma)			Total Ratios				Radiogenic Ratios						
Grain. spot	$^{207}Pb/^{206}Pb$	±	% Disc	$^{238}U/^{206}Pb$	±	$^{207}Pb/^{206}Pb$	±	$^{207}Pb/^{235}U$	±	$^{206}Pb/^{238}U$	±	ρ	$^{207}Pb/^{206}Pb$	±
46.1	1371	21	2	4.316	0.058	0.0881	0.0009	2.792	0.048	0.2315	0.0031	0.775	0.0875	0.0010
14.1	1375	16	-1	4.160	0.049	0.0886	0.0006	2.902	0.042	0.2401	0.0028	0.818	0.0877	0.0007
2.1	1428	22	-7	3.720	0.044	0.0912	0.0006	3.336	0.068	0.2685	0.0033	0.855	0.0901	0.0011
15.1	1429	14	0	4.044	0.047	0.0904	0.0006	3.072	0.042	0.2472	0.0029	0.852	0.0901	0.0006
49.1	1434	21	-8	3.674	0.046	0.0920	0.0008	3.385	0.056	0.2717	0.0034	0.759	0.0904	0.0010
12.1	1435	17	2	4.090	0.052	0.0908	0.0008	3.047	0.047	0.2444	0.0031	0.818	0.0904	0.0008
16.1	1440	13	-1	3.966	0.046	0.0911	0.0006	3.151	0.042	0.2520	0.0029	0.863	0.0907	0.0006
27.1	1444	62	3	4.111	0.055	0.0905	0.0009	3.050	0.130	0.2434	0.0037	0.770	0.0909	0.0030
48.1	1447	18	-4	3.793	0.046	0.0919	0.0007	3.306	0.051	0.2634	0.0032	0.787	0.0910	0.0009
4.1	1624	23	-15	2.959	0.038	0.1026	0.0010	4.645	0.083	0.3369	0.0044	0.725	0.1000	0.0012
42.1	1651	29	-5	3.244	0.055	0.1032	0.0014	4.304	0.100	0.3076	0.0053	0.733	0.1015	0.0016
54.1	1673	13	6	3.598	0.043	0.1032	0.0007	3.934	0.054	0.2778	0.0033	0.869	0.1027	0.0007
7.1	1684	23	-7	3.090	0.035	0.1037	0.0005	4.606	0.091	0.3234	0.0038	0.815	0.1033	0.0013
50.1	1688	10	-6	3.118	0.035	0.1043	0.0005	4.573	0.057	0.3204	0.0036	0.898	0.1035	0.0006
30.1	1694	9	-4	3.188	0.036	0.1043	0.0005	4.488	0.055	0.3135	0.0035	0.910	0.1038	0.0005
59.1	1697	7	-8	3.027	0.033	0.1042	0.0004	4.738	0.055	0.3303	0.0036	0.938	0.1040	0.0004
5.1	1701	9	2	3.366	0.037	0.1054	0.0004	4.264	0.051	0.2967	0.0032	0.906	0.1042	0.0005
37.1	1703	7	2	3.372	0.036	0.1051	0.0003	4.264	0.048	0.2963	0.0031	0.941	0.1044	0.0004
20.1	1705	29	0	3.319	0.042	0.1050	0.0010	4.338	0.107	0.3012	0.0041	0.814	0.1045	0.0016
19.1	1707	8	-3	3.188	0.034	0.1047	0.0004	4.522	0.051	0.3136	0.0033	0.932	0.1046	0.0004
43.1	1708	5	-9	2.976	0.031	0.1047	0.0003	4.848	0.052	0.3360	0.0035	0.965	0.1046	0.0003
1.1	1712	15	-6	3.071	0.037	0.1061	0.0007	4.703	0.069	0.3252	0.0039	0.825	0.1049	0.0009
6.1	1714	8	-8	3.002	0.031	0.1052	0.0004	4.821	0.054	0.3331	0.0035	0.928	0.1050	0.0004
13.1	1715	33	0	3.269	0.038	0.1046	0.0005	4.433	0.112	0.3060	0.0037	0.748	0.1050	0.0019
3.1	1716	7	1	3.315	0.036	0.1052	0.0004	4.369	0.050	0.3016	0.0033	0.938	0.1051	0.0004
11.1	1719	46	6	3.521	0.052	0.1073	0.0025	4.114	0.120	0.2833	0.0042	0.505	0.1053	0.0026
23.1	1720	12	3	3.372	0.041	0.1061	0.0006	4.302	0.060	0.2963	0.0036	0.878	0.1053	0.0007
10.1	1720	8	2	3.333	0.036	0.1059	0.0004	4.354	0.051	0.2998	0.0033	0.924	0.1053	0.0005
41.1	1722	6	-3	3.153	0.033	0.1058	0.0003	4.609	0.051	0.3170	0.0034	0.949	0.1054	0.0004
53.1	1723	13	1	3.305	0.039	0.1064	0.0006	4.398	0.060	0.3023	0.0036	0.861	0.1055	0.0007
31.1	1724	7	-3	3.157	0.034	0.1058	0.0004	4.610	0.053	0.3167	0.0034	0.936	0.1056	0.0004
17.1	1726	9	2	3.348	0.038	0.1061	0.0005	4.349	0.053	0.2985	0.0034	0.923	0.1057	0.0005
57.1	1730	13	6	3.470	0.041	0.1064	0.0007	4.205	0.058	0.2880	0.0034	0.847	0.1059	0.0008
44.1	1731	11	-2	3.174	0.037	0.1066	0.0006	4.600	0.060	0.3148	0.0036	0.885	0.1060	0.0006
32.1	1731	9	-9	2.940	0.032	0.1069	0.0005	4.965	0.060	0.3398	0.0037	0.913	0.1060	0.0005
9.1	1732	9	2	3.301	0.037	0.1064	0.0005	4.426	0.054	0.3028	0.0034	0.913	0.1060	0.0005
40.1	1735	5	-2	3.160	0.033	0.1066	0.0003	4.630	0.050	0.3163	0.0033	0.962	0.1062	0.0003
21.1	1735	8	-7	2.995	0.033	0.1064	0.0005	4.887	0.057	0.3338	0.0036	0.931	0.1062	0.0005
24.1	1735	20	0	3.254	0.036	0.1040	0.0005	4.511	0.089	0.3081	0.0036	0.884	0.1062	0.0012
51.1	1740	13	1	3.271	0.038	0.1070	0.0007	4.486	0.062	0.3055	0.0036	0.850	0.1065	0.0008
35.1	1743	8	-2	3.165	0.034	0.1069	0.0004	4.646	0.054	0.3159	0.0034	0.933	0.1067	0.0004
52.1	1745	43	-9	2.934	0.036	0.0981	0.0006	5.069	0.175	0.3443	0.0048	0.860	0.1068	0.0025
25.1	1754	12	3	3.303	0.039	0.1077	0.0006	4.476	0.061	0.3026	0.0036	0.868	0.1073	0.0007
60.1	1769	9	1	3.185	0.036	0.1083	0.0005	4.683	0.058	0.3139	0.0035	0.912	0.1082	0.0005
58.1	1774	13	-1	3.109	0.035	0.1083	0.0005	4.812	0.077	0.3218	0.0037	0.910	0.1085	0.0008
26.1	1778	10	-2	3.082	0.035	0.1090	0.0006	4.863	0.061	0.3244	0.0037	0.908	0.1087	0.0006
45.1	1780	5	2	3.229	0.033	0.1089	0.0003	4.647	0.050	0.3096	0.0032	0.971	0.1088	0.0003
33.1	1788	5	2	3.218	0.034	0.1094	0.0003	4.684	0.050	0.3107	0.0032	0.969	0.1093	0.0003
47.1	1798	14	-3	3.018	0.038	0.1105	0.0008	5.018	0.075	0.3312	0.0042	0.855	0.1099	0.0009
22.1	1799	75	-10	2.772	0.104	0.1135	0.0043	5.447	0.303	0.3593	0.0134	0.673	0.1100	0.0045
34.1	1821	21	1	3.089	0.043	0.1134	0.0010	4.956	0.090	0.3229	0.0045	0.767	0.1113	0.0013
28.1	1823	30	6	3.296	0.042	0.1036	0.0008	4.703	0.111	0.3061	0.0040	0.730	0.1114	0.0019
39.1	1844	7	-2	2.944	0.032	0.1131	0.0004	5.278	0.060	0.3396	0.0037	0.945	0.1127	0.0004
38.1	2237	13	6	2.582	0.031	0.1412	0.0010	7.516	0.106	0.3871	0.0047	0.852	0.1408	0.0010
55.1	2470	10	5	2.288	0.029	0.1619	0.0009	9.716	0.136	0.4367	0.0056	0.914	0.1614	0.0009
18.1	2568	8	11	2.338	0.029	0.1716	0.0008	10.077	0.136	0.4273	0.0054	0.933	0.1710	0.0008
36.1	2728	15	14	2.267	0.038	0.1901	0.0016	11.439	0.215	0.4404	0.0073	0.881	0.1884	0.0017
8.1	2780	7	10	2.094	0.025	0.1946	0.0008	12.795	0.162	0.4773	0.0057	0.946	0.1944	0.0008
56.1	2820	8	-2	1.772	0.023	0.1999	0.0009	15.491	0.213	0.5639	0.0072	0.934	0.1992	0.0010
29.1	3261	4	11	1.769	0.019	0.2633	0.0006	20.432	0.231	0.5648	0.0062	0.974	0.2624	0.0007

Notes :

APPENDIX D4: Sample DZ_LP_3 SHRIMP DATA
Detrital zircons in Proterozoic Quartzite

DZ_LP_3

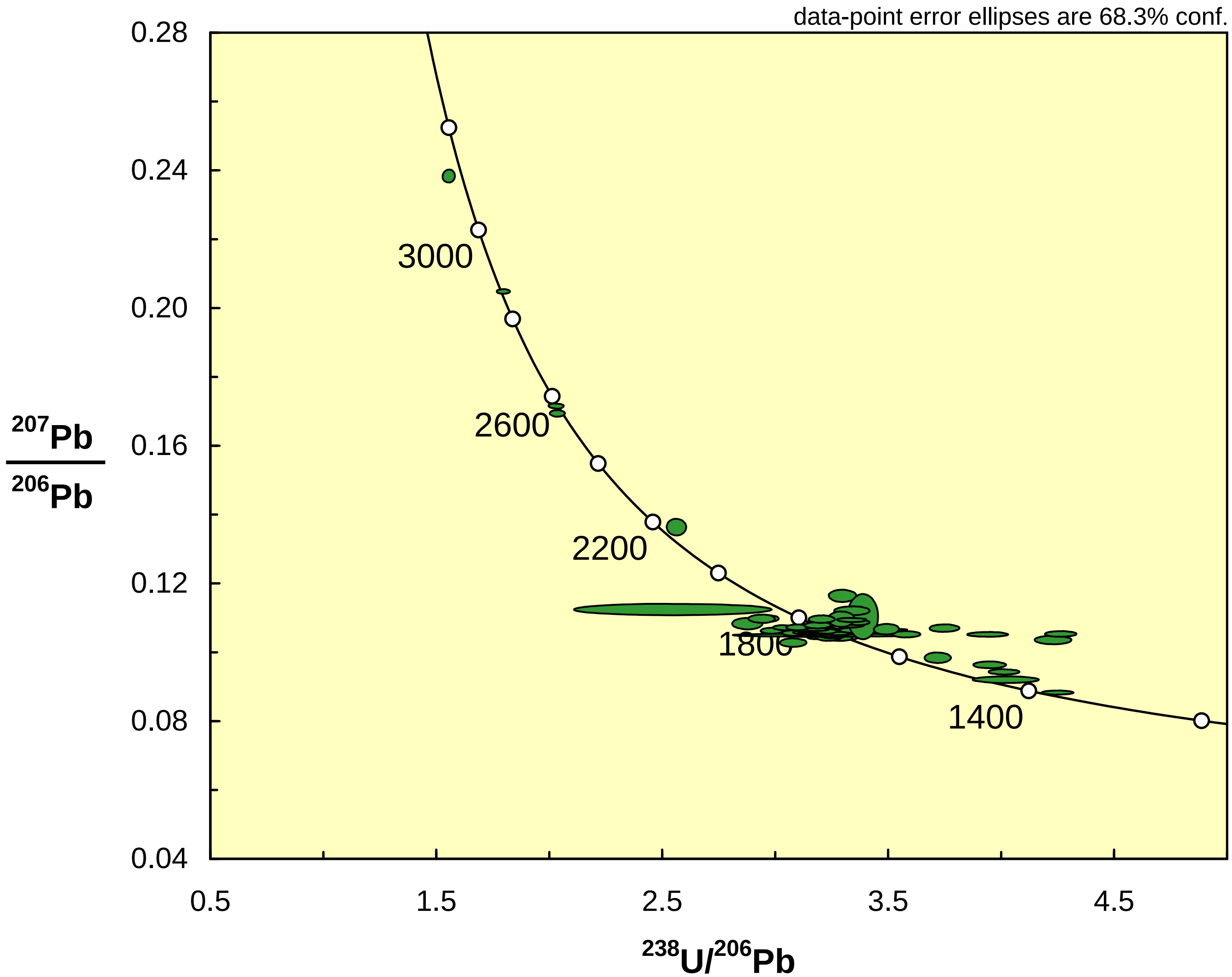

data-point error ellipses are 68.3% conf.
0.28
0.24
0.20
0.16
0.12
0.08
0.04
3000
2600
2200
1800
1400
0.5
1.5
2.5
3.5
4.5
$^{207}Pb/^{206}Pb$
$^{238}U/^{206}Pb$

DZ_LP_3

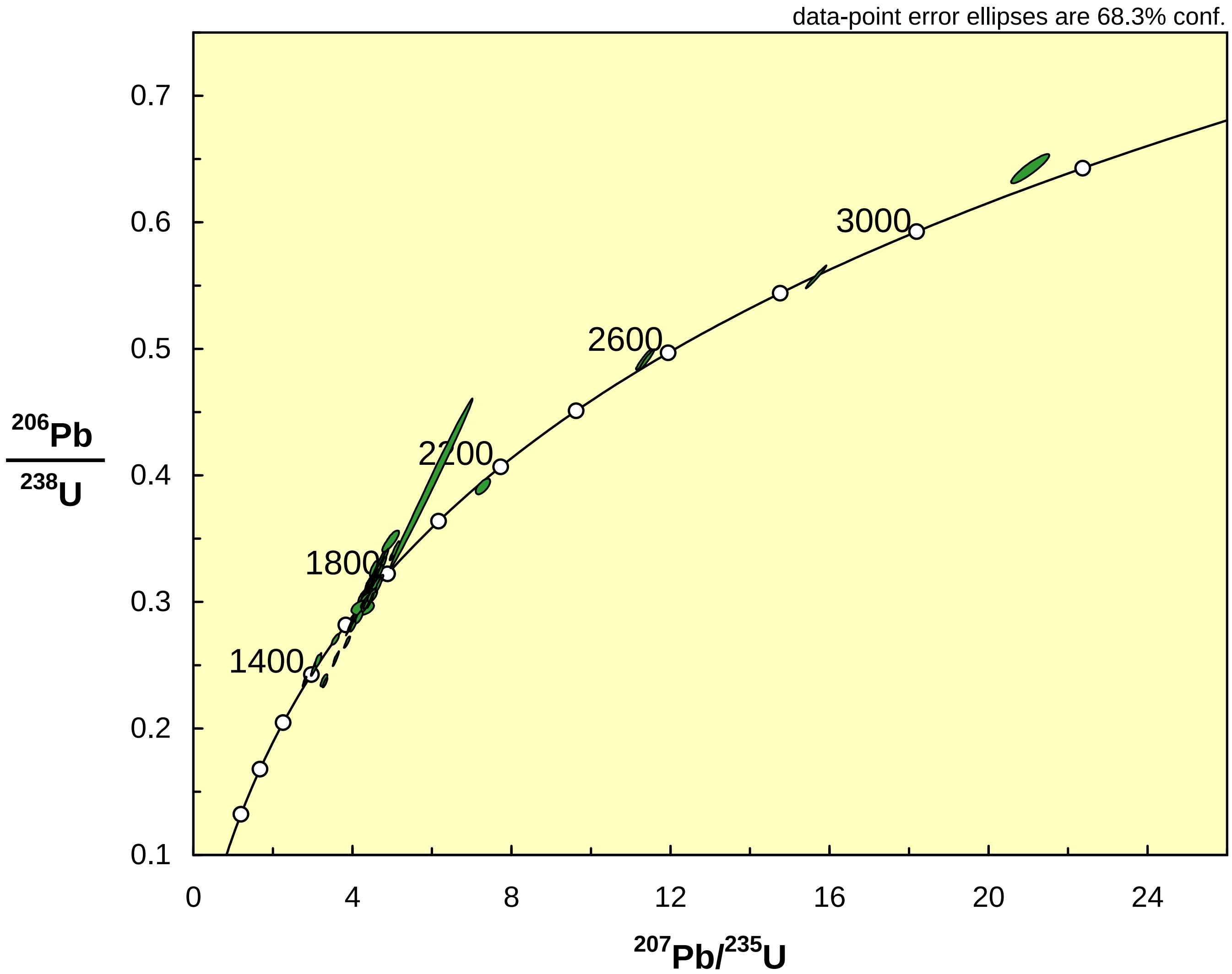

data-point error ellipses are 68.3% conf.
0.7
0.6
0.5
0.4
0.3
0.2
0.1
^{206}Pb / ^{238}U
0
4
8
12
16
20
24
^{207}Pb/^{235}U
1400
1800
2200
2600
3000

DZ_LP_3

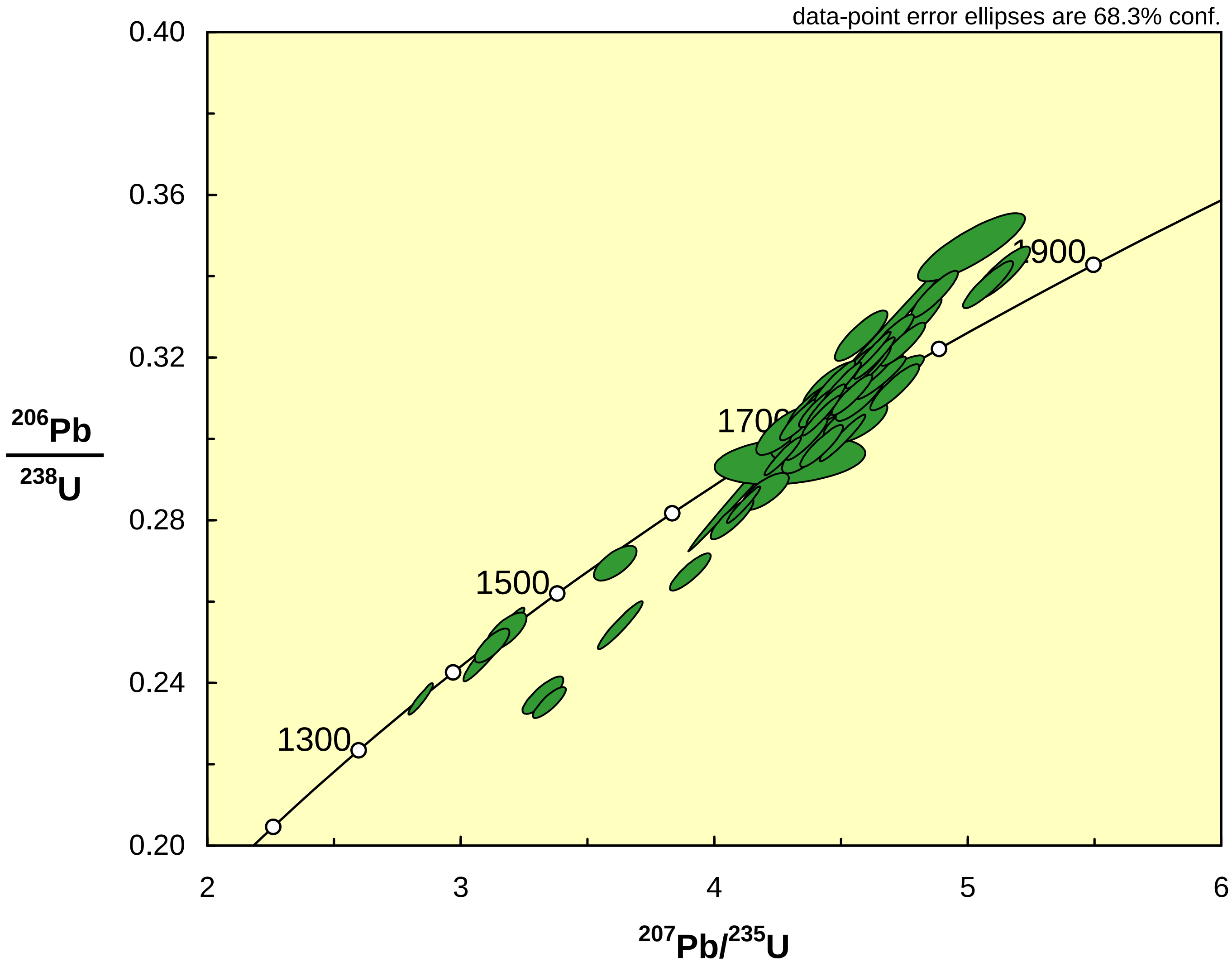

data-point error ellipses are 68.3% conf.
0.40
0.36
0.32
0.28
0.24
0.20
206Pb / 238U
1900
1700
1500
1300
2
3
4
5
6
207Pb/235U

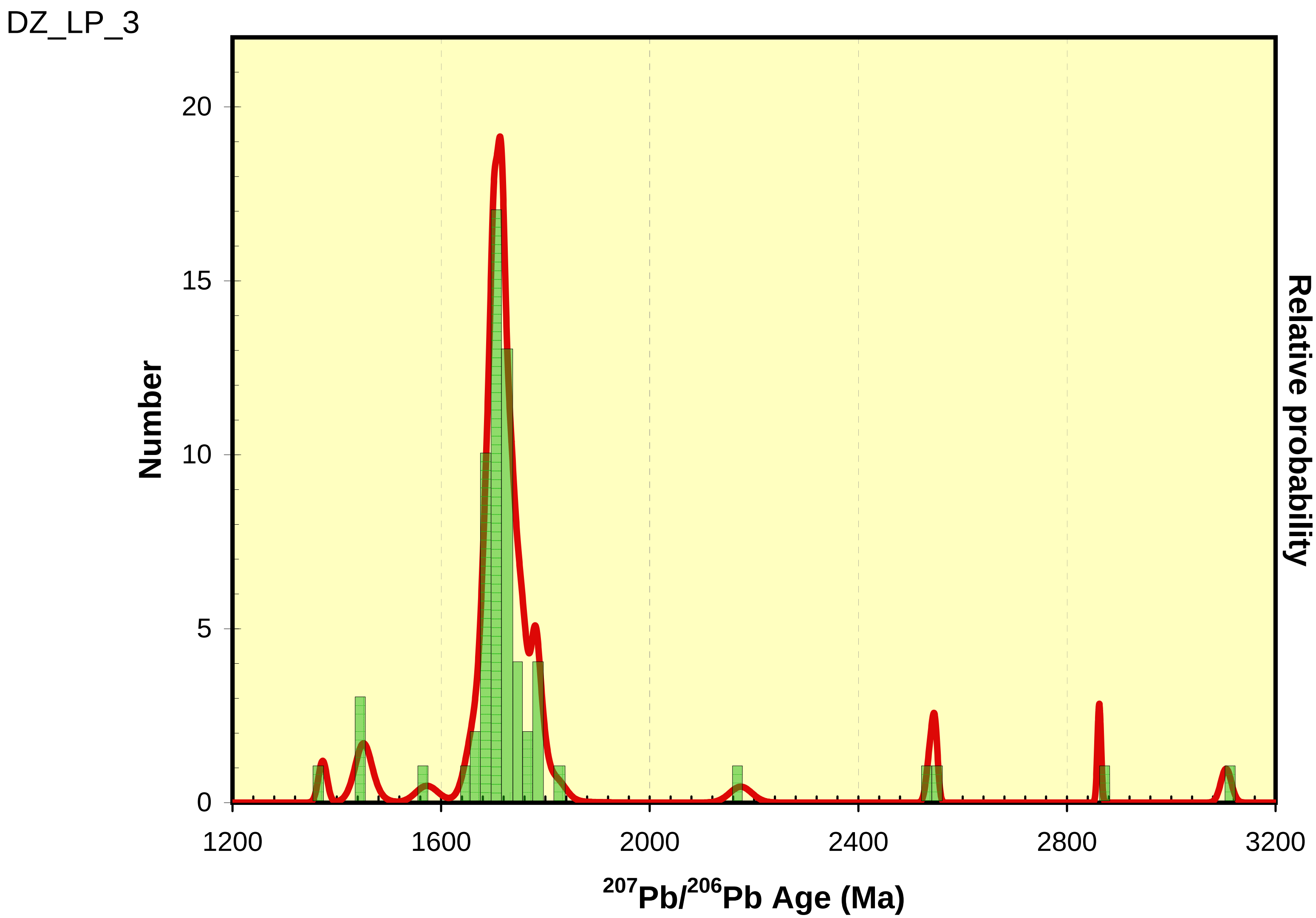
DZ_LP_3
Number
Relative probability
0
5
10
15
20
1200
1600
2000
2400
2800
3200
207Pb/206Pb Age (Ma)

DZ_LP_3

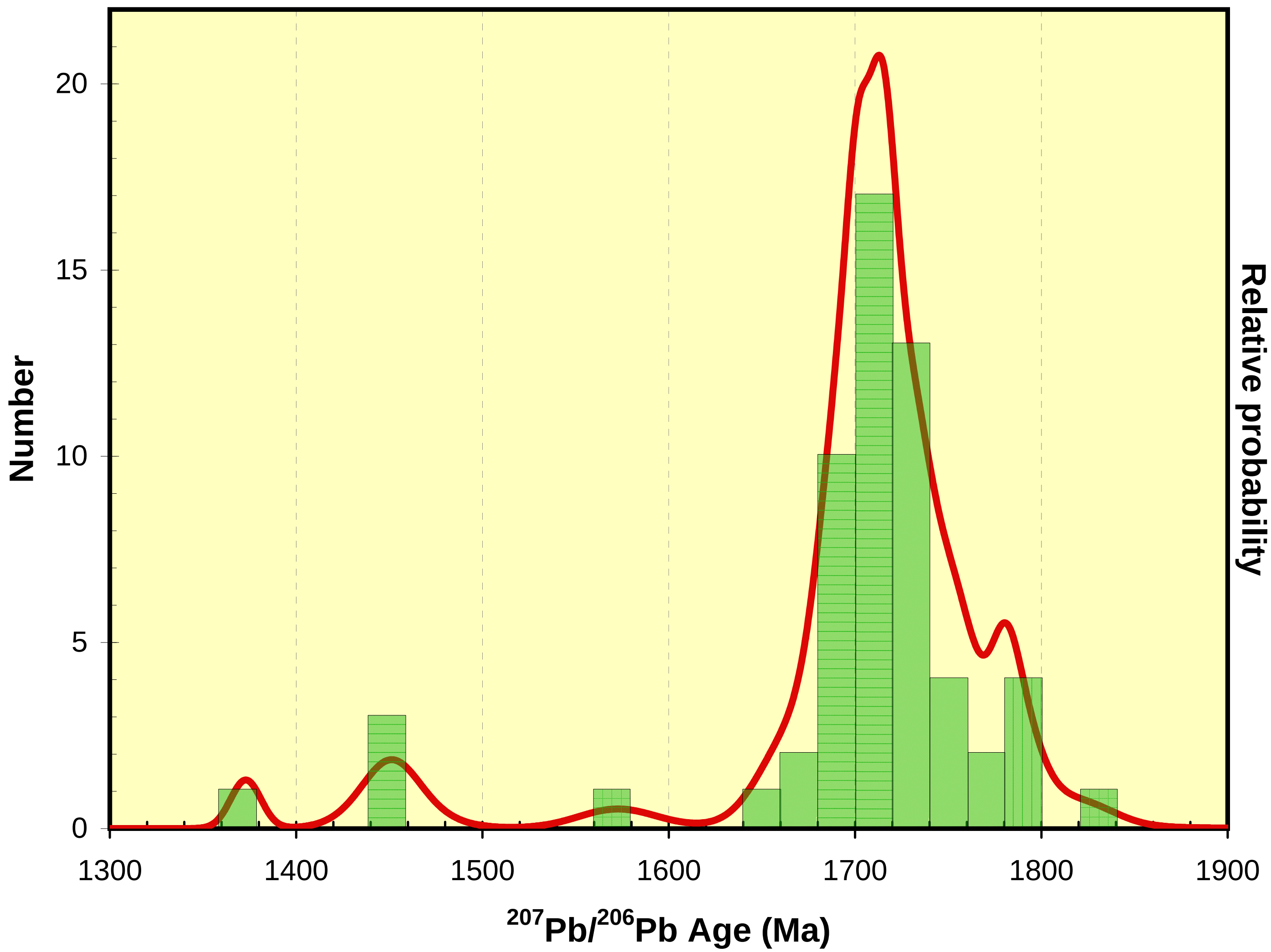

Number
Relative probability
0
5
10
15
20
1300
1400
1500
1600
1700
1800
1900
$^{207}Pb/^{206}Pb$ Age (Ma)

DZ_LP_3

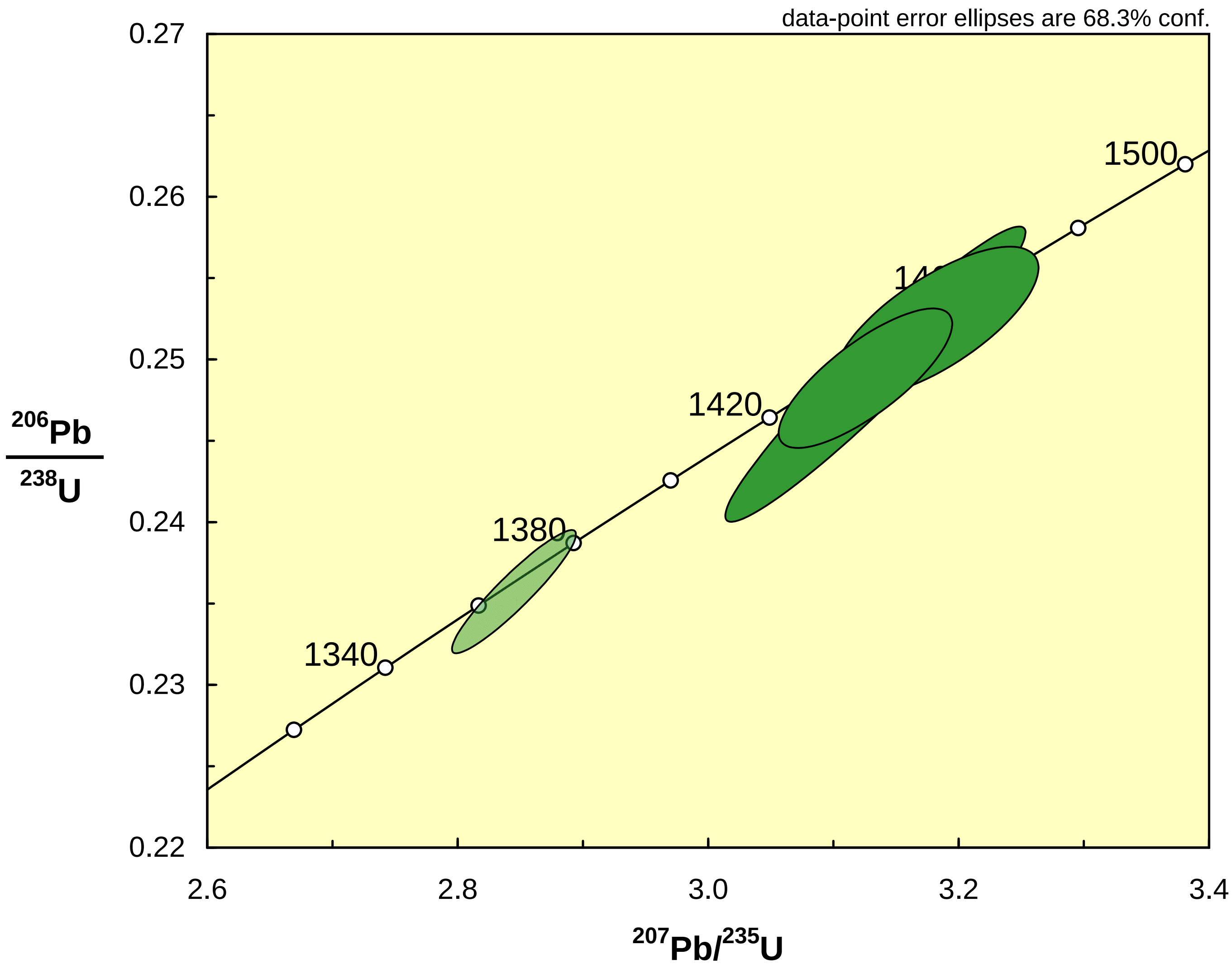

data-point error ellipses are 68.3% conf.
0.27
0.26
0.25
0.24
0.23
0.22
2.6
2.8
3.0
3.2
3.4
1340
1380
1420
1500
^{206}Pb/^{238}U
^{207}Pb/^{235}U

APPENDIX D4 - SHRIMP Sample DZ-LP-3

Table *xyz* . Summary of SHRIMP U-Pb zircon results for sample DZ-LP-3.

Grain. spot	U (ppm)	Th (ppm)	Th/U	^{206}Pb* (ppm)	^{204}Pb/ ^{206}Pb	f_{206} %	Total Ratios ^{238}U/ ^{206}Pb	±	^{207}Pb/ ^{206}Pb	±	Radiogenic Ratios ^{206}Pb/ ^{238}U	±	^{207}Pb/ ^{235}U	±	^{207}Pb/ ^{206}Pb	±	ρ	Age (Ma) ^{206}Pb/ ^{238}U	±	^{207}Pb/ ^{206}Pb	±	% Disc
1.1	274	100	0.36	82	0.000462	0.73	2.872	0.044	0.1079	0.0011	0.3469	0.0056	5.010	0.139	0.1047	0.0017	0.841	1920	27	1710	31	-12
2.1	390	55	0.14	106	0.000144	0.23	3.161	0.035	0.1061	0.0006	0.3157	0.0036	4.542	0.069	0.1043	0.0008	0.881	1769	18	1703	14	-4
3.1	505	238	0.47	138	0.000059	0.09	3.147	0.035	0.1061	0.0004	0.3174	0.0036	4.607	0.057	0.1053	0.0006	0.904	1777	18	1719	10	-3
4.1	123	111	0.91	33	0.000181	0.29	3.191	0.042	0.1060	0.0008	0.3125	0.0041	4.460	0.076	0.1035	0.0011	0.765	1753	20	1688	20	-4
5.1	448	156	0.35	124	0.000022	0.04	3.095	0.034	0.1068	0.0006	0.3230	0.0035	4.741	0.058	0.1065	0.0006	0.895	1804	17	1740	10	-4
6.1	282	139	0.49	73	-	<0.01	3.332	0.038	0.1075	0.0006	0.2997	0.0037	4.400	0.097	0.1065	0.0014	0.878	1690	18	1740	23	3
7.1	537	104	0.19	143	0.000032	0.05	3.234	0.035	0.1053	0.0004	0.3091	0.0034	4.468	0.053	0.1048	0.0005	0.918	1736	17	1712	9	-1
8.1	351	97	0.28	101	0.000038	0.06	2.981	0.034	0.1058	0.0005	0.3353	0.0038	4.865	0.061	0.1052	0.0006	0.899	1864	18	1718	10	-8
9.1	289	79	0.27	84	0.000023	0.04	2.961	0.034	0.1093	0.0006	0.3376	0.0039	5.074	0.064	0.1090	0.0006	0.900	1875	19	1783	10	-5
10.1	682	238	0.35	182	0.000012	0.02	3.219	0.034	0.1062	0.0005	0.3106	0.0033	4.539	0.053	0.1060	0.0005	0.913	1744	16	1732	9	-1
11.1	724	151	0.21	195	0.000027	0.04	3.189	0.034	0.1045	0.0003	0.3134	0.0034	4.500	0.051	0.1041	0.0003	0.955	1758	17	1699	6	-3
12.1	176	30	0.17	47	-	<0.01	3.202	0.039	0.1092	0.0007	0.3124	0.0038	4.709	0.064	0.1093	0.0007	0.886	1752	19	1788	12	2
13.1	277	77	0.28	67	-	<0.01	3.574	0.042	0.1048	0.0006	0.2800	0.0033	4.068	0.055	0.1054	0.0007	0.866	1591	16	1721	12	8
14.1	169	100	0.59	44	0.000125	0.20	3.310	0.042	0.1044	0.0008	0.3015	0.0038	4.268	0.069	0.1027	0.0010	0.782	1699	19	1673	19	-2
15.1	687	439	0.64	182	0.000036	0.06	3.250	0.035	0.1046	0.0006	0.3075	0.0033	4.413	0.054	0.1041	0.0006	0.877	1729	16	1698	11	-2
16.1	324	122	0.38	90	0.000016	0.03	3.079	0.035	0.1050	0.0006	0.3247	0.0037	4.693	0.059	0.1048	0.0006	0.905	1813	18	1711	10	-6
17.1	203	116	0.57	54	0.000070	0.11	3.249	0.039	0.1043	0.0007	0.3074	0.0037	4.379	0.063	0.1033	0.0008	0.844	1728	18	1684	14	-3
18.1	266	65	0.24	73	0.000015	0.02	3.147	0.036	0.1061	0.0006	0.3177	0.0037	4.637	0.060	0.1058	0.0006	0.899	1779	18	1729	10	-3
19.1	695	108	0.15	191	0.000020	0.03	3.128	0.033	0.1053	0.0004	0.3196	0.0034	4.627	0.052	0.1050	0.0004	0.946	1788	17	1714	7	-4
20.1	154	71	0.46	45	-	<0.01	2.937	0.037	0.1092	0.0008	0.3405	0.0043	5.128	0.075	0.1092	0.0008	0.870	1889	21	1787	13	-6
21.1	215	87	0.41	58	0.000031	0.05	3.184	0.038	0.1073	0.0006	0.3143	0.0039	4.677	0.096	0.1079	0.0012	0.877	1762	19	1765	21	0
22.1	655	369	0.56	179	0.000018	0.03	3.151	0.034	0.1053	0.0004	0.3173	0.0034	4.596	0.052	0.1051	0.0004	0.937	1776	17	1716	7	-4
23.1	217	63	0.29	58	0.000012	0.02	3.230	0.038	0.1038	0.0006	0.3095	0.0037	4.422	0.059	0.1036	0.0006	0.887	1738	18	1690	11	-3
24.1	331	327	0.99	71	0.000193	0.31	4.007	0.045	0.0938	0.0005	0.2488	0.0028	3.124	0.046	0.0911	0.0008	0.779	1432	15	1448	17	1
25.1	463	118	0.25	122	-	<0.01	3.250	0.036	0.1043	0.0004	0.3077	0.0034	4.427	0.052	0.1043	0.0004	0.932	1730	17	1703	8	-2
26.1	725	200	0.28	307	0.000180	0.25	2.032	0.022	0.1712	0.0005	0.4908	0.0053	11.432	0.129	0.1689	0.0005	0.960	2574	23	2547	5	-1
27.1	247	124	0.50	64	0.000057	0.09	3.288	0.038	0.1055	0.0006	0.3039	0.0035	4.387	0.058	0.1047	0.0007	0.877	1710	17	1709	12	0
28.1	966	118	0.12	253	0.000006	0.01	3.274	0.035	0.1050	0.0003	0.3054	0.0032	4.418	0.049	0.1049	0.0003	0.956	1718	16	1713	6	0
29.1	228	72	0.31	59	0.000752	1.18	3.293	0.041	0.1159	0.0011	0.3001	0.0038	4.373	0.101	0.1057	0.0020	0.543	1692	19	1726	36	2
30.1	1428	512	0.36	368	0.000359	0.56	3.334	0.052	0.1116	0.0009	0.2983	0.0047	4.388	0.082	0.1067	0.0011	0.835	1683	23	1744	19	3
31.1	201	75	0.37	54	0.000074	0.12	3.225	0.038	0.1081	0.0007	0.3097	0.0037	4.574	0.063	0.1071	0.0008	0.860	1739	18	1751	13	1
32.1	696	234	0.34	177	0.000021	0.03	3.384	0.036	0.1051	0.0004	0.2954	0.0031	4.268	0.048	0.1048	0.0004	0.948	1669	16	1711	7	2
33.1	185	62	0.33	38	0.000081	0.13	4.221	0.055	0.1030	0.0008	0.2366	0.0031	3.325	0.053	0.1019	0.0009	0.815	1369	16	1659	17	18
34.1	298	73	0.25	81	0.000043	0.07	3.150	0.037	0.1048	0.0005	0.3173	0.0037	4.561	0.059	0.1043	0.0006	0.908	1776	18	1701	10	-4
35.1	341	130	0.38	96	0.000056	0.09	3.039	0.035	0.1067	0.0005	0.3287	0.0038	4.801	0.062	0.1059	0.0006	0.909	1832	19	1730	10	-6
36.1	186	115	0.62	50	0.000083	0.13	3.193	0.039	0.1055	0.0008	0.3128	0.0039	4.499	0.068	0.1043	0.0009	0.821	1755	19	1702	16	-3
37.1	147	124	0.84	41	0.000024	0.04	3.074	0.039	0.1024	0.0008	0.3252	0.0041	4.576	0.068	0.1021	0.0008	0.845	1815	20	1662	15	-9
38.1	1137	110	0.10	308	0.000005	0.01	3.167	0.036	0.1059	0.0004	0.3159	0.0037	4.623	0.079	0.1061	0.0011	0.807	1769	18	1734	19	-2
39.1	301	103	0.34	166	0.000006	0.01	1.557	0.018	0.2381	0.0013	0.6420	0.0077	21.048	0.314	0.2378	0.0015	0.913	3197	30	3105	10	-3
40.1	375	126	0.34	98	0.000027	0.04	3.280	0.038	0.1037	0.0005	0.3047	0.0035	4.342	0.056	0.1034	0.0006	0.902	1715	17	1685	10	-2
41.1	511	198	0.39	216	0.000075	0.10	2.035	0.023	0.1690	0.0006	0.4909	0.0055	11.373	0.135	0.1680	0.0007	0.939	2575	24	2538	7	-1
42.1	1476	104	0.07	407	0.000016	0.02	3.115	0.032	0.1045	0.0003	0.3210	0.0033	4.615	0.049	0.1043	0.0003	0.969	1795	16	1702	5	-5
43.1	219	102	0.47	48	0.000312	0.51	3.944	0.047	0.0958	0.0007	0.2522	0.0030	3.181	0.053	0.0915	0.0011	0.717	1450	16	1456	22	0
44.1	378	192	0.51	97	0.000029	0.05	3.336	0.037	0.1060	0.0005	0.2996	0.0033	4.362	0.053	0.1056	0.0005	0.912	1689	17	1725	9	2
45.1	350	74	0.21	118	0.000046	0.07	2.546	0.287	0.1119	0.0011	0.3926	0.0442	6.026	0.681	0.1113	0.0011	0.996	2135	205	1821	18	-17
47.1	715	406	0.57	145	0.000015	0.02	4.243	0.045	0.0878	0.0004	0.2356	0.0025	2.845	0.033	0.0876	0.0004	0.929	1364	13	1373	8	1
48.1	133	37	0.28	34	0.000296	0.47	3.381	0.044	0.1099	0.0043	0.2944	0.0039	4.297	0.195	0.1059	0.0046	0.292	1663	19	1729	80	4
49.1	562	115	0.21	150	0.000046	0.07	3.214	0.266	0.1045	0.0004	0.3109	0.0258	4.454	0.369	0.1039	0.0004	0.999	1745	127	1695	7	-3
50.12	186	87	0.47	40	0.000021	0.03	4.014	0.097	0.0915	0.0006	0.2490	0.0060	3.133	0.079	0.0912	0.0006	0.959	1434	31	1452	14	1
51.1	2341	360	0.15	542	0.000049	0.08	3.713	0.039	0.0979	0.0011	0.2691	0.0028	3.609	0.055	0.0973	0.0011	0.685	1536	14	1572	21	2
52.1	656	458	0.70	132	0.000093	0.15	4.254	0.046	0.1048	0.0005	0.2347	0.0025	3.352	0.043	0.1035	0.0007	0.844	1359	13	1689	13	20
53.1	190	66	0.34	50	0.000037	0.06	3.288	0.039	0.1092	0.0015	0.3039	0.0036	4.555	0.083	0.1087	0.0015	0.643	1711	18	1778	25	4
54.1	414	114	0.28	107	0.000007	0.01	3.334	0.042	0.1089	0.0004	0.2999	0.0038	4.501	0.060	0.1088	0.0004	0.957	1691	19	1780	7	5
55.1	258	75	0.29	66	0.000048	0.07	3.354	0.038	0.1082	0.0006	0.2979	0.0034	4.420	0.056	0.1076	0.0006	0.895	1681	17	1759	10	4
56.1	541	135	0.25	118	0.000077	0.12	3.935	0.060	0.1047	0.0005	0.2538	0.0039	3.629	0.058	0.1037	0.0005	0.950	1458	20	1691	9	14
57.1	1989	117	0.06	485	0.000063	0.10	3.525	0.036	0.1061	0.0003	0.2834	0.0029	4.114	0.044	0.1053	0.0003	0.959	1609	15	1719	6	6
58.1	474	197	0.42	109	0.000034	0.05	3.744	0.043	0.1065	0.0007	0.2670	0.0031	3.904	0.052	0.1061	0.0007	0.861	1525	16	1733	12	12
59.1	565	155	0.27	270	0.000012	0.02	1.798	0.019	0.2046	0.0004	0.5561	0.0059	15.675	0.170	0.2044	0.0004	0.981	2850	25	2862	3	0
60.1	776	162	0.21	207	0.000006	0.01	3.219	0.034	0.1058	0.0005	0.3109	0.0034	4.559	0.069	0.1064	0.0008	0.877	1745	16	1738	14	0
61.1	865	523	0.6	213	0.000002	<0.01	3.487	0.037	0.1063	0.0010	0.2868	0.0030	4.201	0.061	0.1062	0.0010	0.731	1625	15	1736	18	6
62.1	721	132	0.18	195	-	<0.01	3.181	0.034	0.1062	0.0003	0.3148	0.0034	4.656	0.064	0.1073	0.0006	0.933	1764	17	1754	10	-1
63.1	420	31	0.07	113	0.000046	0.07	3.185	0.035	0.1040	0.0004	0.3137	0.0034	4.473	0.053	0.1034	0.0005	0.920	1759	17	1686	9	-4
64.1	512	52	0.10	136	0.000017	0.03	3.246	0.035	0.1047	0.0004	0.3080	0.0033	4.436	0.051	0.1044	0.0004	0.936	1731	16	1704	7	-2
65.1	693	209	0.30	232	0.000009	0.01	2.562	0.027	0.1359	0.0017	0.3902	0.0042	7.308	0.119	0.1358	0.0017	0.658	2124	19	2175	21	2

Notes : 1. Uncertainties given at the one σ level.

2. Error in Temora reference zircon calibration was 0.69% for the analytical session.

(not included in above errors but required when comparing ^{206}Pb/^{238}U data from different mounts).

3. f_{206} % denotes the percentage of ^{206}Pb that is common Pb.

4. Correction for common Pb made using the measured ^{204}Pb/^{206}Pb ratio.

5. For % Disc, 0% denotes a concordant analysis.

Grain. spot	Age (Ma) ^{206}Pb/ ^{238}U	±	^{207}Pb/ ^{206}Pb	±	% Disc	Total Ratios ^{238}U/ ^{206}Pb	±	^{207}Pb/ ^{206}Pb	±	Radiogenic Ratios ^{207}Pb/ ^{235}U	±	^{206}Pb/ ^{238}U	±	ρ	^{207}Pb/ ^{206}Pb	±
47.1	1364	13	1373	8	1	4.243	0.045	0.0878	0.0004	2.845	0.033	0.2356	0.0025	0.929	0.0876	0.0004
24.1	1432	15	1448	17	1	4.007	0.045	0.0938	0.0005	3.124	0.046	0.2488	0.0028	0.779	0.0911	0.0008
50.12	1434	31	1452	14	1	4.014	0.097	0.0915	0.0006	3.133	0.079	0.2490	0.0060	0.959	0.0912	0.0006
43.1	1450	16	1456	22	0	3.944	0.047	0.0958	0.0007	3.181	0.053	0.2522	0.0030	0.717	0.0915	0.0011
51.1	1536	14	1572	21	2	3.713	0.039	0.0979	0.0011	3.609	0.055	0.2691	0.0028	0.685	0.0973	0.0011
33.1	1369	16	1659	17	18	4.221	0.055	0.1030	0.0008	3.325	0.053	0.2366	0.0031	0.815	0.1019	0.0009
37.1	1815	20	1662	15	-9	3.074	0.039	0.1024	0.0008	4.576	0.068	0.3252	0.0041	0.845	0.1021	0.0008
14.1	1699	19	1673	19	-2	3.310	0.042	0.1044	0.0008	4.268	0.069	0.3015	0.0038	0.782	0.1027	0.0010
17.1	1728	18	1684	14	-3	3.249	0.039	0.1043	0.0007	4.379	0.063	0.3074	0.0037	0.844	0.1033	0.0008
40.1	1715	17	1685	10	-2	3.280	0.038	0.1037	0.0005	4.342	0.056	0.3047	0.0035	0.902	0.1034	0.0006
63.1	1759	17	1686	9	-4	3.185	0.035	0.1040	0.0004	4.473	0.053	0.3137	0.0034	0.920	0.1034	0.0005
4.1	1753	20	1688	20	-4	3.191	0.042	0.1060	0.0008	4.460	0.076	0.3125	0.0041	0.765	0.1035	0.0011
52.1	1359	13	1689	13	20	4.254	0.046	0.1048	0.0005	3.352	0.043	0.2347	0.0025	0.844	0.1035	0.0007
23.1	1738	18	1690	11	-3	3.230	0.038	0.1038	0.0006	4.422	0.059	0.3095	0.0037	0.887	0.1036	0.0006
56.1	1458	20	1691	9	14	3.935	0.060	0.1047	0.0005	3.629	0.058	0.2538	0.0039	0.950	0.1037	0.0005
49.1	1745	127	1695	7	-3	3.214	0.266	0.1045	0.0004	4.454	0.369	0.3109	0.0258	0.999	0.1039	0.0004
15.1	1729	16	1698	11	-2	3.250	0.035	0.1046	0.0006	4.413	0.054	0.3075	0.0033	0.877	0.1041	0.0006
11.1	1758	17	1699	6	-3	3.189	0.034	0.1045	0.0003	4.500	0.051	0.3134	0.0034	0.955	0.1041	0.0003
34.1	1776	18	1701	10	-4	3.150	0.037	0.1048	0.0005	4.561	0.059	0.3173	0.0037	0.908	0.1043	0.0006
42.1	1795	16	1702	5	-5	3.115	0.032	0.1045	0.0003	4.615	0.049	0.3210	0.0033	0.969	0.1043	0.0003
36.1	1755	19	1702	16	-3	3.193	0.039	0.1055	0.0008	4.499	0.068	0.3128	0.0039	0.821	0.1043	0.0009
2.1	1769	18	1703	14	-4	3.161	0.035	0.1061	0.0006	4.542	0.069	0.3157	0.0036	0.881	0.1043	0.0008
25.1	1730	17	1703	8	-2	3.250	0.036	0.1043	0.0004	4.427	0.052	0.3077	0.0034	0.932	0.1043	0.0004
64.1	1731	16	1704	7	-2	3.246	0.035	0.1047	0.0004	4.436	0.051	0.3080	0.0033	0.936	0.1044	0.0004
27.1	1710	17	1709	12	0	3.288	0.038	0.1055	0.0006	4.387	0.058	0.3039	0.0035	0.877	0.1047	0.0007
1.1	1920	27	1710	31	-12	2.872	0.044	0.1079	0.0011	5.010	0.139	0.3469	0.0056	0.841	0.1047	0.0017
32.1	1669	16	1711	7	2	3.384	0.036	0.1051	0.0004	4.268	0.048	0.2954	0.0031	0.948	0.1048	0.0004
16.1	1813	18	1711	10	-6	3.079	0.035	0.1050	0.0006	4.693	0.059	0.3247	0.0037	0.905	0.1048	0.0006
7.1	1736	17	1712	9	-1	3.234	0.035	0.1053	0.0004	4.468	0.053	0.3091	0.0034	0.918	0.1048	0.0005
28.1	1718	16	1713	6	0	3.274	0.035	0.1050	0.0003	4.418	0.049	0.3054	0.0032	0.956	0.1049	0.0003
19.1	1788	17	1714	7	-4	3.128	0.033	0.1053	0.0004	4.627	0.052	0.3196	0.0034	0.946	0.1050	0.0004
22.1	1776	17	1716	7	-4	3.151	0.034	0.1053	0.0004	4.596	0.052	0.3173	0.0034	0.937	0.1051	0.0004
8.1	1864	18	1718	10	-8	2.981	0.034	0.1058	0.0005	4.865	0.061	0.3353	0.0038	0.899	0.1052	0.0006
57.1	1609	15	1719	6	6	3.525	0.036	0.1061	0.0003	4.114	0.044	0.2834	0.0029	0.959	0.1053	0.0003
3.1	1777	18	1719	10	-3	3.147	0.035	0.1061	0.0004	4.607	0.057	0.3174	0.0036	0.904	0.1053	0.0006
13.1	1591	16	1721	12	8	3.574	0.042	0.1048	0.0006	4.068	0.055	0.2800	0.0033	0.866	0.1054	0.0007
44.1	1689	17	1725	9	2	3.336	0.037	0.1060	0.0005	4.362	0.053	0.2996	0.0033	0.912	0.1056	0.0005
29.1	1692	19	1726	36	2	3.293	0.041	0.1159	0.0011	4.373	0.101	0.3001	0.0038	0.543	0.1057	0.0020
18.1	1779	18	1729	10	-3	3.147	0.036	0.1061	0.0006	4.637	0.060	0.3177	0.0037	0.899	0.1058	0.0006
48.1	1663	19	1729	80	4	3.381	0.044	0.1099	0.0043	4.297	0.195	0.2944	0.0039	0.292	0.1059	0.0046
35.1	1832	19	1730	10	-6	3.039	0.035	0.1067	0.0005	4.801	0.062	0.3287	0.0038	0.909	0.1059	0.0006
10.1	1744	16	1732	9	-1	3.219	0.034	0.1062	0.0005	4.539	0.053	0.3106	0.0033	0.913	0.1060	0.0005
58.1	1525	16	1733	12	12	3.744	0.043	0.1065	0.0007	3.904	0.052	0.2670	0.0031	0.861	0.1061	0.0007
38.1	1769	18	1734	19	-2	3.167	0.036	0.1059	0.0004	4.623	0.079	0.3159	0.0037	0.807	0.1061	0.0011
61.1	1625	15	1736	18	6	3.487	0.037	0.1063	0.0010	4.201	0.061	0.2868	0.0030	0.731	0.1062	0.0010
60.1	1745	16	1738	14	0	3.219	0.034	0.1058	0.0005	4.559	0.069	0.3109	0.0034	0.877	0.1064	0.0008
6.1	1690	18	1740	23	3	3.332	0.038	0.1075	0.0006	4.400	0.097	0.2997	0.0037	0.878	0.1065	0.0014
5.1	1804	17	1740	10	-4	3.095	0.034	0.1068	0.0006	4.741	0.058	0.3230	0.0035	0.895	0.1065	0.0006
30.1	1683	23	1744	19	3	3.334	0.052	0.1116	0.0009	4.388	0.082	0.2983	0.0047	0.835	0.1067	0.0011
31.1	1739	18	1751	13	1	3.225	0.038	0.1081	0.0007	4.574	0.063	0.3097	0.0037	0.860	0.1071	0.0008
62.1	1764	17	1754	10	-1	3.181	0.034	0.1062	0.0003	4.656	0.064	0.3148	0.0034	0.933	0.1073	0.0006
55.1	1681	17	1759	10	4	3.354	0.038	0.1082	0.0006	4.420	0.056	0.2979	0.0034	0.895	0.1076	0.0006
21.1	1762	19	1765	21	0	3.184	0.038	0.1073	0.0006	4.677	0.096	0.3143	0.0039	0.877	0.1079	0.0012
53.1	1711	18	1778	25	4	3.288	0.039	0.1092	0.0015	4.555	0.083	0.3039	0.0036	0.643	0.1087	0.0015
54.1	1691	19	1780	7	5	3.334	0.042	0.1089	0.0004	4.501	0.060	0.2999	0.0038	0.957	0.1088	0.0004
9.1	1875	19	1783	10	-5	2.961	0.034	0.1093	0.0006	5.074	0.064	0.3376	0.0039	0.900	0.1090	0.0006
20.1	1889	21	1787	13	-6	2.937	0.037	0.1092	0.0008	5.128	0.075	0.3405	0.0043	0.870	0.1092	0.0008
12.1	1752	19	1788	12	2	3.202	0.039	0.1092	0.0007	4.709	0.064	0.3124	0.0038	0.886	0.1093	0.0007
45.1	2135	205	1821	18	-17	2.546	0.287	0.1119	0.0011	~~6.026~~	~~0.681~~	~~0.3926~~	~~0.0442~~	~~0.996~~	0.1113	0.0011
65.1	2124	19	2175	21	2	2.562	0.027	0.1359	0.0017	7.308	0.119	0.3902	0.0042	0.658	0.1358	0.0017
41.1	2575	24	2538	7	-1	2.035	0.023	0.1690	0.0006	11.373	0.135	0.4909	0.0055	0.939	0.1680	0.0007
26.1	2574	23	2547	5	-1	2.032	0.022	0.1712	0.0005	11.432	0.129	0.4908	0.0053	0.960	0.1689	0.0005
59.1	2850	25	2862	3	0	1.798	0.019	0.2046	0.0004	15.675	0.170	0.5561	0.0059	0.981	0.2044	0.0004
39.1	3197	30	3105	10	-3	1.557	0.018	0.2381	0.0013	21.048	0.314	0.6420	0.0077	0.913	0.2378	0.0015

Notes :

APPENDIX E

LP Whole Rock Geochemistry A07-4811

Report Date: 20/12/2007

Analyte Symbol	C-Total	Total S	F	SiO2	Al2O3	Fe2O3(T)	MnO	MgO	CaO	Na2O	K2O	TiO2	P2O5	LOI	Total	Be	V	Co	Ni
Unit Symbol	%	%	%	%	%	%	%	%	%	%	%	%	%	%	%	ppm	ppm	ppm	ppm
Detection Limit	0.01	0.01	0.01	0.01	0.01	0.01	0.001	0.01	0.01	0.01	0.01	0.001	0.01	0.01	0.01	1	5	1	1
Analysis Method	IR	IR	FUS-ISE	FUS-ICP	FUS-ICP	FUS-ICP	FUS-ICP	FUS-ICP	FUS-ICP	FUS-ICP	FUS-ICP	FUS-ICP	FUS-ICP	FUS-ICP	FUS-ICP	FUS-ICP	FUS-ICP	FUS-MS	TD-ICP
JA06-01	0.03	< 0.01	< 0.01	63.48	15.1	8.01	0.044	0.1	0.1	5.78	4.79	0.26	0.06	0.76	98.48	1	18	1	11
JA06-01C	0.02	< 0.01	< 0.01	64.09	13.6	10.77	0.033	0.06	0.1	4.87	4.92	0.296	0.07	0.44	99.24	1	7	< 1	9
BL06-05	0.04	< 0.01	0.04	62.2	16.27	7.88	0.123	0.31	0.32	5.95	5.55	0.305	0.14	0.74	99.79	3	18	1	10
07WP129	0.02	< 0.01	0.05	73.41	12.96	1.95	0.028	0.23	0.18	2.6	6.48	0.339	0.08	0.82	99.08	3	6	2	7
CQ06-25B	0.26	0.11	0.18	46.49	15.27	12.27	0.157	6.98	7.38	3.14	2.75	2.554	0.53	3.39	100.9	3	220	40	107
CQ06-30B	0.33	0.13	0.14	45.25	13.94	11.1	0.186	8.94	9.78	2.78	1.91	1.86	0.51	3.49	99.75	2	205	42	159
BL06-03	0.04	0.02	0.14	44.96	13.44	11.7	0.172	10.35	10.05	2.37	1.68	2.041	0.52	2.35	99.63	2	239	42	176
LH06-23B	3.62	0.05	0.09	41.2	10.82	10.07	0.181	10.68	8.32	1.81	1.96	0.845	0.25	13.44	99.58	2	188	45	218
07WP120	2.45	0.07	0.09	44.65	11.09	10.37	0.193	10.28	8.91	1.83	1.95	0.871	0.26	9.74	100.1	2	193	46	221
LH06-24B	0.02	< 0.01	0.44	48.95	11.99	19.78	0.028	1.89	3.43	5.12	2.86	0.163	3.41	0.77	98.38	1	126	3	21
07WP127B	3.93	0.13	0.5	3.97	0.74	8.03	0.606	1.25	23.35	0.07	< 0.01	0.014	18.92	14.23	71.16	13	61	1	1

Analyte Symbol	Cu	Cd	Zn	S	Ag	Pb	Ga	Ge	Rb	Sr	Y	Zr	Nb	Mo	In	Sn	Sb	Cs	Ba
Unit Symbol	ppm	ppm	ppm	%	ppm	ppm	ppm	ppm	ppm	ppm	ppm	ppm	ppm	ppm	ppm	ppm	ppm	ppm	ppm
Detection Limit	1	0.5	1	0.001	0.3	5	1	1	2	2	2	4	1	2	0.2	1	0.5	0.5	3
Analysis Method	TD-ICP	TD-ICP	TD-ICP	TD-ICP	TD-ICP	TD-ICP	FUS-MS	FUS-MS	FUS-MS	FUS-ICP	FUS-ICP	FUS-ICP	FUS-MS	FUS-MS	FUS-MS	FUS-MS	FUS-MS	FUS-MS	FUS-ICP
JA06-01	9	0.7	58	0.005	0.4	23	54	1	86	27	89	1214	199	< 2	< 0.2	5	< 0.5	0.7	351
JA06-01C	3	0.6	22	0.002	< 0.3	26	32	2	92	23	82	1090	192	< 2	< 0.2	6	< 0.5	0.6	339
BL06-05	5	0.5	146	0.005	0.7	< 5	41	1	257	39	54	836	218	< 2	< 0.2	4	< 0.5	13.2	517
07WP129	5	< 0.5	21	0.002	< 0.3	< 5	21	1	112	79	39	484	67	< 2	< 0.2	4	< 0.5	2.1	839
CQ06-25B	707	0.5	82	0.109	0.3	< 5	19	1	106	730	29	229	67	2	< 0.2	2	< 0.5	6.8	958
CQ06-30B	128	0.6	99	0.133	0.8	6	16	1	71	1029	23	183	72	< 2	< 0.2	1	21.9	4.7	768
BL06-03	59	0.7	74	0.008	0.5	< 5	16	1	55	860	24	166	68	< 2	< 0.2	1	< 0.5	5.3	862
LH06-23B	71	0.6	54	0.037	0.9	7	12	1	55	885	20	115	10	< 2	< 0.2	< 1	< 0.5	14.1	1092
07WP120	75	0.6	63	0.066	0.5	8	13	1	55	629	22	118	9	< 2	< 0.2	< 1	< 0.5	9.1	962
LH06-24B	9	1	33	0.01	< 0.3	48	62	20	124	246	251	8	52	< 2	< 0.2	4	< 0.5	4.6	218
07WP127B	72	0.6	32	0.03	< 0.3	95	449	30	< 2	1758	295	76	4	4	< 0.2	< 1	< 0.5	< 0.5	2789

Analyte Symbol	La	Bi	Ce	Pr	Nd	Sm	Eu	Gd	Tb	Dy	Ho	Er	Tm	Yb	Lu	Hf	Ta	W	Tl	Th	U
Unit Symbol	ppm	ppm	ppm	ppm	ppm	ppm	ppm	ppm	ppm	ppm	ppm	ppm	ppm	ppm	ppm	ppm	ppm	ppm	ppm	ppm	ppm
Detection Limit	0.1	0.4	0.1	0.05	0.1	0.1	0.05	0.1	0.1	0.1	0.1	0.1	0.05	0.1	0.04	0.2	0.1	1	0.1	0.1	0.1
Analysis Method	FUS-MS	FUS-MS	FUS-MS	FUS-MS	FUS-MS	FUS-MS	FUS-MS	FUS-MS	FUS-MS	FUS-MS	FUS-MS	FUS-MS	FUS-MS	FUS-MS	FUS-MS	FUS-MS	FUS-MS	FUS-MS	FUS-MS	FUS-MS	FUS-MS
JA06-01	180	< 0.4	325	38.5	119	20	2.76	15.8	2.5	13.7	2.9	9	1.39	8.9	1.38	25.7	14.8	3	0.4	32.5	7
JA06-01C	131	< 0.4	260	28.9	92.5	16.9	2.37	13.9	2.2	12.5	2.6	7.6	1.16	7.6	1.16	21.5	14.6	2	0.5	25	5.9
BL06-05	150	< 0.4	234	30	90.1	14.6	2.36	11	1.7	8.6	1.8	5.5	0.85	5.6	0.89	18.1	15.5	14	0.9	30.4	7.2
07WP129	58.9	< 0.4	130	15.1	51.5	9.9	2.2	8	1.3	6.5	1.3	3.7	0.54	3.5	0.52	11.1	5.3	< 1	0.4	14.1	3.3
CQ06-25B	48.6	< 0.4	92.5	11.3	38.2	7.4	2.34	6.2	0.9	4.8	0.9	2.5	0.34	2	0.28	5.1	4.5	2	0.7	7.8	1.8
CQ06-30B	60.1	0.6	113	12.8	41.3	7	2.16	5.5	0.8	4.1	0.8	2.1	0.28	1.7	0.24	4.2	4.9	< 1	0.5	9.6	2.2
BL06-03	52.7	< 0.4	101	12.1	41	7.2	2.27	5.9	0.8	4.1	0.8	2.1	0.28	1.6	0.24	3.9	4.4	1	0.4	7.2	1.5
LH06-23B	17	< 0.4	35.8	4.77	18.1	4.2	1.22	3.6	0.6	3.3	0.7	2	0.29	1.8	0.26	2.8	0.5	< 1	0.3	2.7	0.8
07WP120	17.5	< 0.4	37.5	5	18.6	4.2	1.27	3.8	0.6	3.2	0.7	1.9	0.28	1.8	0.27	2.8	0.5	< 1	0.4	2.8	0.8
LH06-24B	658	0.5	4920	1430	8350	1220	165	448	24.1	60.1	8.6	28.9	< 0.05	6.9	0.15	1.4	0.3	3	0.7	2510	17.9
07WP127B	87500	< 0.4	113000	9950	23300	1300	210	208	16	66.2	11.2	34	3.86	13.9	0.4	1.4	< 0.1	1	< 0.1	2810	10.7

Sample ID	Au	As	Br	Cr	Ir	Sb	Sc	Se	Mass
	ppb	ppm	ppm	ppm	ppb	ppm	ppm	ppm	g
JA06-01	-2	13.0	4.9	-5	-5	0.9	1.9	-5	1.243
JA06-01C	11	3.8	-0.5	-5	-5	-0.1	1.5	-5	1.345
BL06-05	-2	4.2	-0.5	-5	-5	-0.1	2.7	-5	1.062
07WP129	-2	-0.5	-0.5	-5	-5	-0.1	4.1	-5	1.329
CQ06-25B	-2	-0.5	-0.5	162	-5	1.1	19.0	-5	1.539
CQ06-30B	-2	20.0	-0.5	306	-5	32.0	23.0	-5	1.271
BL06-03	9	23.0	-0.5	315	-5	0.7	25.0	-5	1.547
LH06-23B	-2	10.0	-0.5	842	-5	-0.1	26.0	-5	1.264
07WP120	-2	14.0	-0.5	850	-5	1.1	27.0	-5	1.260
LH06-24B	65	-1.5	-1.0	27	-10	2.0	5.7	-5	1.394
07WP127B	-400	-200	-50	810	-150	-6.0	7.3	-60	1.102
07WP127B Split PU	-400	-200	-50	920	-150	-6.0	7.7	-60	1.079
BLANK	-5	-0.5	-0.5	-5	-5	-0.1	-0.1	-5	1.000
DMMAS-104	221	1500	-0.5	102	-7	6.1	15.0	-5	1.111
DMMAS104 Accept	229	1570.0		95		6.2	14.1		

Detection limits are elevated due to Th and REEs

	Sample Description	Waypoint #
JA06-01	Syenite at Lemhi Pass, near Continental Divide	88
JA06-01C	Syenite with specular hematite vein	88
BL06-05	Syenite with biotite	99
07WP129	Leadore Granite at Hawley Creek - fresh	129
CQ06-25B	Greenstone Dike - CQ adit outcrop	63
CQ06-30B	Pyroxene Porphyry - unweathered sample from shaft dump	63 to west
BL06-03	Pyroxene Porphyry - Bluebird area, surface	102
LH06-23B	Lucky Horseshoe mafic sill by lower adit	39
07WP120	Lucky Horseshoe mafic sill by lower adit	120
LH06-24B	Lucky Horseshoe, high grade Th-REE ore, hematite, fresh	40
07WP127B	Carbonatite, Roberts South Prospect, North Fork area	127

$^{40}Ar/^{39}Ar$ step heat analysis of Idaho Geological Survey 2007 Samples

For:
Dr. Virginia Gillerman
DGGS

Prepared by:

Paul Layer & Jeff Drake
Geochronology Laboratory
University of Alaska Fairbanks

May 5, 2008

Summary of the Analysis

For $^{40}Ar/^{39}Ar$ analysis, 5 samples were submitted to the Geochronology laboratory at UAF. The samples were crushed, washed and sieved to either 100 – 250 or 250 – 500 micron size fractions, and hand picked for datable mineral phases. The monitor mineral MMhb-1 (Samson and Alexander, 1987) with an age of 513.9 Ma (Lanphere and Dalrymple, 2000) was used to monitor neutron flux (and calculate the irradiation parameter, J). The samples and standards were wrapped in aluminum foil and loaded into aluminum cans of 2.5 cm diameter and 6 cm height. The samples were irradiated in position 5c of the uranium enriched research reactor of McMaster University in Hamilton, Ontario, Canada for 20 megawatt-hours.

Upon their return from the reactor, the samples and monitors were loaded into 2 mm diameter holes in a copper tray that was then loaded in a ultra-high vacuum extraction line. The monitors were fused, and samples heated, using a 6-watt argon-ion laser following the technique described in York et al. (1981), Layer et al. (1987) and Layer (2000). Argon purification was achieved using a liquid nitrogen cold trap and a SAES Zr-Al getter at 400C. The samples were analyzed in a VG-3600 mass spectrometer at the Geophysical Institute, University of Alaska Fairbanks. The argon isotopes measured were corrected for system blank and mass discrimination, as well as calcium, potassium and chlorine interference reactions following procedures outlined in McDougall and Harrision (1999). System blanks generally were $2x10^{-16}$ mol ^{40}Ar and $2x10^{-18}$ mol ^{36}Ar which are 10 to 50 times smaller than fraction volumes. Mass discrimination was monitored by running both calibrated air shots and a zero-age glass sample. These measurements were made on a weekly to monthly basis to check for changes in mass discrimination.

A summary of all the $^{40}Ar/^{39}Ar$ results is given in Table 1, with all ages quoted to the +/- 1 sigma level and calculated using the constants of Steiger and Jaeger (1977). The integrated age is the age given by the total gas measured and is equivalent to a potassium-argon (K-Ar) age. The spectrum provides a plateau age if three or more consecutive gas fractions represent at least 50% of the total gas release and are within two standard deviations of each other (Mean Square Weighted Deviation less than ~2.7). All samples were run three times to check on sample consistency.

Lanphere, M.A., and Dalrymple, G.B., 2000, First-principles calibration of ^{38}Ar tracers: Implications for the ages of $^{40}Ar/^{39}Ar$ fluence monitors, U.S. Geological Survey Professional Paper 1621, 10 p.

Layer, P.W., 2000, Argon-40/argon-39 age of the El'gygytgyn impact event, Chukotka, Russia, Meteroitics and Planatary Science, v. 35, 591-599.

Layer, P.W., Hall, C.M. & York, D., 1987. The derivation of $^{40}Ar/^{39}Ar$ age spectra of single grains of hornblende and biotite by laser step heating, *Geophys. Res. Lett.*, **14**, 757-760.

McDougall, I. and Harrison, T.M., 1999, Geochronology and Thermochronology by the 40Ar/39Ar method-2nd ed, Oxford University Press, New York, 269pp.

Samson S. D., and Alexander E. C. (1987) Calibration of the interlaboratory 40Ar/39Ar dating standard, MMhb1. Chem. Geol. **66**, 27-34.

Steiger, R.H. and Jaeger, E., 1977, Subcommission on geochronology: Convention on the use of decay constants in geo and cosmochronology, Earth and Planet Science Letters, v. 36, p. 359-362.

York, D., Hall, C.M., Yanase, Y., Hanes, J.A. & Kenyon, W.J., 1981. $^{40}Ar/^{39}Ar$ dating of terrestrial minerals with a continuous laser, *Geophys. Res. Lett.*, **8**, 1136-1138.

Preliminary discussion:

Hornblendes: Sample 07LOC77BP is the simplest to interpret. It shows a well-defined plateau on all three runs (although only the third run had an appropriate heating schedule to yield a statistically significant plateau). There is no evidence of argon loss on this sample. Sample 07CQ-09 also shows three reproducible runs, but the interpretation is not straightforward. As with the K-spars (see below), the age and Ca/K spectra show evidence of resetting (and alteration of the hornblende) at 250 – 300 Ma (Triassic), and then step up to early Paleozoic ages that are close to, but most likely younger than the original age of the hornblende.

K-spars: All three K-spar samples show good reproducibility for the three runs each, but the spectra are complicated and do not show recognizable ‘plateaus. All show three-phase age spectrus. The first part is characterized by extremely old ages. These correlate with high Cl/K ratios and are indicative of excess argon in high Cl inclusions, seen in many K-spar samples. From these old ages, the ages drop down to a ‘saddle’ of low ages (late Cretaceous to Tertiary in our case) before rising up to Late Triassic to Early Jurassic maximum ages. We interpret these last two phases as reflecting approximately the original Triassic age of the feldspars (although this age might be a bit young due to argon loss), followed by a resetting event in the Early Tertiary (either complete or partial resetting). These samples would be ideal candidates for K-spar Multi-Domain modeling if more information on thermal histories was desired.

Table 1 Interpretive Details – Hornblendes

Sample	Min.	Integrated Age (Ma)	Plateau Age (Ma)	Information	Other Comments
07CQ-09	HO#1	376.3 ± 1.0	**-**		Maximum age: 420 Ma
	HO#2	328.6 ± 1.0	-		Maximum age: 445 Ma
	HO#3	364.4 ± 0.9	-		Maximum age: 452 Ma
07LOC77BP	HO#1	573.7 ± 1.4	-		Poor heating schedule
	HO#2	567.1 ± 1.8	564.7 ± 2.9	2 fractions 82% ^{39}Ar release MSWD = 2.1	Poor heating schedule
	HO#3	571.7 ± 1.4	**558.3 ± 1.6**	4 fractions 81% ^{39}Ar release MSWD = 0.2	‘good’ plateau

Bold: Preferred age for each sample (ages reported at ±1 sigma)
Plateau: 3+ consecutive fractions, MSWD < ~2.5, more than ~50% 39Ar release.

Table 1 Interpretive Details – K-spars

Sample	Min.	Integrated Age (Ma)	K-Spar saddle Age (Ma)	Information	Other Comments
07LH-02	KS#1	122.1 ± 0.3	55.6 ± 1.1	4 fractions 29% ^{39}Ar release MSWD = 46.7	Maximum age: 175 Ma
	KS#2	134.4 ± 0.3	55.3 ± 0.4	3 fractions 26% ^{39}Ar release MSWD = 3.3	Maximum age: 208 Ma
	KS#3	186.0 ± 0.4	62.6 ± 1.2	2 fractions 17% ^{39}Ar release MSWD = 19.8	Maximum age: 199 Ma
07WP119	KS#1	183.5 ± 0.4	112.3 ± 4.9	6 fractions 31% ^{39}Ar release MSWD = 347	Maximum age: 230 Ma
	KS#2	167.3 ± 0.4	94.2 ± 1.3	3 fractions 22% ^{39}Ar release MSWD = 16.8	Maximum age: 217 Ma
	KS#3	179.8 ± 0.4	103.5 ± 3.0	4 fractions 29% ^{39}Ar release MSWD = 125	Maximum age: 232 Ma
CA06B1	KS#1	136.6 ± 0.3	71.3 ± 1.8	4 fractions 22% ^{39}Ar release MSWD = 102	Maximum age: 183 Ma
	KS#2	161.9 ± 0.4	74.0 ± 1.3	3 fractions 19% ^{39}Ar release MSWD = 14.7	Maximum age: 195 Ma
	KS#3	157.4 ± 0.4	74.7 ± 1.8	3 fractions 19% ^{39}Ar release MSWD = 35.5	Maximum age: 210 Ma

Three hornblende runs

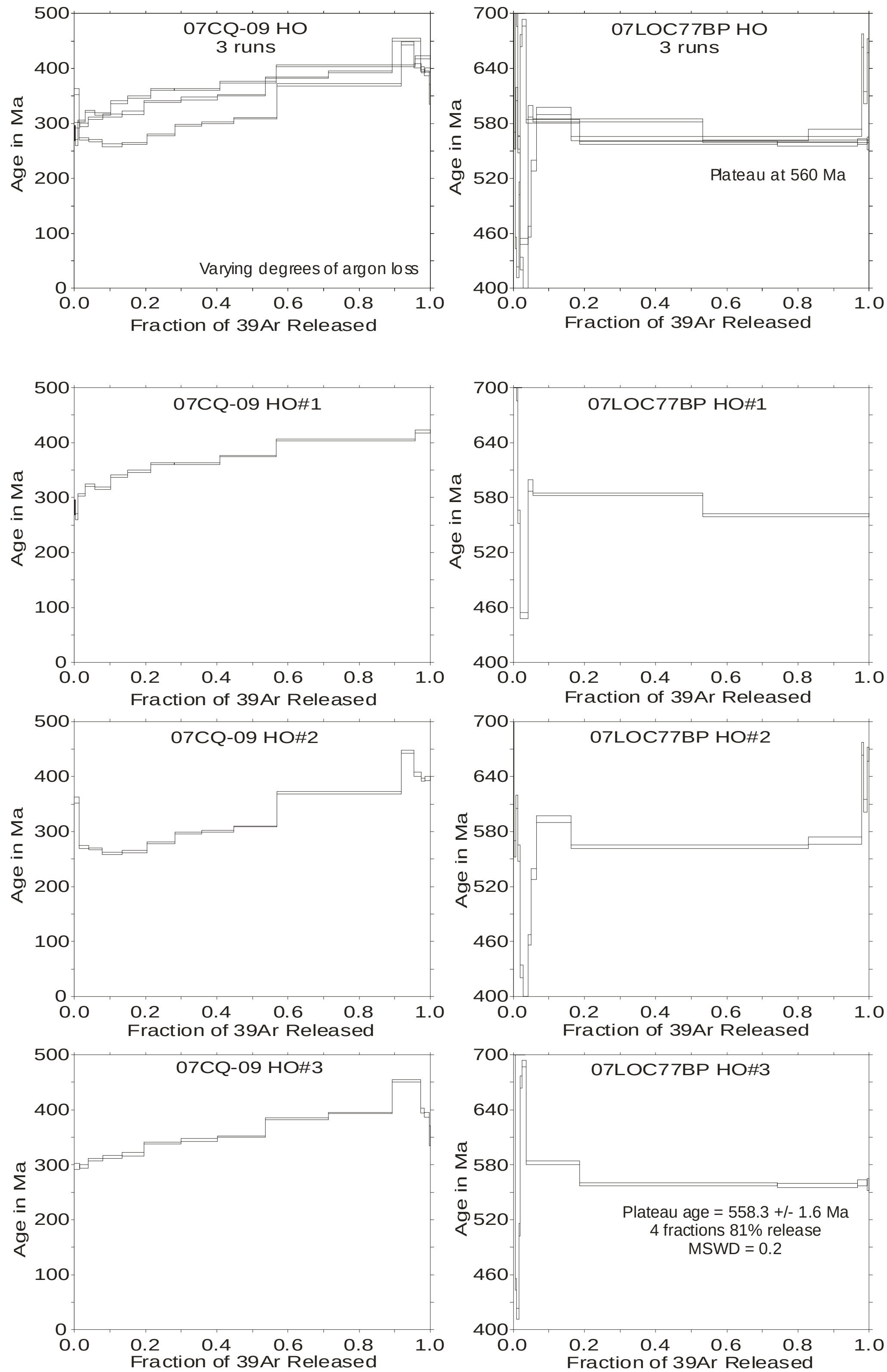

Three runs of each K-spar

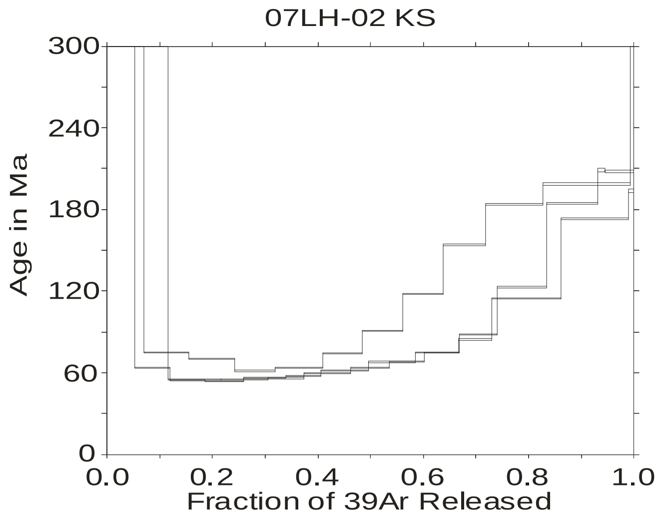

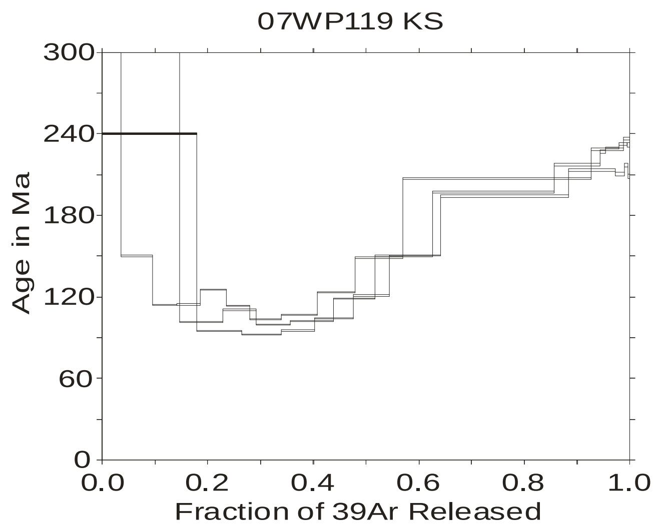

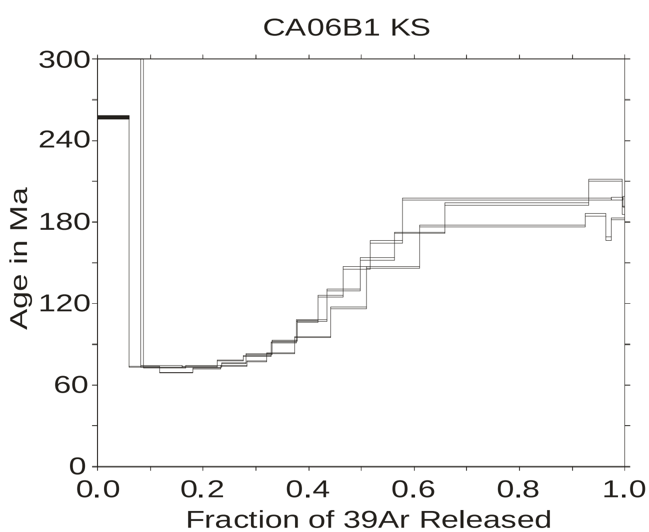

One representative K-spar run from each sample

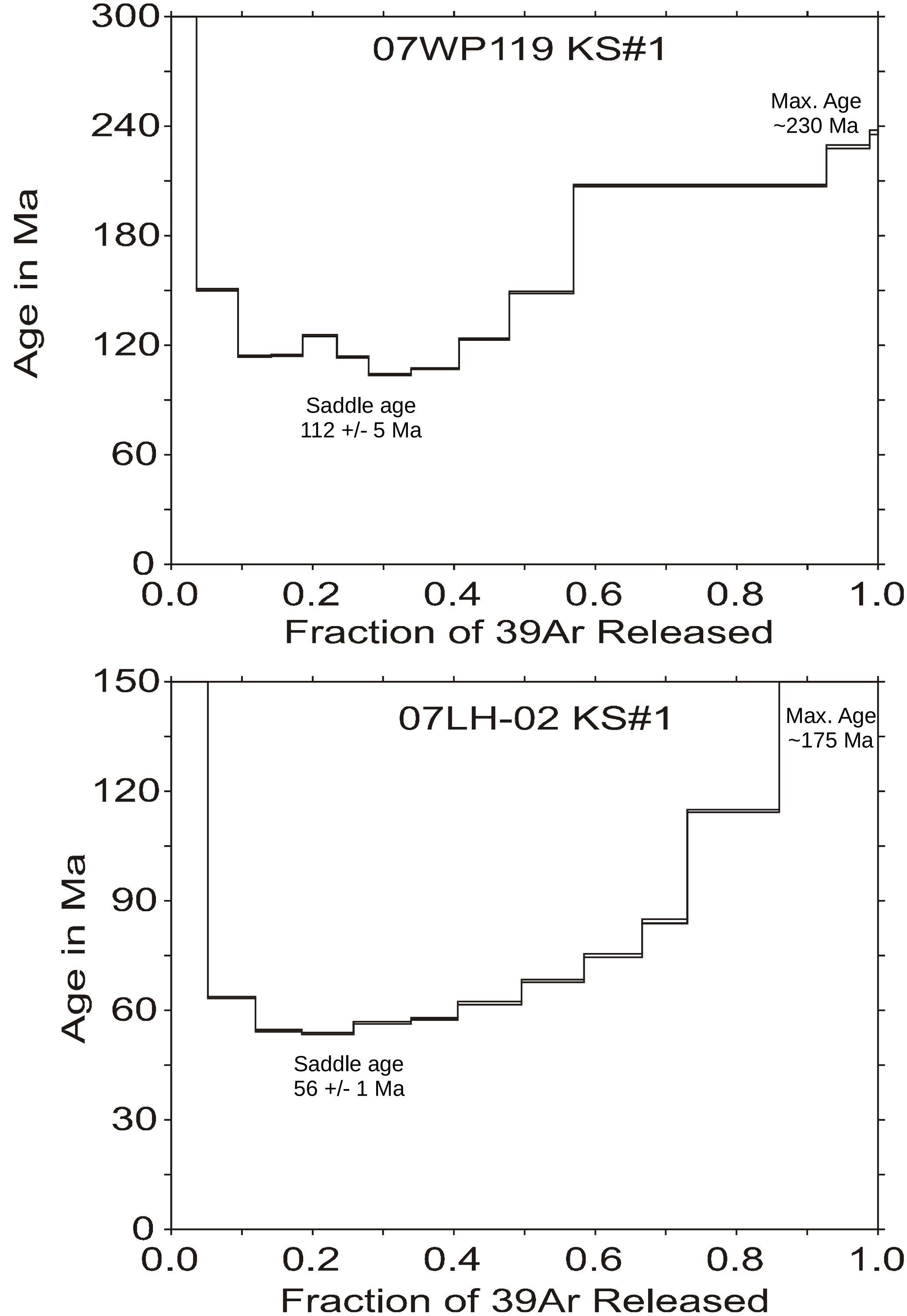

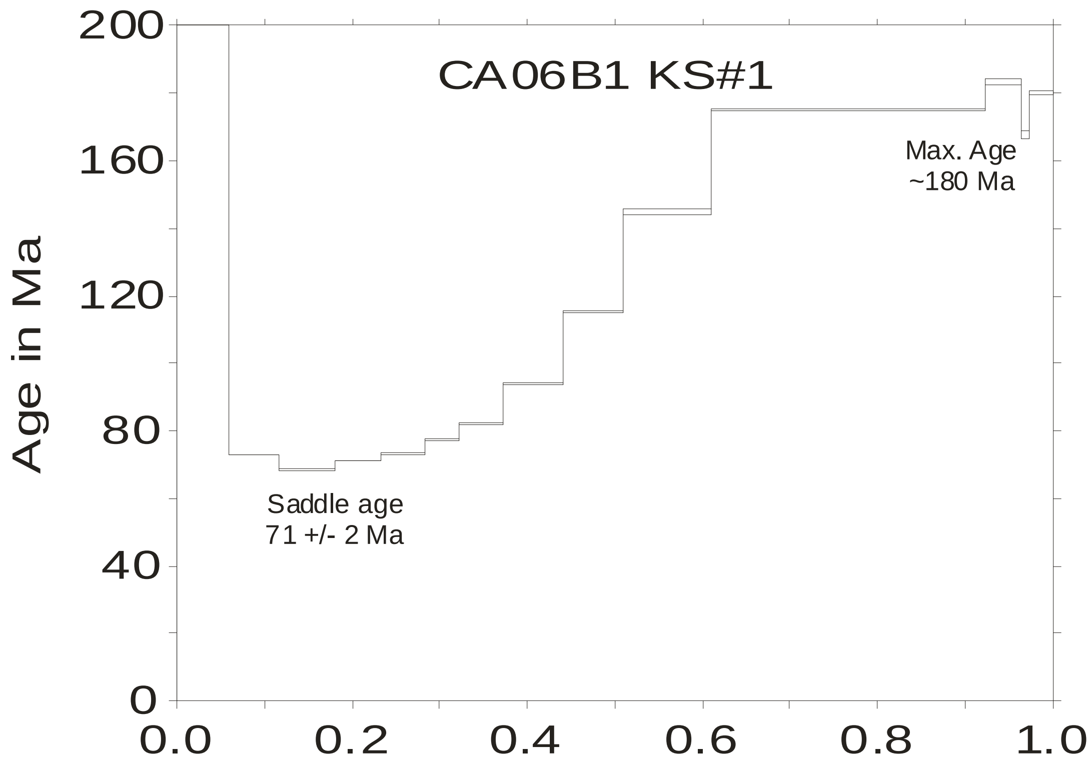

CA06B1 KS#1
Age in Ma
200
160
120
80
40
0
0.0
0.2
0.4
0.6
0.8
1.0
Saddle age
71 +/- 2 Ma
Max. Age
~180 Ma

Lemhi Pass Th-REE District
EPMA geochronology results – preliminary report

Michael J. Jercinovic

Electron Microprobe / SEM Facility
Department of Geosciences, University of Massachusetts
Amherst. MA 01003

Introduction and Methodology

The geochronology of the monazite – thorite deposits in the Lemhi Pass Thorium-Rare Earth District of Idaho and Montana has been difficult to assess, primarily due to the very low actinide content (below 0.5wt.% total) of the abundant monazite, and the inherent difficulties of thorite dating (difficulties chiefly due to metamictization, hydrolysis, and subsequent mobilization of radiogenic Pb). Electron probe microanalysis (EPMA) offers the potential to date such materials by measurement of total radiogenic Pb if a satisfactorily sensitive analysis can be devised. Preliminary reconnaissance work characterizing these materials by EPMA indicated that very thin (several micron) rims and fracture fillings in monazite are somewhat higher in Th (1-2wt.%), permitting better precision and accuracy if the spatial resolution of analysis is sufficient. In addition, there is the potential to find small, un-hydrolyzed domains in thorite, also requiring high spatial resolution, for attempts at accurate dating.

The unique Cameca SX-Ultrachron at the University of Massachusetts is an electron probe designed specifically for trace element microanalysis at high spatial resolution, with an emphasis on Th-U-total Pb geochronology related to monazite, xenotime, thorite, and other natural chronometers. The relatively low common Pb concentrations in these phases, along with high concentrations of actinides (and resulting high radiogenic Pb concentrations) generally allow accurate analysis by this technique. The power of the technique resides in the high spatial resolution afforded by electron probe microanalysis (EPMA), and the in-situ, non-destructive nature of the analysis. Analyses are typically performed on petrographic thin sections, preserving the textural relationships necessary for relating age information with mineral paragenesis, reaction textures, and/or deformation features (e.g., Terry et al., 2000; Shaw et al., 2001; Dahl et al., 2005; Mahan et al. 2006a,b; Dumond et al., 2008). In this way, reactions and kinematic processes can be directly constrained temporally, and polygenetic mineral growth can be evaluated on the micro-scale.

Modern use of EPMA for geochronology was re-introduced by Suzuki and Adachi (1991), Suzuki et al. (1994), and Montel et al. (1996). Compositional mapping, age mapping, and application to tectonic problems by direct, in-situ thin section analysis were discussed by Williams et al. (1999), Williams and Jercinovic (2002), and Goncalves et al. (2005). A recent review of the technique and applications is presented by Williams et al. (2007), and details of analytical issues, strategies, and protocols are presented in Jercinovic and Williams (2005), Jercinovic et al. (2008), Pyle et al. (2002; 2005), and Williams et al. (2006).

Monazite is efficiently located in thin section by full-section compositional mapping. Once locations are documented, all monazite to be analyzed must be compositionally mapped in order to delineate compositional domains. Nearly all natural monazite is compositionally zoned, with zones corresponding in some cases to different ages. The details of compositional zoning are critical for conducting subsequent quantitative analysis, and are also significant for understanding the chemical evolution of the system and correlating reactions to ages (e.g., Williams et al., 2006; 2007). Once mapping has been completed, quantitative analysis can be carried out. Table 1 lists the general EPMA protocol for monazite in thin section.

Quantitative analysis of monazite (REE phosphate) for EPMA geochronology requires the measurement of trace concentrations of Pb and U, and, as is sometimes the case with the monazite in the Lemhi Pass area, minor or trace levels of Th. In most cases, monazite contains Th as a major constituent, but the Lemhi Pass monazite is unusually low in Th, and nearly devoid of U, making analysis particularly challenging. In addition, all major elements must be measured in order for accurate matrix corrections to be applied. The quantitative settings used for this analysis are listed in Appendix A. The PbMα line is used for analysis of Pb in order to maximize count precision (and resulting age precision – see Pyle et al., 2005). The intensity of PbMα, however, must be corrected for overlaps of ThMζ1 and Mζ2, YLγ, and LaLα (2nd order). UMβ is the analytical line for the uranium analysis as the Th interference with UMα is very severe, but there is also Th interference on UMβ that must be corrected for. Therefore, interference calibrations are performed using brabantite for the Th interferences on Pb and U (ThLγ, and family on UMβ), Y-Al-garnet, for interference of YLγ on PbMα, $LaPO_4$ for interference of La on Pb, and K-feldspar, for interference of K Kα on UMβ. Careful selection of peak and background positions for REE analysis avoids most overlaps, however, an overlap of Nd Lβ3 on EuLα must still be accounted for, therefore, an overlap calibration for the Eu measurement is done using synthetic $NdPO_4$.

Background intensities for Pb, Th, and U are obtained by careful WDS scanning (see Jercinovic and Williams, 2005; Jercinovic et al., 2008). Scans for each compositional domain are noise filtered, and selected background wavelength regions are regressed using exponential modeling (see Williams et al., 2007; Jercinovic et al, 2008 for details). The high concentrations of LREEs in the Pb M region of PET, plus occurrences of other interfering lines, sometimes generated by fluorescence at a distance, requires careful evaluation and background modeling to extract appropriate background intensities in monazite. Linear interpolation for background determination will result in very large errors on net intensities for trace element analysis due to both background curvature and potential interferences.

Thorite analysis proceeds by characterizing each potential grain in via backscattered electron imaging to find regions which are not hydrolyzed. Thorite is readily rendered metamict due to very high α-dose, and is then subject to hydrolysis and Pb loss (Lumpkin and Chakoumakos, 1988). High backscatter-brightness regions in thorite tend to remain relatively stoichiometric, and Pb loss is expected to be minimized in these areas. Analyses are confined to these regions. For thorite, Th is present in very high concentration and represents a major element analysis. Radiogenic Pb will reach major element proportions in a few hundred m.y., so peak net intensities are expected to be relatively high. Th interference on PbMα is extreme, so the PbMβ line is selected as the analytical line. The other major issue with thorite analysis relates to the uranium analysis. With such high Th concentrations, the absorption edges corresponding to the Th MIV and ThMV levels will be very significant (Jercinovic and Williams, 2005). The only accurate means of background measurement in this case is to do a single estimate between the two edges, near the low wavelength side of the ThMγ peak. The Th interference on the UMβ line is very large, but can be corrected by interference correction.

Table 1. Summary of analytical procedure for EPMA geochronology as currently implemented at UMass.

Step	Procedure	Explanation
1	Full section map	Carbon coat thin section (vacuum evaporation to ~250Å) and collect map of Ce (and / or La or Nd), Y, and Th, along with base-map reference element (Mg, Al). Typically 1024X512 pixels, 35 µm pixel step size, defocused beam (~ 35 µm). 300 nA, 15kV, 20 msec count time / pixel.
2	Process maps for accessory mineral selection	Import raw maps into image analysis program (Adobe Photoshop or equivalent). Adjust I/O levels to highlight Ce (or La) spots and import adjusted maps as layers into Adobe Illustrator or equivalent. Mark spots from REE, Y and / or Th maps on separate layer with circles, dots, etc. Overlay marked layer on base map (Mg or Al) to identify accessory phases in textural context.
3	Map minerals at high magnification	Map selected grains, usually beam rastering at resolution giving step size <1 µm. Generally YLα, ThMα, UMβ, and CaKα, (and / or other geochemically important elements). 200nA, 100msec/pixel, focused beam.
4	Remove carbon coat, then apply high conductivity coat	Lightly polish section (≤0.3 µm polishing compound) to remove C-coat. Apply Al coat to thin section(s) and standards (stripped of coatings) by high-vacuum thermal evaporation. Should be ~200Å. Follow with ~80Å evaporated carbon. Coated materials must be kept under high vacuum.
5	Collect backgrounds for trace element analysis	Acquire wavelength scans of regions around ThMα, UMβ, and PbMα (8-sinθ steps over 8400 sinθ range, 1500msec/step, 200nA, 15kV, focused beam, differential mode PHA). Collected counts are converted to dead-time corrected cps/nA. Backgrounds should be acquired for each identified compositional domain, particularly guided by thorium variation. All critical domains should have direct background characterization.
6	Extract background intensity from scans	Apply digital noise filter to scan data (Savitsky-Golay ~4% data window with order 3 polynomial), select appropriate background regions (avoiding interferences), and regress included data (exponential best-fit in most cases). Apply regressed line to peak position to calculate intensity of background under peak of interest.
7	Obtain integrated trace and major element analyses.	Calibrate (at 20nA, 15kV, focused beam), YLα, ThMα, UMβ, and PbMα, (see Appendix A). Enter background intensities obtained via above regressions into analysis settings files for each domain. Analyze unknowns (200nA, 15kV, focused beam, 600-900 sec. per point). UMass Moacyr monazite (506 Ma via ID-TIMS and SHRIMP) is analyzed prior unknowns, and is periodically analyzed during the quantitative session to monitor data consistency. For details, see Appendix A for monazite, Appendix B for thorite. Identified compositional domains should be individually analyzed as per Williams et al. (2006). Concentrations are modified by empirical corrections for overlaps (cps-subtraction, matrix iterated). Such corrections are done by interference calibration on appropriate standards. Final concentrations are done via PAP for matrix effects.
8	Calculate ages	Calculate age by iteration (calculating Pb as a function of age with Th and U known, converge to the measured Pb concentration). Analyses confined to a single compositional domain are evaluated for compositional heterogeneity and appropriate errors are calculated using accumulated analyses and propagation of counting statistics (see Williams et al., 2006).

The analytical strategy for both monazite and thorite follows that of Williams et al. (2006). Analyses (individual data points) are confined to a defined compositional domain within a grain.

Points are accumulated within the particular domain in order to build an appropriate statistical precision. Histograms are constructed assuming a normal distribution to illustrate age precision. Weighted means of age populations are calculated for an improved estimate of the age when appropriate. A consistency standard (Moacyr monazite, 506 Ma by ID-TIMS and SHRIMP-II) is analyzed before the unknowns are analyzed as a check of calibration and is run periodically during each session as a consistency standard (Williams et al., 2006).

Detection limits for the geochronologically relevant elements in monazite and thorite are listed in Table 2 for single point analyses and in Table 3 for a population. Approximately 20 points would be required in a domain to obtain population detection limits for Pb in monazite of 5 ppm.

Table 2. Single point detection limits (Ancey, 1978) in ppm.

	Th	U	Pb
Monazite	58	30	25
Thorite	755	91	116

Table 3. Example population detection limits (Ancey, 1978) in ppm. Numbers reported are for monazite N = 8 points, and thorite N = 5 points.

	Th	U	Pb
Monazite	21	**12**	10
Thorite	417	40	62

Instrumentation used includes both the Cameca SX-Ultrachron and Cameca SX50 electron microprobes in the Department of Geosciences at the University of Massachusetts. Mapping was done on all monazite-bearing thin sections and grain mounts using the SX50. This is a 5-WDS spectrometer instrument (with PGT EDS) with LaB_6 cathode, automated via Cameca's SXrayN50 software on a Unix platform. Monazite full section search maps were done using a 15 kV accelerating potential, 200nA beam current, and 35 micron pixel step size. Sections were mapped for Y, Nd (Ce in some cases), Th, and Si. High resolution maps of individual monazite grains or areas were done at 15 kV and 200 nA, with pixel dimensions sufficient to generally achieve sub-micron resolution. Elements mapped include Y, Th, U, and Ca. All quantitative analysis was performed using the Ultrachron. This is also a 5-WDS spectrometer instrument with EDS (Bruker X-Flash SDD), LaB_6 cathode and specially modified gun and optics to achieve optimum beam diameter (smallest possible) over a range of voltage and current, with particular attention to the high current, relatively low voltage requirements for EPMA geochronology. This unique instrument also has two specially constructed VLPET (very-large PET) monochromators with commensurately large flow-proportional counters. These spectrometers have approximately 4x the count rates of traditional PET spectrometers. Automation is done via the PC-based PeakSight™ software. See Appendices A and B for analytical parameters for monazite and thorite.

Samples supplied by Virginia Gillerman were mapped and analyzed. Samples selected for quantitative EPMA geochronology are listed in Table 4 (monazite) and Table 5 (thorite), also listing specific domains analyzed.

Table 4. Samples and domains selected for quantitative monazite EPMA geochronology.

	sample	monazite	domain
Grain mount	LH06-24B	M15	central core
			central low Y core
			high Th rim right
			high Th rim SE
			high Y core SE
			low Th core S
Thin section	06CTCAr	m2a	
		m2b	
		m4a	
		m4b	
Thin section	JA06-01C	m4	SW
		m7	
Thin section	LH06-25	m2	high Th core right
			low Th core
		m3	high Th fracture left
			high Th rim right
			high Y core lower
			low Y core right
Thin section	LH06-A2	m1	area center grain
			higher Th
		m3	high Th
			low Th
Thin section	LH12C	m1	low Th
			high Th
		m2	low Th
			high Th

Table 5. Samples and domains selected for quantitative thorite EPMA geochronology.

	sample	thorite	domain
Grain mount	LH06-24B	14	area 1
		16	area 1
			area 1c
		17	area 1
		18	area 1
			area 2
			area 3
Thin Section	LH06-25	1	area 1
			area 2
		2	area 1
		3	area 1
		4	area 1
		5	area 1
			area 2
			area 3
Thin section	LH06-A2	1	area 1
			area 2
			area 3
			area 4
			area 5
			area 6
		2	area 1
		3	area 1
			area 2
Thin section	LH8c	1	area 1
			area 2
		2	area 2
			area 3
		3	area 1
			area 2
			area 3
Thin section	LH12c	2	area 1
		3	area 1
		4	area 1
		5	area 1
		6	area 1
		7	area 1

Results

Full thin-section monazite search maps are shown in Appendix C. Specific monazites were selected from these maps, and those individual grains were mapped at much higher magnification in order to reveal compositional microstructure. The high resolution monazite compositional maps provide the basis for quantitative analyses of monazite by EPMA as analyses are confined to individual domains (see Table 4 for list of compositional domains analyzed). Figure 1 gives an example of the mapping-based analytical strategy for LH06-25 monazite 3. Figure 2 shows a histogram representation of age results from this sample.

Monazite from the Lucky Horseshoe mine is exceptionally high in Nd and Pr (~ 35wt.% Nd_2O_3, ~ 5wt.% Pr_2O_3), and commensurately low in La and Ce compared to most monazite worldwide (see example analyses, Table 6). Thorium concentrations in the bulk monazite (by far the most volumetrically significant) in the samples for this study is generally below 0.6 wt.% (Table 6). There is also clear evidence, in most monazite samples, of higher Th rims and fracture fillings (see Figure 1). This higher Th monazite (1-2 wt.% in general, see Table 6), can be interpreted as precipitating later than the bulk, low-Th monazite via textural evidence. The Cameca SX-Ultrachron is capable of the spatial resolution necessary to cleanly analyze these relatively high Th rims and fracture fillings, and is also uniquely capable of the count precision necessary to dependably analyze the low-actinide (and very low Pb) bulk monazite. Table 7 summarizes age results from monazite-bearing samples. Table 8 presents weighted means for comparable domains in each sample.

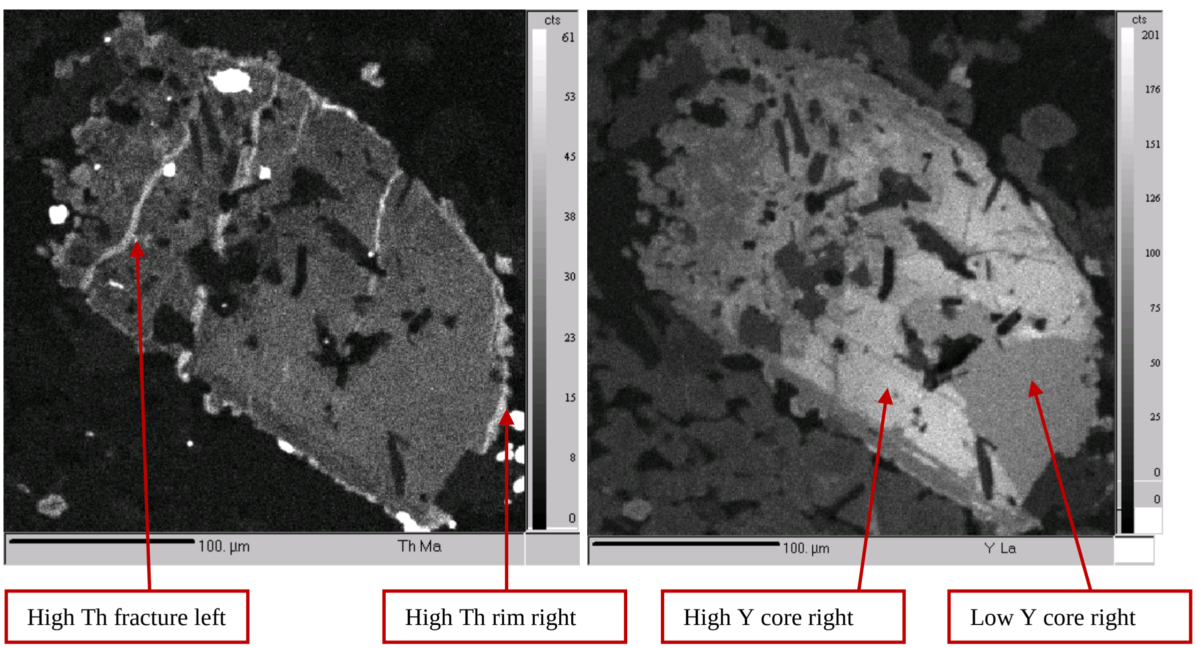

Figure 1. X-ray compositional maps of monazite grain 3 from sample LH06-12, Lucky Horseshoe mine, left = Th, right = Y. Analyzed domains shown below images. See Tables 6 and 7 for results. See Figure 2 for age histograms from this sample. Note small thorite grains (very bright areas) in Th image (left).

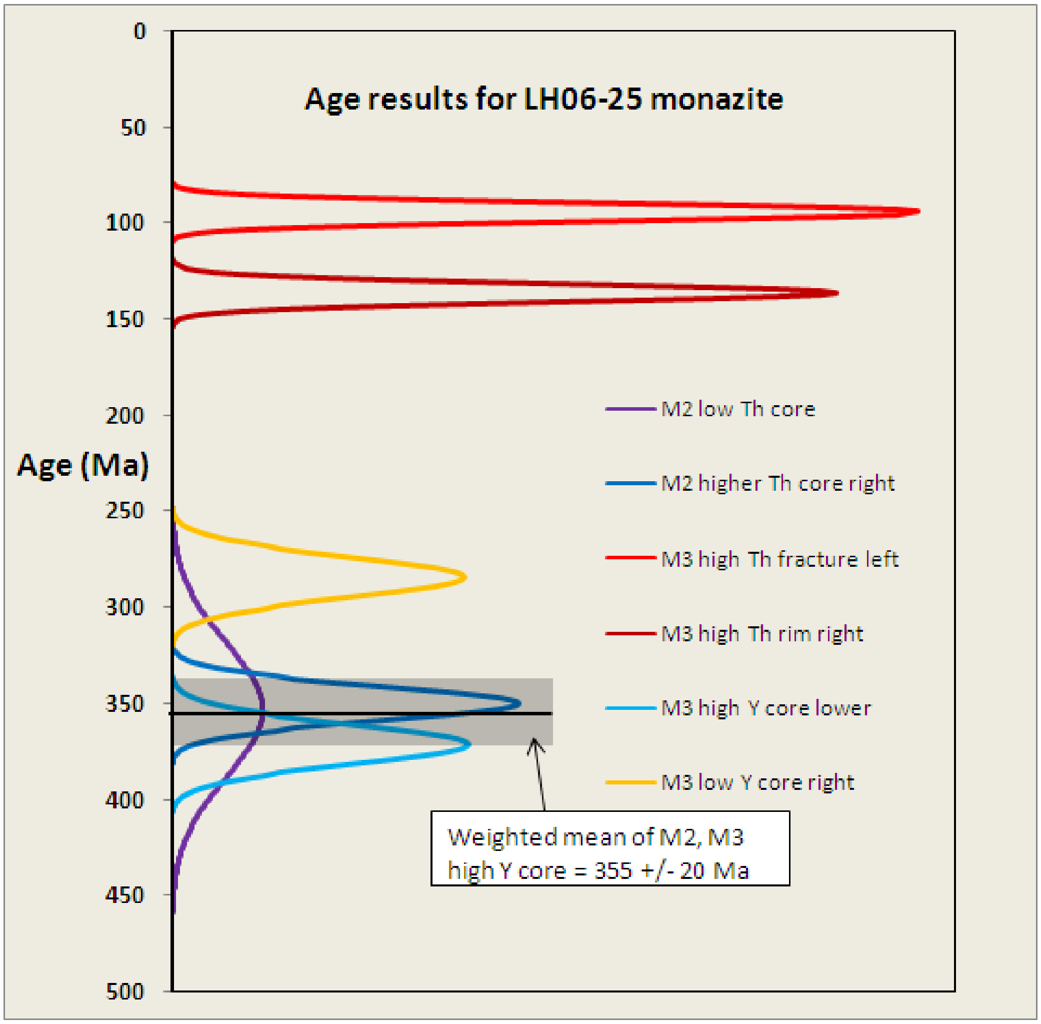

Figure 2. Histogram representation of age results for LH06-25 monazite. Histograms represent age and error as normal distribution around weighted mean age of analyses in each domain. A separate weighted mean of the cumulative results of M2 monazite and M3 high Y core results is shown.

Table 6. Example analyses from low and high Th domains, Lucky Horseshoe mine monazite.

	LH12c M2		LH06-25 M3	
	low Th	high Th	high Y core	high Th fracture
	oxide wt.%	oxide wt.%	oxide wt.%	oxide wt.%
CaO	0.228	0.349	0.310	0.233
K2O	0.011	0.043	0.025	0.039
SiO2	0.198	0.242	0.231	0.285
SrO	0.033	0.031	0.038	0.024
P2O5	28.867	28.963	29.600	29.834
As2O3	0.194	0.044	0.001	0.065
ThO2	0.480	1.838	0.501	1.809
UO2	0.000	0.002	0.000	0.001
Y2O3	1.147	0.800	1.382	0.614
La2O3	3.680	3.493	2.417	2.950
Ce2O3	16.873	16.420	14.275	15.768
Nd2O3	34.774	35.097	35.780	35.460
Pr2O3	5.031	5.018	4.942	5.130
Sm2O3	2.937	2.930	4.243	3.762
Tb2O3	0.000	0.000	0.000	0.000
Gd2O3	1.557	1.605	2.076	1.844
Dy2O3	0.000	0.000	0.028	0.000
Ho2O3	0.020	0.016	0.014	0.000
Er2O3	0.045	0.019	0.037	0.008
Eu2O3	1.213	1.177	1.468	1.342
Tm2O3	0.572	0.583	0.649	0.610
Yb2O3	0.001	0.012	0.005	0.011
SO3	0.106	0.120	0.047	0.068
PbO	0.009	0.010	0.009	0.008
Total	97.979	98.814	98.078	99.865
	ppm	ppm	ppm	ppm
Y	9033	6299	10885	4836
Th	4492	17197	4687	16925
U	3	22	4	7
Pb	82	83	78	70

Table 7. Summary of monazite EPMA geochronology results.

	sample	monazite	domain	Age (Ma +/- SOM)*
Grain mount	LH06-24B	M15	central core	376 +/- 28
			central low Y core	336 +/- 29
			high Th rim right	80 +/- 9
			high Th rim SE	(included in above value)
			high Y core SE	351 +/- 30
			low Th core S	349 +/- 55
Thin section	06CTCAr	m2a		334 +/- 18
		m2b		(included in above value)
		m4a		333 +/- 34
		m4b		(included in above value)
Thin section	JA06-01C	m4	SW	**
		m7		102 +/- 12
Thin section	LH06-25	m2	high Th core right	334 +/- 23
			low Th core	334 +/- 25
		m3	high Th fracture left	81 +/- 12
			high Th rim right	127 +/- 18
			high Y core lower	364 +/- 21
			low Y core right	277 +/- 13
Thin section	LH06-A2	m1	area center grain	341 +/- 36
			higher Th	365 +/- 20
		m3	high Th	343 +/- 30
			low Th	**
Thin section	LH12C	m1	low Th	358 +/- 28
			high Th	118 +/- 15
		m2	low Th	365 +/- 21
			high Th	83 +/- 16

*Age reported = weighted average of analyses +/- 1 standard error of the mean of population of analyses.
** Unacceptable data array

Table 8. Weighted means of monazite EPMA age results.

	sample	monazite	domain	Weighted mean age (Ma +/- 2σ)*
Grain mount	LH06-24B	m15	central core	
			central low Y core	359 +/- 20
			high Y core SE	
			low Th core S	
Thin section	LH06-25	m2	high Th core right	
			low Th core	355 +/- 20
		m3	high Y core lower	
	LH06-25	m3	high Th fracture left	101 +/- 12
			high Th rim right	
Thin section	LH06-A2	m1	area center grain	
			higher Th	352 +/- 31
		m3	high Th	
Thin section	LH12C	m1	low Th	364 +/- 22
		m2	low Th	
	LH12C	m1	high Th	95 +/- 11
		m2	high Th	

*Age reported = weighted average of analyses +/- 2 Std Dev.

Thorite is intergrown with monazite in the Lemhi Pass thin sections from the Lemhi Pass area. Backscattered electron (BSE) imaging reveals small areas in some grains which are clearly of higher average atomic number (significantly brighter in BSE – see Figures 3 and 4) compared to the bulk thorite. Although generally small, these areas are analytically accessible by EPMA, and yield nearly stoichiometric thorite when quantitatively analyzed. Hydrolysis in accompanied by uptake of Ca (Figure 4) and Fe in thorite. Ages obtained by EPMA geochronology for this "unaltered" thorite are given in Table 9.

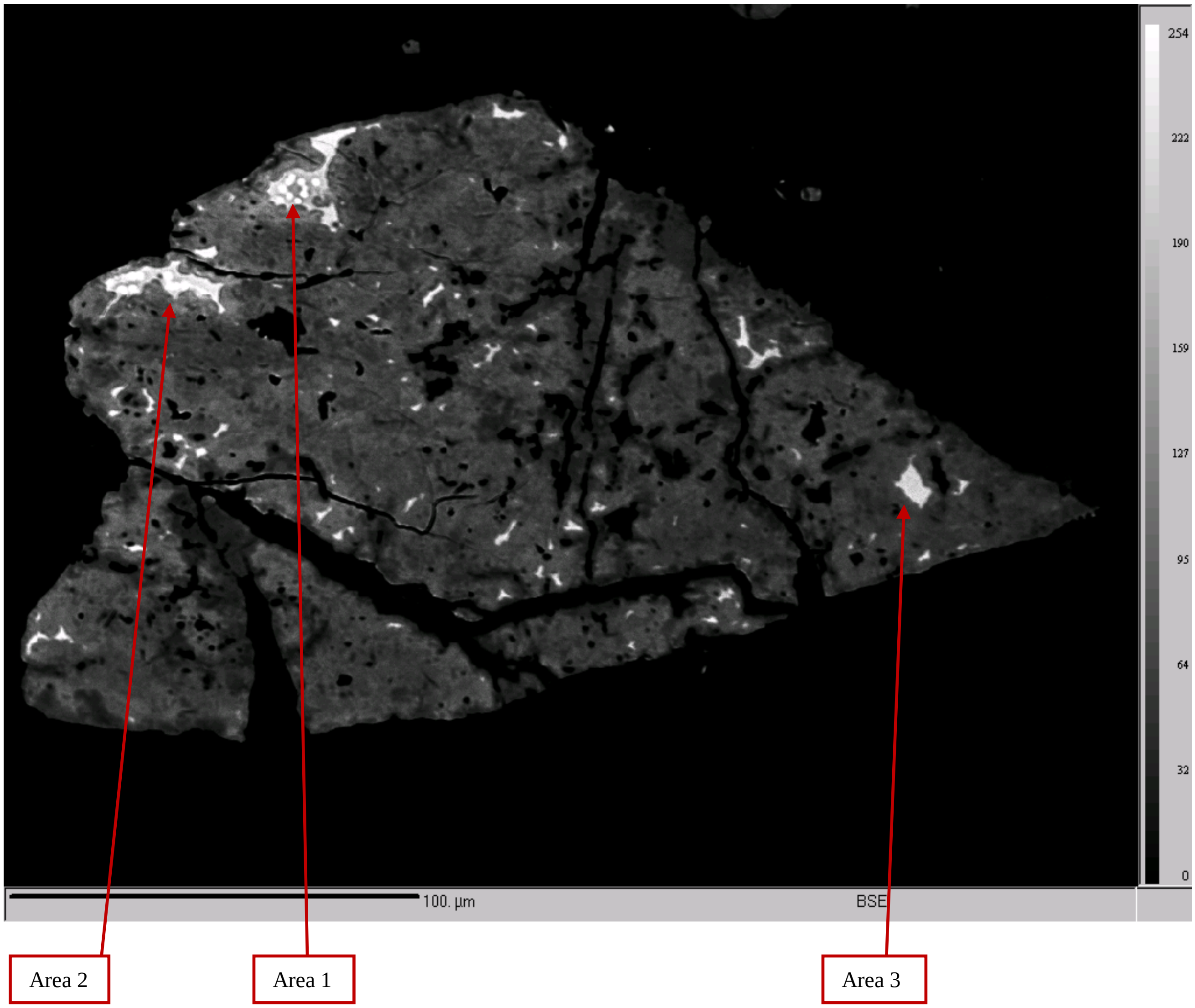

Figure 3. Backscattered electron image of thorite from Lucky Horseshoe (LH06-25, thorite 5). BSE bright areas are remnant, un-hydrolyzed regions (thorite is susceptible to hydrolysis after metamictization). Note scalloped edges of the bright regions, typical of hydrolytic reconstruction front. See Table 9 for results on thorite EPMA geochronology.

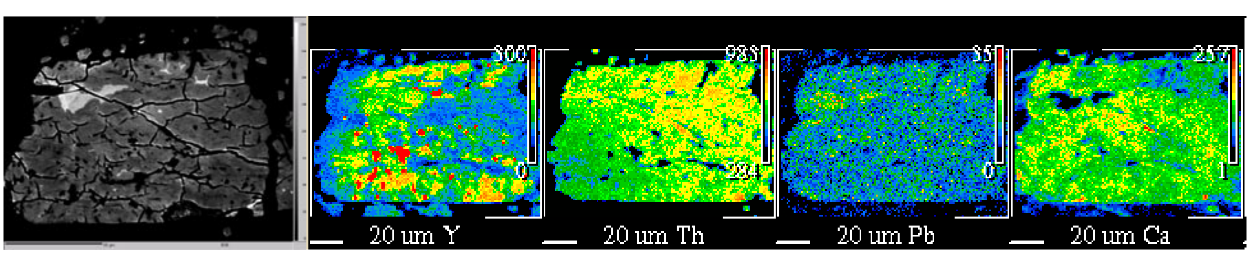

Figure 4. Thorite 3 from LH12c. BSE (left), and compositional maps. BSE bright area in upper left of grain is LH12c Thorite 3 analysis Area 1 in Tables 5 and 9. Note higher Ca in BSE darker (hydrolyzed) areas.

Table 9. Summary of Thorite EPMA age results.

	sample	thorite	domain	Age (Ma +/- SOM)*
Grain mount	LH06-24B	14	area 1	268 +/- 17
		16	area 1	334 +/- 3
			area 1c	323 +/- 6
		17	area 1	350 +/- 12
		18	area 1	344 + /- 6
			area 2	351 +/- 5
			area 3	346 +/- 4
Thin Section	LH06-25	1	area 1	408 +/- 4
			area 2	383 +/- 2
		2	area 1	94 +/- 5
		3	area 1	403 +/- 9
		4	area 1	**
		5	area 1	344 +/- 2
			area 2	334 +/- 2
			area 3	102 +/- 1
Thin section	LH06-A2	1	area 1	100 +/- 1
			area 2	120 +/- 7
			area 3	124 +/- 5
			area 4	139 +/- 8
			area 5	263 +/- 8
			area 6	174 +/- 10
		2	area 1	159 +/- 6
		3	area 1	339 +/- 3
			area 2	332 +/- 2
Thin section	LH8c	1	area 1	288 +/- 15
			area 2	328 +/- 4
		2	area 2	324 +/- 8
			area 3	285 +/- 6
		3	area 1	292 +/- 7
			area 2	289 +/- 12
			area 3	**
Thin section	LH12c	2	area 1	136 +/- 18
		3	area 1	344 +/- 8
		4	area 1	295 +/- 11
		5	area 1	355 +/- 8
		6	area 1	160 +/- 10
		7	area 1	332 +/- 11

*Age reported = weighted average of analyses +/- 1 standard error of the mean of population of analyses.
** Unacceptable data array

Summary

Evidence of two episodes of monazite growth is preserved in samples from the Lemhi Pass Th-REE District of Idaho and Montana, illustrated in Figure 5. The initial episode, at which time the major Th-REE mineralization appears to have taken place, occurred ca. 350 Ma. The actinide content of this monazite is exceptionally low, and the Nd-Pr content exceptionally high, relative to typical igneous or metamorphic monazite (for example, see Williams et al., 2007). Thorium concentrations are generally below 6000 ppm, and concentrations of U generally below 100 ppm in the Lemhi Pass region bulk monazite. This monazite is, however, associated with major mineralization of thorite ($ThSiO_4$). A second episode of ca. 100 Ma monazite growth is also suggested. This monazite occurs generally as thin (less than 5 micrometers) rims on the bulk monazite or as fracture fillings. The later monazite is significantly higher in Th, generally 1-2 wt.% Th, but reaching nearly 5 wt.% in some samples (06CTCAr). There is no suggestion of mineralization older than late Devonian based on monazite EPMA geochronology, and a second episode (although volumetrically minor) of cretaceous mineralization is implied.

EPMA of thorite from the Lemhi Pass Th-REE District yields data compatible with ages suggested by monazite. Although easily rendered metamict with subsequent hydrolyzation (Lumpkin and Chakoumakos, 1988) some small (generally below 10 micrometer) areas within some thorite grains remain. Analysis of these areas yields ages similar to coexisting monazite, and are compatible with mineralization at ca. 350 Ma and ca. 100 Ma (see Figure 5). Radiogenic Pb concentrations in thorite are expected to be somewhat variable due to the effects of metamictization, therefore the spread of apparent ages is correspondingly larger for thorite relative to monazite in Figure 5. There is no suggestion of ages appreciably older than ca.350 Ma, or significantly younger than ca. 100 Ma based on thorite analyses.

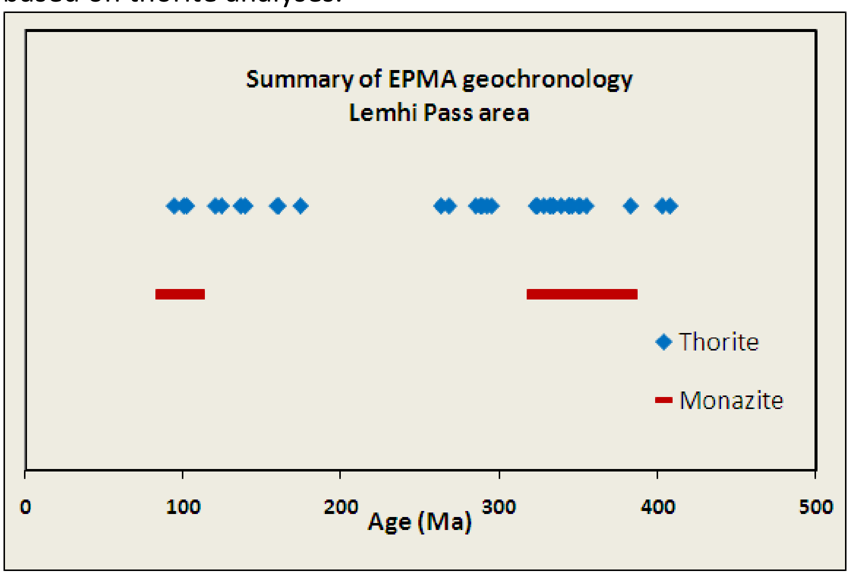

Figure 5. Summary of EPMA geochronology results, analyses from all domains, all samples (see Tables 4 and 5). Monazite data are from Table 8, representative of 2σ errors of weighted means. Thorite values are from Table 9.

References

Ancey M., Bastenaire F., and Tixier R. (1978) Applications of statistical methods in microanalysis. In: Microanalysis and scanning electron microscopy. Pp. 319-343 in *Proceedings of the Summer School at St-Martin-d'Heres*. Maurice, F., Meny L., and Tixier, R. eds. Les Editions de Physique, Orsay, France.

Dahl, P.S., Hamilton, M.A.., Jercinovic, M.J., Terry, M.P., Williams, M.L., and Frei, R. (2005) Comparative isotopic and chemical geochronometry of monazite in metamorphic rocks from the eastern Wyoming province (USA), with implications for U-Th-Pb dating by electron microprobe. *American Mineralogist* **90**, 619-638.

Dumond, G., McLean, N., Williams, M.L., Jercinovic, M.J., and Bowring, S.A. (2008) High-resolution dating of granite petrogenesis and deformation in a lower crustal shear zone, Athabasca granulite terrane, western Canadian Shield. *Chemical Geology* **254**, 175-196.

Goncalves, P., Williams, M.L., and Jercinovic, M.J. (2005) Electron microprobe age mapping. *American Mineralogist* **90**, 578-585.

Jercinovic, M.J., and Williams, M.L. (2005) Analytical perils (and progress) in electron microprobe trace element analysis applied to geochronology: Background acquisition, interferences, and beam irradiation effects. *American Mineralogist* **90**, 526-546.

Jercinovic, M.J., Williams, M.L., and Lane, E.D. (2008) In-situ trace element analysis of monazite and other fine-grained accessory minerals by EPMA. *Chemical Geology* **254**, 197-215.

Lumpkin, G.R. and Chakoumakos, B.C. (1988) Chemistry and radiation effects of thorite-group minerals from the Harding pegmatite, Taos County, New Mexico. *American Mineralogist* **73**, 1405-1419.

Mahan, K.H., Williams, M.L., Flowers, R.M., Jercinovic, M.J., Baldwin, J.A., and Bowring, S.A. (2006) Geochronological constraints on the Legs Lake shear zone with implications for regional exhumation of lower continental crust, western Churchill Province, Canadian Shield. *Contributions to Mineralogy and Petrology* **152**, 223-242.

Mahan, K.H., Goncalves, P., Williams, M.L., and Jercinovic, M.J. (2006) Dating metamorphic reactions and fluid flow: Application to exhumation of high-P granulites in a crustal-scale shear zone, western Canadian Shield. *Journal of Metamorphic Geology* **24**, 193-217.

Montel J., Foret S., Veschambre M., Nicollet C., Provost A. (1996) Electron microprobe dating of monazite. *Chem. Geol*. **131**,37–53.

Pyle J.M, Spear F.S, and Wark D.A. (2002). Electron microprobe analysis of REE in apatite, monazite and xenotime; protocols and pitfalls. See Kohn et al. 2002, pp. 337–62.

Pyle J.M, Spear F.S,Wark D.A, Daniel C.G, and Storm L.C. (2005). Contributions to precision and accuracy of chemical ages of monazite. *American Mineralogist* **90**, 547–577.

Shaw, C.A., Karlstrom, K.E., Williams, M.L., Jercinovic, M.J., and McCoy, A.M. (2001) Electron microprobe monazite dating of ca. 1.71 – 1.63 Ga and ca. 1.45-1.38 deformation in the Homestake shear zone, Colorado: Origin and early evolution of a persistent intracontinental tectonic zone. *Geology* **29**, 739-742.

Suzuki K, Adachi M. (1991) Precambrian provenance and Silurian metamorphism of the Tsubonasawa paragneiss in the South Kitakami terrane, Northwast Japan, revealed by the chemical Th-U-total Pb isochron ages of monazite, zircon and xenotime. *Geochem. J.* **25**:357–76.

Suzuki K, Adachi M, Kajizuka I. (1994) Electron microprobe observations of diffusion in metamorphosed detrital monazites. *Earth Planet. Sci. Lett*. **128**:391–405.

Terry, M.T., Robinson, P., Hamilton, M.A., and Jercinovic, M.J. (2000) Monazite geochronology of UHP and HP metamorphism, deformation, and exhumation, Nordoyane, Western Gneiss Region, Norway. *American Mineralogist* **85**, 1651-1664.

Williams, M.L., and Jercinovic, M.J. (2002) Microprobe monazite geochronology: Putting absolute time into microstructural analysis. *Journal of Structural Geology* **24**, 1013-1028.

Williams ML, Jercinovic MJ, Terry M. (1999). High resolution "age" mapping, chemical analysis, and chemical dating of monazite using the electron microprobe: A new tool for tectonic analysis. *Geology* **27**:1023–26.

Williams, M.L., Jercinovic, M.J., Goncalves, P. and Mahan, K. (2006) Format and Philosophy for Collecting, Compiling, and Reporting Microprobe Monazite Ages. *Chemical Geology* **225**, 1-15.

Williams, M.L., Jercinovic, M.J., and Hetherington, C.J. (2007) Microprobe Monazite Geochronology: understanding geologic processes through integration of composition and chronology. *Annual Review of Earth and Planetary Sciences* **37**, 137-175.

Appendix A. Quantitative settings for monazite analysis.

****
******

Common informations :

File Name : Moacyr TS 11-03-2008.qtiSet
File Date : Nov/03/08-2:43 PM
Comment :

****
******

Column conditions :

Cond 1 :
HV (kV) : 15 I (nA) : 200
Size (µm) : 0.
Scanning : Off
RasterLength (µm) : 16.63

****
******

Xtal informations :

Xtal parameters:

Pb Ma 1	Sp3	LPET	(2d= 8.75	K= 0.000144)
Pb Ma 1	Sp4	LPET	(2d= 8.75	K= 0.000144)
U Mb 1	Sp1	LPET	(2d= 8.75	K= 0.000144)
As Ka 1	Sp5	LLIF	(2d= 4.0267	K= 0.000058)
La La 1	Sp5	LLIF	(2d= 4.0267	K= 0.000058)
Ce La 1	Sp5	LLIF	(2d= 4.0267	K= 0.000058)
Pr Lb 1	Sp5	LLIF	(2d= 4.0267	K= 0.000058)
Nd La 1	Sp5	LLIF	(2d= 4.0267	K= 0.000058)
Sm Lb 1	Sp5	LLIF	(2d= 4.0267	K= 0.000058)
Eu La 1	Sp5	LLIF	(2d= 4.0267	K= 0.000058)
Gd Lb 1	Sp5	LLIF	(2d= 4.0267	K= 0.000058)
Tb La 1	Sp5	LLIF	(2d= 4.0267	K= 0.000058)
Dy La 1	Sp5	LLIF	(2d= 4.0267	K= 0.000058)
Ho Lb 1	Sp5	LLIF	(2d= 4.0267	K= 0.000058)
Er La 1	Sp5	LLIF	(2d= 4.0267	K= 0.000058)
Tm La 1	Sp5	LLIF	(2d= 4.0267	K= 0.000058)
Yb La 1	Sp5	LLIF	(2d= 4.0267	K= 0.000058)
Si Ka 1	Sp2	LPET	(2d= 8.75	K= 0.000144)

Sr La 1	Sp2	LPET	(2d= 8.75	K= 0.000144)
Y La 1	Sp2	LPET	(2d= 8.75	K= 0.000144)
P Ka 1	Sp2	LPET	(2d= 8.75	K= 0.000144)
S Ka 1	Sp2	LPET	(2d= 8.75	K= 0.000144)
Th Ma 1	Sp2	LPET	(2d= 8.75	K= 0.000144)
Ca Ka 1	Sp2	LPET	(2d= 8.75	K= 0.000144)
K Kb 1	Sp1	LPET	(2d= 8.75	K= 0.000144)

Pha parameters :

Elt. Line	Spec	Xtal	Bias (V)	Gain	Dtime (µs)	Blin (mV)	Wind (mV)	Mode
Pb Ma 1	Sp3	LPET	1855	864	3	560	2300	Diff
Pb Ma 1	Sp4	LPET	1865	873	3	560	2300	Diff
U Mb 1	Sp1	LPET	1320	895	2	560	4000	Diff
As Ka 1	Sp5	LLIF	1860	400	3	560	3100	Diff
La La 1	Sp5	LLIF	1860	400	3	560	3100	Diff
Ce La 1	Sp5	LLIF	1860	400	3	560	3100	Diff
Pr Lb 1	Sp5	LLIF	1860	400	3	560	3100	Diff
Nd La 1	Sp5	LLIF	1860	400	3	560	3100	Diff
Sm Lb 1	Sp5	LLIF	1860	400	3	560	3100	Diff
Eu La 1	Sp5	LLIF	1860	400	3	560	3100	Diff
Gd Lb 1	Sp5	LLIF	1860	400	3	560	3100	Diff
Tb La 1	Sp5	LLIF	1860	400	3	560	3100	Diff
Dy La 1	Sp5	LLIF	1860	400	3	560	3100	Diff
Ho Lb 1	Sp5	LLIF	1860	400	3	560	3100	Diff
Er La 1	Sp5	LLIF	1860	400	3	560	3100	Diff
Tm La 1	Sp5	LLIF	1860	400	3	560	3100	Diff
Yb La 1	Sp5	LLIF	1860	400	3	560	3100	Diff
Si Ka 1	Sp2	LPET	1850	895	3	560	2842	Diff
Sr La 1	Sp2	LPET	1850	895	3	560	2842	Diff
Y La 1	Sp2	LPET	1850	895	3	560	2842	Diff
P Ka 1	Sp2	LPET	1850	895	3	560	2842	Diff
S Ka 1	Sp2	LPET	1850	895	3	560	2842	Diff
Th Ma 1	Sp2	LPET	1850	895	3	560	2842	Diff
Ca Ka 1	Sp2	LPET	1850	895	3	560	2842	Diff
K Kb 1	Sp1	LPET	1320	895	2	560	4000	Diff

****

Acquisition informations :

Elt. Line	Spec	Xtal	Peak	Pk Time (S)	Bg Off1	Bg Off2	Slope/IBg (S)	Bg Time	Calibration (cps/nA)	Intensity
Pb Ma 1	Sp3	LPET	60373	700			1.0729	350	Pyromorphite_PbSp3_PbSp4_022	249.1
Pb Ma 1	Sp4	LPET	60349	700			0.950131	350	Pyromorphite_PbSp3_PbSp4_022	262.5
U Mb 1	Sp1	LPET	42452	600			2.17344	300	UO2_U Sp1_007	297.5
As Ka 1	Sp5	LLIF	29194	30	-375	341		15	GaAs_AsSp5_001	59.1
La La 1	Sp5	LLIF	66130	20	-600	600		10	LaPO4_P Sp2_LaSp5_001	84.5
Ce La 1	Sp5	LLIF	63552	10	-1000	1000		5	CePO4_CeSp5_001	93.3
Pr Lb 1	Sp5	LLIF	56076	30	-369	473		15	PrPO4_PrSp5_001	69.4
Nd La 1	Sp5	LLIF	58829	20	-1000	600		10	NdPO4_NdSp5_001	115.5
Sm Lb 1	Sp5	LLIF	49628	40	-1187	806		20	SmPO4_SmSp5_001	86.9
Eu La 1	Sp5	LLIF	52671	40	-888	799		20	EuPO4_EuSp5_001	146.2

Gd Lb 1	Sp5	LLIF	43356	50	-1322	1552		25	GdPO4_GdSp5_001	40.2
Tb La 1	Sp5	LLIF	49071	20	-1209	330		10	TbPO4_TbSp5_001	159.9
Dy La 1	Sp5	LLIF	47406	20	-1120	410		10	DyPO4_DySp5_001	162.7
Ho Lb 1	Sp5	LLIF	40909	20	-200	790		10	HoPO4_HoSp5_001	88.4
Er La 1	Sp5	LLIF	44318	20	-350	1078		10	Er_ErSp5_001	308.4
Tm La 1	Sp5	LLIF	42885	20	-754	813		10	Tm_TmSp5_001	321.2
Yb La 1	Sp5	LLIF	41505	20	-1642	590		10	Yb_YbSp5_001	314.4
Si Ka 1	Sp2	LPET	81514	20	-1170	853		10	Microcline_SiSp2_K Sp1_002146.3	
Sr La 1	Sp2	LPET	78509	40	-496	351		20	SrF2_SrSp2_002	106.5
Y La 1	Sp2	LPET	73700	100	-1089	1005		50	YAG_Y Sp2_005	68.5
P Ka 1	Sp2	LPET	70340	20	-1313	1505		10	LaPO4_P Sp2_LaSp5_001	73.0
S Ka 1	Sp2	LPET	61418	20	-5863	1527		10	Pyrite_S Sp2_002	498.6
Th Ma 1	Sp2	LPET	47255	500			1.1781	250	Brabantite2_ThSp2_40220010140.4	
Ca Ka 1	Sp2	LPET	38390	20	-500	500		10	Wilberforce_CaSp2_001	727.6
K Kb 1	Sp1	LPET	39445	100			2.7068	50	Microcline_SiSp2_K Sp1_00228.4	

Appendix B. Quantitative settings for thorite analysis.

****

Common informations :

File Name : Thorite 10-6-08.qtiSet
File Date : Oct/09/08-12:35 PM
Comment :

****

Column conditions :

Cond 1 :
HV (kV) : 15   I (nA) : 80
Size (µm) : 0.
Scanning : Off
RasterLength (µm) : 18.88

****

Xtal informations :

Xtal parameters:

Th Ma 1	Sp1	LPET	(2d= 8.75	K= 0.000144)
S Ka 1	Sp1	LPET	(2d= 8.75	K= 0.000144)
U Mb 1	Sp1	LPET	(2d= 8.75	K= 0.000144)
As Ka 1	Sp5	LLIF	(2d= 4.0267	K= 0.000058)
La La 1	Sp5	LLIF	(2d= 4.0267	K= 0.000058)
Ce La 1	Sp5	LLIF	(2d= 4.0267	K= 0.000058)
Pr Lb 1	Sp5	LLIF	(2d= 4.0267	K= 0.000058)
Nd La 1	Sp5	LLIF	(2d= 4.0267	K= 0.000058)
Sm Lb 1	Sp5	LLIF	(2d= 4.0267	K= 0.000058)
Eu La 1	Sp5	LLIF	(2d= 4.0267	K= 0.000058)
Gd Lb 1	Sp5	LLIF	(2d= 4.0267	K= 0.000058)
Tb La 1	Sp5	LLIF	(2d= 4.0267	K= 0.000058)
Dy La 1	Sp5	LLIF	(2d= 4.0267	K= 0.000058)
Ho Lb 1	Sp5	LLIF	(2d= 4.0267	K= 0.000058)
Er La 1	Sp5	LLIF	(2d= 4.0267	K= 0.000058)
Tm La 1	Sp5	LLIF	(2d= 4.0267	K= 0.000058)
Yb La 1	Sp5	LLIF	(2d= 4.0267	K= 0.000058)
Si Ka 1	Sp2	LPET	(2d= 8.75	K= 0.000144)

Y La 1	Sp2	LPET	(2d= 8.75	K= 0.000144)
P Ka 1	Sp2	LPET	(2d= 8.75	K= 0.000144)
Ca Ka 1	Sp2	LPET	(2d= 8.75	K= 0.000144)
Pb Mb 1	Sp2	LPET	(2d= 8.75	K= 0.000144)
Pb Mb 1	Sp3	LPET	(2d= 8.75	K= 0.000144)
Pb Mb 1	Sp4	LPET	(2d= 8.75	K= 0.000144)
Fe Ka 1	Sp5	LLIF	(2d= 4.0267	K= 0.000058)

Pha parameters :

Elt. Line	Spec	Xtal	Bias (V)	Gain	Dtime (µs)	Blin (mV)	Wind (mV)	Mode
Th Ma 1	Sp1	LPET	1320	895	2	560	4000	Diff
S Ka 1	Sp1	LPET	1320	895	3	560	4000	Diff
U Mb 1	Sp1	LPET	1320	895	2	560	4000	Diff
As Ka 1	Sp5	LLIF	1860	400	3	560	3100	Diff
La La 1	Sp5	LLIF	1860	400	3	560	3100	Diff
Ce La 1	Sp5	LLIF	1860	400	3	560	3100	Diff
Pr Lb 1	Sp5	LLIF	1860	400	3	560	3100	Diff
Nd La 1	Sp5	LLIF	1860	400	3	560	3100	Diff
Sm Lb 1	Sp5	LLIF	1860	400	3	560	3100	Diff
Eu La 1	Sp5	LLIF	1860	400	3	560	3100	Diff
Gd Lb 1	Sp5	LLIF	1860	400	3	560	3100	Diff
Tb La 1	Sp5	LLIF	1860	400	3	560	3100	Diff
Dy La 1	Sp5	LLIF	1860	400	3	560	3100	Diff
Ho Lb 1	Sp5	LLIF	1860	400	3	560	3100	Diff
Er La 1	Sp5	LLIF	1860	400	3	560	3100	Diff
Tm La 1	Sp5	LLIF	1860	400	3	560	3100	Diff
Yb La 1	Sp5	LLIF	1860	400	3	560	3100	Diff
Si Ka 1	Sp2	LPET	1910	412	3	560	2842	Diff
Y La 1	Sp2	LPET	1850	895	3	560	2842	Diff
P Ka 1	Sp2	LPET	1850	895	3	560	2842	Diff
Ca Ka 1	Sp2	LPET	1850	895	3	560	2842	Diff
Pb Mb 1	Sp2	LPET	1910	412	3	560	2842	Diff
Pb Mb 1	Sp3	LPET	1855	864	3	560	2300	Diff
Pb Mb 1	Sp4	LPET	1865	873	3	560	2300	Diff
Fe Ka 1	Sp5	LLIF	1860	400	3	560	3100	Diff

****
******

Acquisition informations :

Elt. Line	Spec	Xtal	Peak	Pk Time (S)	Bg Off1	Bg Off2	Slope/IBg (S)	Bg Time	Calibration (cps/nA)	Intensity
Th Ma 1	Sp1	LPET	47272	20	-955	1753		10	Brabantite2_ThSp1_014	91.1
S Ka 1	Sp1	LPET	61395	30	-5863	1527		15	Pyrite_S Sp1_001	527.0
U Mb 1	Sp1	LPET	42449	300	-1204	1		150	UO2_U Sp1_007	297.5
As Ka 1	Sp5	LLIF	29194	30	-375	341		15	GaAs_AsSp5_001	59.1
La La 1	Sp5	LLIF	66144	10	-600	600		5	LaPO4_P Sp2_LaSp5_001	84.5
Ce La 1	Sp5	LLIF	63567	10	-1000	1000		5	CePO4_CeSp5_001	93.3
Pr Lb 1	Sp5	LLIF	56076	30	-369	473		15	PrPO4_PrSp5_001	69.4
Nd La 1	Sp5	LLIF	58832	10	-1000	600		5	NdPO4_NdSp5_001	115.5
Sm Lb 1	Sp5	LLIF	49628	40	-1187	806		20	SmPO4_SmSp5_001	86.9
Eu La 1	Sp5	LLIF	52671	40	-888	799		20	EuPO4_EuSp5_001	146.2

Gd Lb 1	Sp5	LLIF	43356	50	-1322	1552	25	GdPO4_GdSp5_001	40.2
Tb La 1	Sp5	LLIF	49071	20	-627	813	10	TbPO4_TbSp5_001	159.9
Dy La 1	Sp5	LLIF	47406	20	-523	1100	10	DyPO4_DySp5_001	162.7
Ho Lb 1	Sp5	LLIF	40909	20	-1016	1157	10	HoPO4_HoSp5_001	88.4
Er La 1	Sp5	LLIF	44318	20	-649	956	10	Er_ErSp5_001	308.4
Tm La 1	Sp5	LLIF	42885	20	-754	813	10	Tm_TmSp5_001	321.2
Yb La 1	Sp5	LLIF	41505	20	-1642	590	10	Yb_YbSp5_001	314.4
Si Ka 1	Sp2	LPET	81454	20	-1170	853	10	Pg721_SiSp2_001	108.2
Y La 1	Sp2	LPET	73746	100	-1089	1005	50	YAG_Y Sp2_005	68.5
P Ka 1	Sp2	LPET	70391	30	-1313	1505	15	LaPO4_P Sp2_LaSp5_001	73.0
Ca Ka 1	Sp2	LPET	38390	20	-500	500	10	Wilberforce_CaSp2_001	727.6
Pb Mb 1	Sp2	LPET	57990	200	-720	734	100	Pyromorphite_PbSp2_PbSp3_PbSp4_001	108.7
Pb Mb 1	Sp3	LPET	57994	340	-720	734	170	Pyromorphite_PbSp2_PbSp3_PbSp4_001	182.7
Pb Mb 1	Sp4	LPET	57963	340	-720	734	170	Pyromorphite_PbSp2_PbSp3_PbSp4_001	195.2
Fe Ka 1	Sp5	LLIF	48092	30	-1187	456	15	Pyrite_FeSp5_001	270.2

Appendix C. Full-section LREE monazite search map results.

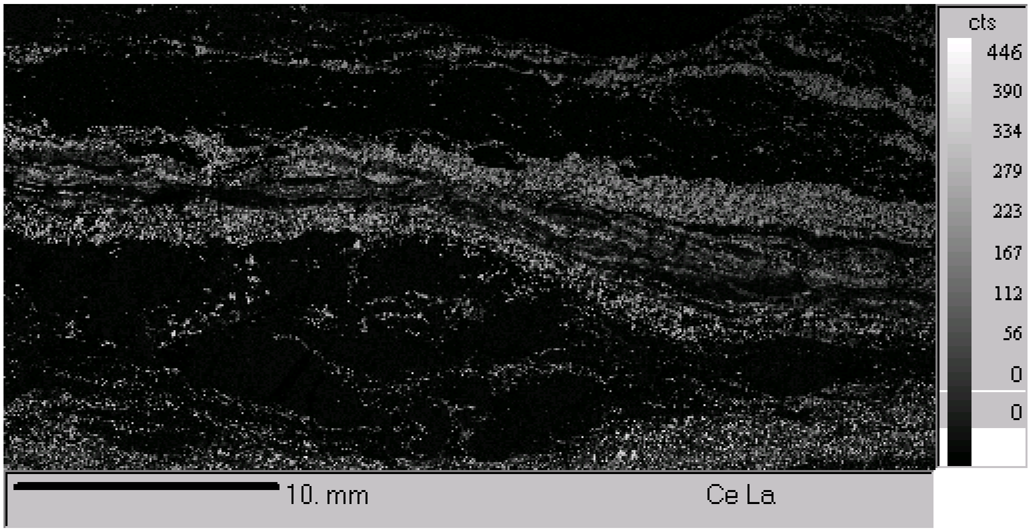

LH12C

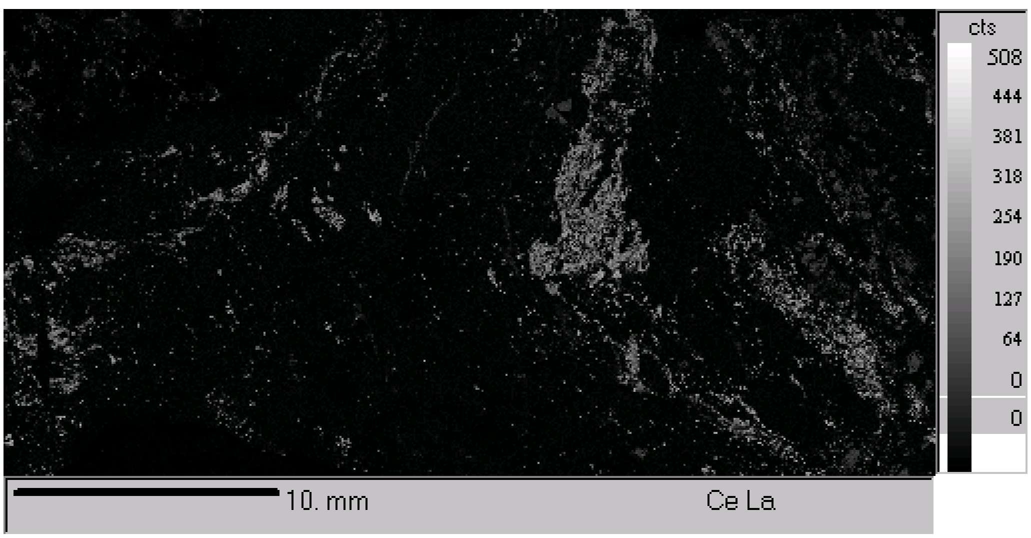

LH8C

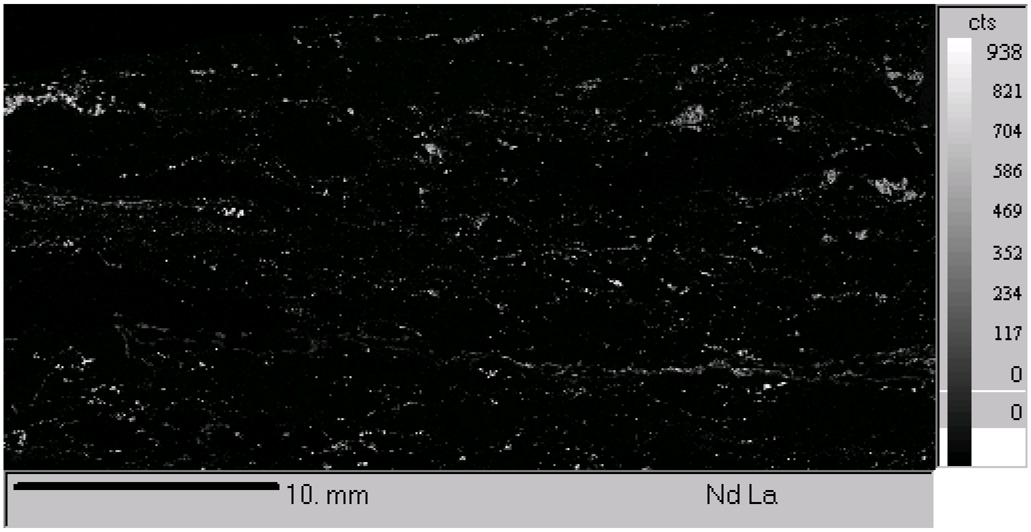

LH06-25

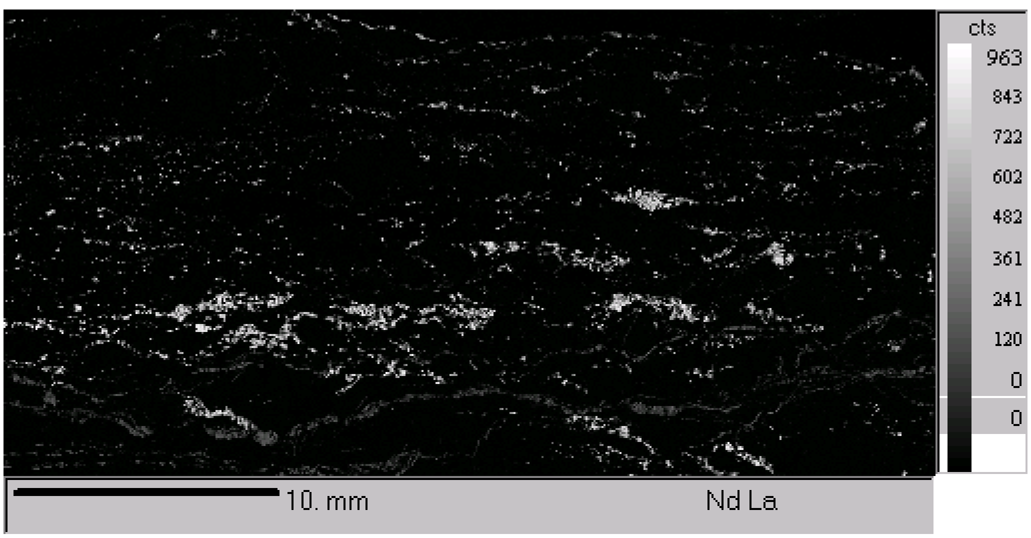

LH06-A2

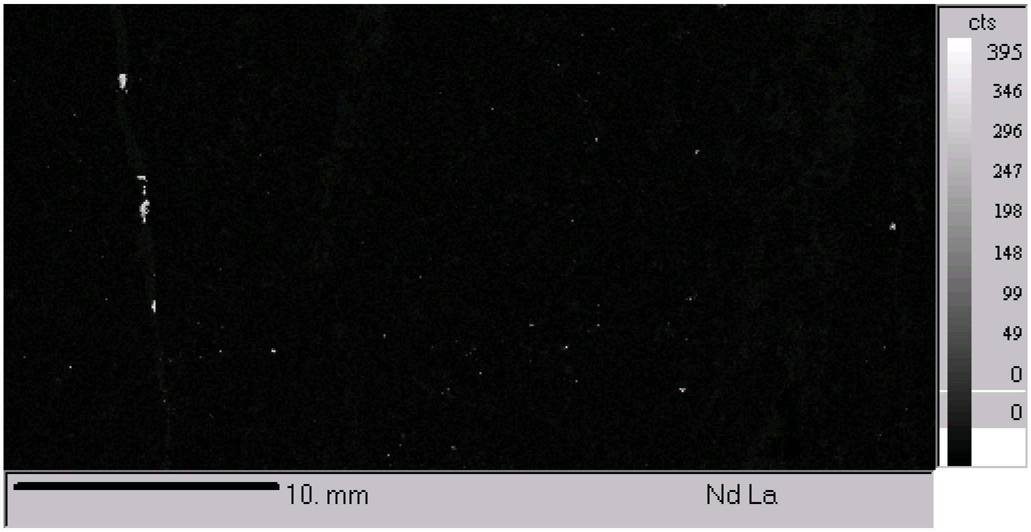

JA06-01C

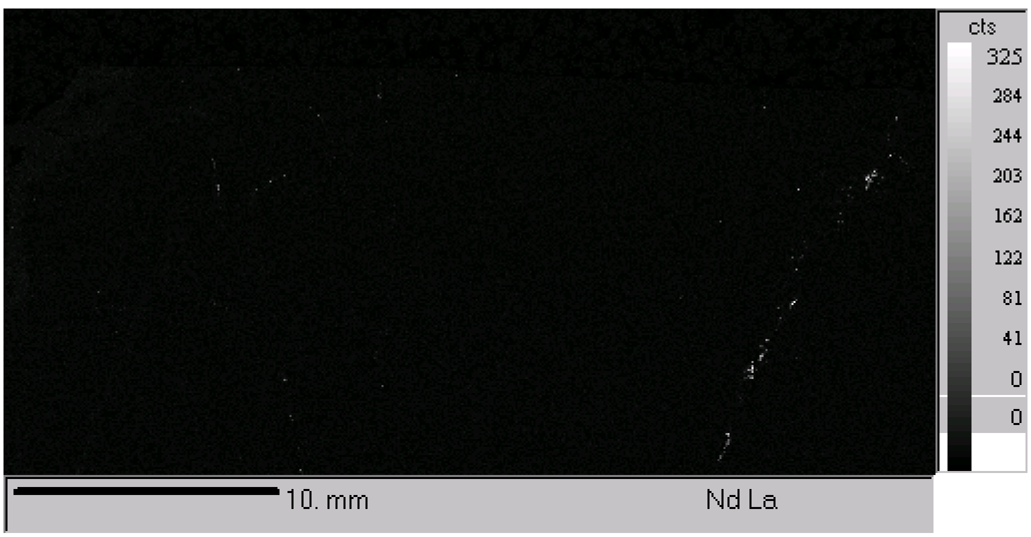

06CTCAr

Lemhi Pass (LP) Lead Isotope Study Samples		APPENDIX H1				V.S. Gillerman, December 16, 2008			
all locations from Lemhi County, Idaho									
Sample Number	**Mine/Location**	**Rock Description**	**Mineral**	**Comments**	**Waypoint #**	**UTM Zone**	**Easting**	**Northing**	
						NAD 27			
07WP129 KF-P L2	Leadore: Hawley Crk. Canyon	Leadore Granite: Pink Granite, coarse-grained, weak c	feldspar, L2		07WP129	12	325189	4947434	
07WP129 KF-M L2	Leadore: Hawley Crk. Canyon	granophyre, perthite, zircon, interstitial quartz	feldspar, L2						
07WP129 KF-C L2	Leadore: Hawley Crk. Canyon		feldspar, L2						
JA06-01A KF-M L2	LP trench W of Cont. Divide	Syenite: 70% feldspar (Or w/ Ab rims), hematite alterat	feldspar, L2	529 Ma U-Pbzircon	06WP088	12	306554	4981060	
JA06-01A KF-C L2	LP trench W of Cont. Divide	Syenite: 70% feldspar (Or w/ Ab rims), hematite alterat	feldspar, L2						
JA06-01C HM	LP trench W of Cont. Divide	Quartz-Hematite veins cutting syenite	hematite						
07WP119 KF-P L2	LP: ThO2 Mine	Th Vein: Qz-pinkKf-Hm-Th; radioactive	feldspar, L2	Dump Open Pit	07WP119	12	302327	4970507	
LH06-24B KF-M L2	LP: Lucky Horseshoe, main pit	ThREE Ore Cataclasite: Fsp-Biot-Apat-Hm-Th-MZ	feldspar, L2	Open Pit - stongly deforme	06WP040	12	303357	4984816	
LH06-24B KF-C L2	LP: Lucky Horseshoe, main pit	high grade Th ore, radioactive	feldspar, L2						
LH06-24B HM	LP: Lucky Horseshoe, main pit		hematite						
CQ06-30B CP	LP: Copper Queen Dump	Qz-Cp-Ga-Po/py vein in altered Pyroxene Porphyry	chalcopyrite	Shaft Dump	surveyed	12	304825	4982275	
CQ06-30B GA	LP: Copper Queen Dump	Qz-Cp-Ga-Po/py vein in altered Pyroxene Porphyry	galena	Shaft Dump					
CQ06-30B PY	LP: Copper Queen Dump	Qz-Cp-Ga-Po/py vein in altered Pyroxene Porphyry	pyrite	Shaft Dump					
CQ06-52 CP	LP: Copper Queen - road?	Qz-Py-Cp in quartzite	chalcopyrite	road area	06WP045	12	304854	4982283	
1CQ-2b MO	LP: Copper Queen Dump	Quartz-Moly vein (cp-bn locally) in quartzite	molybdenite	Shaft Dump		12	304825	4982275	
07CQS-R BN	LP: Copper Queen	Quartz-sulfide vein, mostly bornite in quartzite	bornite	coll. By R. Reed					
085-F	Deep Creek Pluton: ~14 mi. W	Fresh, mg gabbro to mafic syenodiorite;	feldspar, L2	collected off Napias Crk.	06WP085	11	719253	5001925	
099-F	LP: Trench SE of Bluebird	Syenite, fresher, no veins	feldspar, L1	wk. magnetic; concealed	06WP099	12	306078	4982327	
099-F			feldspar, L2						
LH33-F	LP: Lucky Horseshoe mine	Tan Feldspar veins cutting hanging wall schist	feldspar, L2	outer zone of Th-REE ore?	06WP040 + 20	12	303357	4984836	
BC4-F	Bull Canyon Stock, 10 mi. SE (	Red Granite/Syenite- highly altered; high Th, Mz	feldspar, L2	Fsp to sericite + hematite	08BC52	NAD83	W113°10'23"	N44°37'11"	collected by RR/SD
BC1-F	Bull Canyon Stock, 10 mi. SE (	Red Granite/Syenite- highly altered; high Th, Mz	feldspar, L1	Fsp to sericite + hematite	08BC45	NAD83	W113°9'58"	N44°37'52"	collected by RR/SD
BC1-F			feldspar, L2						
CAC-F	LP: Cago Mine	Th vein envelope - white portion	feldspar, L2	outer white envel.	06WP055	12	303964	4980355	
102-F	LP: Trench SE of Bluebird min	Pyroxene Porphyry (same loc. As BL06-03)	feldspar, L1	Oliv altered to Trem.; propy	06WP102	12	305955	4982486	
102-F			feldspar, L2						
120-F	LP: Lower Lucky Horseshoe A	Mafic Sill: carbonate alteration; px, amph fresher	feldspar, L1	Matrix feldspar may be plag	07WP120	12	303477	4984549	
120-F			feldspar, L2						
195-H	Reese Creek Iron Mine	Vein of massive specular hematite, minor white quartz	hematite	Staatz loc. 195	07WP116	12	300690	4967107	
126A-I	Roberts Prospect	Carbonatite Breccia- calcite, Act., coarse ilmenite	ilmenite	North Fork Belt (Anderson,	07WP126	11	718106	5032106	
YJ-G	Yellowjacket mine - ug?	Quartz-galena vein, super fresh	galena	collected by R. Bjorklund		11	694724	4983376	unsure of exact location
YJ1-C	Yellowjacket Open Pit	Partly oxidized breccia with FeOx, Chalcopy matrix	chalcopyrite	in quartzite, coll. 1992		11	695561	4984331	unsure of exact location
1189-C	Napo Canyon, unnamed	Massive chalcopyrite vein, very fresh	chalcopyrite	coll. By R. Reed		12	294143	4973018	
94-18-C	Blackpine Cu-Co prospect, 15	DDH 94-18, Formation Capital, siltite w/qz-cp vein	chalcopyrite	coll. By FCC		11	720389	4991662	for general mine area
PS-1-C	Pope Shenon Mine	Chalcopyrite from vein, from new ug development	chalcopyrite	coll. By D. Krasowski	06WP065	12	275188	4994959	coordinates for reclaimed Adit 2?
B3r-H	LP: Buffalo mine	Vein of massive hematite with Th and trace cp	hematite	coll. By R. Reed	06WP083	12	304672	4983524	general mine coordinates

Lemhi Pb: Gillerman **Appendix H2: Lead Isotope Results**

sample	type	208/204	%se	207/204	%se	206/204	%se	208/206	%se	207/206	%se	Notes
07WP129 KF-P L2	feldspar, L2	**38.132**	**0.047**	**15.631**	**0.046**	**18.093**	**0.046**	**2.1075**	**0.005**	**0.86384**	**0.004**	weak, ran hot at 100 mV 208
07WP129 KF-C L2	feldspar, L2	**37.976**	**0.036**	**15.658**	**0.036**	**18.044**	**0.035**	**2.1049**	**0.004**	**0.86771**	**0.003**	weak, ran hot at 100 mV 208
085-F	feldspar, L2	**39.409**	**0.007**	**15.729**	**0.007**	**19.545**	**0.007**	**2.0163**	**0.001**	**0.80484**	**0.001**	200 ratios at 500mV
BC4-F	feldspar, L2	**44.754**	**0.009**	**15.963**	**0.009**	**23.879**	**0.009**	**1.8743**	**0.002**	**0.66850**	**0.001**	200 ratios at 500mV
102-F	feldspar, L1	**42.604**	**0.005**	**15.861**	**0.004**	**21.388**	**0.004**	**1.9920**	**0.002**	**0.74157**	**0.001**	200 ratios at 1V
099-F	feldspar, L1	**39.628**	**0.002**	**15.672**	**0.002**	**19.354**	**0.002**	**2.0475**	**0.000**	**0.80973**	**0.000**	200 ratios at 3V
JA06-01A KF-C L2	feldspar, L2	**40.293**	**0.016**	**15.809**	**0.015**	**20.361**	**0.015**	**1.9790**	**0.003**	**0.77644**	**0.002**	weak, ran somewhat hot at 300mV 208
JA06-01C HM	hematite	**42.977**	**0.003**	**15.984**	**0.003**	**22.515**	**0.003**	**1.9089**	**0.001**	**0.70994**	**0.001**	3V, somewhat uranogenic?
LH06-24B HM	hematite	**400.057**	**0.016**	**16.364**	**0.016**	**30.014**	**0.016**	**13.3286**	**0.001**	**0.54518**	**0.002**	3V, uranogenic & thorogenic!
B3r-H	hematite	**41.607**	**0.002**	**15.806**	**0.002**	**19.995**	**0.002**	**2.0809**	**0.001**	**0.79502**	**0.001**	200 ratios at 4V
195-H	hematite	**38.288**	**0.002**	**15.655**	**0.002**	**18.688**	**0.002**	**2.0488**	**0.001**	**0.83772**	**0.001**	200 ratios at 4V
126A-I	ilmenite	**38.420**	**0.005**	**15.646**	**0.004**	**18.692**	**0.003**	**2.0638**	**0.002**	**0.84049**	**0.001**	200 ratios at 2V
LH06-24B KF-C L2	feldspar, L2	**97.440**	**0.012**	**15.956**	**0.012**	**23.001**	**0.012**	**4.2364**	**0.001**	**0.69370**	**0.002**	pretty good, 1V 208, thorogenic!
LH33-F	feldspar, L2	**45.897**	**0.006**	**15.988**	**0.006**	**23.123**	**0.006**	**1.9850**	**0.001**	**0.69145**	**0.001**	200 ratios at 800mV
CAC-F	feldspar, L2	**46.264**	**0.011**	**15.871**	**0.010**	**21.370**	**0.010**	**2.1648**	**0.002**	**0.74261**	**0.001**	200 ratios at 500mV
CQ06-30B GA	galena	**41.023**	**0.008**	**15.849**	**0.006**	**20.112**	**0.004**	**2.0397**	**0.004**	**0.78803**	**0.002**	lots of Pb, ran cold at 4V 208
CQ06-30B PY	pyrite	**40.926**	**0.004**	**15.803**	**0.003**	**20.105**	**0.002**	**2.0356**	**0.002**	**0.78598**	**0.001**	lots of Pb, ran cold at 4V 208
CQ06-52 CP	chalcopyrite	**42.316**	**0.001**	**15.881**	**0.001**	**21.564**	**0.001**	**1.9624**	**0.001**	**0.73648**	**0.000**	lots of Pb, ran cold at 4V 208
1CQ-26 MO	molybdenite	**40.337**	**0.005**	**15.745**	**0.004**	**19.487**	**0.002**	**2.0700**	**0.002**	**0.80799**	**0.001**	lots of Pb, ran cold at 3V 208
07CQS-R BN	bornite	**43.577**	**0.002**	**15.964**	**0.002**	**22.317**	**0.002**	**1.9527**	**0.001**	**0.71533**	**0.001**	lots of Pb, ran cold at 4V 208
YJ-G	galena	**39.350**	**0.017**	**15.652**	**0.013**	**17.729**	**0.010**	**2.2194**	**0.008**	**0.88284**	**0.004**	60 ratios at 0.5V
YJ1-C	chalcopyrite	**39.672**	**0.008**	**15.735**	**0.006**	**18.619**	**0.004**	**2.1307**	**0.004**	**0.84507**	**0.002**	200 ratios at 4V
1189-C	chalcopyrite	**38.944**	**0.003**	**15.658**	**0.002**	**18.151**	**0.002**	**2.1455**	**0.001**	**0.86266**	**0.001**	200 ratios at 3V
94-18-C	chalcopyrite	**45.131**	**0.003**	**16.302**	**0.002**	**26.056**	**0.002**	**1.7321**	**0.001**	**0.62566**	**0.001**	200 ratios at 3V
PS-1-C	chalcopyrite	**45.109**	**0.003**	**15.987**	**0.003**	**22.307**	**0.003**	**2.0222**	**0.001**	**0.71668**	**0.001**	200 ratios at 2V

Fractionation Model:

alpha/amu	208/204	207/204	206/204	208/206	207/206
measured*	41.0233	15.8491	20.1123	2.0397	0.7880
-0.003	40.5310	15.7065	19.9916	2.0275	0.7857
-0.0024	40.6295	15.7350	20.0157	2.0299	0.7861
-0.0018	40.7279	15.7636	20.0399	2.0324	0.7866
-0.0012	40.8264	15.7921	20.0640	2.0348	0.7871
-0.0006	40.9248	15.8206	20.0881	2.0373	0.7876
0	41.0233	15.8491	20.1123	2.0397	0.7880
0.0006	41.1217	15.8777	20.1364	2.0422	0.7885
0.0012	41.2202	15.9062	20.1605	2.0446	0.7890
0.0018	41.3187	15.9347	20.1847	2.0471	0.7894
0.0024	41.4171	15.9633	20.2088	2.0495	0.7899
0.003	41.5156	15.9918	20.2329	2.0520	0.7904

blue = best estimate of Pb isotope composition of sample

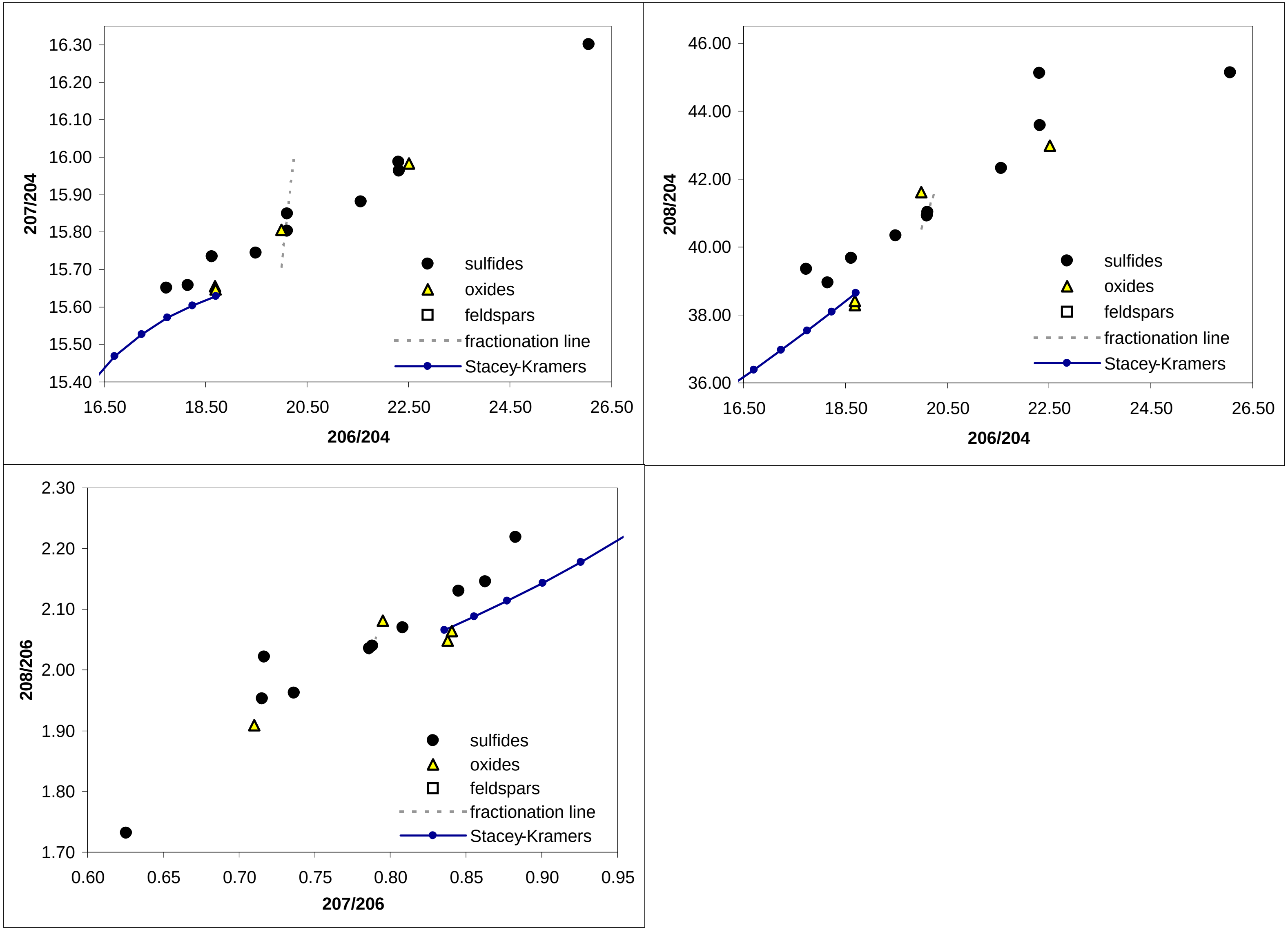
207/204
206/204
sulfides
oxides
feldspars
fractionation line
Stacey-Kramers
208/204
206/204
sulfides
oxides
feldspars
fractionation line
Stacey-Kramers
208/206
207/206
sulfides
oxides
feldspars
fractionation line
Stacey-Kramers

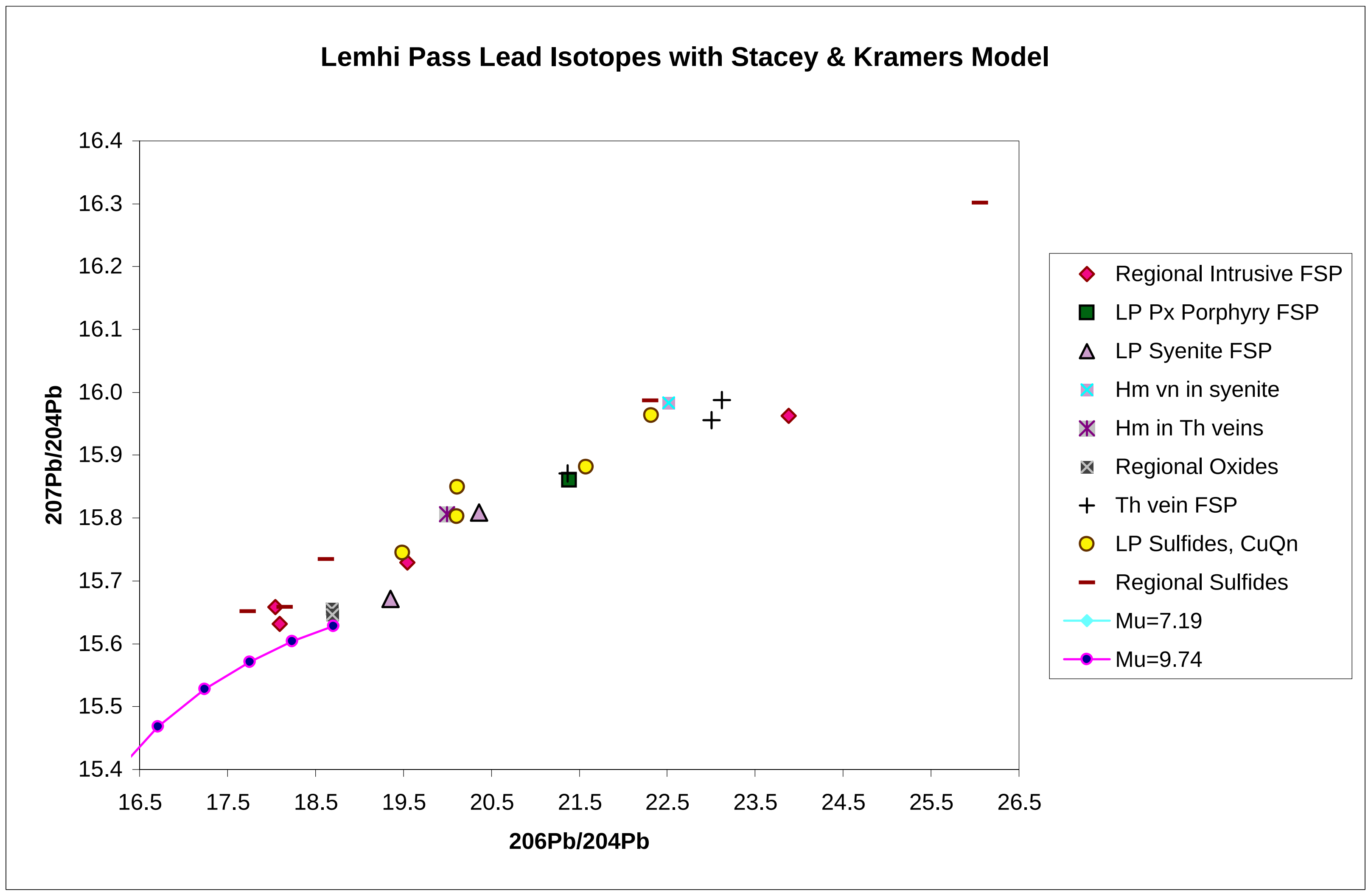
Lemhi Pass Lead Isotopes with Stacey & Kramers Model
207Pb/204Pb
206Pb/204Pb
16.4
16.3
16.2
16.1
16.0
15.9
15.8
15.7
15.6
15.5
15.4
16.5
17.5
18.5
19.5
20.5
21.5
22.5
23.5
24.5
25.5
26.5
Regional Intrusive FSP
LP Px Porphyry FSP
LP Syenite FSP
Hm vn in syenite
Hm in Th veins
Regional Oxides
Th vein FSP
LP Sulfides, CuQn
Regional Sulfides
Mu=7.19
Mu=9.74

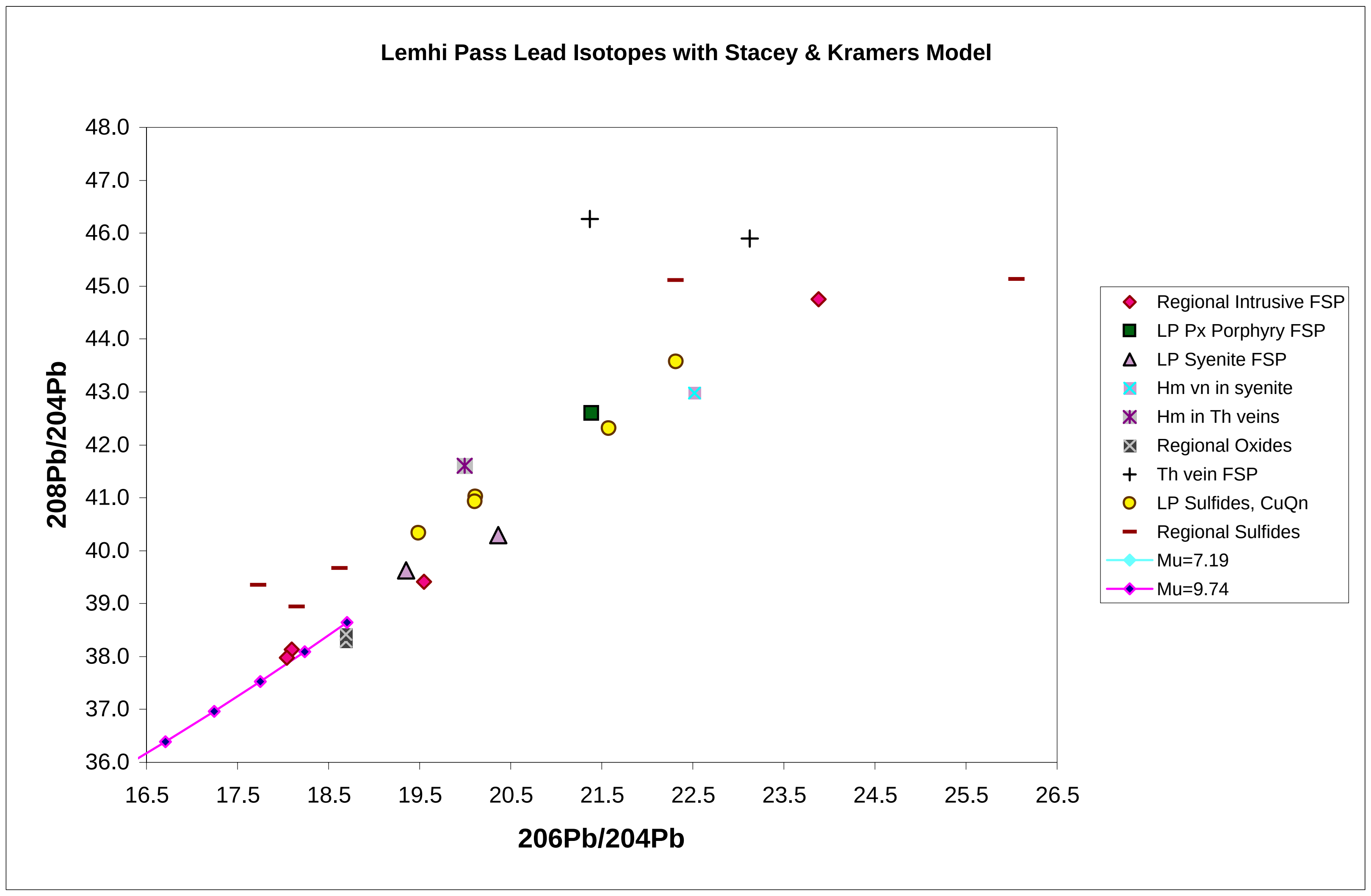
Lemhi Pass Lead Isotopes with Stacey & Kramers Model
208Pb/204Pb
206Pb/204Pb
48.0
47.0
46.0
45.0
44.0
43.0
42.0
41.0
40.0
39.0
38.0
37.0
36.0
16.5
17.5
18.5
19.5
20.5
21.5
22.5
23.5
24.5
25.5
26.5
Regional Intrusive FSP
LP Px Porphyry FSP
LP Syenite FSP
Hm vn in syenite
Hm in Th veins
Regional Oxides
Th vein FSP
LP Sulfides, CuQn
Regional Sulfides
Mu=7.19
Mu=9.74

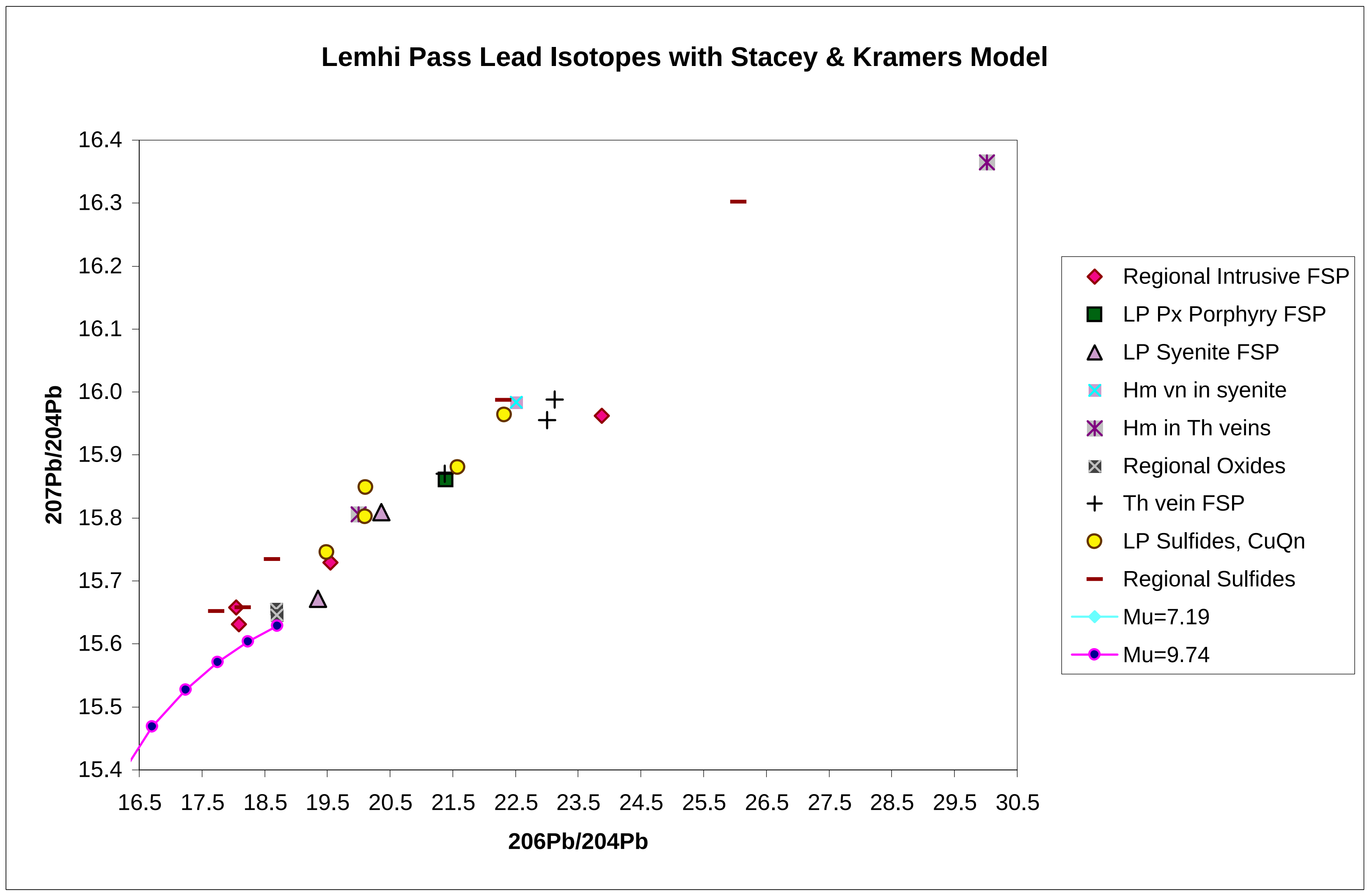
Lemhi Pass Lead Isotopes with Stacey & Kramers Model
207Pb/204Pb
206Pb/204Pb
16.4
16.3
16.2
16.1
16.0
15.9
15.8
15.7
15.6
15.5
15.4
16.5
17.5
18.5
19.5
20.5
21.5
22.5
23.5
24.5
25.5
26.5
27.5
28.5
29.5
30.5
Regional Intrusive FSP
LP Px Porphyry FSP
LP Syenite FSP
Hm vn in syenite
Hm in Th veins
Regional Oxides
Th vein FSP
LP Sulfides, CuQn
Regional Sulfides
Mu=7.19
Mu=9.74

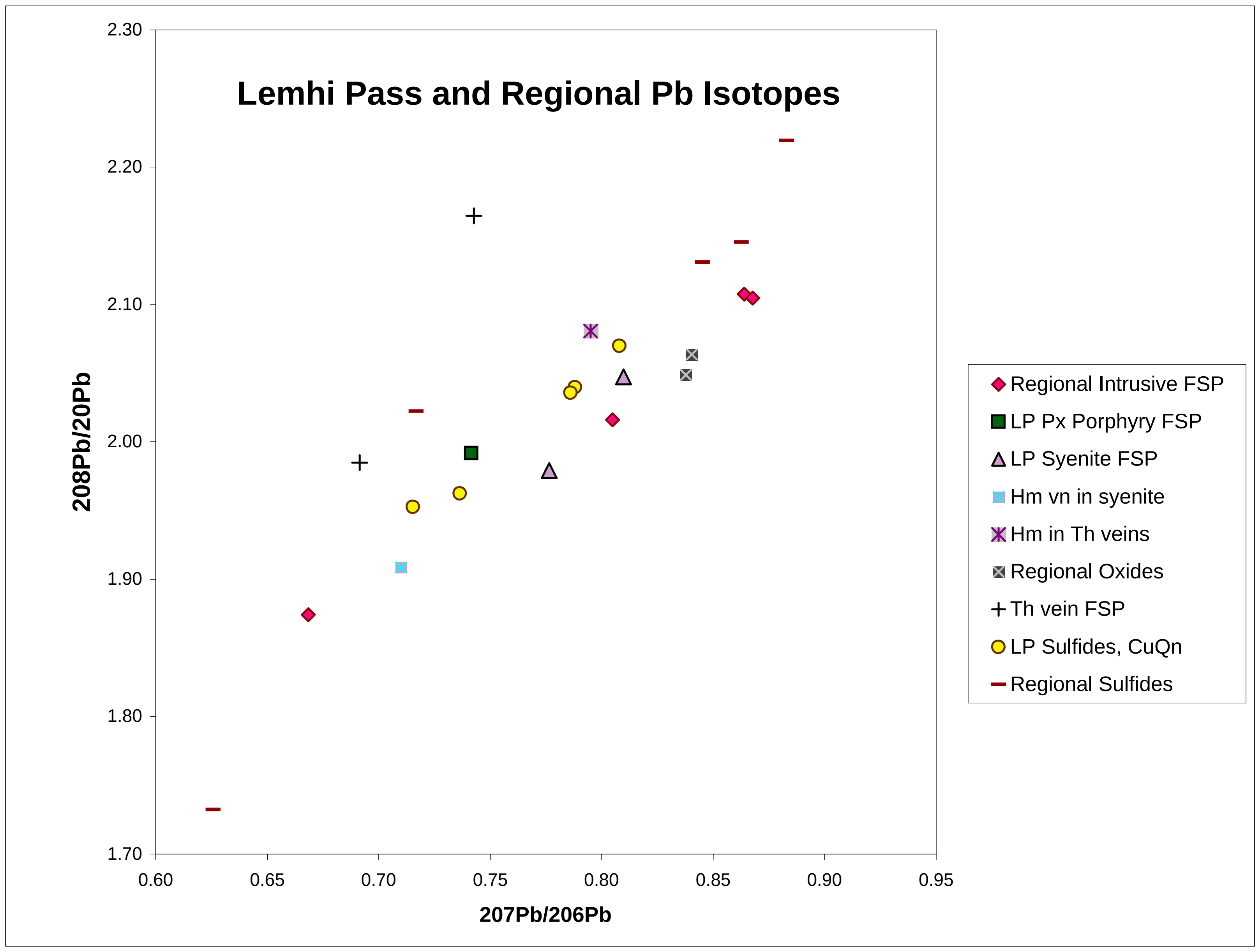
Lemhi Pass and Regional Pb Isotopes
208Pb/20Pb
207Pb/206Pb
2.30
2.20
2.10
2.00
1.90
1.80
1.70
0.60
0.65
0.70
0.75
0.80
0.85
0.90
0.95
Regional Intrusive FSP
LP Px Porphyry FSP
LP Syenite FSP
Hm vn in syenite
Hm in Th veins
Regional Oxides
Th vein FSP
LP Sulfides, CuQn
Regional Sulfides

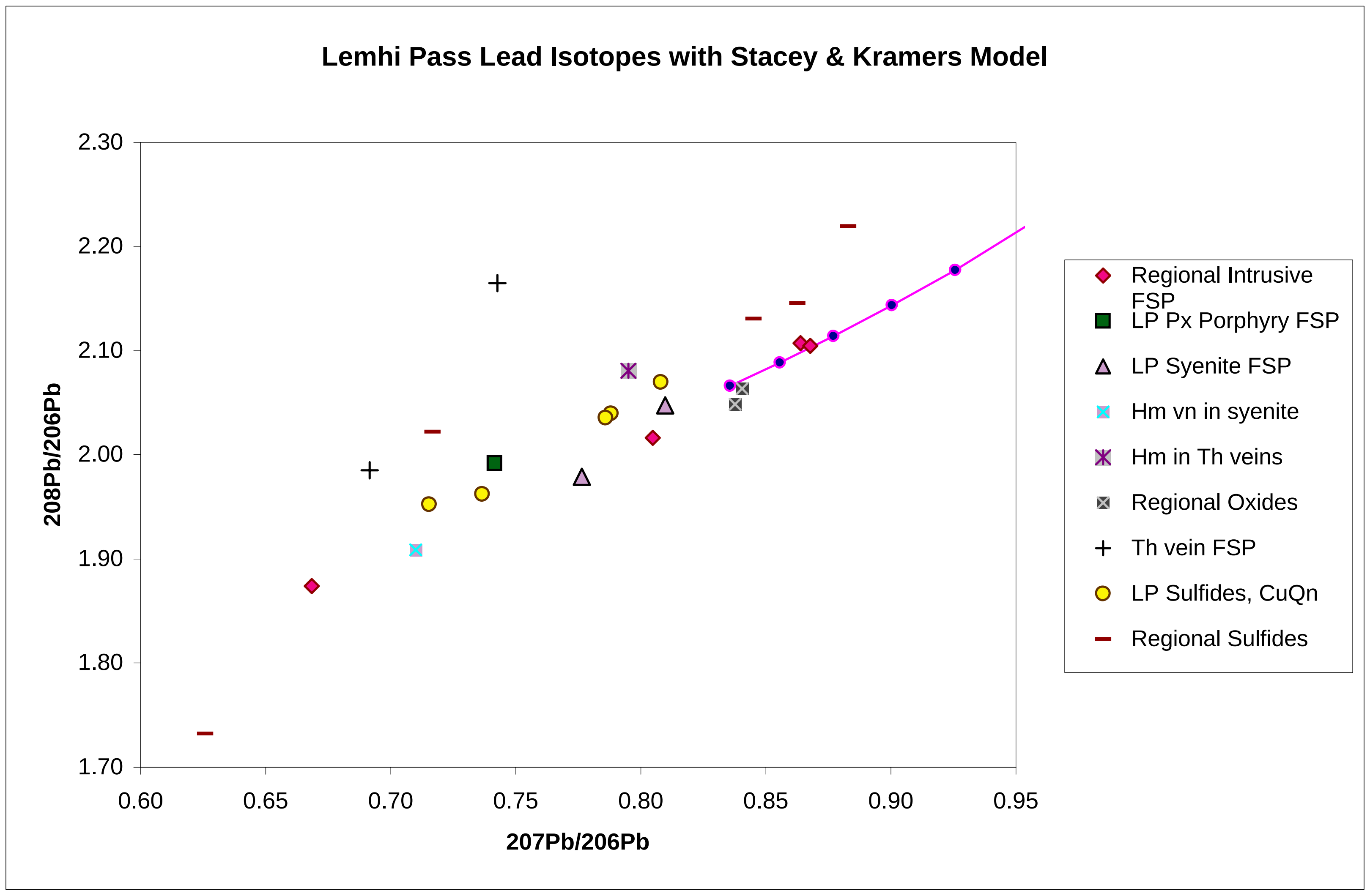
Lemhi Pass Lead Isotopes with Stacey & Kramers Model
208Pb/206Pb
207Pb/206Pb
2.30
2.20
2.10
2.00
1.90
1.80
1.70
0.60
0.65
0.70
0.75
0.80
0.85
0.90
0.95
Regional Intrusive FSP
LP Px Porphyry FSP
LP Syenite FSP
Hm vn in syenite
Hm in Th veins
Regional Oxides
Th vein FSP
LP Sulfides, CuQn
Regional Sulfides

You are asked to plot Pb isotope evolution lines from 4.5 Ga to the present for a variety of μ values on a 207Pb/204Pb versus 206Pb/204Pb diagram...

We need an equation for change in 206Pb/204Pb with time as a function of 238U/204Pb…

... = inputs

(206Pb/204Pb)tot = (206Pb/204Pb)o + (238U/204Pb)*(exp(lambda238*to)-exp(lambda238*tx))

We need another equation for change in 207Pb/204Pb with time as a function of 235U/204Pb…

(207Pb/204Pb)tot = (207Pb/204Pb)o + (238U/204Pb)*(235U/238U)*(exp(lambda235*to)-exp(lambda235*tx))

Stacey and Kramer curve

First Stage:		**lambda*1e9 =**	**1.5513E-01**	**9.8485E-01**	**4.9475E-02**		
		μ =	**7.19**	**0.05214679**	**33.21**	= K	
		initials =	**9.307**	**10.294**	**29.487**		
t (Ga) initial	**t (Ga) from initial**	**t (Ga) before present**	**206/204**	**207/204**	**208/204**	**208/206**	**207/206**
4.57	0	4.57	9.307	10.294	29.487	3.1683	1.1060
	0.1	4.47	9.532	10.735	29.692	3.1151	1.1262
	0.2	4.37	9.753	11.134	29.897	3.0653	1.1416
	0.3	4.27	9.971	11.496	30.100	3.0187	1.1529
	0.4	4.17	10.186	11.824	30.303	2.9750	1.1608
	0.5	4.07	10.397	12.121	30.504	2.9339	1.1658
	0.6	3.97	10.605	12.390	30.705	2.8952	1.1683
	0.7	3.87	10.810	12.634	30.904	2.8588	1.1687
	0.8	3.77	11.012	12.855	31.103	2.8245	1.1674
	0.87	3.7	11.151	12.997	31.241	2.8016	1.1656

Second Stage:		**lambda*1e9 =**	**1.5513E-01**	**9.8485E-01**	**4.9475E-02**		
		μ =	**10**	**0.07252683**	**36.84**	= K	
		initials =	**11.151**	**12.997**	**31.241**		
t (Ga) initial	**t (Ga) from initial**	**t (Ga) before present**	**206/204**	**207/204**	**208/204**	**208/206**	**207/206**
3.7	0	3.7	11.151	12.997	31.241	2.8016	1.1656
	0.5	3.2	12.476	14.076	32.322	2.5907	1.1282
	1	2.7	13.702	14.735	33.377	2.4359	1.0754
	1.5	2.2	14.837	15.138	34.405	2.3189	1.0203
	2	1.7	15.887	15.384	35.409	2.2289	0.9684
	2.5	1.2	16.858	15.535	36.388	2.1585	0.9215
	2.8	0.9	17.406	15.595	36.964	2.1237	0.8960
	3.1	0.6	17.929	15.640	37.532	2.0934	0.8723
	3.4	0.3	18.428	15.674	38.091	2.0670	0.8505
	3.7	0	18.904	15.699	38.642	2.0441	0.8304

Model Age Calculator

t (Ga) initial	**t (Ga) from initial**	**t (Ga) before present**	**206/204**	**207/204**		
	3.197	0.503	18.093	15.652	Leadore WP129	
	3.232	0.468	18.151	15.656	1189 Cp vein	
	4.226	-0.526	19.545	15.729	085 Gabbro is approx. 500N	NO SOLN

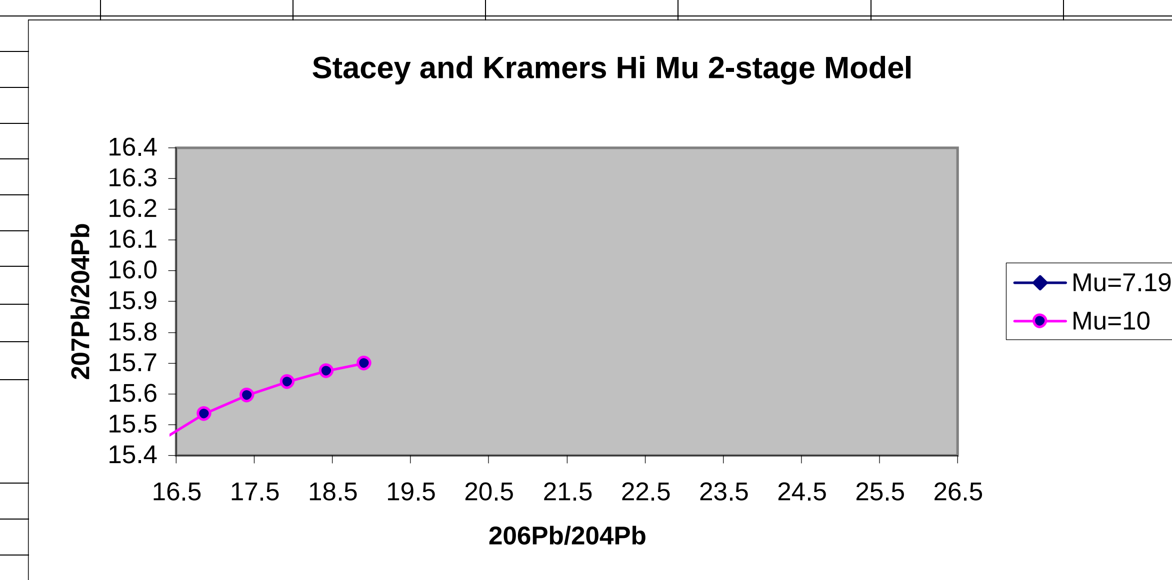

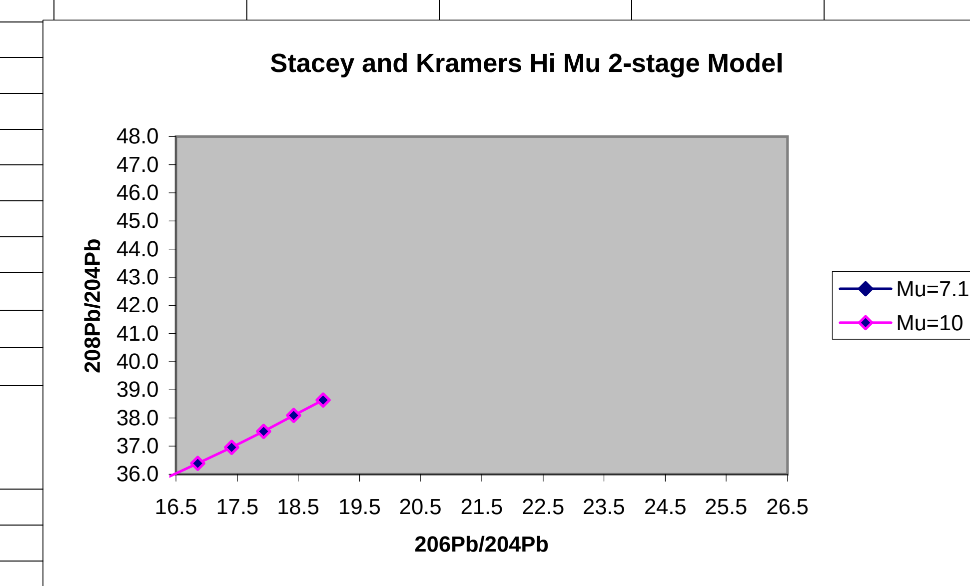

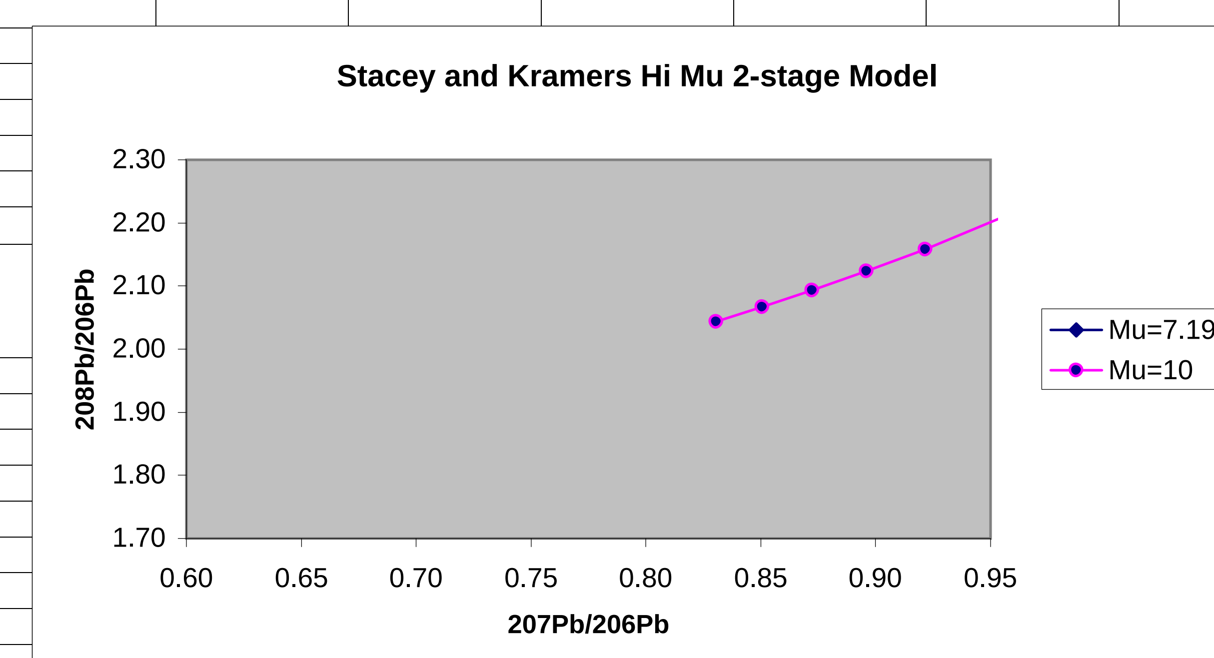

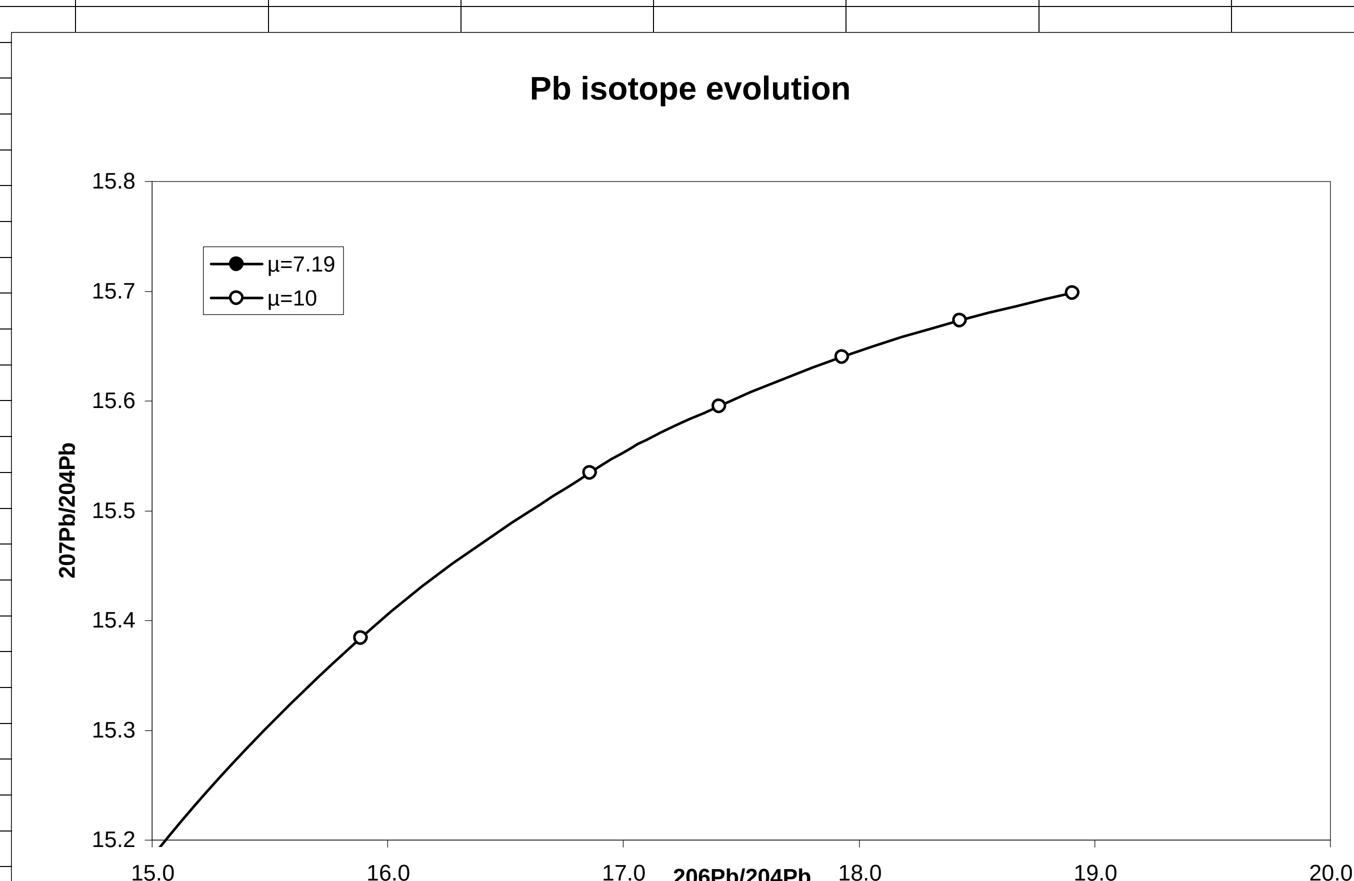

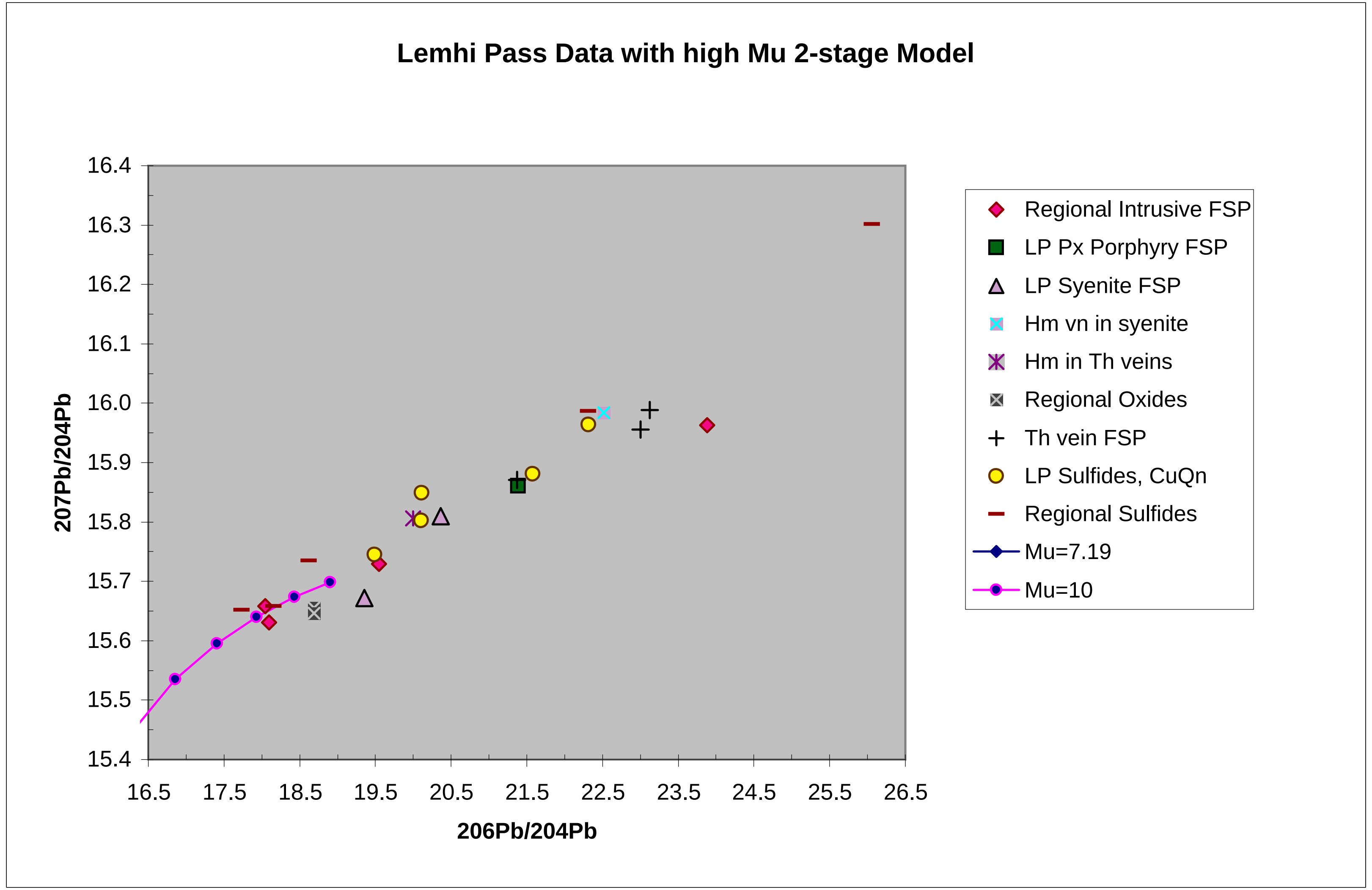

Lemhi Pass Data with high Mu 2-stage Model
207Pb/204Pb
206Pb/204Pb
16.4
16.3
16.2
16.1
16.0
15.9
15.8
15.7
15.6
15.5
15.4
16.5
17.5
18.5
19.5
20.5
21.5
22.5
23.5
24.5
25.5
26.5
Regional Intrusive FSP
LP Px Porphyry FSP
LP Syenite FSP
Hm vn in syenite
Hm in Th veins
Regional Oxides
Th vein FSP
LP Sulfides, CuQn
Regional Sulfides
Mu=7.19
Mu=10

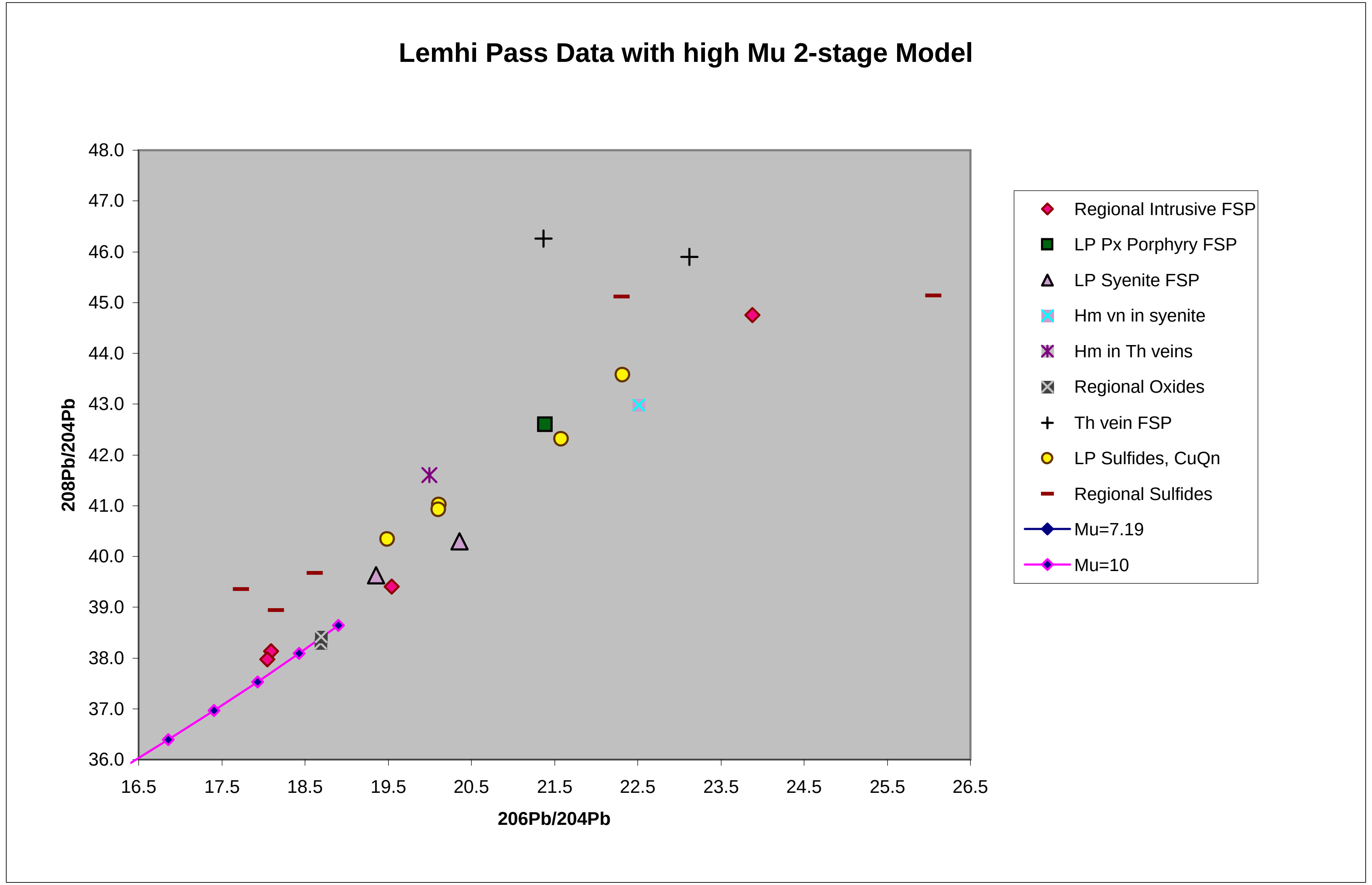

Lemhi Pass Data with high Mu 2-stage Model
208Pb/204Pb
206Pb/204Pb
48.0
47.0
46.0
45.0
44.0
43.0
42.0
41.0
40.0
39.0
38.0
37.0
36.0
16.5
17.5
18.5
19.5
20.5
21.5
22.5
23.5
24.5
25.5
26.5
Regional Intrusive FSP
LP Px Porphyry FSP
LP Syenite FSP
Hm vn in syenite
Hm in Th veins
Regional Oxides
Th vein FSP
LP Sulfides, CuQn
Regional Sulfides
Mu=7.19
Mu=10

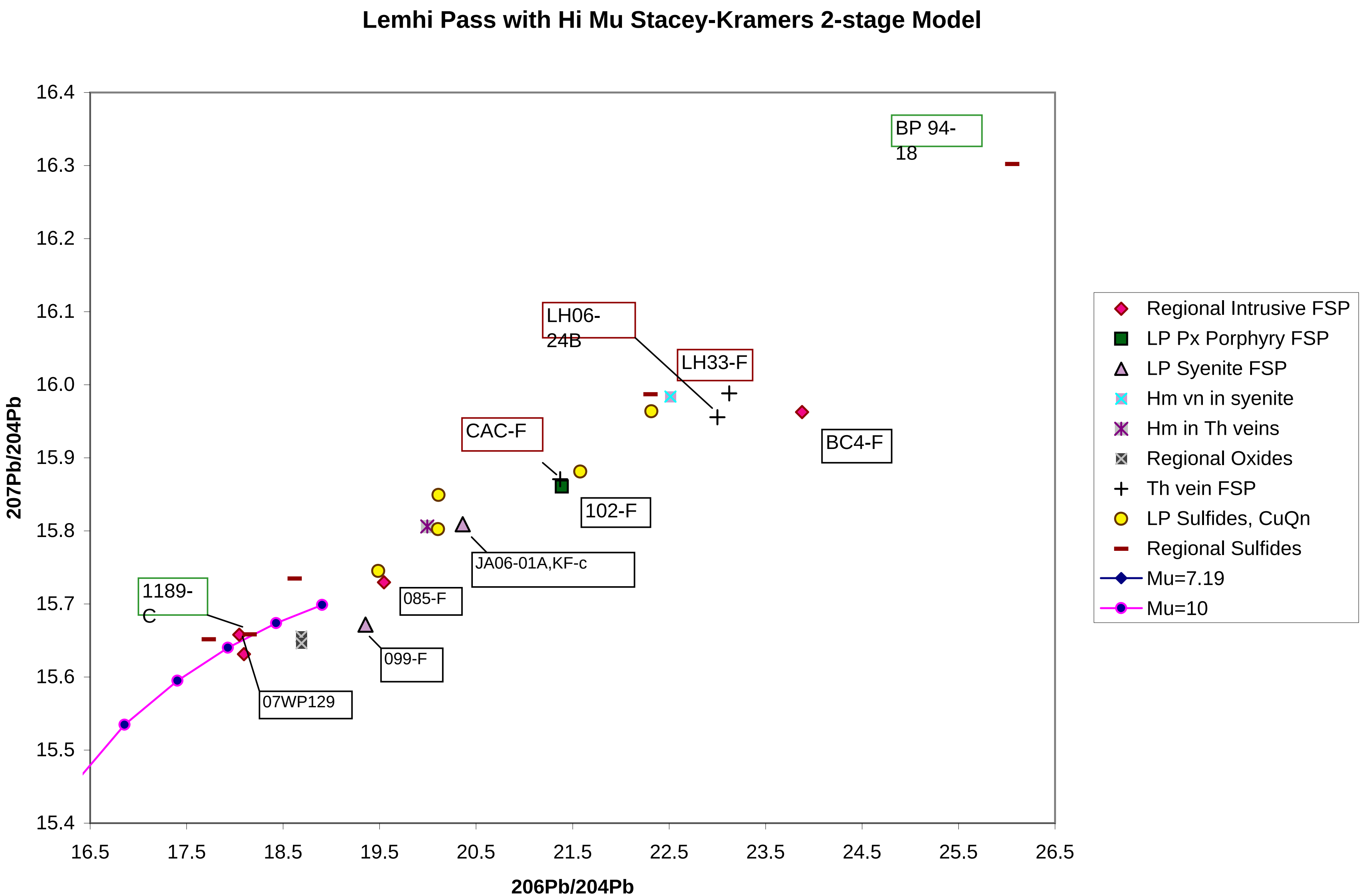

Lemhi Pass with Hi Mu Stacey-Kramers 2-stage Model
207Pb/204Pb
206Pb/204Pb
16.4
16.3
16.2
16.1
16.0
15.9
15.8
15.7
15.6
15.5
15.4
16.5
17.5
18.5
19.5
20.5
21.5
22.5
23.5
24.5
25.5
26.5
BP 94-18
LH06-24B
LH33-F
CAC-F
BC4-F
102-F
JA06-01A,KF-c
085-F
1189-C
099-F
07WP129
Regional Intrusive FSP
LP Px Porphyry FSP
LP Syenite FSP
Hm vn in syenite
Hm in Th veins
Regional Oxides
Th vein FSP
LP Sulfides, CuQn
Regional Sulfides
Mu=7.19
Mu=10